Traces of Exotic Physics in Cosmology

WILLS, DANIELLE,ELIZABETH,STANBR

Traces of Exotic Physics in Cosmology

Danielle Elizabeth Wills

A Thesis presented for the degree of
Doctor of Philosophy

Centre for Particle Theory
Department of Mathematical Sciences
University of Durham
England

March 2015

Dedicated to

Shiva and Shakti

Traces of Exotic Physics in Cosmology

Danielle Elizabeth Wills

Submitted for the degree of Doctor of Philosophy
March 2015

Abstract

In recent years it has become increasingly clear that our universe is far more intricate than we might ever have imagined. While theoretical formulations of the fundamental aspects of Nature have, for many years, hinted at its vast and elusive complexity, suggesting that our known world is but a tiny facet of the greater reality in which it is embedded, it has only been within the last several decades that observations have really begun to confirm this. Indeed, while deep-field surveys of the universe have uncovered myriads of galaxies, constituting an untold number of gravitationally bound microcosms such as ours, precision cosmological measurements have revealed that all of this luminous baryonic matter is a near negligible fraction of the total energy and matter in the universe. The vast majority of our cosmos is a dark universe, comprised of some kind of invisible substances or dark fluids that only interact gravitationally with visible matter.

Even among the objects that are visible to us, there are many mysterious entities which are predicted by theory and which may or may not as yet have been glimpsed in the cosmos. In the first part of this thesis we will study the interactions between two such entities, namely cosmic strings and rotating black holes. In the latter part, we will turn to the invisible sector and explore whether or not the dark phenomena in the universe could in fact be the shadows of fundamental objects moving in higher dimensions beyond our own.

Declaration

The work in this thesis is based on research carried out at the Centre for Particle Theory, Department of Mathematical Sciences, Durham University, England. No part of this thesis has been submitted elsewhere for any other degree or qualification and it is all my own work unless referenced to the contrary in the text.

Chapters 3, 4 and 5 are based on collaborative research papers. The work in Chapter 3 was done in collaboration with Ruth Gregory and David Kubizñák, that in Chapter 4 with Ruth Gregory, David Kubizñák, Robert Mann and Peter Gustainis, and finally that in Chapter 5 with Ivonne Zavala and Tomi Koivisto.

Acknowledgements

First of all I would like to extend my deepest thanks to my supervisor Ruth Gregory, who has inspired, supported and guided me in my studies, provided fantastic and numerous opportunities for me, and most importantly, has really been a friend to me during my time as her student. Thanks to Ruth, my Ph.D life has been full to the brim of diverse research, stimulating research trips, interesting and in-depth discussions, and memorable adventures around the world such as hiking in the Grand Canyon and cross-country skiing in snowy Canada. Both intellectually and personally, I have grown so much as a result of having Ruth as a supervisor.

In addition, I am most grateful to Paul Sutcliffe for being my second supervisor, and for always being so available to me when I have needed advice or guidance.

I would like to thank Ivonne Zavala for introducing me to the world of theoretical physics as a Masters student, and for setting the standard so high as my first research supervisor. I have benefited so much from Ivonne's breath of knowledge and expertise as a theoretical physicist, and have so much enjoyed spending time with her and getting to know her in an informal context. As with Ruth, she is definitely a friend to me.

I would further like to thank Hans Peter Nilles and Stefan Förste for their guidance and support during my MSc, and to my research group in Bonn for two fantastic years.

Thank you to Ivonne along with all my collaborators, David Kubizňák, Robert Mann, Peter Gustainis and Tomi Koivisto, for all their hard work that went into obtaining the results that are presented in this thesis. I feel very privileged to compile together into my own thesis the research and ideas that belong to all of us. In addition, I am deeply grateful to Gianmassimo Tasinato and Simon Ross for their

careful reading and critiquing of this manuscript.

So many people at Durham have made my time as a student so memorable. Thank you to my office mates David Tapp and Paul Jennings, who made the office such an animated and interesting place to be, where there was never a dull moment. Thank you also to Sarah Chadburn, Phillipp Burda, Ben Withers, Simon Gentle and Jonathan Pearson for memorable times in Durham and in Canada at the Perimeter Institute. Thank you also to all my fellow CPT and maths students and to my Durham friends outside of academic life, most notably Natasha Cooper, for adding so many wonderful things to my Ph.D experience.

My family have always provided me with an enormous amount of support and encouragement. I am truly grateful to Liz Evans, John Wills, Natalie Wills, Justin Wills, and Hayley Wills, and later on to Julia Wills and James Laidlaw, for the enumerable ways in which you have all enhanced my life. Liz Evans in particular has shared and fed my passion for uncovering the subtleties of Nature and I thank her for many stimulating philosophical discussions, for the exchanging of ideas and books, and for guiding me to the right path.

Finally, with enormous gratitude and love, I thank my fiancé Mike Pandher, for looking with me from the same place into the vastness of the universe.

Contents

List of Figures

List of Tables

Preface

Impermanent are all component things,
They arise and cease, that is their nature:
They come into being and pass away,
Release from them is bliss supreme.
–Mahaa-Parinibbaana Sutta

The physical universe in which we find ourselves is a vast flux of fleeting forms of energy, where as time progresses, objects arise, interact with other objects, and then dissolve away again in apparently tireless succession. In this sense, what we call time is a measure of the changefulness of the universe.

Hot gases can give birth to stars, a temporary home for planets and lifeforms such as ourselves, which may eventually collapse into black holes, which may themselves ultimately evaporate into radiation. As conscious lifeforms, we are observers of the flux while at the same time, components of it.

From observations we have made of our cosmic environment, we now know that our world of baryonic stars and galaxies is but a small island floating on a sea of more subtle, "dark" forms of energy that are apparently not in communication with our visible world. Visible matter clusters in halos of dark matter, an invisible, gravitating substance whose existence is an inference we have made based on the dynamical and structure-forming behaviour of visible matter. On even larger scales, the dark halos themselves are diluting away within an elusive substance known as dark energy, as is infered from the redshifting of light emitted from the structures contained in the haloes.

The principle of impermanence persists at the quantum level, where quantum particles, tiny packages of energy, are also in a state of flux. As time progresses, particles appear, interact with other particles, and then may either decay into lighter particles, or leave behind a relic density that fades as the universe expands. Thus the particle spectrum of the universe evolves dynamically over time, with its symmetry forged by a series of phase transitions occuring at different cosmological epochs. The changing of microscopic, quantum symmetry at these transitions can result in the formation of macroscopic, classical objects known as cosmic strings, which enter the flux of forms and ultimately interact with other forms that exist at that energy scale.

In the pages that follow, we will theoretically study a subset of interactions that could occur within both the visible sector and the invisible sector of the cosmic flux. We will first examine the possible configurations which can arise from interactions between cosmic strings and rotating black holes in the visible sector, extending this study to the more abstract case of the interactions taking place within a spacetime containing negative vacuum energy. We will then turn to the invisible sector, and explore the possible interactions between the dark fluids in the universe, which will take us into higher dimensions of spacetime and fundamental theories of the natural world.

Chapter 1

Theories of Gravity

We begin with a discussion of the fundamental interaction which governs the behaviour of the universe on cosmological scales, namely the force of gravity. The paradigmatic theory which describes this force is Einstein's classical general theory of relativity. Gravity sculps the cosmic landscape by endowing it with a geometry, along which matter moves. Looking at smaller and smaller scales however, the other fundamental interactions of nature, namely the strong, the weak, and the electromagnetic force, which all have a description as quantum field theories, begin to become more and more relevant for describing the behaviour of matter. On the other hand, the gravitational interaction retreats into the background, becoming irrelevant at the typical energy scales associated with particle physics. In order to smoothly connect these regimes, one must find a deeper theory of nature that contains both general relativity and quantum field theory in suitable limits, but that goes beyond these limits and adequately describes the physics in between, and underpinning, them. The theory that has made the most progress in this regard is string theory, a quantum theory of gravity that unifies all of the known fundamental forces of nature as arising from the vibrations of fundamental strings in a ten dimensional spacetime. Starting from a theory of gravity in ten dimensions, the four dimensional description can contain new couplings between gravity and other fundamental fields which are part of the spectra of the oscillating strings. In this way, general relativity in four dimensions becomes modified by the presence of these fields. Interestingly, these

new interactions can in principle provide a context for understanding some aspects of the most elusive of the cosmological phenomena that have yet been observed, namely the dark sector of the universe.

In Section 1.1 we will discuss general relativity in some detail, beginning with an exposition of the theory in ts Lagrangian formulation in Section 1.1.1, and then describing some important solutions in Sections 1.1.2 and 1.1.3. In Section 1.2 we will then discuss gravity in higher dimensions, outlining some of the key developments in Section 1.2.1 before discussing string theory in Section 1.2.2. Finally, having provided a motivation, in Section 1.3 we will move back to the effective four dimensional description of gravity, and discuss the scalar-tensor class of modified gravity theories.

Units and Conventions

Nature exhibits three fundamental dimensionful constants which are the the speed of light c, Planck's constant $\hbar$, which sets the scale at which the quantum uncertainty principle becomes important, and Newton's constant G, which sets the strength of the gravitational field. In what follows, we will work with natural units such that $c = \hbar = 1$, and $8\pi G = M_p^{-2} = \kappa$ where M_p is the reduced Planck mass, which defines a mass scale of $M_p \approx 2 \times 10^{18}$GeV. We will choose the metric to be of $(-,+,+,+)$ signature.

1.1 General Relativity

1.1.1 Lagrangian formulation

The intricate structural patterns in the large scale structure are produced by luminous galactic fluids that are tracing out the intrinsic curvature of spacetime as they freefall under gravity. Freefalling objects follow paths of minimum distance called geodesics, which are straight lines in a curved space. Formally, spacetime is described by a four dimensional Riemannian manifold with a metric $g_{\mu\nu}$, which allows for a notion of distance in the spacetime. Choosing a path parameterised by

an affine parameter λ, the distance along it is

$$s = \int d\lambda \sqrt{g_{\mu\nu} t^\mu t^\nu} \,, \tag{1.1.1}$$

where $t^\mu = dx^\mu/d\lambda$ is a tangent vector to the path. Extremising this distance gives the geodesic equation,

$$t^\mu \nabla_\mu t^\nu = 0 \,, \tag{1.1.2}$$

where the covariant derivative ∇_μ is the generalisation of the partial derivative in a curved space, $\nabla_\mu t^\nu = \partial_\mu t^\nu + \Gamma^\nu_{\mu\sigma} t^\sigma$, and the connection $\Gamma^\mu_{\sigma\rho}$ is built from the metric and its derivatives,

$$\Gamma^\mu_{\sigma\rho} = \frac{1}{2} g^{\mu\nu} (\partial_\sigma g_{\nu\rho} + \partial_\rho g_{\nu\sigma} - \partial_\nu g_{\sigma\rho}) \,. \tag{1.1.3}$$

The intrinsic curvature of the manifold is characterised by a quantity known as the Riemann curvature tensor, $R^\alpha{}_{\beta\gamma\delta}$, which is constructed from the connection and its derivatives, giving rise to an object which is second order in the metric derivatives,

$$R^\alpha{}_{\beta\gamma\delta} = \Gamma^\alpha_{\beta\delta,\gamma} - \Gamma^\alpha_{\beta\gamma,\delta} + \Gamma^\mu_{\beta\delta}\Gamma^\alpha_{\mu\gamma} - \Gamma^\mu_{\beta\gamma}\Gamma^\alpha_{\mu\delta} \,. \tag{1.1.4}$$

As a clump of matter freefalls under gravity, in addition to its changes in position and velocity, it can also experience changes in its shape and volume as a result of these second order geometrical effects. Changes in volume are quantified by the trace component of the Riemann tensor, known as the Ricci tensor, $R^\sigma_{\mu\sigma\nu} = R_{\mu\nu}$, while changes in shape are quantified by the traceless component, known as the Weyl tensor. If the Riemann tensor vanishes identically, the spacetime is said to be flat, and is thus endowed with a Minkowskian geometry. However, even in the presence of globally non-trival curvature, Riemannian manifolds admit a tangent space at each point where the geometry is locally Minkowskian.

Thus, in a Riemannian spacetime, all geometrical information stems from a single quantity, the metric $g_{\mu\nu}$.

The great insight of Einstein, formalised into the general theory of relativity that constitutes the modern understanding of the gravitational force, is that the intrinsic curvature of spacetime is itself created by the various forms of matter and energy that move along it. The gravitational force that is sourced by matter and energy may then be identified with spacetime geometry, namely the metric $g_{\mu\nu}$. Rather

than fixed and immutable, spacetime then becomes dynamical, thus the metric may be treated as a dynamical field from a classical field theoretic point of view.

Einstein's theory may then be formulated as an action principle for the dynamical field $g_{\mu\nu}$. The action functional is constructed in the standard way, namely from invariant quantities that are formed from the dynamical field and its derivatives. While other quantities are possible, the simplest invariant quantity that can be constructed from the metric and its derivatives is the trace of the Ricci tensor, called the Ricci scalar, $R = g^{\mu\nu}R_{\mu\nu}$. One must then construct an invariant measure on the space. As usual, this is achieved by the invariant volume element, $\sqrt{-g}d^4x$, which in this case, most unlike all other field theory cases, depends itself upon the dynamical field being described by the theory.

Putting these quantities together yields the Einstein-Hilbert action,

$$S_{E.H.} = \frac{1}{2\kappa}\int d^4x\,\sqrt{-g}\,R\,, \tag{1.1.5}$$

which expresses the geometrical content of the theory. To specify the dynamics of $g_{\mu\nu}$ in terms of general equations of motion, one must then write down an action for the matter fields, which act as sources for the geometry. The total action is

$$S = S_{E.H.} + S_m\,, \tag{1.1.6}$$

where

$$S_m = \int d^4x\sqrt{-g}\mathcal{L}(\psi_i, \partial_\mu\psi_i) \tag{1.1.7}$$

is a general action for the matter fields ψ_i. We may now obtain the equations of motion for the gravitational force by a variation of (1.1.6) with respect to a general perturbation of the contravariant metric $\delta g^{\mu\nu}$, which yields

$$\delta S = \frac{1}{2\kappa}\int d^4x\sqrt{-g}\Big(R_{\mu\nu} - \frac{1}{2}g_{\mu\nu}R\Big)\delta g^{\mu\nu} + \int d^4x\frac{\delta S_m}{\delta g^{\mu\nu}}\,\delta g^{\mu\nu}\,. \tag{1.1.8}$$

Defining the *stress energy tensor* as

$$T_{\mu\nu} \equiv -\frac{2}{\sqrt{-g}}\frac{\delta S_m}{\delta g^{\mu\nu}}\,, \tag{1.1.9}$$

the action principle $\delta S = 0$ yields the Einstein field equations,

$$G_{\mu\nu} \equiv R_{\mu\nu} - \frac{1}{2}g_{\mu\nu}R = \kappa T_{\mu\nu}\,, \tag{1.1.10}$$

where $G_{\mu\nu}$ is known as the Einstein tensor.

The geometrical quantities on the left hand side of the field equation (1.1.10) are only those which pertain to the trace part of the Riemann tensor. Thus, we see that non-gravitational[1] matter fields only source the Ricci tensor, $R_{\mu\nu}$. On the other hand, in the case that $T_{\mu\nu} = 0$, and in the absence of a cosmological constant, the field equations read

$$R_{\mu\nu} = 0\,, \tag{1.1.11}$$

which describe the dynamics of the gravitational field in a spacetime devoid of all but geometry. These are known as the vacuum equations. A trivial solution is flat Minkowski spacetime, for which, as we have mentioned, the Riemann curvature tensor vanishes identically. However, more generally, (1.1.11) is simply the statement that the equations of motion do not force the traceless component of the Riemann tensor, namely the Weyl tensor, to vanish. There are in fact many non-trivial solutions to (1.1.11), the most notable of which are the black hole solutions which describe the empty spacetime outside of gravitationally collapsed objects. As there are no matter sources about, the fact that there are non-trivial solutions to (1.1.11) implies that gravity itself can generate gravitational effects, and produce a non-vanishing Weyl tensor. This is a consequence of the non-linearity of the theory, which entails that even in the absence of gravitating matter fields, spacetime may be non-trivially curved because the gravitational field itself contains energy, and thus can produce more gravity.

Going back to our clumps of matter freefalling under gravity, we see that in an empty spacetime, the clumps may experience changes to their shape, while only in the presence of distinct sources for the gravitational field will they experience changes in volume. An example for the latter is an expanding spacetime in cosmology: probe matter is diluted by the expansion, which is sourced by the presence of the cosmological fluid, or by a cosmological constant. An example for the former is the behaviour of matter in the vicinity of black holes, where strong tidal forces act to

[1]By "non-gravitational" we mean that they do not form part of the gravitational sector. This distinction will become important when we discuss modifications of general relativity.

distort the morphology of nearby objects, sourced purely by the non-linear effects of gravity.

Having derived the field equation for $g_{\mu\nu}$, we require further information in order to specify the dynamics of the system, because at this stage we do not have an equation for the non-gravitational degrees of freedom ψ_i which are packaged into $T_{\mu\nu}$. It turns out that by virtue of the properties of Riemannian geometry, this equation is already implicit in the Einstein equations. An important property of the Riemann tensor is the so-called *Bianchi identity*,

$$R^{\sigma}{}_{\rho[\mu\nu;\alpha]} = 0\,, \tag{1.1.12}$$

and contraction of this identity yields a constraint on the Einstein tensor,

$$\nabla_\mu G^{\mu\nu} = 0\,. \tag{1.1.13}$$

From the field equations (1.1.10), this implies that $\nabla_\mu T^{\mu\nu} = 0$, which gives us an equation for ψ_i in the form of a conservation equation for the collective stress-energy of the non-gravitational fields.

From a variational point of view, the contracted Bianchi identity emerges as a natural consequence of general covariance, which is the principle that the laws of physics should be invariant under diffeomorphisms, which are general coordinate transformations. General covariance requires that the action functionals, from which the laws may be derived as equations of motion, are coordinate invariant by construction. Symmetries in the action correspond to conservation laws, thus the Bianchi identity, expressing the conservation of stress-energy, appears as the conservation law associated with the symmetry of S_m under diffeomorphisms.

To derive the conservation law, we perform a general variation of (1.1.7) with respect to the field perturbations $\delta\psi_i$ and $\delta g_{\mu\nu}$, yielding

$$\delta S_m = 0 = \int d^4x \frac{\delta S_m}{\delta \psi_i}\delta\psi_i + \int d^4x \frac{\delta S_m}{\delta g_{\mu\nu}}\delta g_{\mu\nu}\,. \tag{1.1.14}$$

Variation of the matter action with respect to the covariant metric $g_{\mu\nu}$ allows us to define the stress energy tensor with raised indices as

$$T^{\mu\nu} = \frac{2}{\sqrt{-g}}\frac{\delta S_m}{\delta g_{\mu\nu}}\,, \tag{1.1.15}$$

which features the opposite sign to (1.1.9) due to the variational identity $\delta g^{\mu\nu} = -g^{\sigma\mu}g^{\rho\nu}\delta g_{\sigma\rho}$.

For an infinitesimal diffeomorphism $x'^{\mu} = x^{\mu} + \zeta^{\mu}(x^{\alpha})$, the infinitesimal changes in the fields ψ_i and $g_{\mu\nu}$ are given by the Lie derivative, which acts on a general tensor $K_{\alpha\beta}$ as

$$\pounds_{\zeta} K_{\alpha\beta} = K_{\alpha\delta}\zeta^{\delta}_{\ ,\beta} + K_{\delta\beta}\zeta^{\delta}_{\ ,\alpha} + K_{\alpha\beta,\gamma}\zeta^{\gamma}\,, \tag{1.1.16}$$

yielding

$$\delta\psi_i = \pounds_{\zeta}\psi_i = \zeta^{\mu}\partial_{\mu}\psi_i\,, \tag{1.1.17}$$

$$\delta g_{\mu\nu} = \pounds_{\zeta} g_{\mu\nu} = \nabla_{\mu}\zeta_{\nu} + \nabla_{\nu}\zeta_{\mu}\,. \tag{1.1.18}$$

In the case that the second equation (1.1.18) vanishes, the vector ζ^{μ} is called a Killing vector, and represents a symmetry of the metric, which we will discuss in greater detail in Section 1.1.2.

With these specific expressions for the field perturbations, one may use the symmetries of $T^{\mu\nu}$ to obtain

$$\int d^4x \Big(\frac{\partial\mathcal{L}}{\partial\psi_i} - \nabla_{\mu}\frac{\partial\mathcal{L}}{\partial\psi_{i,\mu}}\Big)\zeta_{\nu}\partial^{\nu}\psi_i - \int d^4x \zeta_{\nu}\nabla_{\mu}T^{\mu\nu} = 0\,. \tag{1.1.19}$$

The term in parentheses is the equation of motion for ψ_i, which vanishes identically. Thus, for an arbitrary vector ζ^{μ}, the stress-energy tensor is constrained to be divergence-free, $\nabla_{\mu}T^{\mu\nu} = 0$.

Let us now discuss the general form of the stress-energy tensor. The metric $g_{\mu\nu}$ is a symmetric tensor, thus to reflect the symmetries of spacetime, one usually considers the stress-energy tensor to take the form of a *perfect fluid*,

$$T_{\mu\nu} = \rho u_{\mu}u_{\nu} + P(g_{\mu\nu} + u_{\mu}u_{\nu}) \tag{1.1.20}$$

where ρ is the energy density of the fluid, P is its pressure, and u^{α} is a timelike vector $u^{\mu}u_{\mu} = -1$, which represents the four-velocity of the individual particles which comprise the fluid. Going back to the action 1.1.1, the four-velocity is the tangent vector to a path which is parameterised by the proper time τ.

The equation of motion for the fluid, $\nabla_{\mu}T^{\mu\nu} = 0$, then yields the following two equations:

$$u^{\mu}\nabla_{\mu}\rho + (\rho + P)\nabla_{\mu}u^{\mu} = 0\,, \tag{1.1.21}$$

$$(P+\rho)u^\mu\nabla_\mu u^\nu + (g^{\mu\nu}+u^\mu u^\nu)\nabla_\mu P = 0\,. \tag{1.1.22}$$

For a perfect fluid, (1.1.21) and (1.1.22) completely specify the motion of the fluid, thus the Einstein equations contain all the information about how spacetime and stress-energy behave under the influence of each other. For the case of "dust" particles, $P = 0$ and (1.1.22) then tells us that the individual particles move on geodesics,

$$u^\mu\nabla_\mu u^\nu = 0\,. \tag{1.1.23}$$

This is a very important result as it implies that all test particles, namely particles upon which no other external forces are acting, are constrained by energy conservation to follow geodesics of $g_{\mu\nu}$.

1.1.2 Black holes

Among the most exotic solutions to Einsteins equations are most certainly the black hole solutions, which showcase some of the most interesting and varied ways in which the gravitational field can manipulate the behaviour of matter. In general, these are solutions which describe the empty spacetime outside of gravitationally collapsed objects, but they can also describe the spacetime around very massive objects that totally dominate their local gravitational environment. As with all solutions to Einstein's equations, they are characterised by the various symmetries of the gravitational field, or equivalently, by spacetime symmetries. As mentioned above, such symmetries are described by Killing vectors.

For a general vector k^μ, one can find local coordinates such that $k^\mu = (\partial/\partial\xi)^\mu$, where ξ is one of the coordinates. k^μ is a Killing vector in the case that the Lie derivative acting on the metric satisfies

$$\pounds_k g_{\mu\nu} = \frac{\partial}{\partial\xi} g_{\mu\nu} = 0\,, \tag{1.1.24}$$

thus the metric coefficients are independent of ξ.

For example, spherical symmetry of the spacetime entails that the solution admits an $SO(3)$ rotational symmetry. Then, for the spacetime to be *stationary*, the solution should possess a time-translation symmetry, $t \to t + t_0$, while *static* spacetimes require in addition that time is symmetric under reversal, $t \to -t$. Therefore,

a static solution should admit a timelike Killing vector that is orthogonal to all spacelike surfaces, meaning that there can be no cross terms that mix the timelike and spacelike directions in the metric. On the other hand, stationary spacetimes feature a mixing of the timelike and spacelike directions. In fact, as originally shown by Hawking and Wald, stationarity implies that instead of spherical symmetry, the spacetime is axisymmetric. Working in coordinates $\{t, r, \theta, \phi\}$, there are in general two Killing vectors associated with these symmetries, namely

$$(\partial_t)^\mu \,,\ (\partial_\phi)^\mu \,, \tag{1.1.25}$$

where an additional two Killing vectors are present for full spherical symmetry. These symmetries of the spacetime have corresponding conserved quantities. Each Killing vector k^μ leads to a constant of motion for a particle moving in the spacetime,

$$k_\mu \frac{dx^\mu}{d\lambda} = const. \tag{1.1.26}$$

For the Killing vectors in (1.1.25), this leads to the conservation of energy and of angular momentum.

Schwarzschild

Let us now discuss the particular solutions. The Schwarzschild solution is the unique static and spherically symmetric solution to the vacuum Einstein equations. It describes the gravitational field outside of a static, spherically symmetric body of mass M, such as a star. Within our solar system, where the planets may be considered as test particles moving in the gravitational field exterior to our home star, the sun, it correctly predicts deviations from Newtonian orbital motion, as well as inherently relativistic effects, such as gravitational redshift, time delay and the bending of light.

The Schwarzschild solution is described by the metric

$$ds^2 = -\Big(1 - \frac{2GM}{r}\Big)dt^2 + \Big(1 - \frac{2GM}{r}\Big)^{-1} dr^2 + r^2 d\Omega^2 \tag{1.1.27}$$

where $d\Omega^2 = d\theta^2 + \sin^2\theta d\phi^2$ is the metric on a 2-sphere. This solution asymptotes to flat space at large r, therefore the gravitational effect of a massive object dimishes if one moves far enough away from the object, as one would expect.

The solution becomes singular at the points $r = 2GM$ and $r = 0$. The first of these points defines the Schwarzschild radius,

$$r_S = \frac{2GM}{c^2} \approx 3\Big(\frac{M}{M_\odot}\Big)\,\mathrm{km}\,, \tag{1.1.28}$$

where $M_\odot$ is the mass of the sun. In the case of a typical star, this radius is well within the interior of the star, where the vacuum solution is not expected to be valid. However, very massive stars that undergo complete gravitational collapse will fall well within their Schwarzschild radii, eventually forming a black hole centred at $r = 0$. In this case, the Schwarzschild radius becomes an *event horizon*, a null surface separating regions of spacetime which may and may not causally interact with one another.

A spacetime is said to be geodesically complete if all geodesics are extendable to arbitrarily large values of their affine parameters. A spacetime containing a genuine singularity is geodesically incomplete, meaning that geodesics terminate at the singularity for some finite value of their affine parameter. In the case of the spacetime which is described by (1.1.27), this appears to occur at r_S, because geodesics can reach this singularity at a finite value of their affine parameters. However the Schwarzschild spacetime may be maximally analytically extended beyond r_S by choosing appropriate coordinates. One then sees that r_S is a mere coordinate singularity, and there is no obstruction in continuing the paths of particles beyond this surface. All infalling particles will then travel onwards to $r = 0$, which is a true, irremovable singularity of the spacetime, where the geodesics terminate. However, looking at (1.1.27) one can see that for $r < r_S$, the radial direction becomes timelike. This means that the particles can only move in one direction along the radial path, so that *all* future-directed paths are in the direction of decreasing r. Therefore no particles or signals of any kind may leave the interior region of the black hole, and no information may be glimpsed from beyond r_S.

Reissner-Nordstrom

We mentioned earlier that the Schwarzschild solution is unique. This is a consequence of Birkhoff's theorem, which states that any spherically symmetric vacuum

spacetime solution must be static. In other words, such a solution must be the Schwarzschild solution.

More generally, one can consider spacetimes that contain non-trivial electromagnetic fields. Such spacetimes are no longer vacuum spacetimes, but are sometimes refered to as *electrovacuum* spacetimes, and are solutions of the coupled Einstein-Maxwell equations. One may then generalise Birkoff's theorem to the electrovacuum case, for which it stipulates that the only spherically symmetric solution is the Reissner-Nordstrom solution describing a charged black hole.

The Reissner-Nordstrom solution is the unique spherically symmetric solution to the Einstein-Maxwell system, described by the action

$$S = \frac{1}{2\kappa}\int d^4x\sqrt{-g}\Big(R - F_{\mu\nu}F^{\mu\nu}\Big)\,, \tag{1.1.29}$$

where $F = dA$ is the field strength for the Maxwell potential A. The metric is

$$ds^2 = -\frac{\Delta}{r^2}dt^2 + \frac{r^2}{\Delta}dr^2 + r^2 d\Omega^2 \tag{1.1.30}$$

and the gauge field is

$$A = \frac{q}{r}dt\,. \tag{1.1.31}$$

In these expressions, $\Delta = r^2 - 2GMr + q^2$, where $q \equiv GQ$ and Q is the electric charge of the black hole. The metric function $\Delta = (r - r_+)(r - r_-)$ has two distinct roots,

$$r_\pm = GM \pm \sqrt{(GM)^2 - q^2}, \tag{1.1.32}$$

corresponding to the inner and outer event horizons of the charged black hole. In the case that the two horizons coincide, $r_+ = r_-$, the black hole is said to be *extremal*. This occurs when $GM = q$ and thus $r_+ = GM$. Under a change of coordinates

$$\rho = r - GM\,, \tag{1.1.33}$$

the extremal metric takes the isotropic form

$$ds^2 = -\Big(1 + \frac{GM}{\rho}\Big)^{-2}dt^2 + \Big(1 + \frac{GM}{\rho}\Big)^{2}(d\rho^2 + \rho^2 d\Omega^2)\,. \tag{1.1.34}$$

In these coordinates, the metric becomes singular when $\rho = 0$, thus there is an event horizon located at this point. In the *near-horizon* region where $\rho \to 0$, the metric

becomes

$$ds^2 \approx -\frac{\rho^2}{(GM)^2}dt^2 + \frac{(GM)^2}{\rho^2}d\rho^2 + (GM)^2 d\Omega^2\,, \tag{1.1.35}$$

which, compared with (1.1.43) below, is the line element for $AdS_2 \times S_2$, where the 2-sphere has radius GM. For an observer at a radial point $\rho = \rho_0$, we learn that the event horizon ρ_+ is at an infinite proper distance away,

$$s = \lim_{\rho_+ \to 0} \int_{\rho_+}^{\rho_0} \frac{1}{\rho} d\rho = \lim_{\rho_+ \to 0} [\ln(\rho_0) - \ln(\rho_+)] = \infty\,, \tag{1.1.36}$$

located at the end of an infinite throat-like region in the spacetime.

While the Schwarzschild solution contains only one parameter, the mass of the black hole M, the Reissner-Nordstrom spacetime is then a two parameter family of solutions, where the parameters are M and Q. Together they form the static, spherically symmetric class of black hole solutions.

Kerr and Kerr-Newman

Let us now consider stationarity. As we have mentioned, this implies that the spacetime is axisymmetric, which means that there is a Killing vector ∂_ϕ which is spacelike near infinity, and for which all orbits are closed. As we will elucidate upon, stationary spacetimes are rotating spacetimes. In the presence of pure gravity and no other fields, the unique stationary solution is the Kerr solution, with two parameters, M and J, where J is the total angular momentum of the black hole.

The Kerr geometry in Boyer-Linquist coordinates reads

$$ds^2 = -\frac{\Delta - a^2\sin^2\theta}{\Sigma}dt^2 \; - \; \frac{4GMar\sin^2\theta}{\Sigma}dtd\varphi + \Sigma d\theta^2 \; + \; \frac{\Gamma}{\Sigma}\sin^2\theta\, d\varphi^2 + \frac{\Sigma}{\Delta}dr^2\,, \tag{1.1.37}$$

where $a = J/M$ and

$$\Sigma = r^2 + a^2\cos^2\theta\,, \quad \Delta = r^2 - 2GMr + a^2 \qquad \Gamma = (r^2+a^2)^2 - \Delta a^2\sin^2\theta\,. \tag{1.1.38}$$

The geometry has a coordinate singularity when $\Delta = 0$. As for the Reissner-Nordstrom case, writing $\Delta = (r - r_+)(r - r_-)$ we find that there are in general two distinct event horizons, this time given by

$$r_\pm = GM \pm \sqrt{(GM)^2 - a^2}\,. \tag{1.1.39}$$

For the extremal Kerr, these horizons coincide when $GM = a$. As with the Reissner-Norstrom case above, one can consider the metric in the extremal limit, and show that the spatial distance to the extremal horizon is infinite.

The geometry has a genuine curvature singularity when $\Sigma = 0$, therefore at $r = 0$ and $\theta = \pi/2$. Moving to a different coordinate system, one can show that the singularity in fact takes the form of a "ring", meaning that particles following ingoing radial geodesics on the equator will hit the singularity at $r = 0$, however particles on radial geodesics along the polar axis will instead pass through the ring into another region of the spacetime that can be obtained by analytic continuation. However, just inside the ring singularity the spacetime exhibits closed time-like curves, as the $g_{\phi\phi}$ component of the metric (1.1.37) can change sign, such that a vector ∂_ϕ can become timelike in this region. These curves imply a global violation of causality, which makes this region unphysical.

Let us now discuss the rotational features of the spacetime. Due to the fact that the timelike and azimuthal spacelike directions are mixed in the Kerr spacetime, a particle falling towards the black hole on a radial geodesic will aquire non-vanishing angular momentum and start to rotate, even though no non-gravitational forces are acting on it. This is known as *frame-dragging*, and is a result of the fact that a test particle cannot move in time without also moving in the ϕ-direction. For static spacetimes on the other hand, a particle on a radial geodesic will simply remain on this geodesic as it plummets towards the black hole.

A "non-test" particle falling towards the black hole could however remain stationary with respect to infinity by a way of a sufficient amount of propulsion. This is also true for the static black holes considered above, everywhere outside of the event horizon. However, for the Kerr case, it turns out that even outside of the event horizon, a particle may enter a region within which it is impossible to remain stationary with respect to asymptotic infinity, as remaining stationary would require superluminal propulsion. This occurs within the *ergoregion*.

We mentioned above that within the ring singularity, the $g_{\phi\phi}$ component of the metric can change sign. Even outside of r_+ in this spacetime, another component of the metric may change sign, this time the g_{tt} component. The g_{tt} component in

(1.1.37) is negative only if

$$\Delta - a^2 \sin^2\theta > 0\,, \tag{1.1.40}$$

which implies that

$$r > GM + \sqrt{(GM)^2 - a^2\cos^2\theta}\,. \tag{1.1.41}$$

The boundary of this region is known as the *ergosphere*. Between this boundary and the horizon r_+, in the ergoregion, the vector ∂_t becomes spacelike, meaning that physical particles, which *must* follow timelike paths, can no longer move in time only relative to an asymptotic observer. Instead, regardless of their state of propulsion, they are forced to rotate with the black hole.

As with the static families of solutions, the Kerr spacetime is also subject to a uniqueness theorem. The Carter-Robinson theorem states that any asymptotically-flat stationary and axisymmetric spacetime is a member of the Kerr family. This can be generalised to the stationary electrovacuum case, for which the rotating black hole acquires an extra parameter, namely a charge, Q. The resulting spacetime, known as the Kerr-Newman spacetime, may be described in Boyer-Lindquist coordinates by the metric (1.1.37), but now the metric function Δ becomes

$$\Delta = r^2 + a^2 - 2GMr + GQ^2\,. \tag{1.1.42}$$

The "no-hair" theorems

As it involves no changes in time and thus no evolution is taking place, a stationary configuration is a steady-state configuration that a system could settle down into after gravitational collapse. The uniqueness theorems mentioned above then seem to insist that gravitational collapse to a stationary state leads to the formation of a black hole endowed with mass M, charge Q, and angular momentum J only. In other words, it appears that the black hole cannot pick up any other parameters, which implies that all other information is destroyed during the collapse. These considerations gave rise to a body of classical results known as the black hole "no-hair" theorems, which state that the only long-range information that a black hole can support is its mass, charge, and angular momentum (see [1–4] for a review).

The logic is that the black hole will absorb everything it *can* absorb. However, M, J and Q are "special" because they are conserved quantities associated with the exact local symmetries of the spacetime, such as U(1) symmetry and Poincaré symmetry. Indeed, as we mentioned above, the presence of the Killing vectors ∂_t and ∂_ϕ, which correspond to symmetries of the gravitational field for stationary spacetimes, give rise to the conservation of energy and of angular momentum respectively. Furthermore, in an electrovacuum spacetime, local U(1) symmetry implies the conservation of charge. In fact, the presence of the electrovacuum can itself be viewed as deeply linked to spacetime geometry. As we will review in Chapter 4, Killing vectors can act as a 4-vector potential for an electromagnetic field on Ricci flat backgrounds, which can lead to an initially electrically neutral black hole picking up a charge.

These conserved quantities cannot be destroyed during gravitational collapse. Instead they appear as charges or parameters of the collapsed object that can be measured at spatial infinity by Gauss's law.

Black holes in AdS

Finally, we will briefly mention the non-asymptotically flat classes of black hole solutions. One example is the generalisation of black hole spacetimes to include a non-vanishing cosmological constant.

A spacetime containing a negative cosmological constant is known as an Anti de Sitter (AdS) spacetime. In static coordinates, a general AdS spacetime is described by the line element

$$ds^2 = -\Big(1 + \frac{r^2}{\ell^2}\Big)dt^2 + \Big(1 + \frac{r^2}{\ell^2}\Big)^{-1} dr^2 + r^2 d\Omega^2 \,, \tag{1.1.43}$$

where ℓ is the AdS length. The simplest AdS black hole solution is the Schwarzschild-AdS solution,

$$ds^2 = -\Big(1 - \frac{2M}{r} + \frac{r^2}{\ell^2}\Big)dt^2 + \Big(1 - \frac{2M}{r} + \frac{r^2}{\ell^2}\Big)^{-1} dr^2 + r^2 d\Omega^2 \,, \tag{1.1.44}$$

which is the unique spherically symmetric solution to the Einstein equations in the presence of a negative cosmological constant. This spacetime looks like a Schwarzschild black hole spacetime at low r, but approaches an AdS spacetime at large r.

In Chapter 5 we will look in detail at the spacetime of a rotating, charged black hole in AdS.

1.1.3 Cosmology

When matter is present to source it, the gravitational field acts to change the volume of spacetime. This very simple fact, that the volume of spacetime changes due to the matter distribution it contains, allows for the energy scale of the universe to progressively decrease, and thus for a myriad of physical processes to take place within that volume, which ultimately shape the universe in all its complexity into essentially everything which we observe today. Indeed, this process allows for galaxies to grow from quantum fluctuations, for the standard model gauge group to emerge, and for atoms to form and combine so as to eventually enable complex lifeforms to develop.

The geometry of the universe is characterised by various symmetries in the presence of a matter distribution, which expands the spacetime while respecting the symmetries. The symmetries are large-scale homogeneity and isotropy of the spatial hypersurfaces, meaning that on the largest scales, the universe looks the same at every point, and in every direction. These symmetries, which imply that there is no special place in the universe, are manifest in the cosmic microwave background (CMB), a thermal background of free-streaming photons against which the evolution of all structure takes place, and which may be considered the oldest "object" in the universe.

The scale at which the clustering of matter becomes dominant is about 10 Mpc, where 1 Mpc $= 3.3\times10^6$ light years. Above this scale, the universe is mostly smooth, with the clumpy matter distribution appearing as a perturbation. Below this scale, the non-linear clustering effects of matter become more and more important.

The line element that reflects the large-scale symmetries of the universe is the Friedmann-Robertson-Walker (FRW) metric,

$$ds^2 = -dt^2 + a^2(t)\Big[\frac{dr^2}{1-Kr^2} + r^2 d\Omega^2\Big]\,, \tag{1.1.45}$$

where symmetry restricts the allowable changes in volume to express themselves as a

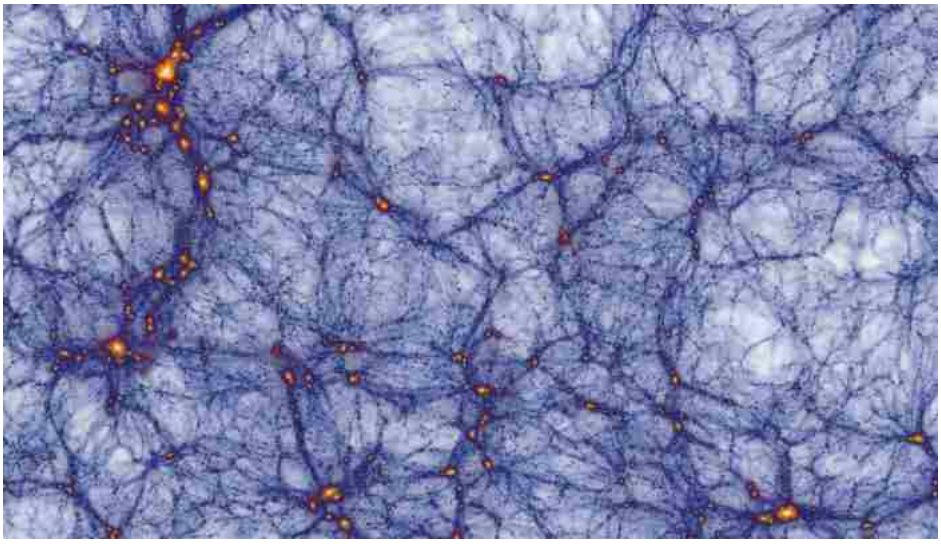

Figure 1.1: A visualisation of the large-scale structure from the *Millennium-XXL Simulation*, on a scale of a few hundred Mpc. The bright regions are very dense clusters of galaxies which form where the filaments intersect each other.

single time dependent scale factor $a(t)$ acting on the spatial hypersurfaces, and K is a constant that quantifies the curvature of the universe. Combining this ansatz with the perfect fluid form for the energy-momentum tensor, and including a cosmological constant Λ, the Einstein equations become

$$H^2 = \frac{\kappa}{3}\rho - \frac{K}{a^2} + \frac{\Lambda}{3}\,, \tag{1.1.46}$$

and

$$\frac{\ddot{a}}{a} = -\frac{\kappa}{6}(\rho + 3P) + \frac{\Lambda}{3}\,. \tag{1.1.47}$$

These two equations are known as the Friedmann equations. They determine the dynamics of the scale factor $a(t)$, where we have defined the Hubble parameter, $H = \dot{a}/a$, which quantifies the rate of the cosmic expansion. They may be supplemented by the (non-independent) conservation equation for matter (1.1.21), arising from the Bianchi identities $\nabla_\mu T^{\mu\nu} = 0$, which for this background becomes

$$\dot{\rho} + 3H(\rho + P) = 0\,. \tag{1.1.48}$$

The relation between the energy density and pressure of the cosmological fluid is

expressed by its equation of state,

$$P = w\rho\,. \tag{1.1.49}$$

Measurements of the CMB indicate that the universe is spatially flat on large scales. For a flat universe, $K = 0$, one can broadly categorise the components of the fluid in (1.1.46) as *radiation*, defined as particles which are either massless, or are moving sufficiently relativistically such that their rest mass is significantly smaller than their kinetic energy, and non-relativistic particles or *matter*. Matter or "dust" particles, in the absence of kinetic energy and thus of pressure, simply follow geodesics of the spacetime, as we saw in Section 1.1.1. In addition, the universe may contain non-trivial vacuum energy Λ, which may also be categorised by its equation of state.

From (1.1.48) one sees that a cosmological constant, for which ρ is constant, implies $\rho = -P$. For pressureless particles, $w = 0$ and thus $\rho_m \sim a^{-3}$ from (1.1.48), therefore the dust particles simply dilute with the expanding three dimensional volume. For radiation, the theory of electromagnetism yields $w = 1/3$, leading to $\rho \sim a^{-4}$, which implies that the radiation particles lose energy quicker than dust particles due to an additional redshifting of their wavelengths or momenta.

Cosmic inflation

From (1.1.47) we see that the expansion rate of the universe will increase with time if $w < -1/3$, therefore if the cosmological constant dominates the energy of the universe, it will *inflate*. This behaviour may seem an usual curiosity associated with the vacuum, however it turns out that certain dynamical fields in the spacetime can produce a similar effect. For example, a canonical scalar field that is moving very slowly along a flat potential can emulate, for a while, the behaviour of a cosmological constant. From the general action

$$S = -\frac{1}{2}\int d^4x\sqrt{-g}\Big[\partial_\mu\phi\partial^\mu\phi + 2V(\phi)\Big]\,, \tag{1.1.50}$$

one can compute the energy momentum tensor

$$T_{\mu\nu} = \partial_\mu\phi\partial_\nu\phi - g_{\mu\nu}\Big[\frac{1}{2}\partial^\alpha\phi\partial_\alpha\phi + V(\phi)\Big]\,, \tag{1.1.51}$$

thus the energy density and pressure of the scalar field in a flat, FRW background are

$$\rho_\phi \equiv -T^0_0 = \frac{1}{2}\dot{\phi}^2 + V(\phi)\,, \qquad P_\phi \equiv T^i_i = \frac{1}{2}\dot{\phi}^2 - V(\phi)\,. \tag{1.1.52}$$

The equation of state for the scalar field is

$$w_\phi = \frac{P_\phi}{\rho_\phi}\,, \tag{1.1.53}$$

for which one finds that $w_\phi \to -1$ in the case that $\dot{\phi}^2 \ll V(\phi)$. This can occur for a very flat potential, $V' \ll V$ thus $V \simeq const.$ Instead of a cosmological constant, we then find that the universe can inflate due to the constant potential energy of a suitable scalar field.

From the Hubble parameter H one may define the inverse quantity, H^{-1}, which is a time scale or length scale, cH^{-1}, known as the Hubble radius. One can then compare the timescale for particle interactions, $t_I \equiv 1/\Gamma$ where Γ is the rate of interactions, with the timescale for expansion, $t_H \equiv 1/H$. As long as

$$t_I \ll t_H\,, \tag{1.1.54}$$

the particles have plenty of time to interact before the expansion acts to dilute them, thus the expansion does not impact microphysical processes such as thermalisation of particles. Equivalently, the length scale for particle interactions is then much smaller than the Hubble radius, thus at the scale relevant for microphysical processes to take place, the expansion of the universe is negligible. On the other hand, for

$$t_I \gg t_H\,, \tag{1.1.55}$$

the interactions of particles are negligible compared to the expansion, with the universe expanding profusely before the particles have had time to interact.

To explain the observed flatness, homogeneity and isotropy of the universe, it is believed that a period of exponential growth took place at very early times. Compellingly, such a paradigm can also explain how the initial conditions for structure formation, the so-called "seeds" of cosmic structure, were originally generated.

The observable universe is thought to have began as a small, causally connected patch within a larger universe. Two regions of spacetime can causally affect each

other if a photon can pass between them, and such regions are said to be within each other's particle horizons. For an observer at a time t_0, the particle horizon is the future light cone emitted from their position at t_0. Therefore, the particle horizon separates regions which have already been observed at t_0 from regions which have not yet been observed at t_0.

The story of cosmology goes that at some very early point in its history, the universe entered a phase of superluminal expansion that drove all scales in this original patch, including quantum scales, outside of the Hubble radius. This period of expansion, known as cosmic inflation, could have been sourced by the presence of a cosmological scalar field as outlined above, as such fields are ubiquitious in high-energy particle theories. During inflation, all particle horizons in the observable patch were expanded enormously, allowing regions of the universe that appear today to have been out of causal contact at the time the CMB was formed, to have had plenty of time to interact and thermalise in the past, thus accounting for the observed homogeneity and isotropy of the CMB.

The expansion was so rapid that a process known as gravitational particle production, a manifestation of Hawking radiation in cosmology, was able to take place. Due to the enormous expansion rate, the timescale associated with quantum fluctuations, t_q, became much longer than the Hubble time during inflation, $t_q \gg t_H$, such that virtual particle pairs which usually bubble in and out of the vacuum could no longer annihilate. Equivalently, the length scale of these fluctuations became much larger than the Hubble radius, which is sometimes called the Hubble horizon. Such fluctuations are then said to be driven to "superhorizon scales" by the expansion. Thus the expanding background "radiates" much like the event horizon of a black hole, when one virtual particle slips beneath the event horizon and its partner accelerates away into the universe. In cosmology, these quantum fluctuations seed the gravitational overdensities that provide the initial conditions for gravitational collapse, and thus for all structure formation in the universe.

At the same time, as mentioned, the expansion smoothed out all inhomogeneities and anisotropies originally present in the observable patch. In addition, the universe become so large that it appears spatially flat at the scales upon which we can observe

it.

At the end of inflation, the universe would have been empty and cold, as other than the tiny density of gravitationally produced particles, all forms of matter that might originally have been present have been diluted away. It is believed that the universe was then reheated by the inflaton field itself, which decayed into a sea of hot thermalised radiation. Stippled across this sea were the quantum fluctuations, producing tiny gravitational perturbations in the uniform energy density of the cosmological fluid, seeding the initial condition for structure growth.

The evolution of particles

As the universe evolves, so it expands and cools, and it does so at various rates depending upon the dominant contribution to the cosmological fluid at a given energy scale. Tracking the expansion backwards in time to the highest possible energy scale permissible by our current understanding of physics, we may reconstruct the full history of the universe up to that scale.

The very earliest times that we can theoretically envisage, earlier than inflation, correspond to a universe in a state of such high curvature that classical general relativity breaks down, and we enter the realm of quantum gravity. The quantum effects of gravity become important at the energy scale M_p, this is the Planck epoch, about which very little is known. At this scale, general relativity must be replaced by an inherently quantum theory of nature. We will return to this in Section 1.2.

Below the Planck scale but above about 10^{16} GeV, which is known as the grand unified theories or GUT scale, it is believed that the electromagnetic, strong and weak interactions are unified, as the coupling constants associated with these interactions, which are energy-scale dependent, appear to meet at this energy. If one includes supersymmetry, a theory which exchanges bosonic and fermionic states, the unification of the gauge couplings is precise, although evidence for supersymmetry has not yet been observed in nature. Due to the fact that the strong and electroweak interactions are unified into a single interaction at energies above the GUT scale, there are additional gauge bosons at this scale which can change quarks into leptons and vice versa, violating the quantum baryon number B. The universe exhibits a

large asymmetry with respect to the number of baryons versus anti-baryons which it contains. It is possible that the physical process which created the asymmetry, known as barogenesis, took place at this energy scale, as this process requires baryon number to be violated.

As the energy of the universe fell below the GUT scale, a phase transition occured during which the additional GUT bosons acquired masses, making them too heavy to be excited in the cosmological fluid. The removal of a number of gauge bosons from the particle spectrum of the universe corresponds to a breaking of a particle gauge group into smaller subgroups that have less bosons, thus the grand unified interaction was broken apart into the strong and the electroweak interactions. As we will discuss in detail in Chapter 2, this is accomplished by a process known as spontaneous symmetry breaking, for which a natural consequence in cosmology is the production of topological defects, such as cosmic strings, domain walls and monopoles. Monopoles and domain walls are problematic for cosmology as they totally dominate the energy density, giving rise to a universe with a very different expansion and structure formation history than the one we observe today. However, if cosmic inflation takes place around the GUT scale, then they too will be diluted away by the expansion. From observations of the density perturbations generated during inflation, which are etched into the CMB, one can discern the energy scale of the universe at the time that these perturbations crossed the Hubble horizon. It turns out that for most viable inflation models, this scale is consistent with the scale of grand unified theories.

At around 100 GeV, a second phase transition occured during which the electroweak interaction split up into the weak and electromagnetic interactions, and the standard model particles received their masses via the Higgs mechanism, which we will review for the abelian case in Section 2.3. There may also have been a production of cosmic strings at this scale.

The interaction between electrically charged particles becomes stronger at shorter separation distances. The opposite turns out to be true for quarks, which are charged under the strong force, mediated by gluons. At energies above 50 GeV, the interaction between quarks and gluons is very weak, and they form a quark-gluon plasma.

At around 50 GeV however, a further phase transition took place, the QCD phase transition, which led to the confinement of the quarks and gluons into bound states, and thus baryons and mesons were born.

At around 1 MeV, neutrinos decoupled from the thermal sea of particles. This was followed by the annihilation of electrons and positrons into photons exclusively, causing the photon temperature to become slightly higher than the termperature of the decoupled neutrinos. Finally, at energies of 100 keV, Big Bang Nucleosynthesis took place, and all the light nuclei were formed as protons and neutrons were able to combine. The energy density in radiation and matter then became equal at 0.75 keV, with matter, or non-relativistic particles, starting to dominate the cosmological fluid as the energies decreased further. Neutral hydrogen then formed during Recombination at 0.26-0.33 eV, when protons and electrons combined. The free electron density then rapidly declined, meaning that Thompson scattering between electrons and photons, the dominant process which couples photons to the primordial plasma, became inefficient and the photons decoupled at around 0.23-0.28 eV. These photons free-stream towards us today in the form of the cosmic microwave background. Without the pressure of the coupled photons around to prevent the baryonic fluid from gravitationally collapsing into the overdensitiies, matter then began to cluster, and over time grew linearly and then non-linearly into stars, galaxies, and eventually entire clusters of galaxies that are knotted across the universe as we observe it today.

The cosmological dark sector

We will now discuss the particular quantities that appear in the Friedmann equation (1.1.46) which govern the dynamics of the universe today. As we have mentioned, observations indicate that we live in a flat universe, $K = 0$, so there is no curvature-driven contribution to the cosmological expansion. On the other hand, it is now widely accepted that a cosmological constant Λ, or a mysterious unknown fluid that behaves very much like one, is strongly influencing the evolution of the universe today.

At the closing of last century, astronomers discovered, from observations of high

redshift Type Ia supernovae, that the universe is currently entering an accelerating epoch [5,6]. Type Ia supernovae are produced when white dwarf stars undergo gravitational collapse, a process which is believed to be independent of the environment of the white dwarf, thus the light emitted from the resulting explosion, the supernovae, is considered to be a "standard candle". This means that these objects have the same intrinsic brightness regardless of their redshift z. The observed brightness as a function of redshift then probes the geometry of spacetime. The observations of these objects turned out to be consistent only with those cosmological models which include a cosmological constant that constitutes about 70 percent of the total energy in the universe today, in other words, with models which describe an accelerating universe.

Further evidence for cosmic acceleration comes in the form of the estimates for the age of the universe. Based on a cosmological model for which the universe is matter dominated today, which would be the case if there were only matter and radiation species about, the age of the universe is found to be less than the age of the oldest stars. This paradox is resolved if one instead considers that the universe is accelerating, as then it would take longer for the expansion to slow down to the observed rate, thus lengthening the calculated age of the universe. Finally, observations of the shape of the CMB power spectrum [7] and of the matter power spectrum in the large-scale structure [8] are all consistent with an accelerating cosmological model.

However, it should be mentioned that there are alternative ways to interpret the data, which have been widely explored. The most popular rival hypothesis to cosmic acceleration is the idea that our universe constains large-scale inhomogeneities, and our galaxy happens to be situated in the centre of a very large cosmic void [9].

The simplest way to explain the acceleration is to attribute it to the presence of a cosmological constant, as this is already present in general relativity and does not invoke the presence of new fields. However as we will see, there are good reasons to go beyond this simple picture. More generally, one can describe the acceleration as being driven by an unidentified and possibly unknown source of energy in the cosmological fluid for which $w < -1/3$ today, which we refer to as *dark energy*

(see [10] for a review). The cosmological constant case, for which $w = -1$, is then a candidate for dark energy, but there are many alternatives. In what follows we will focus on a particular brand of dark energy models known as quintessence models. Note however that the latest observations from the Planck satellite constrain the equation of state of dark energy to be $w = 1.006 \pm 0.045$ [11], which is consistent with a cosmological constant, or with a field that *very* closely mimics one.

Let us now discuss ρ in the Friedmann equation (1.1.46). It turns out that if ρ were comprised entirely of visible "baryonic" matter at the time that the CMB was formed, then the photon-baryon fluid in the early universe would not be sufficient to account for early structure formation. In order to adequately explain the observed spectrum of primordial fluctuations in the CMB, the gravitational overdensities must be enhanced by a pressureless or "cold", non-interacting or "dark" fluid, which is present in a greater quantity than, and couples only gravitationally, to baryonic matter. Matter will then naturally cluster in the gravitational potential wells of this fluid, and eventually stars and galaxies will form there. Indeed, measurements of the rotation curves of galaxies have revealed that, if the Newtonian r^{-2} law for the gravitational force is correct, then these luminous structures must be freefalling under the influence of a gravitational field that is largely external to their own. If this were not the case, then the large momenta of stars in the galaxies would cause the galaxies to fly apart. However, as with the cosmic acceleration there are alternative interpretations of the data in this case, the most widely studied being the possibility that our law of gravity for galaxies should be modified [12, 13], but one must then still account somehow for the observed spectrum of overdensities in the CMB.

Perhaps the greatest direct evidence for the existence of a large quantity of collisionless, dark matter in galaxy structures comes from the 1E0657-56 "Bullet Cluster" of galaxies [14]. Observations clearly indicate that within this cluster, a smaller galaxy has collided with a larger galaxy, causing a separation of the mass components of the two galaxies. In particular, due to the collisionless nature of dark matter, the dark mass appears to have simply passed through the locus of the collision, while the hot X-ray gas experienced drag forces which caused it to

slow down relative to the dark mass, thus producing the separation. Gravitational lensing of the cluster has indeed revealed that most of the gravitating mass is off-set from the X-ray gas, which believed to be the most dominant baryonic contribution to the gravitational wells of clusters.

Finally, if there are dark, non-relativistic particles in the universe, it is plausible that there are also relativistic dark particles, or "dark radiation", although compelling observational evidence for such a species has not yet been found.

With ρ consisting mainly then of cold dark matter (CDM), and strong evidence for a cosmological constant Λ or dark energy, our universe today is almost entirely a *dark* universe, and thus our modern standard model of cosmology has been appropriately christened ΛCDM.

Let us now discuss the reasons to go beyond Λ. The cosmological constant corresponds to a non-vanishing vacuum energy, whose magnitude should be derivable from quantum field theory calculations based on an accurate model of particle physics. The vacuum energy arises from the zero-point energies of the fields in the theory, and depends upon the cut-off scale at which the theory is expected to no longer be reliable. For the standard model of particle physics, one would derive the vacuum energy density to be at least of order the electroweak symmetry-breaking scale, $\rho^{-1/4} \sim TeV$, if supersymmetry replaces the standard model above that scale. In fact, if supersymmetry were an exact symmetry of nature, the zero-point energies would cancel out, leading to $\Lambda = 0$. However, we do not see superparticles accompanying particles, therefore the symmetry must be broken, making the superparticles too massive to be observed. Therefore the vacuum energy is not cancelled by supersymmetry. Rather, the observed value is $\rho^{-1/4} \sim 10^{-3}eV$, a disparity between the theoretical prediction and the observed value of 10^{60} orders of magnitude. This is in fact a best case scenario, for if one extends the theory up to the Planck scale, the discrepancy becomes $\mathcal{O}(10^{120})$. If we use renormalisation to cancel the divergences by counter terms, the disparity of energy scales translates into a fine-tuning of the same severity.

A second problem with the cosmological constant picture is that it comprises 70% of the energy budget today, not effectively 100% or 0%. Given the vastly different

dilution rates of the various fluids, this percentage is highly unnatural.

To illustrate this, it is useful to reformulate the Friedmann equation into a dimensionless constraint, by introducing the energy density parameters

$$\Omega_X = \frac{\kappa\rho_X}{3H^2} \quad \Omega_\Lambda = \frac{\Lambda}{3H^2} \quad \Omega_K = -\frac{K}{H^2a^2}\,, \tag{1.1.56}$$

where X denotes matter m and radiation r. Using these quantities, the Friedmann equation (1.1.46) becomes

$$\sum_X \Omega_X + \Omega_\Lambda + \Omega_K = 1\,. \tag{1.1.57}$$

The behaviour of the various energy densities with the scale factor a for the ΛCDM model is plotted in Figure 1.2. We see that while Ω_Λ and Ω_X are vastly different in magnitude as we look into the past and into the future, with Ω_Λ being totally negligible at all times in the past while totally dominant at all times in the future, they happen to be of the same order of magnitude today, right when we happen to measure them. This seems to be an uncanny coincidence. Another way to phrase this is that the energy density of the cosmological constant, albeit really tiny, eventually catches up with the cosmological fluid, and the fact that the initial conditions in the early universe were such that Λ could catch up *today* is quite remarkable.

The two problems mentioned above can be addressed, or ameliorated, by considering a dynamical form of dark energy. In what follows, as mentioned, we will look in detail at quintessence models of dynamical dark energy.

A quintessence field is a scalar field that drives late-time cosmic expansion in an analogous way to scalar field models of early universe inflation, namely by evolving along a suitable potential that allows its energy density to become close to time independent for some portion of its evolution. In the simplest case, the theory could take precisely the same form as (1.1.50). For quintessence fields, the potential could be such that the field experiences a large degree of time dependence early on in its history, but approaches a regime in which the time dependence drops away at late times. Thus, such a field could evolve over a large range of scales during its history, making it less of a surprise that it appears to take on such a tiny value today, easing the cosmological constant or fine-tuning problem. In particular, for models that

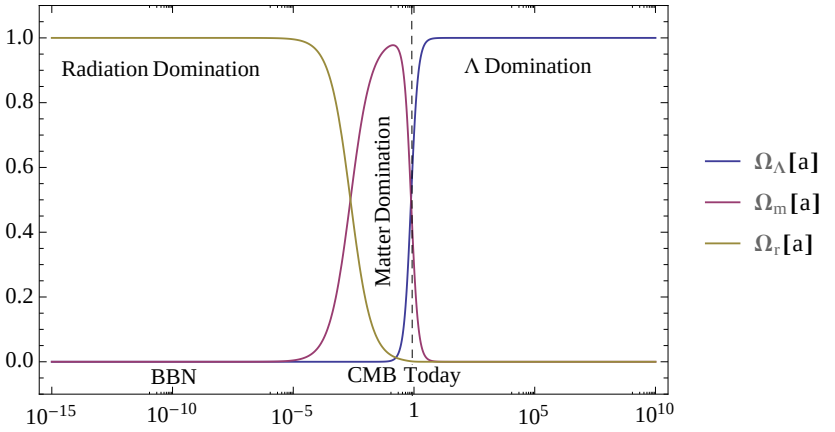

Figure 1.2: Coincidence problem: Ω_Λ and Ω_X, the fractional energy of the cosmological constant and the fractional energy of the cosmological fluid, are of the same order of magnitude only during a tiny window of the cosmological evolution, yet we happen to measure them to be right within that window today.

exhibit *tracker* behaviour [15,16], the potential is such that at late times, dark energy will always evolve towards a tiny magnitude, independently of initial conditions. This allows for dark energy to eventually catch up with the cosmological fluid and ultimately come to dominate the energy density of the universe. Tracker behaviour occurs for certain exponential and inverse power law potentials. For models that do not exhibit this behaviour, the fine-tuning problem of the cosmological constant can translate into the problem of fine-tuning the mass of the quintessence field.

However, there is still the problem of explaining why the field happened to catch up with the cosmological fluid *today*, precisely when we are around to measure it. Quintessence models can address this coincidence problem if they possess so-called *scaling solutions* [17–19], for which the energy density of the quintessence field becomes proportional to that of the cosmological fluid,

$$\frac{\Omega_{DE}}{\Omega_m} = const\,, \tag{1.1.58}$$

allowing these fluids to dilute at the same rate for some part of their evolution. On the other hand, for ΛCDM,

$$\frac{\Omega_\Lambda}{\Omega_m} \sim a^3\,. \tag{1.1.59}$$

One way that this scaling behaviour can arise is if the quintessence field is coupled

to the cosmological fluid in such a way as to allow for an energy exchange between them[2]. For example, dark energy could lose energy to the cosmological fluid, giving it less accelerating power, while the cosmological fluid would be boosted by the exchange, making it dilute slower. This could lead to a regime in which the effective equations of state for each of the fluids, which take into account the energy exchange, become equal for some part of the evolution, allowing the energy densities to be proportional over a range of efolds, rather than at a point in cosmological time.

Therefore, while a simple cosmological constant Λ is consistent with observations, it seems to require some kind of magical fine-tuning in both its magnitude as well as in the initial conditions of the universe for it to manifest to us in the precise way it does today. On the other hand, moving to dynamical dark energy can in principle allow for this precise manifestation to become more natural. In practise however, it is not easy to find suitable candidates for dark energy in realistic particle and high-energy theories. Instead of focussing on finding a candidate within a complete theory, another approach is to consider an effective theory, such as a theory of modified gravity in which scalar fields are abundant, and construct a model for dark energy from this purely phenomenological point of view. In Chapter 6 we will discuss a naturally unified picture of the cosmological dark sector which in fact connects these two independent approaches.

1.2 Quantum gravity in higher dimensions

We will now take a glimpse into the inner workings of the universe, which give rise to the vast and varied physical phenomena that we observe on the surface of nature. As we have mentioned, general relativity, as a classical theory of the gravitational field in a four dimensional spacetime, cannot be reconciled with quantum theory. While these theories may appear to be disconnected in four dimensions, we will see in what follows that they may turn out to be naturally connected in higher dimensions. After reviewing some important developments in the theory of gravity in higher dimensions, we will discuss a particularly successful fundamental theory of the

[2]Coupled quintessence models have been studied in Refs. [20–28].

gravitational field, and of all other known fields, which is the theory of superstrings oscillating in a ten dimensional spacetime.

1.2.1 A history of extra dimensions

While it may seem a step in the direction away from simplicity, naturalness and uniqueness, which are three of the most highly valued guiding principles in theoretical physics, the driving philosophy behind the introduction of new dimensions into some kind of invisible sector is to seek a deeper context in which all the four dimensional phenomena may turn out to be unified. Therefore, the idea is that while the physics may appear to be unnecessarily complicated in the four dimensional description, this complexity is merely a projection arising from a more fundamental description which is simple, natural and unique.

The concept that spacetime may admit an extra, hidden dimension made its devut in the early part of the twentieth century when Kaluza [29] demonstrated that general relativity in five dimensions contains four dimensional general relativity as well as an electromagentic field, although a scalar field with unusual couplings also emerges, preventing the four dimensional theory from being straight-forwardly interpretable as general relativity plus electromagnetism. While the idea that one can obtain a spectrum of matter fields in four dimensions from pure gravity in higher dimensions is a very compelling one, this has to be reconciled with the fact that our universe does not appear to contain an extra dimension. Kaluza's idea was to impose that all derivatives of the fields with respect to the extra coordinate are vanishing, meaning that the four dimensional laws of physics do not notice the extra dimension, except for the emergence of the new fields themselves. This is known as the cylindrical condition. One can imagine for example that our four dimensional universe is a hypersurface in five dimensions, where all the particles and their various interactions are bound by some mechanism to the hypersurface. While the cylindrical condition found a different interpretation in terms of compactification, the idea that certain fields and gauge groups are confined to a hypersurface in spacetime has found a realisation within string theory. These hypersurfaces are known as *D-branes*, which we will review in detail in what follows.

Electromagnetism in four dimensions is known to arise from a local U(1) gauge symmetry. From the five dimensional point of view, there are only spacetime symmetries, and the U(1) symmetry can be interpreted as arising from diffeomorphism invariance with respect to the fifth dimension. This suggests that what we view as "internal symmetries" in four dimensions could all in fact descend from purely geometrical symmetries in a higher dimensional spacetime, and prompts the search for the ultimate unification of all the fundamental forces in higher dimensions rather than simply at higher energies.

The cylindrical condition remained a puzzle until Klein [30] was able to show that if the extra dimension had a circular topology, this condition would naturally arise. This entails that while the other spacetime dimensions are extended, the fifth dimension is compactified. If this is so, then the fields will be periodic functions of the fifth dimension, and one can expand them into a series of Fourier modes. If the radius of the compact dimension is small enough, the energies of all modes except the zero mode will be very high, thus acquire large masses and are not dynamical in the low energy universe. For example, a scalar field $\phi(x^\mu, y)$, where y is the compact dimension, may be expanded as

$$\phi(x^\mu, y) = \sum_{n=-\infty}^{\infty} \phi_n(x^\mu) e^{iny/R} \,. \tag{1.2.60}$$

From the equation of motion $\nabla^2\phi = 0$, one sees that the masses are $M_n = n/R$, therefore for $R \ll 1$ all modes except the zero mode $n = 0$ will be too heavy to be observed. Unfortunately, for general higher dimensional theories one cannot simply impose compactification on which ever directions one chooses. A spacetime with four large dimensions and one or more curved compact dimensions must be a solution of the higher dimensional Einstein equations. It often occurs that to obtain such a spacetime, one must add in other non-gravitational fields to the higher dimensional Lagrangian, which spoils the principle that all physics in four dimensions descends fundamentally from higher dimensional gravity. Nevertheless, a natural way to obtain extra matter fields along with gravity in higher dimensions is to consider supergravity theories, which are theories with *local* supersymmetry. This has the added benefit of adding fermions to the theory, thus making it phenomenologically

viable, as Kaluza-Klein reduction of pure gravity only gives rise to bosons.

Although one has now incorporated more structure into the initially purely gravitational theory, this in fact turns out to endow the higher dimensional theory with uniqueness. While it would appear that one can add an arbitrary number of extra dimensions in this way, for the special case of eleven dimensional supergravity, the combination of supersymmetry and Kaluza-Klein theory conspire to uniquely fix the number of spacetime dimensions. Namely, the maximum number of dimensions which are consistent with a single graviton in a supergravity theory is eleven [31], while at the same time, the minimum number of dimensions which allow for a Kaluza-Klein theory to unify all of the Standard model interactions into a single gauge group is eleven [32]. Furthermore, compactification of the eleven dimensional supergravity theory to an extended four dimensional spacetime and a compact seven dimensional spacetime is a solution of the equations of motion, therefore the theory decomposes naturally down to four dimensions.

While all of these successes indicated that at the classical level, eleven dimensional supergravity must be the long sought-after fundamental theory of nature which unifies all physical phenomena, it unfortunately does not contain chiral fermions, and therefore cannot give rise to the Standard model. Chirality can be obtained by switching down to ten dimensions, however the special uniqueness of the number of spacetime dimensions is then lost. In addition, the ten dimensional theory does not split up naturally into the desired structure of four large dimensions and six compact dimensions, but instead one must add new fields to obtain this structure. Finally, the ten dimensional chiral theory contains anomalies.

It seems then that all of the appeal of seeking unification in higher dimensional theories is lost, as the ten dimensional theory is not natural nor unique. Much to the contrary however, Green and Schwartz [34] were able to show that there are in fact only two ten dimensional supergravity theories which are free of anomalies, these being precisely those theories that are based on the gauge groups $SO(32)$ and $E_8 \times E_8$. One must also include additional fields, however this is not *ad hoc* if these theories arise as low energy limits of superstring theories, which include all the desired fields that are missing in the supergravity theories. These fields *must* be

there in that case. There are five string theories, however, these all arise as different limits of a single deeper theory, which is eleven dimensional M-theory, for which the low energy limit is eleven dimensional supergravity. Therefore, quite miraculously, we are lead once again to the special case of eleven dimensions where not only are the forces unifiable, but the underlying theory admits naturalness and uniqueness, in the sense described above.

String theory makes much use of the mechinary developed for purely gravitational theories in higher dimensions, such as Kaluza-Klein theory and braneworld theories. Therefore, it will be very useful and instructive to recapitulate some of the features of these theories before moving on to discussing string theory, where the simple physics can be eclipsed in the presence of a large number of extra fields and mathematical structure associated with all their various properties and dynamics.

Kaluza Klein theory

Let us consider the case of adding just one more dimension to our four dimensions, and let us assume that we have pure gravity in five dimensions. The action then takes the form of a five dimensional Einstein-Hilbert action,

$$S = \frac{1}{2\kappa_5}\int R\sqrt{-g_5}\, d^5x\,. \tag{1.2.61}$$

Projected into four dimensions, the five dimensional metric g_{ab} may be decomposed into four-dimensional fields $\{g_{\mu\nu}, A_\mu, \phi\}$ as

$$g_{ab}dx^a dx^b = g_{\mu\nu}dx^\mu dx^\nu + \phi^2(dy + kA_\mu dx^\mu)^2\,. \tag{1.2.62}$$

Solving the five dimensional vacuum equations using the ansatz (1.2.62), and compactifying the fifth dimension, we can compute the precise interactions between the fields that would emerge in the four dimensional theory. The four dimensional action turns out to be

$$S = \int d^4x\sqrt{-g}\phi\Big[\frac{R}{2\kappa_4^2} - \frac{1}{4}\phi^2 F_{\alpha\beta}F^{\alpha\beta} - \frac{2}{3k^2}\frac{\partial_\alpha\phi\partial^\alpha\phi}{\phi^2}\Big]\,, \tag{1.2.63}$$

where we have integrated over the extra dimension and absorbed it into the definition of κ_4,

$$\kappa_4^2 \equiv \frac{\kappa_5^2}{\int dy}\,. \tag{1.2.64}$$

Upon a conformal rescaling of the metric $g_{\mu\nu} \to \phi^{-1} g_{\mu\nu}$ and a redefinition of the scalar field, this can be brought into the more familiar form, where the gravitational part of the action is a pure Einstein-Hilbert term, and the scalar field has a canonical kinetic term. The new action is

$$S = \int d^4x \sqrt{-g} \Big[\frac{R}{2\kappa_4} - \frac{1}{4}\phi(\sigma) F_{\alpha\beta} F^{\alpha\beta} - \frac{1}{2} \partial_\alpha \sigma \partial^\alpha \sigma \Big] . \tag{1.2.65}$$

We see then that starting with pure gravity in five dimensions, we have obtained a theory of gravity plus matter fields in four dimensions. The gauge symmetry of the vector field A_μ can then be understood as descending from higher dimensional spacetime symmetry, namely diffeomorphism invariance with respect to the fifth dimension. The trade-off is that there is now an additional scalar field, which couples to the gauge field such that standard electrodynamics can only be obtained in the case that $\phi = const.$ However, there is no potential for ϕ, indeed it is a massles scalar field which parameterises geometric deformations of the extra dimension. Thus one cannot fix the value of ϕ.

Braneworlds

Another very compelling mechanism to conceal the presence of an extra dimension without compactifying it arises in the context of braneworld scenarios. A braneworld is a physical universe or "world" that is confined to a hypersurface, known as a brane, embedded in higher dimensions. In a braneworld scenario, the reason we do not see the extra dimension is because spacetime is *warped*.

A p-brane is then a p-dimensional object that generalises the concept of a point particle, a 0-brane, to higher dimensions. The action for a point particle is the dimensionless integral over the one dimensional particle worldline,

$$S = -m \int ds = -m \int \sqrt{-g_{\mu\nu} \dot{x}^\mu \dot{x}^\nu} d\tau . \tag{1.2.66}$$

In flat space, choosing to set $\tau = t$, this may be written as

$$S = -m \int \sqrt{1 - \vec{v}^2}\, dt , \tag{1.2.67}$$

where a timelike particle must obey $\vec{v} < 1$, where $\vec{v}$ is the velocity of the particle, and thus the Lorentz factor $\gamma = 1/\sqrt{1 - \vec{v}^2}$ is always real.

Analogously, the action for a p-brane is given by the dimensionless integral over the $(p+1)$-dimensional worldvolume,

$$S_p = -T_p \int \sqrt{-\det \gamma_{\alpha\beta}}\, d^p\xi \,, \tag{1.2.68}$$

where ξ^α are coordinates on the brane, $x^a(\xi^\alpha)$ are spacetime embedding functions. The induced metric on the brane is given by the pullback of the spacetime metric onto the brane worldvolume,

$$\gamma_{\alpha\beta} = g_{ab} \frac{\partial x^a}{\partial \xi^\alpha} \frac{\partial x^b}{\partial \xi^\beta} \,, \tag{1.2.69}$$

where the derivatives are generalisations of the four-velocity of the point particle.

Let us consider a stationary 3-brane in a five dimensional spacetime with a cosmological constant Λ_5. Analogously to setting $\tau = t$ for the point particle in four dimensions, in five dimensions one can choose to align the coordinates on the brane with the four dimensional space-time coordinates, $\xi^\mu = x^\mu$. Positioning the brane at $x^5 = 0$, where x^5 extends to postive and negative infinity, the action is

$$S = -\int d^5x \sqrt{-g_5} \Big[\frac{R}{2\kappa_5} + \Lambda_5 \Big] - T_3 \int d^4x \sqrt{-g_4} \,, \tag{1.2.70}$$

where T_3 is the tension of the 3-brane. The Einstein equations derived from this action admit a *warped solution* of the form

$$ds^2 = h^{-1/2}(x^5) \eta_{\mu\nu} dx^\mu dx^\nu + dx^5 dx^5 \,, \tag{1.2.71}$$

where h is the warp factor. For the solution to be static, it is required that the cosmological constant must be negative. The resulting five dimensional spacetime on either side of the brane at is AdS_5.

Because of the warp factor, four dimensional gravity is localised on the brane at $x^5 = 0$. One can add a second brane that contains the standard model gauge fields, which is located at a certain distance from the original brane at $x_5 = 0$, and the warping will then have the effect of redshifting the energies associated with interactions on the standard model brane relative to the "Planck" brane at $x^5 = 0$. This amounts to introducing a gauge hierarchy, offering a solution to the hierarchy problem of particle physics in extra dimensions of spacetime.

1.2.2 Superstring theory

General relativity is a classical theory of the gravitational force. In keeping with all other known fundamental forces of Nature, gravity is believed to be mediated by a quantum particle, the spin-2 graviton. One would hope to then write down a sensible quantum theory for gravitons. There are a number of conceptual puzzles which make it really difficult, if not impossible, to extraplote the theoretical framework of general relativity all the way down to the quantum realm. The main issue is that quantum corrections to the Einstein-Hilbert action are suppressed by powers of the Planck mass, M_P, therefore one would have to access regimes in which the energies are of order 10^{18} GeV to see the quantum effects of gravity play themselves out in the world. For a particle with a Planck scale mass, the Schwarzschild radius is of order the Compton wavelength, $\hbar/mc$. Therefore, at ambient energies around the Planck scale, which we expect to be present at the birth of the universe, spacetime could become a sea of quantum black holes, and even *virtual* black holes [35], objects which general relativity cannot help us to understand. Furthermore, the quantum fluctuations of light cones would make it very difficult to understand causality. Even the concept of spacetime becomes ambiguous, because while we usually think of spacetime as a smooth manifold, if the energies of quantum fluctuations become high enough, they could turn the small scale structure of spacetime into a foam-like substance [36]. The only way forward in such a context is to seek out a new quantum description of gravity which allows us to meaningfully reformulate the laws of physics and carry out reliable computations at high energies, and which smoothly connects with general relativity as the energies are lowered.

A second more practical issue which makes it impossible to write down a quantum version of general relativity is its lack of renormalisability. In quantum field theory, loop momentum integrals are divergent in the ultraviolet, as the momenta of virtual particles in the loops are able to grow without bound. For quantum scattering process involving fundamental interactions other than gravity, we know how to deal with these infinities by redefining or renormalising parameters in the theory. However, in the case of gravitational scattering process, the momenta diverge so badly that we cannot control the theory using renormalisation techniques.

Therefore, one cannot compute gravitational scattering amplitudes using the tools of quantum field theory.

As mentioned, the hope is that we find out that Nature is better described at high energies by a deeper theory, for which general relativity emerges as a low energy limit. There are many interesting proposals for such a theory, however, the theory which has made the most progress in incorporating gravity along with all the other fundamental interactions into a unified quantum framework is *string theory*.

String theory, as the name is suggests, is a theory for which the fundamental constituents of Nature are one-dimensional strings, instead of zero-dimensional point-particles, with a fundamental length scale ℓ_s. The strings can have their endpoints free, or they can form closed loops. As they move through spacetime, they oscillate in various ways, and the oscillation modes produce a rich spectrum of bosonic quantum fields with masses that are integer multiples of the string scale, $M_s = 1/\ell_s \lesssim M_p$. For the low energy universe, the only dynamical degrees of freedom are the massless modes, among which is a rank-2 symmetric tensor field, which may naturally be identified with the graviton of general relativity. In addition, there are scalar and vector fields, which are essential for building the Standard model of particle physics. Realistic particle theories contain fermions in addition to bosons. For the case of oscillating strings, bosons can be paired with fermions via supersymmetry. The resulting theory is known as a *superstring theory*.

A very exotic aspect of string theory is the appearance of extra dimensions of space, which we reviewed in Section 1.2.1 above. For superstrings, worldsheet conformal invariance demands that the theory is formulated in a ten dimensional spacetime.

As one dimensional objects, strings trace out a two-dimensional surface, the string worldsheet, as they move through spacetime. This has surprising consequences for one of the long-standing problems of gravity, namely the lack of renormalisability.

For point particles, divergent behaviour at loop level in scattering processes arises because interactions can take place at a point. The uncertainty principle relates distances to momenta,

$$\Delta L = \frac{\hbar}{p}\,, \tag{1.2.72}$$

thus as $\Delta L \to 0$, the momentum diverges. In string theory on the other hand, interactions take place over a smooth 2D surface, the string worldsheet, thus preventing the divergence of momenta. Therefore, simply increasing the dimensionality of the fundamental object to one dimension higher has the effect of removing one of the major obstructions in formulating a quantum theory of gravitational interactions.

We will now briefly mention what string theory has to say about gravity at the Planck scale. Instead of appearing as a final force to be unified with the forces of particle physics at a high enough energy scale, string theory suggests that gravity should instead be viewed as a *dual* description of a gauge theory living in one dimension lower. This constitutes a significant paradigm shift in the way we view gravity and particle physics, and is currently the subject of very active research worldwide. In fact, it turns out the duality is such that weakly coupled gauge theories correspond to strongly coupled gravity theories and vice versa, allowing the difficult non-perturbative regions of both gravity and gauge theories to be probed on the other side of the duality, in a much more controlled perturbative regime. To date, the exploration of the physics of quantum gravity at the Planck scale using the correspondence is still in its infancy, however significant progress has been made in our understanding of strongly coupled gauge theories.

We will now describe the theory in more detail. We have mentioned that strings can be open or closed, producing different vibrational spectra. This in fact leads to a variety of different types of string theories, which corresponds to the various limits of M-theory, existing in eleven dimensions. It has been shown that the various superstring theories, or M-theory limits, can be related to one another via a system of dualities. The topology of the closed string worldsheet can either preserve or reverse the orientation of a closed string as it moves through spacetime, leading to oriented and unoriented closed string theories respectively. Further distinct classes then arise from adding open strings. Type II and heterotic string theories contain only closed, oriented strings, whereas Type I theories contain unoriented strings which may be open or closed. In fact, Type I theory is really an open string theory, but open strings can form loops by joining their endpoints and thus turn into closed strings, which may split open again. On the other hand, pure closed strings cannot

split open into open strings. When supersymmetry is included, the Type II theories can be subdivided into Type IIA, which is a non-chiral theory, and Type IIB, which is chiral.

Type IIB flux compactifications

We will now focus exclusively on Type IIB theory. Distinct closed string sectors arise when boundary conditions are imposed for the left and right moving oscillations along the string. States with periodic boudary conditions are are classified as being in the Neveu-Schwarz sector, while states with antiperiodic boundary conditions are in the Ramond sector. The massless bosonic spectrum includes a rank-2 symmetric tensor which we identify with the ten dimensional graviton, G. There are two scalar fields, the dilaton ϕ which parameterises the string coupling, $g_s = e^{\phi}$, and a second scalar C_0. There are two antisymmetric 2-form fields, C_2 and B_2, and finally, an antisymmetric 4-form C_4. The n-forms C_n constitute the Ramond sector, while the remaining fields constitute the Neveu-Schwarz sector.

The closed string spectrum does not contain any gauge fields, which are essential for building the Standard model of particle physics. On the other hand, the massless open string spectrum contains a U(1) gauge boson, therefore one can introduce gauge theories into Type IIB by adding in open strings. There is a subtlety to this, as one must specify boundary conditions for the end points of the open string. Imposing boudary conditions in fact amounts to introducing entirely new $(p+1)$-dimensional objects into string theory, known as Dp-branes, which can be thought of in terms of their primary task, namely as surfaces upon which open strings can end, or as new solitonic objects that have a life and story of thier own. We already encountered these sorts of objects in Section 1.2.1 in the context higher dimensional gravity theories: they are the branes of string theory. With the open strings attached to them, one can now split up the degrees of freedom of the ten dimensional U(1) gauge boson into those that propagate along, and those that propagate transverse to, the Dp-brane worldvolume. The former combine into a $(p+1)$-dimensional worldvolume gauge field, while the latter are a collection of $9-p$ scalars. These scalars parameterise the motion of the brane in the directions tranverse to its worldvolume. Having

introduced D-branes into the theory, we now have a useful way to think about the other form fields in the spectrum. As we have mentioned, branes can be thought of as higher dimensional generalisations of point particles. Therefore, a Dp-brane can couple electrically to a $(p+1)$-form potential in the same way as a charged particle couples to a vector field. For example, the 4-form C_4 can be interpreted as the charge of a D3-brane.

The action for a D-brane contains two pieces, namely the DBI action and the Wess-Zumino action, where the first encodes the couplings of the open strings to the Neveu-Schwarz sector closed strings, and the second, the couplings to the Ramond sector closed string fields in the background,

$$S = S_{DBI}[G, \phi, B] + S_{WZ}[C_n]\,. \tag{1.2.73}$$

The DBI action takes the form

$$S_{\rm DBI} = -\mu_p \int d^{p+1}\xi e^{\frac{(p-3)}{4}\phi}\sqrt{-\det(\gamma_{ab} + e^{-\frac{\phi}{2}}\mathcal{F}_{ab})}\,, \tag{1.2.74}$$

where

$$\mu_p = (2\pi)^{-p}(\alpha')^{-\frac{(p+1)}{2}}, \qquad T_p = \mu_p e^{\frac{(p-3)}{4}\phi}, \tag{1.2.75}$$

with T_p being the tension of the brane, where $\alpha' = \ell_s^2$, γ_{ab} is the induced metric, and $\mathcal{F}_{ab} = \mathcal{B}_{ab} + 2\pi\alpha' F_{ab}$ is the gauge invariant combination of the pullback of B_2 and the field strength of the world-volume $U(1)$ gauge field.

The Wess-Zumino (WZ) action takes the form

$$S_{WZ} = \mu_p \int_{\mathcal{W}_{p+1}} \sum_n \mathcal{C}_n \wedge e^{\mathcal{F}}\,, \tag{1.2.76}$$

where $\mathcal{W}_{p+1}$ is the world-volume of the brane, and $\mathcal{C}_n$ are the pullbacks of the C_n forms to which the brane couples. In this expression, the wedge product picks out the relevant terms in the exponential.

With open strings included, we now have a theory that includes $U(1)$ gauge fields, but still no higher gauge groups that could accommodate the Standard model. In Type IIB theory, gauge groups can be enhanced by stacking or intersecting the branes together in various ways.

To make contact with the real world, six of the ten space-time dimensions must now be concealed. In string theory, this is accomplished by compactification, much

like in Kaluza-Klein theory. However, instead of a circle, we now have a six dimensional compact space, which can admit a huge variety of cycles. The ten-dimensional graviton gives rise to a four-dimensional graviton plus a collection of massless scalar fields which descend from its compact components, and which parameterise changes in the shape and volume of the compact dimensions.

In order to stabilise these scalar moduli fields, one must in fact encorporate the braneworld picture and compactify on a *warped geometry*, with the general ansatz

$$ds^2 = h^{-1/2}(x^m)g_{\mu\nu}dx^\mu dx^\nu + h^{1/2}(x^m)g_{mn}dx^m dx^n\,, \tag{1.2.77}$$

where h is the warp factor, $g_{\mu\nu}$ is the four dimensional metric and g_{mn} is the compact metric. Non-trivial warping can arise in the compact dimensions only when there are sources of positive as well as negative tension about, as for positive tension sources alone, the warped regions are always non-compact. In Type IIB theory, negative tension sources are present in the form of solitonic objects called orientifold planes. The stabilisation of geometric moduli occurs because in a warped compactification, the flux lines of the various form fields can be non-vanishing, and they thread through the cycles in the compact space. The compact flux lines are quantised, thus once they settle into a minimum energy configuration, any further deformations of the geometry will come with an energy cost.

With a warped geometry in the compact space, Type IIB string theory is naturally endowed with a gauge hierarchy, making it even more attractive as a theory of particle physics. Furthermore, D-branes can move as probes in the warped geometry, which has interesting implications for cosmology in the four-dimensional universe.

D-brane inflation and cosmic strings

In Chapter 6, we will look in detail at the cosmology of moving D-branes in strongly warped regions of the compact space. However, we will briefly mention here how cosmic inflation can arise in such a context. The mechanism can be illustrated by simply considering the restrictions on the motion of the branes. In particular, just like point-particles, D-branes can move relativistically, and as they do so, they must obey causality in the compact dimensions. As we have discussed, the motion of a

D-brane gives rise to a scalar fields in four dimensions which parameterise its motion in the compact space. For a cosmological background in four dimensions, a D-brane moving in a single compact direction in a warped region has a Lorentz factor of the form

$$\gamma = \frac{1}{\sqrt{1 - h\dot{\phi}^2}}\,, \tag{1.2.78}$$

where h is the warp factor and $\phi(t)$ is the scalar position field. The brane must move on a timelike trajectory, therefore $h\dot{\phi}^2 < 1$ such that γ is always real. For strongly warped regions where $h \gg 1$, the brane is thus forced to slow down, $\dot{\phi}^2 \ll 1$, in order to remain on a timelike trajectory. Therefore, even though the potential may be very steep, the brane moves very slowly along it, as its velocity is strongly suppressed by the warping. This leads to a nearly constant energy density for the scalar field, and hence the field may drive cosmic acceleration. This type of D-brane inflation is known as *DBI inflation* [37, 38], which is distinct from slow-roll inflation because even though the brane is moving very slowly, it is still moving relativistically, as $\gamma \gg 1$. Slow-roll inflation can then be realised in the D-brane context as the non-relativistic limit of DBI inflation[3].

Another interesting aspect of D-brane inflation is the production of cosmic strings [44–46]. We will see in Chapter 2 that cosmic strings can be formed during symmetry breaking processes such as the abelian Higgs mechanism, when a U(1) gauge field obtains a mass due to the Higgs field acquiring a vacuum expectation value. In the context of string theory, brane inflation as outlined above can arise when a D-brane is attracted to an anti-D-brane situated at the tip of a warped region, which ultimately ends in the annihilation of the two objects. The annihilation of the pair of branes corresponds to a symmetry breaking process, analogous to the abelian Higgs mechanism, that can produce cosmic strings. In this simple example of a pair of branes, the gauge group is $U(1) \times U(1)$, and the scalar field, which is tachyonic, and which parameterises the motion of one of the branes, is charged under a linear combination of the two gauge fields associated with the branes. When the branes annihilate, the tachyon acquires a vacuum expectation value, thus giving a mass to

[3]For reviews on D-brane inflation along with other aspects of string cosmology, see Refs. [39–43]

the gauge field combination under which it is charged, and breaking the original symmetry of the system.

1.3 Scalar-tensor theories

In general relativity, there are no non-minimal couplings between gravity and the other fields in the spacetime, thus we may write down, in a completely unambigious way, a gravitational action which is purely geometrical, and a matter action which constrains the matter fields to freefall along that geometry. However, things are not so simple once GR appears as a low energy limit of more UV-complete theory, or as a reduction from a gravitational theory in higher dimensions. As we have discussed in detail, these theories generically unleash a plethora of new fields into the four dimensional description, which may introduce a direct coupling of a scalar field to R, or influence the geodesics of matter fields. Inspired by these deeper descriptions of nature are the so-called *scalar-tensor* class of gravitational theories, which, due to the new interactions with gravity, choose to incorporate scalar degrees of freedom into the gravitational sector of the universe. For the simplest case of a single additional degree of freedom, the gravitational sector is then a doublet of fields, $(g_{\mu\nu}, \phi)$. The prototypical action takes the form

$$S = \frac{1}{2\kappa}\int d^4x\sqrt{-g}\Big(f(\phi)R + \mathcal{L}_\phi(\phi, \phi_{,\mu})\Big) + S_m(g_{\mu\nu}, \psi_i, \psi_{i,\mu})\,, \tag{1.3.79}$$

where a Langrangian for the dynamical scalar field $\mathcal{L}_\phi$ has been added to the gravitational part of the action. The matter action is, as before, a functional of $g_{\mu\nu}$ and the fields ψ_i and their derivatives, and does not contain the scalar field. Featuring a direct coupling of a scalar field to R, such an action is said to be in the *Jordan frame*.

Since the scalar field does not couple to matter in this frame, variation of (1.3.79) with respect to $g^{\mu\nu}$ will lead to a stress-energy tensor for matter that has the same form as (1.1.9), and one can further show that this stress-energy tensor is conserved, following precisely the same procedure as for the purely GR case. However, both sides of the Einstein equation are modified in this frame.

To make contact with general relativity, one can choose to transform the gravitational sector to the so-called *Einstein frame*, $(g_{\mu\nu}, \phi) \to (\bar{g}_{\mu\nu}, \bar{\phi})$, in which the gravitational action assumes the Einstein-Hilbert form. This is accomplished by a conformal transformation of the metric,

$$\bar{g}_{\mu\nu} = f(\phi) g_{\mu\nu} \,, \tag{1.3.80}$$

and a canonical redefinition of the scalar field $\phi \to \bar{\phi}$. The action is then

$$S = \frac{1}{2\kappa} \int d^4x \sqrt{-\bar{g}} \Big(\bar{R} + \mathcal{L}_{\bar{\phi}}(\bar{\phi}, \bar{\phi}_{,\mu}) \Big) + S_m(f^{-1}(\bar{\phi}) \bar{g}_{\mu\nu}, \psi_i, \psi_{i,\mu}) \,. \tag{1.3.81}$$

We have seen an explicit example of this in Section 1.2.1 above, in the context of Kaluza-Klein theory. Thus these theories are *conformally equivalent* to GR. However, this does not mean that they are the same as GR, as the matter fields now couple to an *effective metric* which depends upon the scalar field ϕ.

This has consequences for the conservation of energy-momentum. Variation of this action with respect to $\bar{g}^{\mu\nu}$ yields the familiar quantities in the new frame, $\bar{G}_{\mu\nu}$ and $\bar{T}_{\mu\nu}$, but the conservation equation for matter is now modified. This is due to the fact that, as ϕ now appears in S_m, a general variation yields

$$\delta S_m = 0 = \int d^4x \frac{\delta S_m}{\delta \psi_i} \delta \psi_i + \int d^4x \frac{\delta S_m}{\delta \bar{\phi}} \delta \bar{\phi} + \int d^4x \frac{\delta S_m}{\delta g_{\mu\nu}} \delta g_{\mu\nu} \,, \tag{1.3.82}$$

while the equation of motion for $\bar{\phi}$ reads

$$\bar{\nabla}_\mu \frac{\partial \mathcal{L}_{\bar{\phi}}}{\partial \bar{\phi}_{,\mu}} - \frac{\partial \mathcal{L}_{\bar{\phi}}}{\partial \bar{\phi}} + \bar{\nabla}_\mu \frac{\partial \mathcal{L}_m}{\partial \bar{\phi}_{,\mu}} - \frac{\partial \mathcal{L}_m}{\partial \bar{\phi}} = 0 \,. \tag{1.3.83}$$

Therefore, whereas the first term in (1.3.82) vanishes by virtue of the equation of motion for ψ_i, the second term is just one part of the equation of motion for $\bar{\phi}$, thus does not vanish. This leads to a modified conservation equation of the form

$$\bar{\nabla}_\mu \bar{T}^{\mu\nu} = \Big(\bar{\nabla}_\mu \frac{\partial \mathcal{L}_{\bar{\phi}}}{\partial \bar{\phi}_{,\mu}} - \frac{\partial \mathcal{L}_{\bar{\phi}}}{\partial \bar{\phi}} \Big) \partial^\nu \bar{\phi} \,. \tag{1.3.84}$$

It should be noted however that the *total* stress-energy, namely the sum of the stress energy tensors for the scalar and matter fields, is conserved in this frame, a consequence of the diffeomorphism invariance of $S_{\bar{\phi}}$ and S_m.

We see then that theories with extra fields in the gravitational sector lead to new effective metrics for matter fields in the Einstein frame, which implies the

emergence of two geometries that are conformally related to one another. One geometry determines the curvature of spacetime, the other controls how matter moves in the spacetime.

While this is different from general relativity, which treats spacetime as being endowed with a single Riemannian geometry, it is still in accordance with the foundations of general relativity. Absolutely central to general relativity is the *Einstein equivalence principle*, according to which all test particles freefall in the same way once an initial position and velocity has been specified, and in local freefalling frames, the laws of special relativity are recoverable. As long as the geometry is Riemannian, we may locally choose coordinates which place us in an inertial frame, in which the laws of special relativity may be retrieved. Then, as long as all of the matter fields couple to the same Riemannian metric, one can derive geodesic equations for the test particles and show that all such particles freefall in the same way. This is because in the case of Riemannian geometry, the contracted Bianchi identity ensures that matter is conserved, and thus test particles follow geodesics, as we have seen in Section 1.1.1.

The disformal relation

The example above features a spacetime-dependent conformal relation between the physical metric and the effective metric in the Einstein frame. Keeping things as general as possible, one could write down an Einstein-frame formulation of a scalar-tensor theory schematically as

$$S = \frac{1}{2\kappa}\int d^4x\sqrt{-g}R + S_\phi(g_{\mu\nu},\phi,\phi_{,\mu}) + S_m(\bar{g}_{\mu\nu},\psi_i,\psi_{i,\mu})\,, \tag{1.3.85}$$

where the matter fields couple to some unspecified effective metric,

$$\bar{g}_{\mu\nu} = f(g_{\mu\nu},\phi,\partial\phi...)\,. \tag{1.3.86}$$

One could then ask, what would be the most general and physically consistent relation between $g_{\mu\nu}$ and $\bar{g}_{\mu\nu}$ that could be given by the scalar field and its derivatives? This question was originally addressed in Ref. [49], but here we will follow the argument in Ref. [47]. Constructing a rank (0,2) symmetric tensor out of $g_{\mu\nu}$, ϕ

and its derivatives restricts us to three possible terms,

$$\bar{g}_{\mu\nu} = f_1(\phi, X, \Box\phi ...)g_{\mu\nu} + f_2(\phi, X, \Box\phi ...)\partial_\mu\phi\partial_\nu\phi + f_3(\phi, X, \Box\phi ...)\partial_\mu\partial_\nu\phi\,, \quad (1.3.87)$$

where the functions f_i must not contain any non-contracted indices, but may contain all possible coordinate invariants that can be contructed from $g_{\mu\nu}$, ϕ and its derivatives. Physical consistency then demands that we set $f_i = f_i(\phi, X)$ and $f_3 = 0$, in order to avoid instabilities in the equations of motion via Ostrogradski's theorem[4] [48]. We are thus left with the *disformal relation* [49],

$$\bar{g}_{\mu\nu} = C(\phi, X)g_{\mu\nu} + D(\phi, X)\partial_\mu\phi\,\partial_\nu\phi\,, \quad (1.3.88)$$

where the first term is the familiar spacetime-dependent conformal transformation of the physical metric, and the second term involving first derivatives of the scalar field is the purely "disformal" contribution. For clarity, the scalar factors have been relabelled as C and D to indicate the conformal and disformal factors respectively.

The purely conformal transformation, for which $D = 0$, characterises the Brans-Dicke class of scalar-tensor theories, for which the f(R) gravity theories are a widely studied example [50,51]. On the other hand, the disformal transformation in (1.3.88) is generic in extensions of general relativity. In fact, it must appear in the Einstein frame formulation of any more general Horndeski-type scalar-tensor theory [52–54]. Another very active area of study in which the disformal coupling makes an appearance is in the field of non-linear massive gravity theories [55, 56]. Finally, studies of disformal couplings in a variety of contexts have demonstrated that these couplings exhibit a diverse phenomenology[5].

We have seen that the purely conformal coupling may be understood as arising from fundamental scalar fields that couple to four-dimensional gravity due to compactification effects from a higher dimensional theory. While the disformal coupling

[4]Note that for $f_3 \neq 0$, it might still be possible to avoid instabilities due to a cancellation of terms in the equations of motion, however, we will restrict ourselves to the simpler case $f_3 = 0$ which is trivially instability-free.

[5]For applications in relativistic MOND theories, see for example Refs. [13, 57–60]. For varying-speed-of-light theories, see Refs. [61–63]. For cosmological and astrophysical applications, see for example Refs. [64–71].

may appear to be more abstract, it can in fact also be interpreted as arising due to the four-dimensional projection of a higher dimensional theory. Indeed, it may be realised in the higher dimensional context as the induced metric on a brane that is moving in the extra dimensions. We will see this explicitly in Chapter 6 in the context of Type IIB string theory.

Chapter 2

Cosmic Strings

In the early universe, while most of the matter is in the form of a coupled cosmological fluid of fundamental particles that hasn't yet had time to form macroscopic structures, macroscopic objects called topological defects can emerge from cosmological phase transitions. These objects, which we mentioned briefly in Section 1.1.3, can be in the form of cosmic strings, domain walls and monopoles[1]. In this Chapter, we will discuss these objects in more detail, focussing in particular on cosmic strings.

We will begin with a review in Section 2.1 of the symmetry breaking process that can lead to the formation of these objects, and will then describe the objects themselves in more detail in Section 2.2. Following this, we will focus exclusively on cosmic strings. Realistic strings may be composed of a scalar Higgs condensate core threaded with magnetic flux lines. In Section 2.3 will review the abelian Higgs model which describes these sorts of strings, and discuss the most simple topologically non-trivial solution, the Nielsen–Olesen vortex solution [77], in Section 2.4.

Defect objects can have a significant gravitational influence on the spacetime through which they are traversing. Domain walls can act as a spacetime "mirror" [75, 76], while cosmic strings can produce a conical deficit effect in the spacetime [77–81]. Even more exotic spacetimes can arise when a defect object comes into contact with black holes, as in that case, the features of the spacetimes associated with each object essentially blend into each other, producing a new spacetime that

[1]For a thorough review on the subject of topological defects, see [72, 73]

reflects the gravitational impact of the combined objects.

In Section 2.4 we will review the gravitational effect of the Nielsen–Olesen string in isolation, demonstrating how the conical effect arises. We will then go on to discuss strings and black holes in Section 2.5, wherein we will review some aspects of cosmic string phenomenology in Schwarzschild and Reissner–Nordstrom spacetimes.

2.1 Symmetry breaking in the universe

Perhaps some of the earliest scientific observations of Nature were that it appears to contain four basic "elements", which were classified as air, water, earth and fire. In the modern context we can understand the first three of these elements as the various phases of matter, namely the gaseous, liquid and solid phases, as a function of the fourth element, energy. Naively, as energy decreases, a substance undergoing changes in its phase appears to progressively acquire a definite, fixed shape. In the gaseous phase at high energy, we cannot assign any kinds of spatial relations or proportions to the substance, whereas by the time it reaches the solid phase at low energy, these sorts of structural properties are distinctly definable. At a more fundamental level, where the substance is undergoing changes to its intermolecular structure, a similar principle is in fact operating.

Take the example of water, which is composed of the molecule H_2O. In its steam phase, neighbouring molecules are not bound to one another in any way, thus a volume filled with steam consists of many individual molecules with completely random orientations. In the liquid phase, the hydrogen atoms on the water molecule point towards the oxygen molecules on neighbouring molecules, such that the overall structure is based on a tetrahedral shape. However, this is simply a time-averaged approximate structure, as the molecules in the liquid phase of water are continuously rotating and moving, causing these hydrogen bonds between neighbouring molecules to break apart and form again in quick succession. When water boils, these bonds are broken completely. When water freezes on the other hand, the intermolecular hydrogen bonds cause the molecules to align themselves into a fixed hexagonal lattice structure, which, for example, produces the hexagonal, 6-fold symmetry of

snowflakes.

We can then think about the phases of water, and matter in general, as simply being different states of symmetry. The high temperature state has the most symmetry, as the individual molecules have not chosen any particular directions to point towards and are, collectively, invariant under the SO(3) rotation group. As the temperature cools, the substance undergoes a phase transition during which some of the symmetry is lost, as the new phase exhibits some tendancies of the molecules to align in certain ways. During the final phase transition to the solid phase, even more symmetry is lost, as now all of the molecules have chosen a definite, fixed alignment.

Now lets take this principle to the level of fundamental particles. The water example is in fact a microcosmic manifestation of a process known as spontaneous symmetry breaking that takes place macroscopically as the whole universe evolves towards a low energy state. We saw in Section 1.1.3 that the universe undergoes a series of phase transitions in its early history, during which a large gauge group with enough symmetry to unify the strong, weak and electromagnetic interactions is believed to be progressively broken down to subgroups with a lower degree of symmetry, eventually evolving dynamically to the symmetries of the standard model. The symmetries that are broken by the phase transitions are therefore internal particle symmetries. The loss of symmetry manifests itself as the disappearance of a number of gauge bosons from the particle spectrum of the universe, as during the phase transition, these gauge bosons acquire masses that correspond to the energy scale of the universe at the time of the phase transition. Therefore, at energies below the phase transition scale, they are too heavy to be excited. The remaining massless gauge bosons correspond to those symmetries that were preserved during the transition, and these mediate the interactions associated with the smaller subgroups.

One phase can transform smoothly into another phase, just like water turning into ice, or the phase transition can occur discontinuously via the formation of bubbles containing the new phase, just like water boiling into steam. The latter is described as being a first-order phase transition, and the former, as a second-order phase transition.

The gauge bosons acquire masses due to the presence of scalar Higgs field in the symmetry group which obtains a vacuum expectation value during the phase transition. Symmetry breaking occurs when the Higgs field migrates from an unstable vacuum to a true vacuum along a potential of the form

$$V(\phi) = \lambda\Big(|\phi|^2 - \eta^2\Big)^2 , \tag{2.1.1}$$

where $|\phi^2| \equiv \phi^\dagger\phi$. The true vacuum corresponds to the minimum of this potential, where ϕ aquires a vacuum expectation value

$$|\phi_0|^2 = \eta^2 . \tag{2.1.2}$$

On the other hand, the unstable vacuum corresponds to $\phi = 0$. The Higgs field can move smoothly between the two phases, giving rise to a second-order phase transition. Interactions with other particles can however contribute new effective terms to the Higgs potential, possibly changing the nature of the phase transition.

If the theory is $\mathbb{Z}_2$ invariant, and therefore $\phi \in \mathbb{R}$ such that $|\phi|^2 = \phi^2$ in (2.1.1), the vacuum configuration is discrete, and can only be one of two values, $\phi_0 = \pm\eta$. On the other hand, if the theory is U(1) invariant, $\phi \in \mathbb{C}$ and thus the vacuum configuration is a continuous circle manifold defined by $\phi_0 = \eta e^{i\alpha}$, where $\alpha \in \mathbb{R}$ is an arbitrary phase. The potential (2.1.1) for a U(1) invariant theory is depicted in figure 2.1. In both cases, the symmetry of the theory is *spontaneously broken* at the level of the vacuum, meaning that while the theory respects the symmetry, the vacuum configuration does not.

One can consider excitations around the vacuum expectation value of the Higgs in the true vacuum. For the case of a vacuum manifold defined by $\phi_0 = \eta e^{i\alpha}$, perturbations in the radial direction are massive, as the potential curves upwards, $V'' > 0$, in this direction. An excitation would thus require energy, or mass, to move along it. On the other hand, excitations along the vacuum manifold are massless, as the potential is flat in this direction, $V'' = 0$, meaning that these excitations require no energy to move along it.

This gives rise to a massive scalar Higgs excitation mode and a massless Goldstone mode. The latter always appear when a continuous symmetry is spontaneously broken, as note that for a discrete symmetry, there is no massless direction in the

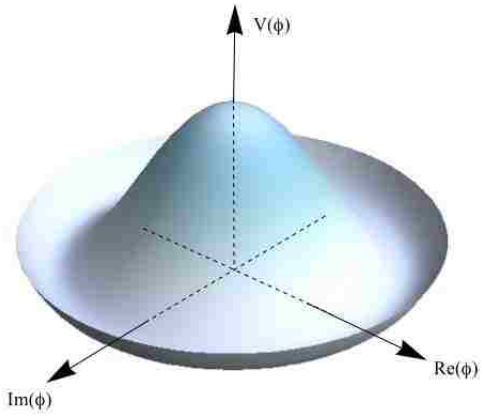

Figure 2.1: Potential for the Higgs field: When the Higgs field sits at $\phi = 0$, the unstable vacuum state respects the U(1) symmetry of the potential, as rotations about the z-axis do not change the location of the Higgs field. Once the Higgs field rolls down into the true vacuum, the symmetry is broken, as rotations about the z-axis now "move" the Higgs field around the circle.

vacuum state. The Goldstone mode is the additional degree of freedom that can give a mass to a gauge boson that is coupled to the theory.

2.2 Topological defects

An interesting possibility arises when the topology of the vacuum is non-trivial. This implies that there can be field configurations that contain regions or domains in which the symmetry is left unbroken, namely, in which $\phi = 0$ locally, even when the true vacuum state is attained globally. These regions correspond to localised concentrations or clumps of energy, called topological defects, where the energy of the metastable vacuum is trapped and cannot dissipate away.

The objects that are formed depend upon the type of symmetry that is spontaneously broken. In three dimensional space, one can form codimension one defects, known as domain walls, if a discrete symmetry is broken. In that case, $\phi \in \mathbb{R}$ and therefore $\phi(\mathbf{x}) = 0$ defines a two-dimensional hypersurface, which is the wall. On the other hand, one can obtain codimension two defects, known as vortex lines or cosmic strings, if a U(1) symmetry is broken. We then have $\phi \in \mathbb{C}$, and thus $\phi(\mathbf{x}) = 0$

reduces to two equations for three spatial coordinates, $\Re\mathrm{e}\,\phi = 0$ and $\Im\mathrm{m}\,\phi = 0$, thus the solution is the intersection between the two-dimensional hypersurfaces defined by these equations, a one-dimensional object. Finally, a codimension three object, called a monopole, can arise if an $SO(3)$ symmetry is broken. In that case, $\boldsymbol{\phi}$ is a three-dimensional vector and thus $\boldsymbol{\phi} = 0$ is a set of three equations defining three two-dimensional hypersurfaces. The solution is thus the intersection of these, which defines a point.

In a cosmological context, topological defects can be produced by the co-called Kibble mechanism [74], which generically predicts the formation of these objects during all phase transitions in the universe. The idea behind this mechanism is that different regions of spacetime can only know about each other at a given timescale if a photon can pass between them on that timescale. During a phase transition, the Higgs field chooses one particular vacuum state out of the set of all possible vacuum states, which is the vacuum manifold. Regions of the universe which are outside of causal contact with one another during the phase transition will acquire different vacuum states, as the choice of state picked out in one region cannot be communicated to all neighbouring regions on the timescale of the transition. The boundaries between regions with different vacua appear as defects. At these boundaries, no choice of vacuum is made, and the universe is instead trapped in the symmetric, "old" phase.

Returning to the topology of the vacuum, a domain wall defect can arise if the vacuum manifold is disconnected, whereas cosmic strings and monopoles can form if the vacuum manifold contains non-contractable loops or spheres respectively. This implies that the boundary between different vacua, namely the defect, cannot be deformed away. As we have seen, for a vortex line, corresponding to a broken U(1) symmetry, the vacuum manifold corresponds to all the possible directions in which the phase of the Higgs field can point, which form a circle. After a phase transition, the Higgs field will thus point in all sorts of different directions across all different regions of the universe. Joining up different regions by loops, along each loop the phase of the Higgs will vary randomly. However, if there is a loop along which the phase of the Higgs happens to vary by an integer multiple n of 2π, then such a

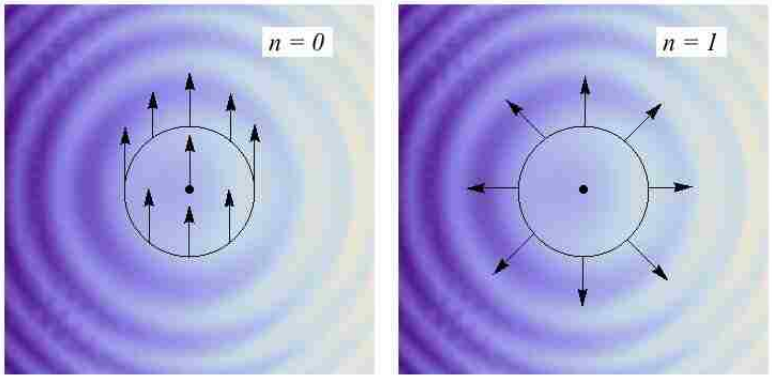

Figure 2.2: Formation of vortices: The Kibble mechanism for the simple cases of $n = 0$ and $n = 1$. If around a closed loop the phase of the Higgs does not vary ($n = 0$), then one can contract that loop to a point by defining a phase at that point. On the other hand, for $n = 1$ the phase is not definable at the central point. This means that the Higgs field must vanish at that point, which then corresponds to a vortex.

loop winds around a vortex, and cannot be contracted to a point. This is because contracting the loop to a point means contracting the phase to a point, but if the phase varies by $2\pi n$ around the loop, then there is no way to smoothly deform it to a particular, average value at the point. To avoid a singularity at that point, the Higgs field must vanish there, which means it is in the metastable vacuum state. The integer n is then called the winding number of the vortex. This situation is illustrated in figure 2.2.

Cosmic strings are amoung the most interesting of topological defects in a cosmological context, as their emergence does not pose any problems for the evolution of the universe. On the other hand, the energy of domain walls and monopoles can over-close the universe, thus if these defects are produced during a phase transition they must be diluted away by cosmic inflation. Cosmic strings on the other hand are able to break apart into smaller and smaller loops, which radiate and eventually disappear. The loops form because strings that cross each other exchange their end-points, a process known as intercommutation. In this way, if a large network of strings is produced in the early universe, it will naturally dilute itself by breaking up into small loops that decay away into gravitational radiation, leaving only a few

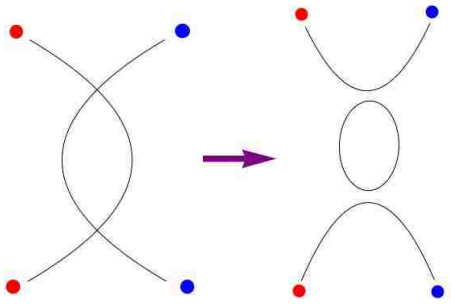

Figure 2.3: Intercommutation of strings: Two strings cross and exchange end-points, leading to the formation of a loop and two smaller strings.

complete strings. Eventually, the string density evolves into a scale-invariant state, such that the network no longer changes as time progresses.

2.3 Abelian Higgs model

As we have seen, cosmic strings or vortices can be produced when a U(1) symmetry is spontaneously broken in the presence of non-trivial topology. For global symmetries the core of the string is composed of a Higgs condensate. If the theory is gauged, and hence the string forms from the breaking of a local U(1) symmetry, the Higgs-condensate core will be threaded with magnetic flux lines associated with the gauge boson that couples to the Higgs. The latter case is typical in realistic symmetry breaking schemes such as grand unification and electroweak breaking, where the symmetry breaking process is invoked to break large particle gauge groups by giving masses to gauge bosons.

In what follows we will consider only gauged strings. We begin by reviewing the Abelian Higgs theory.

The Abelian-Higgs action in the full four-dimensional theory is

$$S = -\int d^4x\sqrt{-g}\left[D_\mu\Phi^\dagger D^\mu\Phi + \tfrac{1}{4}\tilde{F}_{\mu\nu}\tilde{F}^{\mu\nu} + V(\Phi)\right], \tag{2.3.3}$$

where the potential is

$$V(\Phi) = \frac{1}{4}\lambda\left(\Phi^\dagger\Phi - \eta^2\right)^2, \tag{2.3.4}$$

matching (2.1.1) up to a numerical prefactor. The fields in the theory are the complex Higgs field Φ, with two degrees of freedom, and the massless gauge field

A_μ, with field strength $\tilde{F}_{\mu\nu}$, and two degrees of freedom. The covariant derivative is $D_\mu = \nabla_\mu + ieA_\mu$, and the action is invariant under the U(1) gauge transformation

$$A_\mu(x) \to A_\mu(x) - \partial_\mu \alpha(x)\,, \tag{2.3.5}$$

$$\phi(x) \to e^{ie\alpha(x)}\phi(x). \tag{2.3.6}$$

It is useful to express the theory in terms of the physical degrees of freedom in the broken symmetric phase. Using the radial decomposition for the Higgs field, we extract these degrees of freedom as

$$\Phi(x^\alpha) = \eta X(x^\alpha) e^{i\chi(x^\alpha)}\,, \tag{2.3.7}$$

$$A_\mu(x^\alpha) = \frac{1}{e}\big[P_\mu(x^\alpha) - \nabla_\mu \chi(x^\alpha)\big]\,, \tag{2.3.8}$$

where X is the massive Higgs boson, χ is the Goldstone boson, and P_μ is the massive gauge boson. In terms of these fields, the Lagrangian becomes

$$\mathcal{L} = -\eta^2 \nabla_\mu X \nabla^\mu X - \eta^2 X^2 P_\mu P^\mu - \frac{1}{4e^2} F_{\mu\nu}F^{\mu\nu} - \frac{\lambda\eta^4}{4}(X^2-1)^2\,, \tag{2.3.9}$$

thus it is explicit that the Goldstone degree of freedom has been removed from the theory, and the gauge boson has obtained a mass. Namely, we now have a massive Higgs field with one degree of freedom, and a massive gauge boson with three degrees of freedom. Note that although we are casting the theory in terms of the dynamical variables in the broken phase, we do not set $X = 1$ which would amount to the Higgs field being in the true vacuum, as for a vortex, X has a spatial profile from the metastable vacuum in the core of the string out to the true vacuum at some distance away from the core. This is most unlike the topologically trivial Higgs theory, where the symmetric phase and broken symmetric phase do not exist simultaneously.

In terms of these variables, the equations of motion are

$$\nabla_\mu \nabla^\mu X - P_\mu P^\mu X - \frac{\lambda\eta^2}{2} X(X^2-1) = 0\,, \tag{2.3.10}$$

$$\nabla_\mu F^{\mu\nu} - \frac{X^2 P^\nu}{\beta} = 0\,, \tag{2.3.11}$$

where $\beta = \lambda/2e^2$ is the Bogomol'nyi parameter [108], and $F_{\mu\nu}$ is the field strength of P_μ.

The inverse masses of the Higgs and gauge bosons determine the width of the scalar and magnetic core of the string respectively. These widths are

$$w_H = m_H^{-1} \equiv \frac{1}{\sqrt{\lambda}\eta}\,, \qquad w_g = m_g^{-1} \equiv \frac{1}{\sqrt{2}e\eta}\,. \tag{2.3.12}$$

In general, the two cores have different widths, and the ratio determines whether the vortex is type I, II, or supersymmetric (Bogomolnyi limit, [108]).

2.4 The Nielsen–Olesen vortex

The Nielsen-Olesen vortex [77] is the simplest topologically non-trivial solution of the Abelian Higgs system. It represents a static, cylindrically symmetric vortex solution in flat space, where the core of the vortex is aligned with the z-axis. Therefore, the four dimensional problem can be reduced to determining the profiles of the fields in the $\{r, \varphi\}$ plane, where symmetry restricts them to depend on the radial direction only, and then extending these trivially along the z-direction. In the plane, the gauge field has two components, A_r and A_φ. For the Nielsen-Olesen solution, the gauge field has only one component, A_φ, which gives rise to a constant magnetic field in the z-direction. While this is all that is required for the static straight vortex, starting with both components, rotational invariance implies that

$$\partial_\varphi A_r = \partial_\varphi A_\varphi = 0\,, \tag{2.4.13}$$

therefore one may always perform an r-dependant gauge transformation to set A_r to zero, without introducing any dependence upon φ.

Working with the degrees of freedom in the broken symmetric phase, the Nielsen–Olesen vortex solution may be expressed in cylindrical polar coordinates by the fields

$$X = X_0(R)\,, \qquad P_\mu = nP_0(R)\,\partial_\mu\varphi\,, \qquad \chi = n\varphi\,, \tag{2.4.14}$$

where $R = r\sqrt{\lambda}\eta$ is a rescaled radial coordinate, and n is the winding number of the string. The functions X_0 and P_0 satisfy the vortex equations (2.3.10) and (2.3.11), which for $n = 1$ become

$$-X_0'' - \frac{X_0'}{R} + \frac{X_0 P_0^2}{R^2} + \tfrac{1}{2}X_0(X_0^2 - 1) = 0\,, \tag{2.4.15}$$

$$-P_0'' + \frac{P_0'}{R} + \frac{X_0^2 P_0}{\beta} = 0\,. \tag{2.4.16}$$

One must now specify boundary conditions which capture the effects of the non-trivial topology, namely that there is finite energy trapped in the core that cannot dissipate to the vacuum which surrounds it. For the Higgs field Φ, we then require that it vanishes in the core and lies in vacuum at spatial infinity. These conditions are met if $X(0) = 0$ and $X(\infty) = 1$, for then $\Phi(0) = 0$ and $|\Phi(\infty)| = \eta$. For the gauge field A_μ we have

$$A_\varphi \equiv \frac{1}{e}\big[P_\varphi - \nabla_\varphi \chi\big] = \frac{1}{e}\big[P_0(R) - 1\big]\,, \tag{2.4.17}$$

where we require that $A_\varphi(0) = 0$ for the energy of the vortex to be finite in the core. Therefore, we set $P_0(0) = 1$. Finally, in order for the energy of the vortex to be minimised at spatial infinity, we require that $P_0(\infty) = 0$. Then all the terms in the Lagrangian (2.3.9) vanish individually, and the true vacuum state for all fields is attained. If instead the Higgs field were to be in vacuum at spatial infinity but $P_0(\infty) \neq 0$, one would be able to measure energy arbitrarily far away from the vortex, implying that its total energy is infinite.

With these boundary conditions, the solutions to the Nielsen–Olesen equations (2.4.15) must be found numerically. However, the fields do admit the following asymptotic behaviour:

$$\begin{aligned} X_0(R \to \infty) &= \begin{cases} 1 - x_\infty \frac{e^{-R}}{\sqrt{R}}, & \text{for } \beta \lesssim 4. \\ 1 - p_\infty^2 \frac{\beta e^{-2R/\sqrt{\beta}}}{R(\beta - 4)}, & \text{for } \beta > 4\,, \end{cases} \\ P_0(R \to \infty) &= p_\infty \sqrt{R} e^{-R/\sqrt{\beta}} \end{aligned} \tag{2.4.18}$$

where p_∞ and x_∞ are constants of $\mathcal{O}(1)$. Therefore we see that the fields fall off exponentially fast to the vacuum state.

Figure 2.4 displays the numerically obtained profiles of X_0 and P_0 for the case of $\beta = 1$. We see that the fields are highly localized around $R = 0$, as expected from their asymptotic behaviour.

So far, we have considered the vortex to be a probe configuration in a flat background. However, we know that it is composed of energy, therefore we should consider its gravitational effects. To couple the Abelian-Higgs system to gravity, we

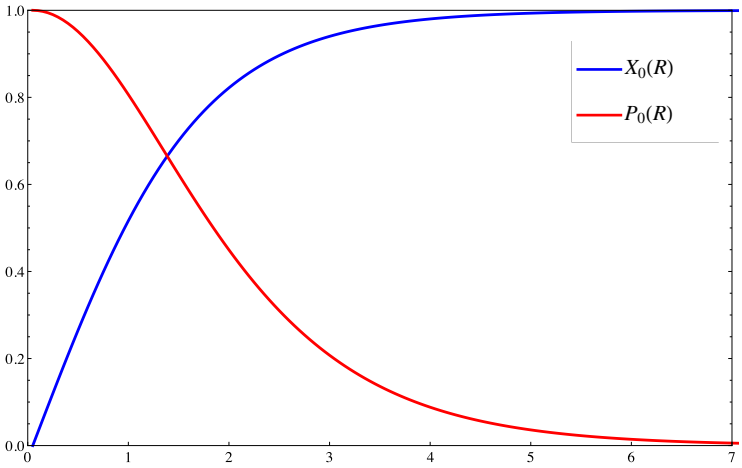

Figure 2.4: Numerical solution of the Nielsen-Olesen vortex: X_0 (blue) and P_0 (red).

may write the total action as

$$S = \frac{1}{2\kappa}\int \sqrt{-g}Rd^4x + \int \sqrt{-g}\mathcal{L}d^4x\,, \tag{2.4.19}$$

where $\mathcal{L}$ is given by (2.3.9). Setting the Higgs mass to unity, $\lambda\eta^2 = 1$, the Einstein equation takes the form

$$R_{\mu\nu} - \frac{1}{2}R\,g_{\mu\nu} = \kappa\eta^2\,T_{\mu\nu}\,, \tag{2.4.20}$$

where the energy-momentum tensor for the vortex is

$$T_{\mu\nu} = -2\nabla_\mu X\nabla_\nu X - 2X^2P_\mu P_\nu - 2\beta\,F_{\mu\sigma}F^\sigma_\nu - \mathcal{L}g_{\mu\nu}\,. \tag{2.4.21}$$

Thus we see that the gravitational coupling of the vortex is determined by

$$\epsilon \equiv 8\pi\,G\eta^2\,, \tag{2.4.22}$$

which will typically be of order $10^{-7} - 10^{-12}$ for cosmic strings of cosmological relevance.

To compute the gravitational effect of the string, we will therefore use a perturbative technique, where we expand the Ricci curvature to first order in ϵ as

$$R_{\mu\nu} \to R_{\mu\nu} + \delta R_{\mu\nu}\,, \tag{2.4.23}$$

where $\delta R_{\mu\nu}$ is linear in ϵ. We will solve the Einstein equations in trace-reversed form, namely

$$R_{\mu\nu} = \epsilon\Big(T_{\mu\nu} - \frac{1}{2}Tg_{\mu\nu}\Big)\,. \tag{2.4.24}$$

At zeroth order in ϵ, the Einstein equations are then just the vaccum equations,

$$R_{\mu\nu} = 0\,. \tag{2.4.25}$$

At linear order on the other hand, they become

$$\delta R_{\mu\nu} = \epsilon\Big(T_{\mu\nu} - \frac{1}{2}T g_{\mu\nu}\Big)\,, \tag{2.4.26}$$

therefore the energy momentum of the flat-space vortex gives rise to a gravitational correction to the curvature at linear order in ϵ.

We will therefore solve the Einstein equations up to linear order in ϵ, where the energy-momentum tensor is built from the Nielsen–Olesen fields.

To compute these leading order corrections to the curvature, we need to select a convenient set of coordinates, which reflect the axial symmetry of the vortex. An appropriate set is the Weyl system, with metric

$$ds^2 = -e^{2\lambda}dt^2 + e^{2(\nu-\lambda)}\left[dz^2 + dR^2\right] + \alpha^2 e^{-2\lambda}d\varphi^2\,. \tag{2.4.27}$$

The Ricci curvature is

$$\sqrt{-g}(R^t_t + R^\varphi_\varphi) = \alpha''\,, \tag{2.4.28}$$

$$\sqrt{-g}R^t_t = [\alpha\lambda']'\,, \tag{2.4.29}$$

$$\sqrt{-g}R^z_z = [\alpha(\nu-\lambda)']'\,, \tag{2.4.30}$$

$$\sqrt{-g}R^R_R = \alpha'' + \alpha(\nu''-\lambda'') - \alpha'(\lambda'+\nu') + 2\alpha\lambda'^2\,, \tag{2.4.31}$$

where $\sqrt{-g} = \alpha\, e^{2(\nu-\lambda)}$ and for the background vacuum spacetime, $\alpha = R$ and $\lambda = \nu = 0$. The components of the energy-momentum tensor (2.4.21) are given by

$$T^t_t = T^z_z = X_0'^2 + \frac{X_0^2P_0^2}{R_0^2} + \beta\frac{P_0'^2}{R^2} + \frac{1}{4}(X^2-1)^2 = \mathcal{E}\,, \tag{2.4.32}$$

$$T^R_R = -X_0'^2 + \frac{X_0^2P_0^2}{R^2} - \beta\frac{P_0'^2}{R^2} + \frac{1}{4}(X_0^2-1)^2 = -\mathcal{P}_R\,, \tag{2.4.33}$$

$$T^\varphi_\varphi = X_0'^2 - \frac{X_0^2P_0^2}{R^2} - \beta\frac{P_0'^2}{R^2} + \frac{1}{4}(X_0^2-1)^2 = -\mathcal{P}_\varphi\,. \tag{2.4.34}$$

Due to the fact that $T^t_t = T^z_z$ in the above, we can see immediately that $R^t_t = R^z_z$ and thus we deduce that $\nu = 2\lambda$, up to a possible constant.

To compute the leading order correction to α, we see from (2.4.28) that we simply need to solve

$$\frac{\alpha''}{R} = -\epsilon(\mathcal{E} - \mathcal{P}_R), \tag{2.4.35}$$

leading to

$$\alpha = R - \epsilon \int\int R(\mathcal{E} - \mathcal{P}_R) dR \tag{2.4.36}$$

$$= \left[1 - \epsilon \int R(\mathcal{E} - \mathcal{P}_R) dR\right] R + \epsilon \int R^2(\mathcal{E} - \mathcal{P}_R) dR\,, \tag{2.4.37}$$

where we have integrated by parts to obtain the second line.

Turning to λ, for which the background value vanishes, (2.4.29) yields

$$\lambda'' + \frac{\lambda'}{R} = \frac{\epsilon}{2}(\mathcal{P}_R + \mathcal{P}_\varphi)\,, \tag{2.4.38}$$

which is solved by

$$\lambda = \frac{\epsilon}{2} \int \frac{1}{R} \int R(\mathcal{P}_R + \mathcal{P}_\varphi) dR\,. \tag{2.4.39}$$

Then, using the equations of motion for X_0 and P_0, one can show that

$$\frac{d}{dR}(R\mathcal{P}_R) = \mathcal{P}_\varphi\,, \tag{2.4.40}$$

and upon inserting this identity into (2.4.39) and integrating by parts, we find

$$\lambda = \frac{\epsilon}{2} \int R\mathcal{P}_R dR\,. \tag{2.4.41}$$

Inserting (2.4.41) into (2.4.30) then yields $\nu = 2\lambda$.

We will now demonstrate that these corrections to the flat-space metric functions give rise to an asymptotically conical spacetime. As can be seen from the asymptotic behaviour of the fields, X_0 and P_0 fall off rapidly to their constant vacuum values outside of the core, and indeed from figure 2.4 we see they have already settled into the vacuum state at a radial distance of $R < \mathcal{O}(10)$. Thus the integrals in the metric functions above converge rapidly to their asymptotic, constant values. Let us then define these constant forms of the integrals as

$$\epsilon \int R(\mathcal{E} - \mathcal{P}_R) dR \equiv A, \quad \epsilon \int R^2(\mathcal{E} - \mathcal{P}_R) dR \equiv B, \quad \epsilon \int R\mathcal{P}_R dR \equiv C, \tag{2.4.42}$$

such that asymptotically,

$$\alpha \to R(1 - A + B/R), \quad \lambda = 2\nu \to C. \tag{2.4.43}$$

The asymptotic form of the metric then becomes

$$ds^2 = e^C[-dt^2 + dR^2 + dZ^2] + R^2(1 - A + B/R)^2 e^{-C} d\varphi^2, \tag{2.4.44}$$

and upon a rescaling of the coordinates such that $\tilde{t} = e^{C/2}t$, $\tilde{z} = e^{C/2}z$ and $\tilde{R} = e^{C/2}(R + B/(1 - A))$, the conical nature of the metric is made explicit,

$$ds^2 = -d\tilde{t}^2 + d\tilde{R}^2 + d\tilde{z}^2 + \tilde{R}^2(1 - A)^2 e^{-2C} d\varphi^2 \tag{2.4.45}$$

where we may write $g_{\varphi\varphi}$ to linear order as

$$\tilde{R}^2(1 - (A + C))^2 \,. \tag{2.4.46}$$

This gives a conical deficit angle in the azimuthal direction which may be expressed as

$$\Delta = 2\pi(A + C) = 2\pi\epsilon \int R\mathcal{E} dR = 8\pi G\mu \,, \tag{2.4.47}$$

where μ is the energy per unit length of the string.

We see then that radial stresses $\mathcal{P}_R$ do not contribute to the deficit angle, as the sum of A and C cancels them out. However, they may lead to a red or blue-shifting of spacetime at infinity relative to the core of string, as the values of the integrals are different in these regions. For the so-called Bogomolyni limit for $\beta = 1$, one may write the vortex equations succintly as

$$X_0' = \frac{X_0 P_0}{R} \,, \qquad P_0' = \frac{R}{2}\Big(X_0^2 - 1\Big) \,, \tag{2.4.48}$$

and one can easily show that the radial stresses vanish identically.

To summarise, we see that an isolated, self-gravitating vortex affects the ambient spacetime around it by asymptotically inducing a conical deficit angle in the azimuthal direction.

The physical effect is that photons travelling around the string from a distant source will not experience a gravitational attraction towards the string, as locally the spacetime around the string is Minkowskian, however, due to the global properties of the spacetime which is conical, such photons will form two images on either side of the string due to gravitational lensing [72, 78]. Thus the presence of a cosmic string may be distinguished observationally by a gravitational lensing signature.

2.5 Strings and black holes

In addition to defects, the universe contains other exotic, classical objects, most notably black holes. It is interesting then to examine how these objects might interact with one another. Indeed, as galaxies are believed to host supermassive black holes in their centres, if a vortex were to drift into a galaxy it would no doubt soon come into contact with a black hole.

In Section 1.1.2 we briefly discussed the black hole "no hair" conjecture. To summarise the discussion therein, the idea is that the only long-range information that a black hole can support is its mass M, charge Q, and angular momentum J. While all else is believed to be destroyed or lost during the accretion process, these particular properties cannot be destroyed because they correspond to conserved quantities associated with the exact symmetries of the spacetime. Therefore, the only allowable black hole spacetimes are the Kerr-Newman family, no other charge or new parameter can be associated with a black hole.

To show that the conjecture is false, one simply has to provide a counter-example. Taking black hole hair to then refer to a long-range, stable property or charge of the black hole spacetime[2], we will see shortly that hair in this very sense can indeed arise when a vortex pierces through a black hole.

The history of vortices and black holes cohabiting the same spacetime began with a study of the gravitational impact of an infinitely thin string threading through a black hole [80], however the first example of a realistic, finite-width string threading through a black hole was given in [83, 84]. We will review some aspects of this work in Section 2.5.1. These early studies were later generalised to the case of a vortex ending on a black hole [85–88], as well as to spacetimes containing positive and negative cosmological constants [89–91]. When the charged black hole case was considered, it was discovered that such a black hole exhibits a phenomenon known

[2]Sometimes the no-hair theorems are taken to mean that a black hole cannot support a non-trivial field configuration on the event horizon. However, this has turned out to be too restrictive, and indeed many physically interesting field configurations have in fact been studied in the literature. See for example [99–105].

as flux-expulsion [92–96], more commonly referred to as the Meissner effect. This interesting effect will be reviewed in Section 2.5.2. However, the rotating black hole case remained elusive, as the conventional field ansatz for the vortex seemed to be inconsistent with angular momentum, while at the same time, the conventional conical gravitational effect of the string, in the presence of rotation, seemed to lead to a divergence of energy-momentum [97].

Understanding the behaviour of vortices in rotating spacetimes is a primary focus of the research which is detailed in this thesis. We will return to this topic in Chapters 3 and 4.

2.5.1 Vortex in a Schwarzschild spacetime

We will first consider the simplest species of black hole, namely the Schwarzschild family. We will review the work of [83], in which it is conclusively demonstrated that a vortex can coexist in a state of static equilibrium with a Schwarzschild black hole, where the vortex pierces through the poles of black hole, and does not become accreted by the black hole. As a stable, long-range field configuration in a black hole spacetime, the vortex amounts to a "property" of the black hole that is measurable at spatial infinity, therefore it qualifies as genuine black hole *hair*. This is confirmed by the fact that the parameters associated with the presence of the vortex, namely the masses of the Higgs field and gauge field, cannot be absorbed into the one parameter that characterises the Schwarzschild black hole, its mass M.

Corresponding to the three parameters of the Schwarzschild vortex spacetime are three length scales, the width of the scalar core w_H, the width of the gauge core, w_g, and the black hole horizon radius,

$$r_+ = 2GM\,. \tag{2.5.49}$$

To obtain the field profiles for the composite vortex and black hole system, one follows the same protocol as for the Nielsen–Olesen vortex, and solves the vortex equations on the background spacetime, treating the vortex as a probe. This approach is sensible because as we have seen, the gravitational effect of the vortex is given by the parameter ϵ, which is very small for physical cosmic strings.

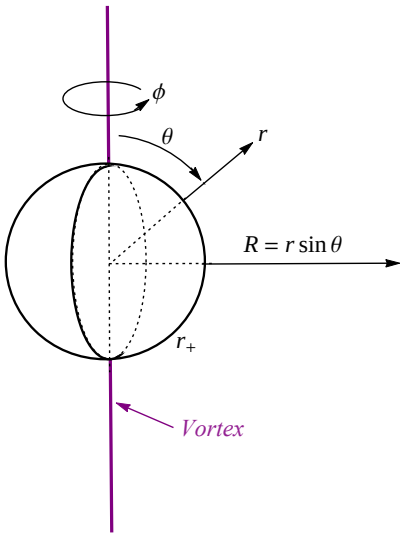

Figure 2.5: A vortex piercing a Schwarzschild black hole, illustrating the alignment of the two objects.

We once again consider the vortex to be static and cylindrically symmetric, however the background is spherically symmetric. Thus the ordinary differential equations that arose for the Nielsen-Olesen vortex become partial differential equations in the Schwarzschild context. The Schwarzschild metric is

$$ds^2 = -\Big(1-\frac{2GM}{r}\Big)dt^2 + \Big(1-\frac{2GM}{r}\Big)^{-1}dr^2 + r^2(d\theta^2+\sin^2\theta d\phi^2)\,. \qquad (2.5.50)$$

In this background, the vortex equations (2.3.10)-(2.3.11) become

$$\begin{aligned} &-\Big(1-\frac{r_+}{r}\Big)X_{,rr} - \frac{2r-r_+}{r^2}X_{,r} - \frac{X_{,\theta\theta}}{r^2} - \frac{\cot\theta X_{,\theta}}{r^2} + \frac{1}{2}X(X^2-1) + \frac{XP_\phi^2}{r^2\sin^2\theta} = 0\,,\\ &\Big(1-\frac{r_+}{r}\Big)\,\partial_r\partial_r P_\phi + \frac{1}{r^2}\partial_\theta\partial_\theta P_\phi + \frac{r_+}{r^2}\partial_r P_\phi - \frac{\cot\theta}{r^2}\partial_\theta P_\phi - \frac{X^2P_\phi}{\beta} = 0\,, \end{aligned} \qquad (2.5.51)$$

In order to proceed analytically, we may then approximate the width of the string as being very small compared to the radius of curvature of the event horizon. This is the "thin string" limit. Having set the Higgs mass to unity, this limit implies that $r_+ \gg 1$. Furthermore, we will restrict ourselves to the region within and very near to the core of the vortex, as we expect the fields to fall off rapidly to their vacuum values, based on the behaviour of the vortex in flat space. These simplifcations mean that we are in a regime where the curvature is not significantly felt by the vortex fields as they fall from the core to their vacuum values. Within these limits, we

thus expect the Schwarzschild vortex to closely resemble the Nielsen-Olesen vortex, which depends only upon the radial direction in cylindrical coordinates. Thus we may try an ansatz of the form

$$X = X_0(R)\,, \quad P_\phi = P_0(R)\,, \quad R \equiv r\sin\theta \tag{2.5.52}$$

where X_0 and P_0 are the Nielsen-Olesen fields, and R is the radial distance that is orthogonal to the axis of the vortex in Schwarzschild coordinates (see figure 2.5 for a depiction). With this ansatz, the vortex equations become

$$-X_0'' - \frac{X_0'}{R} + \frac{1}{2}X_0(X_0^2-1) + \frac{X_0 P_0^2}{R_0^2} + \frac{r_+\sin^2\theta}{r}\Big(X_0'' + \frac{X_0'}{R}\Big) = 0\,, \tag{2.5.53}$$

$$P_0'' - \frac{P_0'}{R} - \frac{X_0^2 P_0}{\beta} + \frac{r_+\sin^2\theta}{r}\Big(-P_0'' + \frac{P_0'}{R}\Big) = 0\,. \tag{2.5.54}$$

We see then that the Schwarzschild vortex equations have a very good approximate solution of the form (2.5.52), as long as $\frac{r_+}{r}\sin^2\theta \ll 1$. Now, since $r\sin\theta = R \sim \mathcal{O}(1)$ in (and very near to) the core of the vortex, $\sin\theta \sim \mathcal{O}(1/r)$. Therefore the corrections are $\mathcal{O}(r_+/r^3) < \mathcal{O}(1/r_+^2) \ll 1$ for the thin string limit.

For the thin, probe vortex, we see that the fields do not mind touching the event horizon of a black hole, indeed the presence of the horizon is a higher-order effect that can be suitably diluted away. While one may suspect this to be a mere artefact of the thin string limit, full numerical solutions also suggest that the vortex remains largely indifferent to the presence of the horizon. Figure 2.6 depicts the numerical solution for a vortex piercing through a black hole of mass $GM = 5$. The morphology of the vortex seems unaffected by the black hole, indeed the contour lines remain very straight as they approach and intersect the horizon.

While the probe vortex has no apparent problem in piercing the horizon, this can become a more delicate issue when the energy of the vortex is taken into account. For a stable and static solution, the vortex should not disturb the structure of the horizon, a null surface which is free of shear stresses. We saw in (2.4.32) that for the flat-space vortex, the energy and the tension along the core balance each other, $T^z_z = T^t_t$. This means that as the core touches the horizon at $\theta = 0$ and π, the horizon feels no energy-momentum and thus is undisturbed. However, the physical vortex is not infinitely thin, therefore one must address what happens at the horizon

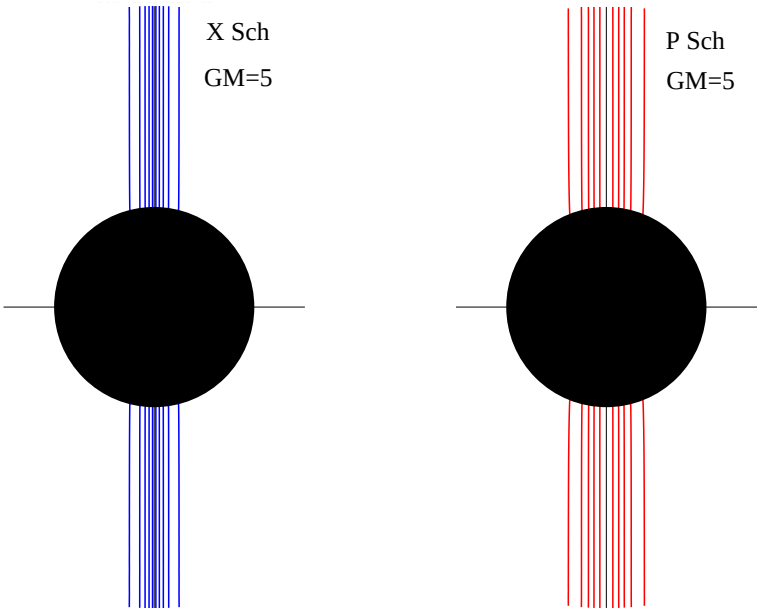

Figure 2.6: The equipotentials of the vortex in the Schwarzschild background. The Higgs contours are in blue, and the P_ϕ contours are in red. In each case contours are shown for $X, P_\phi = 0.1, 0.3, 0.5, 0.7, 0.9$.

as we move off of the poles. In fact, the authors of [83] were able to show that this same balance is also maintained on the horizon, therefore there is no backreaction as the vortex touches the null surface, and no obstruction, in this sense, to it remaining there in a static fashion.

So then, what happens gravitationally when a string sits through a Schwarzschild black hole? We saw in Section 2.4 above that the presence of the vortex in flat space induces a conical effect in the azimuthal direction. Considering the case of an infinitely thin vortex, the metric for the string and black hole system becomes [80]

$$ds^2 = -\left(1-\frac{2GM}{r}\right)dt^2+\left(1-\frac{2GM}{r}\right)^{-1}dr^2+r^2d\theta^2+r^2(1-4G\mu)^2\sin^2\theta d\phi^2\,, \quad (2.5.55)$$

namely, a conical deficit angle is removed from the azimuthal direction in the Schwarzschild spacetime. The authors of [83] demonstrated conclusively that the geometry described by (2.5.55) does indeed correspond to the infinitely-thin string limit of a physical vortex piercing through a Schwarzschild black hole.

2.5.2 Flux expulsion in Reissner-Nordstrom

As with the Schwarzschild black hole, the vortex has no trouble entering into a state of static equilibrium with the charged black hole, where it pierces through the poles of the black hole. A very important difference between the two cases is that the Reissner-Nordstrom black hole admits two horizons r_+ and r_-, which coincide only in the extremal limit. In the context of extremality, a very interesting effect arises for the vortex: if the black hole is small enough, then instead of piercing through it, the flux lines of the vortex sweep over the horizon and regroup again at the other side. This phenomenon is known as flux expulsion, or the Meissner effect. Rather than doing so exclusively at the poles, the fields in the flux-expelling state remain in their metastable vacuum states, $X = 0$, $P = 1$, across the full two-dimensional surface of the extremal horizon, and fall to the vacuum only away from the horizon. Therefore, the gauge field is long-range all across the horizon, allowing the corresponding magnetic flux lines to engulf it.

Energetically, this implies that there are regimes in which it is favourable for the fields approaching the black hole along the z-direction to veer off track and avoid the black hole. We will return to the physics of the flux-expelled state in Chapter 4 when we discuss rotating black holes.

An analytic proof for the existence of expulsion for low mass black holes, as well as a derivation of the precise bounds on the mass required for this phenomenon, was presented in [95], and we will now review their work. Therefore, we will leave the physics aside for now, and look in detail at the mathematics underlying this phenomenon.

As is reviewed in Section 1.1.2, the Reissner-Nordstrom geometry is described by the metric

$$ds^2 = -\frac{\Delta}{r^2}dt^2 + \frac{r^2}{\Delta}dr^2 + r^2[d\theta^2 + \sin^2\theta d\phi^2], \tag{2.5.56}$$

where $\Delta = r^2 - 2mr + q^2 = (r - r_+)(r - r_-)$, and q is proportional to the charge of the black hole. For extremal black holes the inner and outer horizons coincide, and thus the metric function Δ has a double root, $\Delta = (r - r_+)^2$, leading to the vanishing of Δ as well as Δ' on the horizon.

The vortex field equations in the Reissner-Nordstrom background read

$$-\frac{1}{r^2}\partial_r(\Delta X_{,r}) - \frac{1}{r^2\sin\theta}\partial_\theta(\sin\theta X_{,\theta}) + \frac{XP_\phi^2}{r^2\sin^2\theta} - \frac{1}{2}X(1-X^2) = 0\,, \quad (2.5.57)$$

$$\partial_r\left(\frac{\Delta}{r^2}\partial_r P_\phi\right) + \frac{\sin\theta}{r^2}\partial_\theta\left(\frac{\partial_\theta P_\phi}{\sin\theta}\right) - \frac{X^2P_\phi}{\beta} = 0\,. \quad (2.5.58)$$

To study flux expulsion we need to look at the fields on, and in the close vicinity of, the extremal horizon r_+. We therefore expand the fields near the horizon as

$$X = \xi_0(\theta) + (r-r_+)\xi_1(\theta)\,, \quad P_\phi = \pi_0(\theta) + (r-r_+)\pi_1(\theta)\,, \quad (2.5.59)$$

where ξ_1 and π_1 are bulk fields. With these expansions, we see that due to the fact that $\Delta' = \Delta = 0$, the horizon equations in fact decouple from the exterior geometry, yielding

$$\begin{aligned} \xi_0'' + \cot\theta\xi_0' - \frac{\xi_0\pi_0^2}{\sin^2\theta} + \frac{r_+^2}{2}\xi_0(1-\xi_0^2) = 0\,, \\ \pi_0'' - \cot\theta\pi_0' - \frac{r_+^2}{\beta}\xi_0^2\pi_0 = 0\,. \end{aligned} \quad (2.5.60)$$

The constraints on the field are that they must be in the unstable vacuum state in the core, $\xi_0 = 0, \pi_0 = 1$ for $\theta = 0, \pi$, and they must be symmetric around $\pi/2$. It is then obvious that the flux-expelled state, $\xi_0(\theta) = 0$ and $\pi_0(\theta) = 1\ \forall\,\theta \in (0,\pi)$, solves the horizon equations[3], regardless of the value of r_+ and hence of the black hole mass. However, it must be demonstrated that this solution extends to the bulk. Following the argument in [95] closely, we see that this is only possible for horizon radii below a certain critical value, $r_+ < r_c$.

To find the value of r_c, let us suppose that expulsion occurs, therefore on the horizon, $X \equiv 0$ and $P_\phi \equiv 1$, with X increasing and P_ϕ decreasing towards their vacuum values away from the horizon. Now consider a region very close to the horizon such that $X^2 \ll 1$, $P < 1$, and $\partial_r(\Delta X_{,r}) > 0$. Then from (2.5.57) we see that

$$X > XP_\phi^2 > \sin\theta\partial_\theta(\sin\theta X_{,\theta}) + \frac{1}{2}r_+^2\sin^2\theta X\,. \quad (2.5.61)$$

[3]Note that for a Schwarzschild black hole, for which $\Delta' \neq 0$ on the horizon, the bulk quantities ξ_1 and π_1 would appear in the horizon equations, thus the flux expelled solutions $\xi_0 = 0$, $\pi_0 = 1$ obviously would not solve the horizon equations. Therefore we see that the double root structure of Δ, namely the existence of an extremal limit, is crucial for flux-expelled states to arise.

This condition must hold for a flux-expelled solution. Now, since $\sin\theta = 0$ at $\theta = 0$ and $X_{,\theta} = 0$ at $\theta = \pi/2$ where it reaches its maximum value, the product $\sin\theta X_{,\theta} = 0$ at $\theta = 0, \pi/2$. In addition, it is positive for small θ, as both X and $\sin\theta$ are increasing. Therefore, its derivative must have at least one zero on $(0, \pi/2)$. Let us then define $\theta_0 < \pi/2$ as the first value of θ at which $\partial_\theta(\sin\theta X_{,\theta}) = 0$. From (2.5.61) we then find that

$$\frac{1}{2} r_+^2 \sin^2\theta_0 < 1\,, \tag{2.5.62}$$

which is manifestly true for $r_+ < \sqrt{2}$.

Let us now consider a larger black hole with $r_+ > \sqrt{2}$, and define $\alpha > \theta_0$ by $r_+^2 \sin^2\alpha = 2$. Then, integrating (2.5.61) on the range $(\theta, \pi/2)$, for $\theta > \alpha$ gives

$$X_{,\theta}(\theta) > \frac{1}{\sin\theta}\int_\theta^{\pi/2} d\theta' X(\theta')\left(\frac{r_+^2}{2}\sin\theta' - \frac{1}{\sin\theta'}\right) > \frac{X(\theta)}{\sin\theta}\int_\theta^{\pi/2} d\theta'\left(\frac{r_+^2}{2}\sin\theta' - \frac{1}{\sin\theta'}\right)\,,$$

where we have obtained a lower bound on the integral by using the fact that $X(\theta) < X(\theta')$. This gives

$$X_{,\theta}(\theta) > X(\theta)\left[\frac{r_+^2}{2}\cot\theta + \frac{\ln\tan(\theta/2)}{\sin\theta}\right]\,. \tag{2.5.63}$$

We can further bound this expression by using the fact that because $\partial_\theta(\sin\theta X_{,\theta}) = \cos\theta X_{,\theta} + \sin\theta X_{,\theta\theta} = 0$ at θ_0 and < 0 on $(\theta_0, \pi/2]$, $X_{,\theta\theta} < 0$ on $[\theta_0, \pi/2]$ and hence $X_{,\theta}(\theta) < \frac{X(\theta)-X(\alpha)}{\theta-\alpha} < \frac{X(\theta)}{\theta-\alpha}$, leading to

$$1 > (\theta - \alpha)\left[\frac{\cot\theta}{\sin^2\alpha} + \frac{\ln\tan(\theta/2)}{\sin\theta}\right] \tag{2.5.64}$$

over the range $\theta \in (\alpha, \pi/2)$. One finds this is violated for $r_+^2 > 8.5$. Hence for $r_+ \geq \sqrt{8.5} \approx 2.92$ the vortex must pierce the horizon. This gives us an upper bound on r_c.

We can in fact also derive a lower bound on r_+. We know that flux expulsion is always a solution on the horizon. Therefore, to find this lower bound, we will instead assume that a piercing solution exists for equations (2.5.60), and derive a minimum requirement on r_+ for this solution. Turning this bound around will give the parameter space for which a piercing solution *cannot* exist on the horizon, and thus flux expulsion *must* happen: this will give us the lower bound.

Thus we begin by assuming that a piercing solution exists, namely that ξ_0 and π_0 have non-trivial profiles on the horizon, where ξ_0 increases from its zero value at

the poles to its maximum at the equator, while π_0 decreases from unity at the poles to its minimum value at the equator.

At $\pi/2$, we then have

$$\xi_0'' = \xi_0\pi_0^2 - \frac{r_+^2}{2}\xi_0(1-\xi_0) \leq 0 \Rightarrow \pi_0^2 \leq \frac{r_+^2}{2}(1-\xi_0^2) \leq \frac{r_+^2}{2}\,, \tag{2.5.65}$$

therefore

$$\pi_0'' = \frac{r_+^2}{\beta}\xi_0^2\pi_0 \leq \frac{r_+^3}{\sqrt{2}}\frac{\xi_0^2}{\beta}\sqrt{1-\xi_0^2} \leq \frac{\sqrt{2}}{3\sqrt{3}}\frac{r_+^3}{\beta}\,, \tag{2.5.66}$$

where in the final step we have maximised over ξ_0, with the maximum occurring at $\xi_0 = \sqrt{2/3}$. This gives us an upper bound on π_0'' at the equator. We will now find a lower bound on the same quantity, and later we will match these bounds to obtain the domain in r_+ for which a piercing solution can exist.

From the horizon equations (2.5.60), we see that finiteness requires that $\pi_0'(0) = 0$. Given that $\pi_0'(\pi/2) = 0$ as well, there must exist a θ_0 for which $\pi_0''(\theta_0) = 0$. This is where π_0', which is negative on $(0, \pi/2)$, takes its largest value:

$$\pi_0' = -\tan\theta\Big(\frac{r_+^2}{\beta}\xi_0^2\pi_0 - \pi_0''\Big) \Rightarrow |\pi_0'(\theta_0)| = \tan\theta_0\Big(\frac{r_+^2}{\beta}\xi_0^2\pi_0\Big) \leq \frac{r_+^2}{\beta}\tan\theta_0\,. \tag{2.5.67}$$

Then, we note that the value of π_0 at its minimum must be larger than it would be if π_0 were able to decrease linearly from unity at the poles, with the highest possible slope, which is $|\pi_0'(\theta_0)|$. Thus we may estimate,

$$\pi_0(\pi/2) > 1 - \frac{\pi}{2}|\pi_0'(\theta_0)|\,, \tag{2.5.68}$$

and combining this result with (2.5.66) gives

$$\frac{r_+^2}{2} \geq \pi_0(\pi/2) > 1 - \frac{\pi}{2}|\pi_0'(\theta_0)| \Rightarrow |\pi_0'(\theta_0)| > \frac{2}{\pi}\Big(1 - \frac{r_+^2}{2}\Big)\,. \tag{2.5.69}$$

Then, assuming $r_+ < \sqrt{2}$ such that the bound is meaningful, and using (2.5.67), we obtain

$$\frac{\pi r_+^2}{2\beta\Big(1-\frac{r_+^2}{\sqrt{2}}\Big)} > \cot\theta_0 > \frac{\pi}{2} - \theta_0, \tag{2.5.70}$$

where in the last step we have simply expanded around $\tan(\pi/2 - \theta_0)$. We are now ready to write down a lower bound on $\pi_0''(\pi/2)$. Noting that $\pi_0''(\theta_0) = 0$ where π_0' is

maximally negative, while $\pi_0''(\pi/2) = r_+^2\xi_0^2\pi_0/\beta \geq 0$, we see that π_0'' on $[\theta_0, \pi/2]$ is maximum at the equator, thus

$$\pi_0''(\pi/2) \geq \frac{\pi_0'(\pi/2) - \pi_0'(\theta_0)}{\pi/2 - \theta_0} \;\Rightarrow\; \pi_0''(\pi/2) > \Big(\frac{2}{\pi}\Big)^2 \frac{\beta}{r_+^2}\Big(1 - \frac{r_+}{\sqrt{2}}\Big)^2 . \tag{2.5.71}$$

Combining the bounds, we arrive at

$$\frac{r_+^3}{\beta}\frac{\sqrt{2}}{3\sqrt{3}} \;>\; \pi_0''(\pi/2) \;>\; \Big(\frac{2}{\pi}\Big)^2 \frac{\beta}{r_+^2}\Big(1 - \frac{r_+}{\sqrt{2}}\Big)^2 , \tag{2.5.72}$$

and finally,

$$\frac{\Big(\frac{r_+}{\sqrt{2}}\Big)^5}{\Big(1 - \frac{r_+}{\sqrt{2}}\Big)^2} \;>\; \frac{3\sqrt{3}\beta^2}{2\pi^2} \approx \frac{\beta^2}{4} . \tag{2.5.73}$$

Turning this bound around, we conclude that the flux lines *must* expel if

$$r_c^5/(\sqrt{2} - r_c)^2 \;>\; \beta^2/\sqrt{2} , \tag{2.5.74}$$

which gives $r_c \simeq 0.7$ for $\beta = 1$.

Therefore, following [95], we see that small mass extremal charged black holes can support a Meissner effect. In particular, for $\beta = 1$, the flux can be expelled from the interior of the black hole if

$$0.7 < r_+ < \sqrt{8.5} . \tag{2.5.75}$$

In summary, cosmic strings and black holes can form very interesting systems. From a gravitational point of view, the conical effect of the string can be woven into the deep potential well of the black hole, such that the light from stars and other objects in these wells could potentially exhibit an additional lensing effect due to the presence of the string. From a field theoretic point of view, when a charge is added to the black hole, a new class of phenomena opens up for small mass black holes, in which they may experience two separate phases of cosmic string hair.

While these arguments paint a compelling picture, it remains to be seen whether or not this picture may indeed be realised in natural systems. Most notably, natural, astrophysical black holes are rotating objects, which, as mentioned earlier, turns out to add quite a level of subtlety and complexity to the study of these systems.

Chapter 3

Rotating Black Hole Hair

Astrophysically, black holes are formed when very massive stars collapse under their own gravity. A gravitationally collapsed object can only settle down into a static final state if the collapse is completely spherical, which is very unrealistic for gargantuan, hugely energetic astrophysical objects. Physical black holes are then much more likely to be stationary objects, which are described by the Kerr family of black hole spacetimes, parameterised by M and J.

In this Chapter, we will discuss the possible interacting states of cosmic strings with rotating black holes, therefore we make contact with cosmology. As we have discussed in detail in Section 2.5, previous studies involving static black holes have demonstrated that in these simple cases, vortices and black holes can form stable configurations [83, 95]. While this points to the fact that physical, *videlicet* rotating, black hole vortices could exist in Nature, it turns out that the conventional field ansatz $\{X, P_\phi\}$ is inconsistent with the presence of rotation. This is because the timelike Killing vector is not orthogonal to the spacelike hypersurfaces for a stationary spacetime, indeed, the time and azimuthal directions are mixed.

For the vortex, this implies that the usual azimuthal form of the gauge vector field P_ϕ is coupled to the zeroth component P_t, and the two cannot be considered independently. We will see in what follows that the norm of the gauge boson cannot in fact be finite on the horizon unless a P_t component is present to counter the P_ϕ component. Taking this into account, we will show that a vortex with three non-trivial spatially varying fields, X, P_ϕ and P_t, has the correct structure to form a

stable, composite state with a black hole. We will explore this system in both the nonextremal and extremal cases, and show that a Meissner effect arises for the low mass extremal Kerr vortex. The physics of the phase transition is however quite different to the Reissner-Nordstrom case, once again due to the presence of an additional field required for the description. The presence of P_t leads to a discontinuity between the piercing and expelling phases, such that a first order phase transition takes place, and the black hole bubbles its way down to expulsion as the horizon radius shrinks.

Most interesting, however, is the way in which the non-trivial mixing of t and ϕ expresses itself gravitationally in the Kerr vortex spacetime. We have seen that a self-gravitating vortex induces a conical deficit angle in the azimuthal direction, and that this effect is preserved when one threads the vortex through the centre of a static spacetime. In the stationary case, we will show in what follows that the azimuthal conical effect is itself twisted into the timelike direction by the rotation: the angle that is removed by the string is from the perspective of an azimuthal coordinate that is co-rotating with the black hole. Asymptotic observers therefore see a spacetime in which both the timelike and azimuthal directions, as well as their intersection, are reshaped by a conical effect.

This Chapter is based on the work done in Ref. [98].

3.1 Higgs hair for the Kerr black hole

We begin by expressing the vortex equations in the Kerr geometry, treating the vortex as a probe.

The geometry reads

$$ds^2 = -\frac{\Delta - a^2\sin^2\theta}{\Sigma}dt^2 - \frac{4GMar\sin^2\theta}{\Sigma}dtd\varphi + \Sigma d\theta^2 + \frac{\Gamma}{\Sigma}\sin^2\theta\, d\varphi^2 + \frac{\Sigma}{\Delta}dr^2\,, \qquad (3.1.1)$$

where $a = J/M$ and

$$\Sigma = r^2 + a^2\cos^2\theta\,, \quad \Delta = r^2 - 2GMr + a^2 \qquad \Gamma = (r^2+a^2)^2 - \Delta a^2\sin^2\theta\,. \quad (3.1.2)$$

We will align the vortex in such a way as to respect the symmetries of the spacetime. This means that as with the Schwarzschild and Reissner-Nordstrom cases, the core

of the vortex is aligned along the polar axis of the black hole. The system is thus symmetric with respect to a reflection about the equatorial plane. The string is considered to be straight and extends along the polar axis to spatial infinity, where the ambient spacetime is asymptotically flat.

As we see in the metric (3.1.1), the t and ϕ directions are mixed due to rotation, thus we expect a mixing between the t and ϕ degrees of freedom in the gauge field, as we have discussed. Therefore we consider an ansatz which includes a nonzero P_ϕ *and* P_t. Indeed, inserting an azimuthal gauge field component P_ϕ into the equation for the gauge field (2.3.11), we see that this equation implies that a second component, P_t, is automatically generated:

$$\nabla_\mu F^{\mu\phi} + \frac{X^2 P^\phi}{\beta} = \nabla_\mu g^{\mu\alpha} g^{\phi\beta} F_{\alpha\beta} + \frac{X^2 g^{\phi\alpha} P_\alpha}{\beta} = 0\,. \tag{3.1.3}$$

The vortex equations thus become

$$\begin{aligned}
\frac{X^2}{\beta}P_\phi &= \frac{\Delta}{\Sigma}\partial_r\partial_r P_\phi + \frac{1}{\Sigma}\partial_\theta\partial_\theta P_\phi + \frac{2GM\rho^2}{\Sigma^3}(r^2 - a^2\cos^2\theta)\partial_r P_\phi \\
&\quad -\frac{\cot\theta}{\Sigma^3}(\Sigma^2 + 4GMra^2\sin^2\theta)\partial_\theta P_\phi - \frac{4a^3GMr}{\Sigma^3}\cos\theta\sin^3\theta\partial_\theta P_t \\
&\quad +\frac{2GMa\sin^2\theta}{\Sigma^3}\big[2r^2\Sigma + \rho^2(r^2 - a^2\cos^2\theta)\big]\partial_r P_t\,, \qquad (3.1.4)\\
\frac{X^2}{\beta}P_t &= \frac{\triangle}{\Sigma}\partial_r\partial_r P_t + \frac{1}{\Sigma}\partial_\theta\partial_\theta P_t + \frac{4GMra}{\Sigma^3}\cot\theta\left(\partial_\theta P_\phi + a\sin^2\theta\partial_\theta P_t\right) + \frac{\cot\theta}{\Sigma}\partial_\theta P_t \\
&\quad +\frac{2GMa}{\Sigma^3}(\Sigma - 2r^2)\partial_r P_\phi - \frac{1}{\Sigma^3}\big[2GM(2r^2\rho^2 - a^2\sin^2\theta\Sigma) - 2r\Sigma^2\big]\partial_r P_t\,, \qquad (3.1.5)\\
0 &= \frac{\Delta}{\Sigma}X_{,rr} + \frac{\Delta'}{\Sigma}X_{,r} + \frac{X_{,\theta\theta}}{\Sigma} + \frac{\cot\theta X_{,\theta}}{\Sigma} + \frac{1}{2}X(1 - X^2) + XP_\mu^2\,, \qquad (3.1.6)
\end{aligned}$$

where $\rho^2 = r^2 + a^2$ has been introduced for visual clarity, and the gauge boson norm is

$$P_\mu^2 = \frac{(\rho^2 P_t + aP_\phi)^2}{\Sigma\Delta} - \frac{(P_\phi + a\sin^2\theta P_t)^2}{\Sigma\sin^2\theta}\,. \tag{3.1.7}$$

We now see explicitly why we needed to introduce the P_t field (indeed, this was first noted by Wald [109] who found an expression for constant probe magnetic flux field through a Kerr black hole). For non-vanishing P_ϕ, the P_t equation (3.1.5) does not allow $P_t = 0$ unless $a = 0$. Furthermore, setting $P_t = 0$, the gauge field norm becomes

$$P_\mu^2 = \frac{P_\phi^2}{\Sigma}\Big(\frac{a^2\sin^2\theta - \Delta}{\Delta\sin^2\theta}\Big)\,, \tag{3.1.8}$$

which is divergent on the horizon where $\Delta \to 0$. Therefore, consistency imposes that in a rotating spacetime, the vortex always picks up an extra component, P_t.

3.1.1 Approximate solution

The vortex equations (3.1.4)-(3.1.6) must be solved numerically, however as for the static case, one can search for an approximate analytic solution to these equations, using the flat-space vortex as a blueprint. The idea is that in a suitable limit in which the effects of curvature are largely negligible, the vortex in the black hole spacetime should strongly resemble the flat-space vortex. The corollary in the Kerr case, however, is that in general there will always be a P_t component of the gauge field, as the discussion above implies that the only consistent limit in which $P_t \to 0$ is the limit in which $a \to 0$.

At spatial infinity, the ambient spacetime becomes locally flat and therefore in the limit that one is very far away from the black hole, one can expect the vortex to be well approximated by the flat-space vortex. Indeed, in that case, $a \to 0$ and thus we expect the P_t component of the gauge field to be strongly suppressed. However, this limit is not very interesting as it doesn't capture any of the distinguishing features of the black hole spacetime. As discussed in Section 2.5.1, the other sensible limit which allows one to remain right in the heart of the black hole spacetime, is the limit in which the string width is much smaller than the black hole. In this case, at the scale relevant for the fields to transition from their core to their vacuum values, the effects of curvature are not yet felt, and the horizon appears to be flat as the string touches it.

The Nielsen-Olesen fields depend only upon the radial distance in cylindrical coordinates, namely the distance orthogonal to the core of the vortex. Therefore, in the Kerr case, we can consider the function

$$R = \rho \sin\theta \,, \tag{3.1.9}$$

which gives the radial distance which is orthogonal to the polar axis in Boyer-Lindquist coordinates. For our approximate solution, we will consider the fields to depend upon this precise combination of r and θ.

We will now make further simplifications based on the discussion above. The first is that we will treat the vortex as being much thinner than the black hole horizon r_+. Having set the Higgs mass and thus the core width to unity, this entails that $r_+ \gg 1$. This "thin string limit" implies that $\rho \gg 1$, as the smallest value that ρ can take is when $r = r_+$ and $a = 0$, then $\rho_{min} = r_+ \gg 1$. The second simplification is that we only consider the region within and close to the core of the string, as we can expect the fields to fall off rapidly to their vacuum values outside of the string, based on the behaviour of the vortex in flat space. Thus we consider the region $R < \mathcal{O}(10)$. This implies that $\sin\theta = R/\rho \ll 1$, whereas $\cos\theta \simeq 1$.

Using these simplifications, we can expand the functions Σ and Γ as

$$\Sigma = \rho^2\Big(1 - \frac{a^2R^2}{\rho^4}\Big) \simeq \rho^2\,, \qquad \Gamma = \rho^4\Big(1 - \frac{\Delta a^2R^2}{\rho^6}\Big) \simeq \rho^4\,. \tag{3.1.10}$$

Furthermore, the derivatives become

$$\begin{gathered}\frac{\partial}{\partial r} = \frac{rR}{\rho^2}\frac{d}{dR}\,, \qquad \frac{\partial}{\partial\theta} = \rho\cos\theta\frac{d}{dR} \simeq \rho\frac{d}{dR}\,,\\ \frac{\partial^2}{\partial r^2} = \frac{r^2R^2}{\rho^4}\frac{d^2}{dR^2} + \Big(\frac{R}{\rho^2} - \frac{Rr^2}{\rho^4}\Big)\frac{d}{dR} \simeq \frac{R^2}{\rho^2}\frac{d^2}{dR^2}\,,\\ \frac{\partial^2}{\partial\theta^2} \simeq \rho^2\Big(1 - \frac{R^2}{\rho^2}\Big)\frac{d^2}{dR^2} - R\frac{d}{dR}\,.\end{gathered} \tag{3.1.11}$$

Using these expressions, the derivative operator becomes

$$\frac{\Delta}{\Sigma}\frac{\partial^2}{\partial r^2} + \frac{1}{\Sigma}\frac{\partial^2}{\partial\theta^2} \simeq \Big(1 + \frac{\Delta R^2}{\rho^4}\Big)\frac{d^2}{dR^2} - \frac{R^2}{\rho^2}\frac{d}{dR}\,. \tag{3.1.12}$$

We may now expand equation (3.1.6) for the Higgs field, keeping terms only up to order $\mathcal{O}(r_+^{-2})$, remembering that $\Delta = \mathcal{O}(\rho^2)$ away from the horizon, and $R \simeq \mathcal{O}(1)$. This yields

$$\Big(1 + \frac{\Delta R^2}{\rho^4}\Big)X'' + \Big(1 - \frac{R^2}{\rho^2} + \frac{rR^2\Delta'}{\rho^4}\Big)\frac{X'}{R} + \frac{X}{2}(1 - X^2) + XP_\mu^2\,, \tag{3.1.13}$$

where

$$P_\mu^2 = \frac{\rho^2}{\Delta}P_t^2 + \frac{4GMar}{\rho^2\Delta}P_t\,P_\phi - \frac{P_\phi^2}{R^2}\,. \tag{3.1.14}$$

Comparing this with the equation of motion for the Nielsen-Olesen Higgs field in (2.4.15), we see that at leading order, this equation is solved by fields of the form

$$X \simeq X_0(R)\,, \quad P_\phi \simeq P_0(R)\,, \quad P_t \simeq -\frac{2GMar}{\rho^4}P_0(R)\,, \quad R \equiv \rho\sin\theta. \tag{3.1.15}$$

where to obtain the form of P_t we set the sum of the first two terms in (3.1.14) to zero, so as to obtain the Nielsen–Olesen gauge boson norm at leading order. In figure 3.1, the approximation is compared to the numerical solution for the same values of the parameters. For low mass black holes, the discrepancies between the solutions should become more pronounced, as the thin string limit $r_+ \gg 1$ is then starting to break down. The figure shows black holes with masses just three times the string scale, and still the corrections are only dicernable close to the horizon, where the vortex contour lines of the full solution exhibit slight curvature. Therefore one can appreciate that the approximate solution is in fact only mildly approximate, and is in excellent agreement with the full solution across almost all working scales of the problem.

We see from the figure that the P_t field remains close to the horizon, thus there is no electric field asymptotically far from the black hole. On the other hand, the Higgs field X and gauge field component P_ϕ retain the same behaviour here as they exhibited for the static case.

3.1.2 Numerical solution

We have seen that in the thin string limit, the vortex equations may be solved to leading order by the functions (3.1.15). We would now like to obtain general solutions to these equations. In this case, the fields will no longer be functions of a single combination of r and θ, and the full non-linear coupled system must be solved numerically.

The vortex equations (3.1.4)-(3.1.6) form an elliptic system. To solve them, we implement a gradient flow technique on a two-dimensional polar grid, for which $r \in [r_+, r_\infty]$ and $\theta \in [0, \pi]$. The basic idea is that we begin by assigning a value of each of the three fields to each grid point, using the approximate analytic solutions for the fields, (3.1.15). We then evolve these values using the equations of motion on the grid, and use the result to update the values of the fields at each grid point. We repeat this procedure until the updated values are no longer changing, thus we have reached a steady-state configuration and the equations of motion are satisfied. The principle behind this method is that energy in a non-minimal configuration will

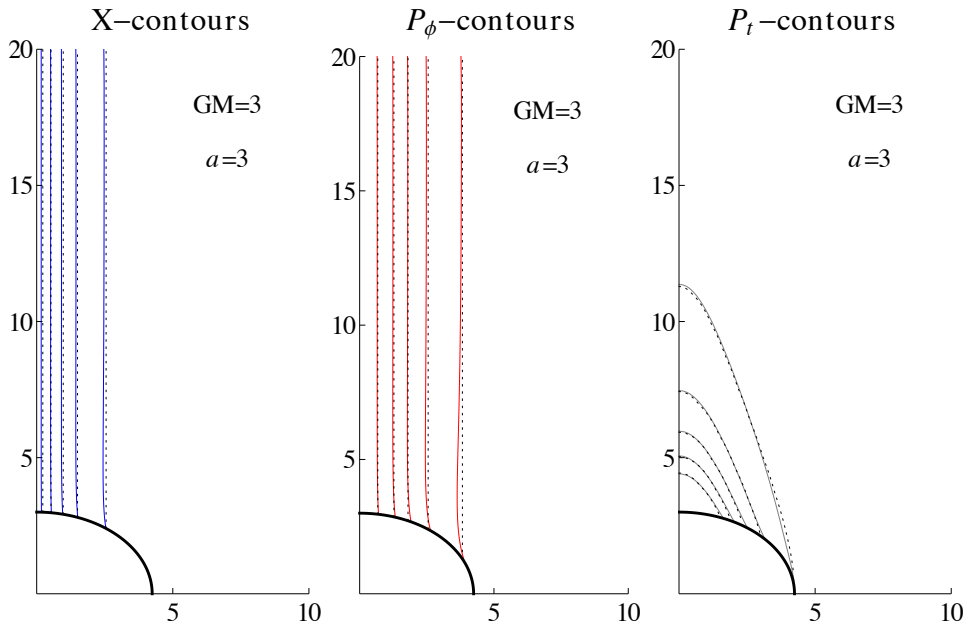

Figure 3.1: A comparison of the approximate and exact numerical solutions for an extremal $GM = a = 3$ Kerr black hole. In spite of the low value of black hole mass, (3.1.15) is still an extremely good approximation to the actual result. Here, the Higgs contours are in blue, the P_φ contours in red, the P_t contours in grey, and all the corresponding approximate solution contours in dashed black. Contours are shown for X, P_φ =0.1, 0.3, 0.5, 0.7, 0.9, and for P_t= -0.099, -0.077, -0.055, -0.033, -0.011.

dissipate until it attains a minimal, steady-state configuration. For our system, the minimum energy configuration corresponds to the state in which the equations of motion are satisfied, but the actual system has no time-dependance. Therefore, to implement this process numerically, we introduce a fictitious time variable, with the "rate of change" of our fields being proportional to the actual elliptic equations we wish to solve:

$$\dot{Y}^i = \Delta Y^i + F^i(\mathbf{Y}, \nabla \mathbf{Y}) \,, \tag{3.1.16}$$

where Δ^i represents a second order (linear) elliptic operator and F is a (possibly nonlinear) function of the variables $Y^i \equiv (X, P_\phi, P_t)$ and their gradients, such that the right hand side is our system of elliptic equations. Therefore, our equations are now in the form of diffusion equations. Solutions to these new equations eventually "relax" to a steady state in which the variables are no longer changing with each time step, thus $\dot{Y}^i = 0$, and the solutions Y^i satisfy our elliptic equations.

The presence of the event horizon makes this treatment a little more subtle, as our elliptic system then has one boundary upon which the equations become parabolic. To deal with this, the fields on the horizon are updated as well, using the equations on the horizon supplemented by the constraint

$$P_t(r_+) = -\frac{a P_\phi(r_+)}{r_+^2 + a^2} \,, \tag{3.1.17}$$

which is necessary for the gauge field to have a finite norm on the horizon as per equation (3.1.7). As we have explained, we use the approximate analytic solution for the fields as an initial condition for the integration. The approximate solution is accurate to $\mathcal{O}(r_+^{-2})$, therefore we choose our outer radial boundary r_∞ to be sufficiently far from the horizon such that the analytic approximation can be extremely well trusted. On axis we impose the standard vortex boundary conditions, $X = 0$ and $P_\phi = 1$, however these conditions do not restrict the form of P_t. Indeed, we have seen that P_t is in fact "generated" or conjured into the vortex equations by the rotation, and thus represents a dyonic degree of freedom that is introduced to the vortex solution by the presence of the black hole. In the case of a Schwarzschild black hole on the other hand, the electric and magnetic degrees of freedom of the gauge boson, if both are present, are decoupled, and only the latter is relevant for

the static vortex solution. Taking this into account, it is not surprising that P_t cannot be constrained by the standard, static vortex boundary conditions. Since we do not wish to pick up a spurious charge of the black hole, we allow the P_t field to relax freely across the grid, and update it along the axis by continuity.

A sample of solutions for $GM = 5$ are displayed in figure 3.2, showing both the nonextremal and extremal cases.

3.2 Extremal Kerr black holes

As we reviewed in Section 2.5, previous studies have shown that a vortex may coexist in a state of static equilibrium with a black hole [83, 95]. In the present work, we have, at this stage, proven the principle that a vortex can coexist in a state of *stationary* equilibrium with a black hole, at the cost of introducing some electric flux close to the black hole horizon. We will now examine in detail the extremal limit of the composite Kerr-vortex system.

As we saw in Section 2.5.2, for the case of Reissner-Nordstrom black holes of small mass, the vortex flux can be expelled from the interior of the black hole [95]. We would now like to explore whether or not this phenomenon of flux expulsion can occur for the extremal Kerr vortex. There is in fact good reason to believe that this phenomenon can be expected, based on the work of Wald pertaining to the behaviour of uniform magnetic fields around rotating black holes. In fact, the physics behind the expelling of vortex flux lines by an extremal horizon, rotating or not, is made particularly transparent by Wald's construction.

Wald demonstrated that Killing vectors can generate electromagnetic fields on Ricci flat backgrounds [109]. A Killing vector k^μ satisfies

$$k_{\mu;\nu} + k_{\nu;\mu} = 0\,. \tag{3.2.18}$$

After differentiating and commuting the derivatives several times, and making use of the Einstein equation $R_{\mu\nu} = 0$, this equation can be reduced to the expression

$$k^{\mu;\nu}{}_{;\nu} = 0\,, \tag{3.2.19}$$

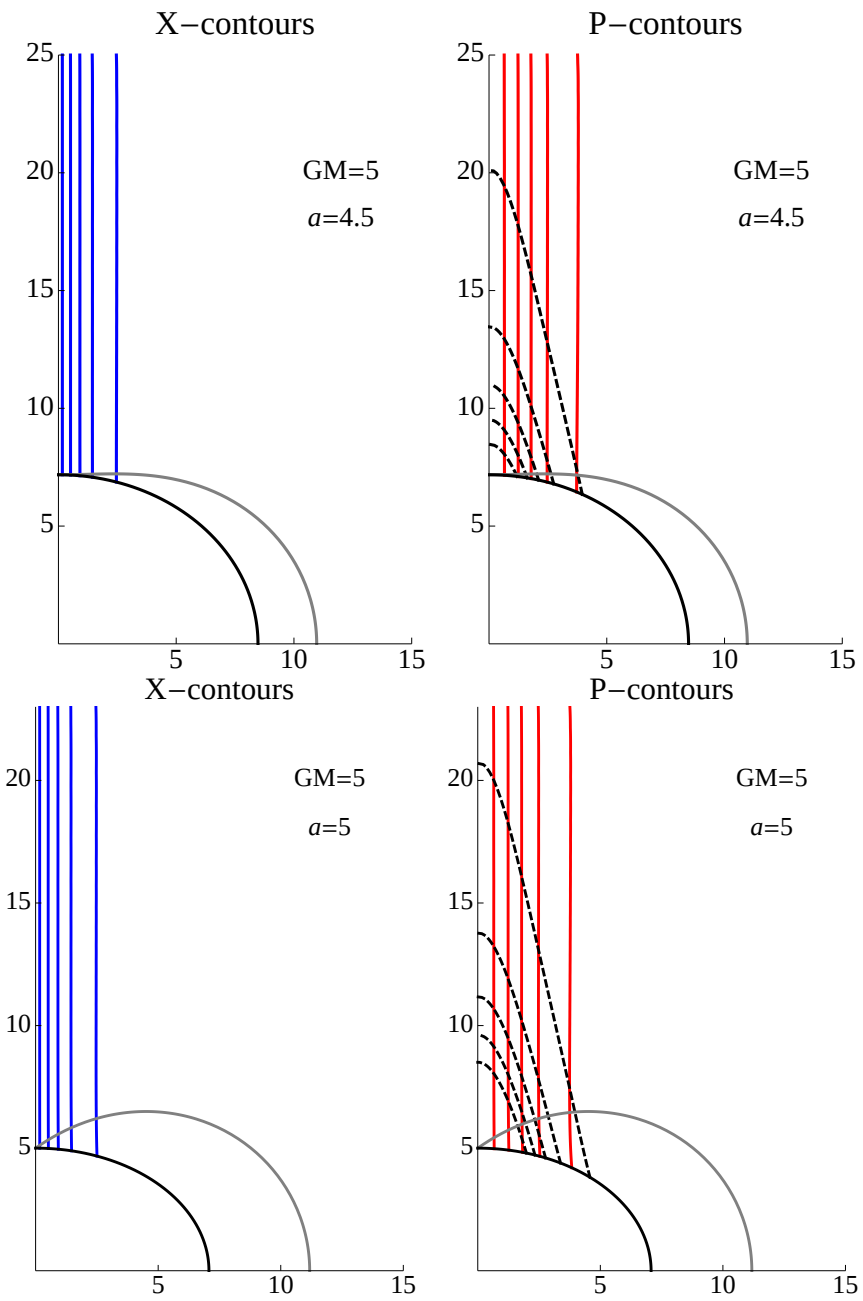

Figure 3.2: Numerical solution for a Kerr black hole with the values of GM and a indicated. On the left, the $X = 0.1, 0.3, 0.5, 0.7, 0.9$ contours are plotted in blue. On the right, the $P_\varphi = 0.1, 0.3, 0.5, 0.7, 0.9$ contours are in red, and the $P_t = -0.045, -0.035, -0.025, -0.015, -0.005$ contours are in dashed black. The horizon is shown in black, and the edge of the ergosphere in grey.

which is precisely the equation for the 4-vector potential A^μ of an electromagnetic field in the Lorentz gauge $A^\nu{}_{;\nu} = 0$, namely

$$A^{\mu;\nu}{}_{;\nu} \equiv F^{\mu\nu}{}_{;\nu} = 0\,. \tag{3.2.20}$$

Therefore, each Killing vector, which characterises a symmetry of the gravitational field, has a corresponding electromagnetic field, which is then intricately linked to spacetime geometry.

For the Kerr spacetime, the potential is then a linear combination of the Killing vectors $\partial_t{}^\mu$ and $\partial_\phi{}^\mu$. Wald's solution is

$$A^\mu \propto (2a\partial_t + \partial_\varphi)^\mu\ , \tag{3.2.21}$$

which represents a constant axial magnetic field B_z threading a rotating black hole, and an electic field that sweeps down the axes and out along the equator of the black hole [109]. The black hole thus acquires an electric charge $Q = 2JB$ as measured by Gauss's law,

$$4\pi Q = \oint_S F^{\mu\nu}\, d^2S_{\mu\nu} \equiv \oiint_S \mathbf{E}\cdot\hat{\mathbf{n}}\, dS \tag{3.2.22}$$

and hence this mechanism can provide a way to "charge up" a black hole.

Physically, we can understand the appearance of the electric field as a consequence of Faraday's law in a cosmological setting: rotation in the presence of a magnetic field induces an electric field. This field may then give rise to an isolated electric charge. For the magnetic field on the other hand, Gauss's law for magnetism states that the magnetic field B is divergence-free, $\nabla^z B_z = 0$. In integral form this is

$$\oiint_S B_z \hat{n}^z dS = 0\,, \tag{3.2.23}$$

so the net flux of the magnetic field out of the surface S should vanish, otherwise the surface contains an isolated magnetic charge, namely, a magnetic monopole. To respect this law, the extremal black hole must exhibit a Meissner effect, and expel the magnetic flux from its interior. In the case of the Wald solution, the flux lines then cross the horizon for nonextremal black holes, while for *all* extremal black holes, the flux is expelled.

The Meissner effect for extremal black holes can be understood as follows. In the special case of the extremal limit, we saw in Section 1.1.2 that in the near-horizon region of a black hole the proper distance along a radial geodesic becomes infinite,

$$\int_{r_+}^{r_++\epsilon} \sqrt{g_{\tilde{r}\tilde{r}}} d\tilde{r} \;\sim\; \int_{r_+}^{r_++\epsilon} \frac{1}{\tilde{r}} d\tilde{r} \;\to\; \infty\,, \tag{3.2.24}$$

where $\tilde{r} = r - r_+$. Now, as a simple example, consider a disc in the equatorial plane extending outwards from r_+ to $r_+ + \epsilon$. As a result of (3.2.24), such a surface has infinite area. If the constant magnetic field lines in the z-direction were to cross this surface, then the magnetic flux leaving the disc would be infinite. To obey Gauss's law in (3.2.23), and thus avoid producing a magnetic monopole, the magnetic field must then vanish on the horizon, giving rise to a Meissner effect. Specifically we require that $B_z \to 0$ faster than $\Delta \to 0$. The effect is depicted in figure 3.3.

Note that for a vortex rather than a uniform magnetic field, the magnetic flux is also set to zero when the gauge field goes to vacuum, $P_\phi \to 0$. Therefore, if the fields are already in vacuum at the equator, or before, such as is the case for larger mass black holes, then the magnetic flux cannot sweep over the horizon as $P_\phi = 0$ along sections of it. The vacuum is the lowest energy state, thus the fields cannot be pulled out of vacuum so that the flux lines can engulf the horizon. The field lines have then nowhere to go unless they pierce the black hole.

The Wald solution (3.2.21) thus provides a hint of what we might expect for the Kerr vortex in the limit that the horizon is well below the scale of the string. In that case, the black hole would be situated sufficiently deep within the core that it feels only a uniform magnetic field B_z around its exterior, associated with the massless gauge boson. However, we cannot simply use the Wald solution as an approximate solution in the core, because the electric field is very different. In particular, due to the fact that the photon is massless throughout the whole of spacetime for the Wald solution, the field lines can sweep outwards from the equator, whereas our photon is massive beyond the core, thus these lines must be contained within the core. That is why our approximate solution for P_t in (3.1.15) does not converge to the Wald solution in the appropriate small mass limit.

In what follows we will show, using analytic arguments, that the Meissner effect indeed arises for the Kerr vortex. This effect, as for the Reissner-Nordstrom case,

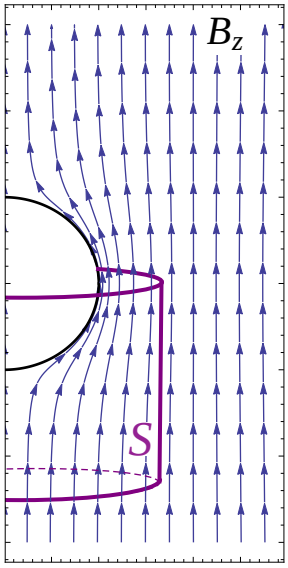

Figure 3.3: The Meissner effect for an extremal black hole: The net magnetic flux leaving the surface S must vanish. Therefore, the magnetic field B_z must vanish on the horizon such that the flux passing through a near-horizon equatorial surface (upper purple disc), which has infinite area, does not diverge.

only occurs for sufficiently small black holes, which makes perfect sense in the light of Wald's construction. As for the Reissner-Nordstrom case in Section 2.5.2, we will derive the limits on the masses required for expulsion and penetration.

3.2.1 Near horizon expansion

We see from the form of the gauge boson norm P_μ^2 in (3.1.7) that one combination of P_ϕ and P_t must vanish on the horizon in order for the system to remain finite, while another combination does not vanish. To study the near horizon limit, it is then useful to rewrite the vector field in terms of the alternative variables P and Q, where

$$\begin{aligned} P &= P_\varphi + a\sin^2\theta P_t\,, \\ Q &= \rho^2 P_t + a P_\varphi\,, \end{aligned} \tag{3.2.25}$$

giving

$$\Big[\frac{P^2}{\Sigma\sin^2\theta} - \frac{Q^2}{\Sigma\Delta}\Big]X = \frac{\Delta}{\Sigma}X_{,rr} + \frac{2(r-GM)}{\Sigma}X_{,r} + \frac{X_{,\theta\theta}}{\Sigma} + \frac{\cot\theta X_{,\theta}}{\Sigma} + \frac{1}{2}X(1-X^2)\,, \tag{3.2.26}$$

$$\frac{X^2P}{\beta} = \frac{\Delta}{\Sigma}P_{,rr} + \frac{P_{,\theta\theta}}{\Sigma} - \frac{\cot\theta P_{,\theta}}{\Sigma}\Big(1 - \frac{2a^2\sin^2\theta}{\Sigma}\Big) + \frac{2P_{,r}}{\Sigma^2}\big[\Sigma(r-GM) - r\Delta\big] + \frac{2a\sin^2\theta}{\Sigma^2}\Big(rQ_{,r} - \cot\theta Q_{,\theta} + aP - Q\Big)\,, \tag{3.2.27}$$

$$\frac{X^2Q}{\beta} = \frac{\Delta}{\Sigma}Q_{,rr} + \frac{Q_{,\theta\theta}}{\Sigma} - \frac{\cot\theta Q_{,\theta}}{\Sigma}\Big(1 - \frac{4GMr}{\Sigma}\Big) + \frac{2\Delta}{\Sigma^2}\big[\cot\theta(Q_{,\theta} - aP_{,\theta}) - r(Q_{,r} - aP_{,r}) + Q - aP\big]\,. \tag{3.2.28}$$

For the extremal Kerr black hole the metric function Δ has a double root, $\Delta = (r-r_+)^2$, and so as with the Riessner-Nordstrom case in Section 2.5.2, we expand the fields near the horizon as

$$\begin{aligned} X &= \xi_0(\theta) + (r-r_+)\xi_1(\theta) + \dots\,, \\ P &= \pi_0(\theta) + (r-r_+)\pi_1(\theta) + \dots\,, \\ Q &= \psi_0(\theta) + (r-r_+)\psi_1(\theta) + \dots\,. \end{aligned} \tag{3.2.29}$$

Eq. (3.2.27) (or finiteness of energy on horizon) then implies that $\psi_0 = 0$. To leading order, the equations then read

$$\xi_0'' + \cot\theta\xi_0' + \frac{r_+^2}{2}(1+\cos^2\theta)\xi_0(1-\xi_0^2) - \Big[\frac{\pi_0^2}{\sin^2\theta} - \psi_1^2\Big]\xi_0 = 0\,, \tag{3.2.30}$$

$$\pi_0'' - \cot\theta\frac{3\cos^2\theta - 1}{1+\cos^2\theta}\pi_0' + \frac{2\sin^2\theta}{1+\cos^2\theta}(\psi_1+\pi_0) - \frac{r_+^2}{\beta}\xi_0^2\pi_0(1+\cos^2\theta) = 0\,, \tag{3.2.31}$$

$$\psi_1'' + \cot\theta\frac{3-\cos^2\theta}{1+\cos^2\theta}\psi_1' - \frac{r_+^2}{\beta}\xi_0^2\psi_1(1+\cos^2\theta) = 0\,. \tag{3.2.32}$$

Note that although the expansion does not in general decouple from the bulk (because of the appearance of the bulk field ψ_1 in the equation for ξ_0) it does form a closed system in this extremal case, as we have an equation for each of the three fields, ξ_0, π_0 and ψ_1. The constraints on the solutions are that they must be symmetric around $\theta = \pi/2$, and obey $\xi_0 = 0$, $\pi_0 = 1$ at $\theta = 0, \pi$.

3.2.2 Flux penetration and expulsion

Let us first show that for large black holes, a string will always penetrate the black hole horizon. Similar to the extremal Reissner-Nordstrom case, we proceed by contradiction. Returning to the full bulk equation (3.2.27), let us assume that flux expulsion occurs, i.e. at $r_+ = a = GM$ we have $X = 0$ and $P_\varphi = 1$ (with $P_t = -1/2r_+$ from (3.1.17)) leading to $P \equiv \pi_0 = (1+\cos^2\theta)/2$, and hence (3.2.31) yields $\psi_1 \equiv Q'(r_+) = -1$.

Therefore near r_+ where $X > 0$, $P < 1$ and $X^2 \ll 1$, both $\partial_r(\Delta\partial_r X) > 0$ and $(Q^2/\Delta\Sigma - X^2/2) > 0$. Hence Eq. (3.2.27) implies

$$\begin{aligned}\frac{1}{2}r_+^2\sin^2\theta X \;&+\; \sin\theta\partial_\theta(\sin\theta\partial_\theta X)\\ &\leq\; \frac{1}{2}r_+^2(1+\cos^2\theta)\sin^2\theta X + \sin\theta\partial_\theta(\sin\theta\partial_\theta X) < XP^2 < X\,. \end{aligned}\tag{3.2.33}$$

However, this is the same equation as the one obtained for the Reissner-Nordstrom black hole in (2.5.61), which is extensively discussed in Section 2.5.2, and the discussion therein therefore applies. Hence we conclude that for any $r_+ > \sqrt{8.5} \approx 2.92$ the vortex must pierce the extremal Kerr black hole.

Let us now look more closely at what happens on the horizon. An inspection of (3.2.32) shows that if $\xi_0 \neq 0$, then $\psi_1 = 0$. Specifically, at the turning points $\psi_1' = 0$, we find

$$\psi_1'' = \frac{r_+^2}{\beta}\xi_0^2\psi_1(1+\cos^2\theta)\,. \tag{3.2.34}$$

All quantites on the right hand side of this expression are always positive except for ψ_1, thus we see that ψ_1 has a maximum $\psi_1'' > 0$ (minimum $\psi_1'' < 0$) only when it is negative (positive). Now, if $\theta = 0$, the second term in (3.2.32) is divergent unless it corresponds to a turning point, $\psi_1'(0) = 0$. As $\xi_0(0) = 0$, we then find that[1] $\psi_1''(0) = 0$. Then, as we move away from $\theta = 0$, if $\psi_1(0)$ is negative then $\psi_1'' < 0$, thus ψ_1 is always decreasing and can never reach a minimum, as this would require

[1] To confirm that the second term does not diverge, we could use l'Hopital's rule to show that

$$\lim_{\theta\to 0}\frac{\psi_1'(\theta)}{\sin\theta} = \lim_{\theta\to 0}\frac{\psi_1''(\theta)}{\cos\theta} = \psi''(0)\,, \tag{3.2.35}$$

then (3.2.32) yields $\psi''(0) = 0$.

ψ_1 to be positive. The reverse occurs for positive ψ_1, namely it aways stays positive. The fields should be symmetric around $\pi/2$, and this is only possible if ψ_1 can have a turning point there. However we have shown this to be impossible, as long as $\xi_0 \neq 0$, which it isn't as long as $\theta \neq 0$. Therefore we see that $\psi_1 = 0$ as long as $\xi_0 \neq 0$.

Eqs. (3.2.30) and (3.2.31) now read

$$\begin{aligned} \xi_0'' + \cot\theta\xi_0' + \frac{r_+^2}{2}(1+\cos^2\theta)\xi_0(1-\xi_0^2) - \frac{\pi_0^2\xi_0}{\sin^2\theta} = 0\,, \\ \pi_0'' - \cot\theta\frac{3\cos^2\theta - 1}{1+\cos^2\theta}\pi_0' + \frac{2\sin^2\theta}{1+\cos^2\theta}\pi_0 - \frac{r_+^2}{\beta}\xi_0^2\pi_0(1+\cos^2\theta) = 0\,, \end{aligned} \tag{3.2.36}$$

and form a pair of coupled equations for the two purely horizon fields ξ_0 and π_0, decoupled from the bulk. Based on energetic considerations, let us assume that these fields have only one turning point on the horizon. In this case, the field ξ_0 would start from zero at $\theta = 0$ and monotonically increase to reach its first maximum at $\theta = \pi/2$, $\xi_0(\pi/2) < 1$, while the value of π_0 would monotonically decrease to reach its first minimum $\pi_0(\pi/2) < 1$. Since $\pi_0''(\pi/2) > 0$, the second equation at $\theta = \pi/2$ implies that $r_+^2\xi_0(\pi/2)^2 - 2\beta > 0$, and therefore, $r_+^2 > 2\beta$. Thus we see that for $r_+ < \sqrt{2\beta}$ the penetrating solution cannot exist and the black hole must expel the flux.

We will now demonstrate that flux expulsion is indeed a solution of our near horizon equations (3.2.30)–(3.2.32). Consider the flux-expelling case for which $\xi_0 \equiv 0$. Using the boundary condition $\psi_1'(0) = 0$, (3.2.32) solves to $\psi_1 = const.$, and (3.2.31) has the general solution $\pi_0 = \lambda\sin^2\theta + \gamma\cos\theta - \psi_1$. Applying the boundary condition $\pi_0(0) = 1$, and using the fact that the solution must be symmetric around $\pi/2$, then yields $\gamma = 0$, $\psi_1 = -1$. Then, using the fact that $P(r_+) \equiv \pi_0 = (1 + \cos^2\theta)/2$, we find that $\lambda = -1/2$. Therefore the solution reads $\pi_0 = -\frac{1}{2}\sin^2\theta + 1$ and $\psi_0 = 0$. In the original variables this corresponds to

$$P_\phi = 1\,, \qquad P_t = -\frac{1}{2r_+}\,, \tag{3.2.37}$$

on the horizon and hence represents a flux-expelled solution. Let us point out that if there is a phase transition between the flux penetration and expulsion, the value of ψ_1 on the horizon necessarily suffers from a discontinuity: $\psi_1 = 0$ for flux

penetration, for which $\xi_0 > 0$, whereas for $\xi_0 = 0$, the case of expulsion, ψ_1 jumps to $\psi_1 = -1$. Therefore

$$\lim_{\xi_0 \to 0^+} \psi_1 \neq \psi_1\Big|_{\xi_0=0}. \tag{3.2.38}$$

Our analytic arguments suggest that similar to the Reissner-Nordstrom case, there exists a critical radius r_c, $1.41 < r_c < 2.92$ for $\beta = 1$, below which the flux is necessarily expelled. Numerical investigations actually indicate $r_c \approx 1.912$.

Figure 3.4 displays a comparison between the Kerr and Reissner-Nordstrom phase transitions for several values of β, where the maximum value of the Higgs field, $\xi_0(\pi/2)$, which is the order parameter for the transition, is plotted against the horizon radius r_+. We see that the nature of the phase transition is different for the two black holes, and furthermore, the two cases exhibit a different response to a variation of the Bogomolyni parameter β. The Bogomolyni paramater governs the ratio between the Higgs and gauge field masses, therefore a drop in β corresponds to a narrowing of the gauge core. This leads to a lowering of the critical radius for flux expulsion, which both black holes exhibit. However, the Kerr black hole has a higher critical radius when β increases. In fact, we see from (3.2.36) that π_0 now has two contributions to its effective mass that come with opposite signs, while the Reissner-Nordstrom Higgs field has only a single, negative contribution. For Kerr, the positive contribution is purely geometric, and disappears at $\theta = 0$ as it should. The negative contribution comes from the Higgs field ξ_0, and this contribution must dominate to prevent the flux of π_0 from being expelled. Due to the fact that this contribution includes a factor of the form r_+^2/β, it is clear that an increase in β will dampen this term and thus increase the critical radius at which expulsion happens.

3.3 Backreaction of the vortex on the black hole

We have seen that while the spacetime around a cosmic string is locally flat, globally it is not Euclidean: instead, the string cuts out an azimuthal deficit angle at infinity. When a cosmic string is threaded through a black hole, one must essentially combine the spacetimes associated with the two objects in some appropriately stable way. For static black holes, intuitively it is easy to imagine that the conical effect of the

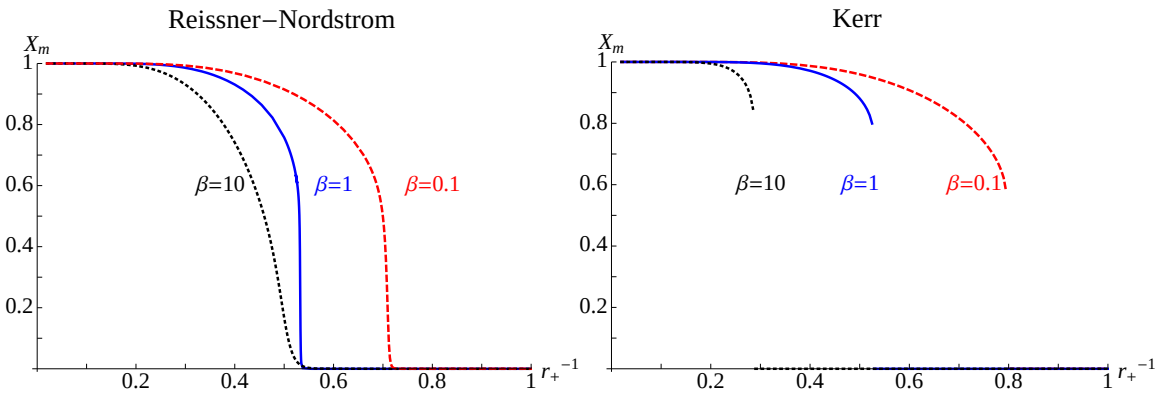

Figure 3.4: Phase plots for the RN and Kerr extremal black holes. The maximum value of the Higgs field, $X_m = \xi_0(\pi/2)$, is plotted against the horizon radius r_+. The transition is shown for different values of the Bogomolnyi parameter: $\beta = 10$ in dotted black, $\beta = 1$ in solid blue, and $\beta = 0.1$ in dashed red.

string is simply centred on the black hole, and this is precisely what studies have revealed [80, 83]. However, in the Kerr spacetime such a conical effect could not be consistently quarantined away from the time direction, as this direction is not orthogonal to the azimuthal direction. Nevertheless, in the literature it is often simply assumed that the effect of a cosmic string in a rotating background is to induce the usual azimuthal deficit angle at infinity [97, 110].

In fact, what occurs in the Kerr spacetime is much more interesting: we will show in what follows that the string induces a conical deficit angle from the perspective of an azimuthal coordinate that is co-rotating with the black hole. This means that the black hole horizon, a rotating 2-sphere, will feel an azimuthal section cut out of it as a result of the string.. Seeing as the horizon is rotating with respect to an asymptotic observer, such an observer sees a deficit angle in the union of the time and azimuthal directions. Only at spatial infinity, where the rotation is no longer felt, will the deficit angle emerge entirely in the azimuthal direction.

We will now derive this effect concretely. We have demonstrated above that the analytic approximations for the fields (3.1.15) are in excellent agreement with their numerical counterparts, therefore, in order to proceed analytically, we will henceforth make use of these approximate solutions. Our approach is then to follow the perturbative procedure which we used for the self-gravitating vortex in Section

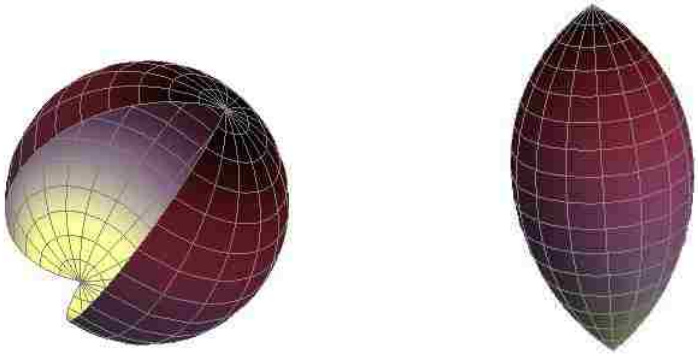

Figure 3.5: The black hole horizon shown with a wedge removed as a result of the gravitational effect of the string.

2.4, namely, we expand the Einstein equations in powers of $\epsilon = 8\pi G\eta^2$, and use the probe vortex solution to compute the leading order gravitational correction to the Kerr spacetime.

We first need to select an appropriate set of coordinates for the problem, which reflects the axial symmetry of the Kerr-string system. A convenient choice for the metric is (see e.g. [111])

$$ds^2 = e^{2\lambda}dt^2 - \alpha^2 e^{-2\lambda}\big[d\varphi + Bdt\big]^2 - e^{2(\nu-\lambda)}(dx^2+dy^2)\,, \tag{3.3.39}$$

where the functions α, B, ν and λ are functions of the x and y coordinates only. The Ricci tensor of this metric is given by:

$$\begin{aligned}
R^{\varphi}_{\varphi} + R^{t}_{t} &= e^{2(\lambda-\nu)}\frac{\nabla^2\alpha}{\alpha}\,, && (3.3.40)\\
R^{t}_{\varphi} &= \frac{\alpha}{2}e^{-2(\lambda+\nu)}\Big[-3\nabla\alpha\cdot\nabla B + 4\alpha\nabla B\cdot\nabla\lambda - \alpha\nabla^2 B\Big]\,, && (3.3.41)\\
R_{\varphi\varphi} &= -\frac{\alpha}{2}e^{-2\nu}\Big[\alpha^3 e^{-4\lambda}(\nabla B)^2 + 2\nabla^2\alpha - 2\nabla\alpha\cdot\nabla\lambda - 2\alpha\nabla^2\lambda\Big]\,, && (3.3.42)\\
R^{x}_{x} + R^{y}_{y} &= \frac{e^{2(\lambda-\nu)}}{2\alpha}\Big[2\nabla^2\alpha - \alpha^3 e^{-4\lambda}(\nabla B)^2 + 4e^{\lambda}\nabla\cdot\big(\alpha\nabla e^{-\lambda}\big)\\
&\qquad +4\alpha\nabla^2\nu\Big]\,, && (3.3.43)\\
R_{xy} &= \frac{1}{2\alpha}\big[\alpha^3 e^{-4\lambda}B_x B_y - 4\alpha\lambda_x\lambda_y + 2(\alpha_x\nu_y + \alpha_y\nu_x) - 2\alpha_{xy}\Big]\,, && (3.3.44)\\
R^{y}_{y} &= \frac{e^{2(\lambda-\nu)}}{2\alpha}\Big[-\alpha^3 e^{-4\lambda}B_y^2 + 2\alpha\nabla^2(\nu-\lambda) - 2(\alpha_y\nu_y - \alpha_x\nu_x)\\
&\qquad -2\nabla\alpha\cdot\nabla\lambda + 4\alpha\lambda_y^2 + 2\alpha_{yy}\Big]\,, && (3.3.45)
\end{aligned}$$

In the above, $\sqrt{-g} = \alpha\, e^{2(\nu-\lambda)}$, the two-dimensional gradient operator $\nabla = (\partial_x, \partial_y)$, and the Laplace operator $\nabla^2 = \nabla \cdot \nabla = \partial_x^2 + \partial_y^2$. In particular, defining[2]

$$x = \int \frac{dr}{\sqrt{\Delta}}\,, \quad y = \theta\,, \tag{3.3.46}$$

the background (Kerr) solution can be written as

$$\alpha_0 = \sqrt{\Delta}\sin\theta\,, \quad B_0 = -\frac{2aGMr}{\Gamma}\,, \quad e^{2\nu_0} = \frac{\Delta\Sigma^2}{\Gamma}\,, \quad e^{2\lambda_0} = \frac{\Delta\Sigma}{\Gamma}\,. \tag{3.3.47}$$

The Einstein equations take the form

$$R_{\mu\nu} = \epsilon\Big(T_{\mu\nu} - \frac{1}{2}T g_{\mu\nu}\Big)\,, \tag{3.3.48}$$

where the Ricci tensor is expanded as $R_{\mu\nu} \to R_{\mu\nu} + \delta R_{\mu\nu}$ around the background Kerr solution, which is given by the Weyl expressions (3.3.47), and the energy momentum tensor is built from the energy of the probe vortex. The components of the energy

[2]Note this is not the usual Weyl gauge, in which the α variable is typically equal to one of x or y, however, this choice proves easier to analyse, and is closer to the standard Boyer Lindquist Kerr gauge.

momentum tensor take the form

$$
\begin{aligned}
T^t_t &= \frac{1}{\Sigma}(X^2_{,\theta}+\Delta X^2_{,r})+\frac{1}{4}(X^2-1)^2+\frac{X^2}{\Delta\Sigma}\left[\Gamma P_t^2+\Omega P_\phi^2\right] \\
&\quad +\frac{\beta}{\Delta\Sigma^2}\left[\Gamma(P^2_{t,\theta}+\Delta P^2_{t,r})+\Omega(P^2_{\phi,\theta}+\Delta P^2_{\phi,r})\right], && (3.3.49)\\
T^t_\phi &= \frac{2\beta}{\Delta\Sigma}\Big[\Gamma(P_{t,\theta}P_{\phi,\theta}+\Delta P_{t,r}P_{\phi,r})+2GMar(P^2_{\phi,\theta}+\Delta P^2_{\phi,r})\Big] \\
&\quad +\frac{2X^2}{\Delta\Sigma}(\Gamma P_tP_\phi+2GMarP_\phi^2), && (3.3.50)\\
T^\phi_\phi &= \frac{1}{\Sigma}(X^2_{,\theta}+\Delta X^2_{,r})+\frac{1}{4}(X^2-1)^2-\frac{X^2}{\Delta\Sigma}\left[\Gamma P_t^2+\Omega P_\phi^2\right] \\
&\quad -\frac{\beta}{\Delta\Sigma^2}\left[\Gamma(P^2_{t,\theta}+\Delta P^2_{t,r})+\Omega(P^2_{\phi,\theta}+\Delta P^2_{\phi,r})\right], && (3.3.51)\\
T^x_x &= \frac{1}{\Sigma}(X^2_{,\theta}-\Delta X^2_{,r})+\frac{1}{4}(X^2-1)^2-\frac{X^2}{\Delta\Sigma}\Big[\Gamma P_t^2-\Omega P_\phi^2+\frac{4GMar}{\Delta\Sigma}P_tP_\phi\Big] \\
&\quad +\frac{\beta}{\Delta\Sigma^2}\Big[\Gamma(\Delta P^2_{t,r}-P^2_{t,\phi})+\Omega(P^2_{\phi,\theta}-\Delta P^2_{\phi,r}) && (3.3.52)\\
&\quad +4GMar(\Delta P_{t,r}P_{\phi,r}-P_{t,\theta}P_{\phi,\theta})\Big], \\
T_{xy} &= 2\sqrt{\Delta}X_\theta X_r-\frac{2\beta}{\sqrt{\Delta}\Sigma}\Big[\Gamma P_{t,\theta}P_{t,r}+2GMar(P_{t,\theta}P_{\phi,r}+P_{\phi,\theta}P_{t,r}) && (3.3.53)\\
&\quad -\Omega P_{\phi,\theta}P_{\phi,r}\Big], \\
T^y_y &= -\frac{1}{\Sigma}(X^2_{,\theta}-\Delta X^2_{,r})+\frac{1}{4}(X^2-1)^2-\frac{X^2}{\Delta\Sigma}\Big[\Gamma P_t^2-\Omega P_\phi^2+\frac{4GMar}{\Delta\Sigma}P_tP_\phi\Big] \\
&\quad -\frac{\beta}{\Delta\Sigma^2}\Big[\Gamma(\Delta P^2_{t,r}-P^2_{t,\phi})+\Omega(P^2_{\phi,\theta}-\Delta P^2_{\phi,r}) && (3.3.54)\\
&\quad +4GMar(\Delta P_{t,r}P_{\phi,r}-P_{t,\theta}P_{\phi,\theta})\Big],
\end{aligned}
$$

where for compactness we have introduced the function

$$\Omega=\frac{\Delta-a^2\sin^2\theta}{\sin^2\theta}\,.$$

In the thin string limit, using the approximate solution (3.1.15), these become

$$
\begin{aligned}
&T^t_t\approx T^x_x\approx X_0'^2+\frac{X_0^2P_0^2}{R^2}+\beta\frac{P_0'^2}{R^2}+\frac{1}{4}(X_0^2-1)^2\equiv\mathcal{E}\,,\\
&T^y_y\approx -X_0'^2+\frac{X_0^2P_0^2}{R^2}-\beta\frac{P_0'^2}{R^2}+\frac{1}{4}(X_0^2-1)^2\equiv-\mathcal{P}_R\,,\\
&T^\varphi_\varphi\approx X_0'^2-\frac{X_0^2P_0^2}{R^2}-\beta\frac{P_0'^2}{R^2}+\frac{1}{4}(X_0^2-1)^2\equiv-\mathcal{P}_\phi\,, && (3.3.55)\\
&T_{xy}\approx\frac{\sqrt{\Delta}r}{\rho}R(\mathcal{E}+\mathcal{P}_R)\,,\\
&T^t_\varphi\approx-\frac{4GMra}{\rho^8}\left[(\rho^2-4r^2)RPP'-a^2R^2(X^2P^2+P'^2)\right]\approx0\,,
\end{aligned}
$$

where $\mathcal{E}$ etc. denote the energy-momentum components of the Nielsen-Olesen vortex, defined in (2.4.32), which are simply functions of $R = \rho \sin\theta$. Because these components are functions of R only, this leads to a modification of the Kerr geometry which is also dependent on R.

Note that far away from the black hole in the polar direction $r\cos\theta$, the perturbed Kerr metric should asymptote towards the metric of the self-gravitating vortex. Thus we expect the corrections to take the form that $\delta\alpha = \epsilon\alpha_0\alpha_1(R)$, $\delta\lambda = \delta\nu/2 = \epsilon\lambda_1(R)$. We will therefore consider general perturbations of the form

$$\alpha = \alpha_0\Big(1 + \epsilon\alpha_1(R) + O(\epsilon^2)\Big)\,, \qquad \alpha = B_0\Big(1 + \epsilon B_1(R) + O(\epsilon^2)\Big)\,, \tag{3.3.56}$$

$$\lambda = \lambda_0 + \epsilon\lambda_1(R) + O(\epsilon^2)\,, \qquad \nu = \nu_0 + \epsilon\nu_1(R) + O(\epsilon^2)\,. \tag{3.3.57}$$

Using these expressions, we find for the curvature:

$$\begin{aligned}
\delta(R^\phi_\phi + R^t_t) &= \epsilon\frac{e^{2(\lambda_0-\nu_0)}}{\alpha_0}\Big[2\nabla\alpha_0\cdot\nabla\alpha_1 + \alpha_0\nabla^2\alpha_1\Big] && (3.3.58)\\
\delta(R^t_\phi) &= -\epsilon\frac{e^{2(\lambda_0-\nu_0)}}{2\alpha_0}\Big[\alpha_0^3 e^{-4\lambda_0}\nabla B_0\cdot(3\nabla\alpha_1 - 4\nabla\lambda_1)\\
&\quad +\alpha_0^3 e^{-4\lambda_0}\nabla B_0\cdot\nabla B_1 + \nabla\cdot(\alpha_0^3 e^{-4\lambda_0}B_0\nabla B_1)\Big] && (3.3.59)\\
\delta(R_{\phi\phi}) &= -\epsilon\frac{\alpha_0 e^{-2\nu_0}}{2}\Big[\alpha_0^3 e^{-4\lambda_0}((\nabla B_0)^2(2\alpha_1 - 4\lambda_1)\\
&\quad +2\nabla B_0\cdot\nabla(B_0B_1)) - 2\alpha_0\nabla\alpha_1\cdot\nabla\lambda_0 - 2\nabla\alpha_0\cdot\nabla\lambda_1\\
&\quad +4\nabla\alpha_1\cdot\nabla\alpha_0 + 2\alpha_0\nabla^2\alpha_1 - 2\alpha_0\nabla^2\lambda_1\Big] && (3.3.60)\\
\delta(R^x_x + R^y_y) &= \epsilon\frac{e^{2(\lambda_0-\nu_0)}}{2\alpha_0}\Big[2\alpha_0\nabla^2\alpha_1 + 4\nabla\alpha_0\cdot\nabla\alpha_1 + 4\alpha_0\nabla^2\nu_1\\
&\quad -\alpha_0^3 e^{-4\lambda_0}((\nabla B_0)^2(2\alpha_1 - 4\lambda_1) + 2\nabla B_0\cdot\nabla(B_0B_1))\\
&\quad +4e^{\lambda_0}(\alpha_0\nabla\alpha_1\cdot\nabla e^{-\lambda_0} - \nabla\cdot(\alpha_0 e^{-\lambda_0}\nabla\lambda_1))\Big] && (3.3.61)\\
\delta(R_{xy}) &= \epsilon\frac{1}{2\alpha_0}\Big[\alpha_0^3 e^{-4\lambda_0}(B_{0x}(B_0B_1)_y + B_{0y}(B_0B_1)_x + (2\alpha_1 - 4\lambda_1)B_{0x}B_{0y})\\
&\quad -4\alpha_0(\lambda_{0x}\lambda_{1y} + \lambda_{1x}\lambda_{0y}) + \alpha_{0x}\nu_{1y} + \alpha_{0y}\nu_{1x} + \alpha_0\alpha_{1x}\nu_{0y}\\
&\quad \alpha_0\alpha_{1y}\nu_{0x} - 2(\alpha_{0x}\alpha_{1y} + \alpha_{0y}\alpha_{1x} + \alpha_0\alpha_{1xy})\Big] && (3.3.62)\\
\delta(R^y_y) &= \epsilon\frac{e^{2(\lambda_0-\nu_0)}}{2\alpha_0}\Big[-\alpha_0^3 e^{-4\lambda_0}((2\alpha_1 - 4\lambda_1)(B_{0y})^2 + 2B_{0y}(B_0B_1)_y)\\
&\quad +2\alpha_0(\nabla^2\nu_1 - \nabla^2\lambda_1) - 2\alpha_0(\alpha_{1y}\nu_{0y} - \alpha_{1x}\nu_{0x})\\
&\quad -2(\alpha_{0y}\nu_{1y} - \alpha_{0x}\nu_{1x}) - 2(\alpha_0\nabla\alpha_1\cdot\nabla\lambda_0 + \nabla\alpha_0\cdot\nabla\lambda_1)\Big] && (3.3.63)
\end{aligned}$$

Notice that the perturbations of the B function always come with prefactors of the derivatives of B_0, which is $\mathcal{O}(\rho^{-3})$. Given that the overall prefactor

$$\alpha_0^3 e^{-4\lambda_0} \;=\; \frac{\Gamma^2 \sin^3\theta}{\sqrt{\Delta}\Sigma^2} \;=\; \mathcal{O}(1)\,, \tag{3.3.64}$$

we see that B_1 terms are always subdominant.

To expand the equations, we make use of the derivatives given in (3.1.11) to obtain the following expressions:

$$\nabla \equiv \Big(\frac{\partial}{\partial x}, \frac{\partial}{\partial y}\Big) = \Big(\frac{\sqrt{\Delta} r R}{\rho^2}\frac{d}{dR}, \rho\frac{d}{dR}\Big)\,, \tag{3.3.65}$$

$$\frac{\partial^2}{\partial x^2} \simeq \frac{\Delta R^2}{\rho^2}\frac{d^2}{dR^2} + \frac{rR\Delta'}{2\rho^2}\frac{d}{dR}\,, \qquad \frac{\partial^2}{\partial y^2} \simeq \rho^2\Big(1-\frac{R^2}{\rho^2}\Big)\frac{d^2}{dR^2} - R\frac{d}{dR}\,, \tag{3.3.66}$$

$$\nabla^2 \equiv \partial_x^2 + \partial_y^2 \simeq \rho^2\Big(1+\frac{\Delta R^2}{\rho^4}\Big)\frac{d^2}{dR^2} + \Big(\frac{rR\Delta'}{2\rho^2} - R\Big)\frac{d}{dR}\,. \tag{3.3.67}$$

First, consider the Einstein equation (3.3.40),

$$\delta(R_t^t + R_\varphi^\varphi) = -\epsilon\,(\mathcal{E} - \mathcal{P}_R)\,. \tag{3.3.68}$$

Expanding (3.3.58), the right-hand-side becomes

$$\begin{aligned}\delta(R_t^t + R_\varphi^\varphi) &= \epsilon\,\frac{\rho^2}{\Sigma}\Big[\Big(1+\frac{\Delta R^2}{\rho^4}\Big)\alpha_1'' + \Big(2 - \frac{R^2}{\rho^2} + \frac{3rR^2\Delta'}{2\rho^4}\Big)\frac{\alpha_1'}{R}\Big] \\ &= \epsilon\,\Big[\alpha_1'' + \frac{2}{R}\alpha_1' + \mathcal{O}(\rho^{-2})\Big]\,,\end{aligned} \tag{3.3.69}$$

yielding a simple ordinary differential equation for α_1 at leading order,

$$\alpha_1'' + 2\frac{\alpha_1'}{R} = -(\mathcal{E} - \mathcal{P}_R)\,, \tag{3.3.70}$$

which is solved by

$$\alpha_1 = -\int_0^R R(\mathcal{E}-\mathcal{P}_R)dR + \frac{1}{R}\int_0^R R^2(\mathcal{E}-\mathcal{P}_R)dR\,. \tag{3.3.71}$$

At leading order, this is in fact identical in form to the self-gravitating correction (2.4.36).

Next, recalling that B and its derivatives are subdominant, we obtain for the Einstein equations (3.3.42), (3.3.43) and (3.3.45)

$$\delta R_{\varphi\varphi} \;=\; -\epsilon R\,[R\alpha_1'' + 2\alpha_1' - R\lambda_1'' - \lambda_1'] = R^2\left[\mathcal{E} + \frac{1}{2}(\mathcal{P}_\phi - \mathcal{P}_R)\right]\,, \tag{3.3.72}$$

$$\delta(R_x^x + R_y^y) \;=\; \epsilon\left[\alpha_1'' + \frac{\alpha_1'}{R} + 2\nu_1'' - 2\lambda_1'' - 2\frac{\lambda_1'}{R}\right] = -\epsilon\,[\mathcal{E} - \mathcal{P}_\phi]\,, \tag{3.3.73}$$

$$\delta R_y^y \;=\; \epsilon\left[\alpha_1'' + \frac{\alpha_1'}{R} + \nu_1'' - \lambda_1'' - \frac{\nu_1'}{R} - \frac{\lambda_1'}{R}\right] = -\epsilon\left[\mathcal{E} - \frac{1}{2}(\mathcal{P}_\phi - \mathcal{P}_R)\right] \tag{3.3.74}$$

Inserting (3.3.71) into the first of the above equations yields precisely the expression (2.4.38) which we obtained for the self-gravitating vortex,

$$\lambda_1'' + \frac{\lambda_1'}{R} = \frac{1}{2}(P_\phi + P_R)\,, \tag{3.3.75}$$

and thus as we have seen, is solved by

$$\lambda_1 = \frac{1}{2}\int_0^R R\mathcal{P}_R dR\,. \tag{3.3.76}$$

Finally, subtracting (3.3.75) from both sides of (3.3.73) yields

$$\epsilon\Big[\alpha'' + \frac{2\alpha'}{R} + 2\nu'' - 3\lambda'' - \frac{3\lambda'}{R}\Big] = -\epsilon\Big[\mathcal{E} - \frac{1}{2}(\mathcal{P}_\phi - \mathcal{P}_R)\Big]\,, \tag{3.3.77}$$

and consistency with (3.3.74) then implies that $\nu_1 = 2\lambda_1$, just as we found for the self-gravitating case.

We can now check the remaining equations:

$$\begin{aligned}
\delta R_{xy} &= -\epsilon\sqrt{\Delta}\,\frac{r}{\rho}\left[R\alpha_1'' + 2\alpha_1' - 4\lambda_1'\right] = \epsilon\sqrt{\Delta}\,\frac{r}{\rho}\left[\mathcal{E} + \mathcal{P}_R\right]\,, && (3.3.78)\\
\delta R^t_\varphi &= \epsilon\frac{GMra}{\rho^8}\left(\rho^2 - 4r^2 + 2a^2\right)R^3\left[3\alpha_1' - 4\lambda_1'\right] && (3.3.79)\\
&= -\epsilon\frac{4GMra}{\rho^8}\left[(\rho^2 - 4r^2)RPP' - a^2R^2(X^2P^2 + P'^2)\right] = \mathcal{O}(r_+^2/r^5)\,.
\end{aligned}$$

Pulling all the details together, and looking outside the core of the vortex, we see the leading order asymptotic form of the Kerr-vortex is

$$\begin{aligned}
ds^2 = &\left(1 - \frac{2GMr}{\Sigma} + \frac{8(GMar\sin\theta)^2}{\Gamma\Sigma}\epsilon\hat{\mu}\right)dt^2 - \Sigma d\theta^2 - \frac{\Sigma}{\Delta}dr^2\\
&- \frac{\Gamma}{\Sigma}(1 - 2\epsilon\hat{\mu})\sin^2\theta\, d\varphi^2 + \frac{4GMar\sin^2\theta}{\Sigma}(1 - 2\epsilon\hat{\mu})dtd\varphi\,,
\end{aligned} \tag{3.3.80}$$

where

$$\hat{\mu} = \int_0^\infty R\mathcal{E}dR \tag{3.3.81}$$

is the renormalised energy per unit length of the string.

Thus we see that in Boyer-Lindquist coordinates, the conical effect of the string emerges in the time *and* azimuthal directions. On the other hand, transforming to a to a frame co-rotating with the black hole, $\varphi_H = \varphi - \Omega_H t = \varphi - B(r_+)$, we see that the conical effect is then indeed confined to a purely angular direction, namely the azimuthal direction in the co-rotating frame, such as on the horizon. Note that

this is not inconsistent with the conical effect in the static case, as in that case, there is simply no difference between the azimuthal coordinate at infinity and on the horizon.

3.4 Discussion

In this Chapter we have seen that a vortex in a rotating spacetime necessarily picks up a time component P_t, and this significantly enhances the phenomenology of these composite vortex and black hole systems compared to their purely static counterparts. Importantly, including rotation has enabled the interactions between vortices and black holes to become relevant for cosmology and astrophysics. As we have shown, a vortex is quite able to form a stable state with a rotating black hole, which implies that these objects do not repel one another, nor does a black hole accrete a string that pierces it axially. Therefore, it would be interesting to look for signs of these composite objects in galactic systems, now that we know that they are possible.

While conventional strings do not feature an electric field, as even if one considers a time component of the gauge field to be present, it is not relevant for the description of the static vortex, we see that in the rotating context, an electric field is necessarily generated. That this is a genuine electric flux, and not some frame dragging transformation effect is easily verified by computing

$$|F \wedge F| \sim \mathbf{E} \cdot \mathbf{B} \sim \frac{8GMaP_0(R)P_0'(R)(3r^2 - a^2)}{R\rho^6} \tag{3.4.82}$$

for the approximate solution, which is clearly a nonvanishing quantity. The emergence of electric flux is thus a frame-independent effect, and as we mentioned earlier, can be viewed as a manifestation of Faraday's law in astrophysical systems.

Given that a Kerr black hole admits an extremal limit, we explored the possible emergence of a Meissner effect for low mass black holes, as such an effect is known to arise for low mass extremal Reissner-Nordstrom black holes [95]. We confirmed that the Meissner effect appears for the Kerr black hole, however in contrast to the Reissner-Nordstrom case, the transition between piercing and expelling phases is discontinuous.

It is worth mentioning that a large degree of sensitivity arose in the numerics for the extremal Kerr black hole at low mass, which points to a possible physical instability in the system for these regions of the parameter space. We conjecture that this could be due to a super-radiant instability analogous to the instability in Kerr-AdS [106, 107]. For the latter case, perturbations can be amplified due to the confinement of the AdS spacetime, which our system in some sense replicates as a result of the confining nature of the core of the string, which is the only massless region in our spacetime along which perturbations can freely propagate.

Finally, we explored the gravitational backreaction of the Kerr vortex, which revealed perhaps the most important implications of these systems for cosmology. We found that the rotation mixes the azimuthal conical effect of the string into the time direction. This is particularly interesting because it implies that the ergosphere is shifted, as well as, possibly, the innermost stable circular orbits of objects close to the black hole. The behaviour of test objects around this system is still to be explored, however based on the above, such a study is indeed compelling.

To summarise, the Kerr vortex system has turned out to be quite surprising in its degree of phenomenological intricacy. Coupled with the fact that it is precisely the rotating system which is physically relevant, this certainly warrants further study of these objects in the light of the observations made herein.

Chapter 4

Vortex Hair for AdS Black Holes

In Chapter 4 we studied the composite Kerr-vortex system, and saw that not only can a stable, time-independent configuration of the two objects exist, but furthermore, the addition of cosmic string hair to the rotating black hole opens up a new branch of phenomenology in these spacetimes.

Formally, we saw that a rotating black hole can only consistently accommodate a cosmic string piercing through it if the gauge field picks up a time component. This component produces an electric field close to the horizon. One can think about this as a cosmological manifestation of Faraday's law, namely that rotation in the presence of an external magnetic field produces an electric field. Indeed, the timelike direction is not orthogonal to the azimuthal spacelike direction in the Kerr spacetime, therefore one cannot think about quantities associated with the azimuthal direction independently from those associated with the time direction. Another consequence of this emerged in the way that the cosmic string perturbs the Kerr spacetime. In a static background, it is well known that a cosmic string produces a conical deficit angle in the azimuthal direction. However, in the Kerr spacetime, we demonstrated that the metric is conical with respect to a local co-rotating frame, which includes the time direction. Finally, an exploration of low mass extremal black holes confirmed that these black holes are able to expel the vortex flux from their cores, exhibiting a Meissner effect. Unlike Reissner-Nordstrom black holes, the transition between expulsion and piercing turns out to be first order, once again due to the presence of the additional degree of freedom in the gauge field.

We will now investigate the impact of a negative cosmological constant on the black hole and vortex system. To be completely general, we will consider Kerr-Newman AdS black holes, therefore we cover all previously studied cases in various limits when the AdS length is taken to infinity.

While the inclusion of a negative cosmological constant may not be relevant for cosmology, from a theoretical perspective the system is very interesting: In holography, a vortex in the bulk has an interpretation as a defect in the dual CFT [91, 112], corresponding in the dual superfluid to heavy pointlike excitations around which the phase of the condensate winds.

In the current work, we will treat the vortex as a probe, and obtain approximate analytic as well as full numerical forms for the profiles of the vortex fields. We will then study the Meissner effect in detail.

This Chapter is based on the work done in Ref. [116].

4.1 Vortices in AdS

We have thus far been discussing vortices in black hole backgrounds which are asymptotically flat. Therefore, far away from the black hole, the system will closely resemble the Nielsen–Olesen vortex in flat space. For the AdS black hole, the background is not asymptotically flat, but rather far away from the black hole, one will feel a negative cosmological constant in an otherwise empty spacetime. Therefore, before discussing black holes, our first task is to understand what the vortex would look like in a pure AdS geometry.

The AdS background may be described by

$$\begin{aligned} ds^2 &= -\Big(1+\frac{r^2}{\ell^2}\Big)dt^2 + \frac{dr^2}{\big(1+\frac{r^2}{\ell^2}\big)} + r^2 d\theta^2 + r^2\sin^2\theta d\phi^2 \\ &= -\frac{\ell^2+R^2}{\ell^2(1-Z^2)}dt^2 + \frac{\ell^2+R^2}{(1-Z^2)^2}dZ^2 + \frac{\ell^2 dR^2}{\ell^2+R^2} + R^2 d\phi^2\,. \end{aligned} \tag{4.1.1}$$

By writing the AdS metric in this second, cylindrical, form it becomes clear that if we align the vortex in the $\{R, \phi\}$ plane, the equations of motion will be independent of Z, and hence as with the case in flat space, our vortex (2.3.10)-(2.3.11) can be represented by a set of ordinary differential equations.

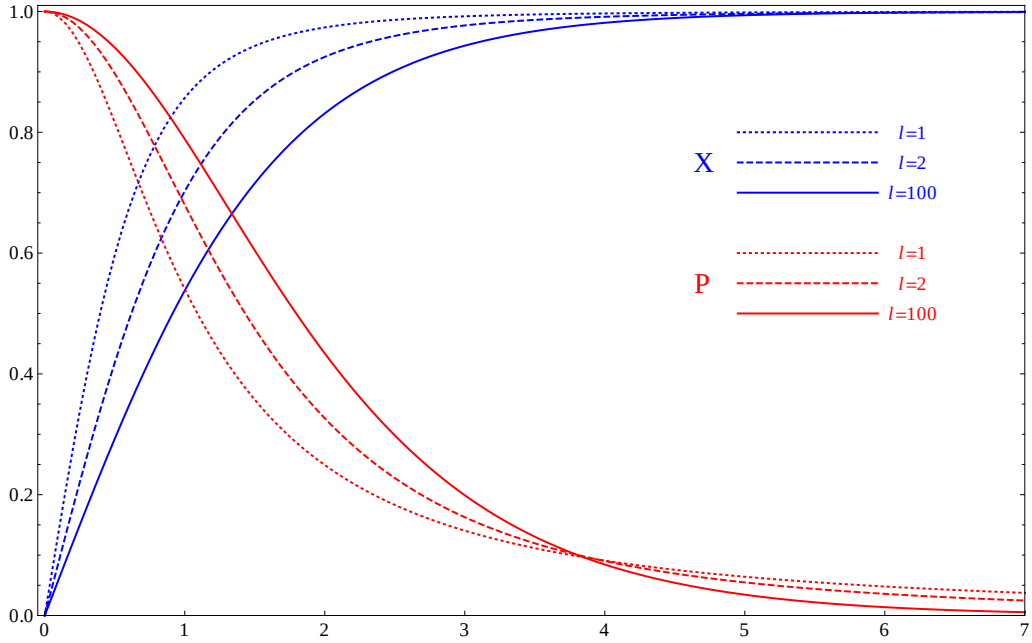

Figure 4.1: **AdS-NO vortex:** The values of X and P for the AdS NO vortex are depicted as functions of R.

Employing the Nielsen–Olesen ansatz for the fields in (2.4.14), these equations take the form

$$\begin{aligned} \left(1+\frac{R^2}{\ell^2}\right)X_0''+\left(\frac{4R}{\ell^2}+\frac{1}{R}\right)X_0'-\frac{P_0^2X_0}{R^2}-\frac{1}{2}X_0(X_0^2-1)=0\,, \\ \left(1+\frac{R^2}{\ell^2}\right)P_0''+\left(\frac{2R^2}{\ell^2}-1\right)\frac{P_0'}{R}=\frac{X_0^2P_0}{\beta}\,. \end{aligned} \tag{4.1.2}$$

For $R \to 0$, we see that the effects of the negative cosmological constant on the vortex drop away, and the equations in the AdS background resemble the Nielsen-Olesen vortex equations in (2.4.15). Therefore, the innermost core region of the string does not notice the effects of ℓ. For $R \gtrsim \ell$ however, the functions X_0 and P_0 are modified by the cosmological constant. In particular, one can see that their asymptotic profiles become power law rather than exponential.

Figure 4.1 displays the profiles of the Higgs and gauge fields for the AdS vortex, across two orders of magnitude for the AdS length ℓ. At large ℓ, the vortex closely resembles the flat-space Nielsen–Olesen vortex, whereas as ℓ drops down towards the scale of the vortex, we see that the profiles become much more narrow, with the power law fall-off to vacuum becoming more pronounced. Note that while it is

possible to solve the equations at a scale of $\ell \lesssim 1$, in this region a physical vortex might not in fact arise. This is due to the fact that the false vacuum of the Higgs field becomes stable for Compton wavelengths above the AdS scale [113].

4.2 Vortices in Kerr-AdS

We will now study two limits of the vortex and black hole system analytically. The first is the thin string limit, which should allow us to obtain an analytic approximation to the full vortex solution that can only be found numerically. The second is the extremal limit, which should allow us to investigate the Meissner effect, and construct a proof for its existence.

We begin by writing down the charged rotating black hole solution [114]

$$ds^2 = -\frac{\Delta}{\Sigma}\left[dt - \frac{a\sin^2\theta}{\Xi}d\phi\right]^2 + \frac{\Sigma}{\Delta}dr^2 + \frac{\Sigma}{S}d\theta^2 + \frac{S\sin^2\theta}{\Sigma}\left[adt - \frac{r^2+a^2}{\Xi}d\phi\right]^2 , \quad (4.2.3)$$

where

$$\begin{aligned} \Sigma &= r^2 + a^2\cos^2\theta\,, \quad \Xi = 1 - \frac{a^2}{\ell^2}\,, \quad S = 1 - \frac{a^2}{\ell^2}\cos^2\theta\,, \\ \Delta &= (r^2+a^2)\Big(1+\frac{r^2}{\ell^2}\Big) - 2mr + q^2\,, \end{aligned} \quad (4.2.4)$$

and the $U(1)$ potential is

$$A = \frac{qr}{\Sigma}\left(dt - \frac{a\sin^2\theta}{\Xi}d\phi\right) . \quad (4.2.5)$$

The mass M, the charge $\mathcal{Q}$, and the angular momentum J are related to the parameters m, q, and a as follows:

$$GM = \frac{m}{\Xi^2}\,, \quad G\mathcal{Q} = \frac{q}{\Xi}\,, \quad GJ = \frac{am}{\Xi^2}\,. \quad (4.2.6)$$

The ergosphere is located at $\Delta = a^2 S\sin^2\theta$, and the horizon at $\Delta = 0$. Note that there is a restriction on the values of a, namely that they should always lie below the scale of ℓ. This restriction impacts the ϕ direction, and, on the equator, the θ direction. Furthermore, it affects all parameters associated with the spacetime as defined above, as well as the $U(1)$ gauge potential. Solving $\Delta = 0$, which is a quartic function of r, the outer horizon r_+ corresponds to the largest real root. The

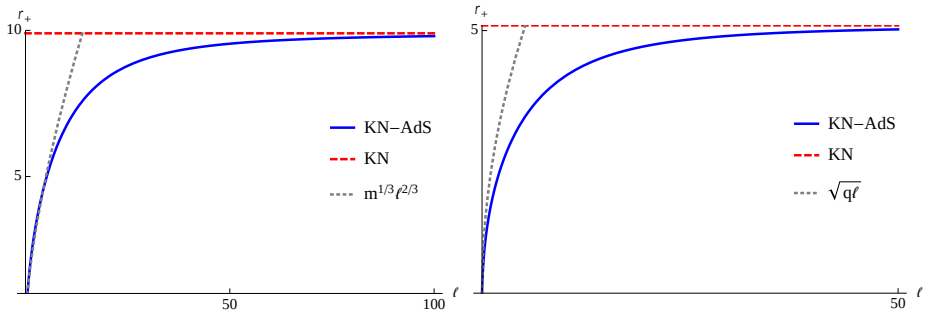

Figure 4.2: **Behaviour of the horizons:** The behaviour of the non-extremal horizon (Left) for $m = 5$, $a = 1$ and $q = 0$, and of the extremal horizon (Right) for $a = 1$ and $q = 5$, as functions of ℓ.

functional form of $r_+(m, a, q, \ell)$ is complicated, however in the extremal limit where $r_+ = r_-$ it reduces to a more tractable form, $r_+(a, q, \ell)$, namely

$$r_+ = \frac{\ell}{\sqrt{6}}\left[\left(\left(1+\frac{a^2}{\ell^2}\right)^2 + 12\left(\frac{a^2+q^2}{\ell^2}\right)\right)^{1/2} - \left(1+\frac{a^2}{\ell^2}\right)\right]^{1/2}. \tag{4.2.7}$$

The extremal horizon shrinks significantly as ℓ falls to low values, and in the presence of a charge q asymptotes to $\sqrt{q/\ell}$. This is also true for the outer horizon radius (which asymptotes to $m^{1/3}\ell^{2/3}$ in the absence of a charge). Finally, for large ℓ the outer and extremal horizons asymptote to their Kerr-Newman counterparts. The generic behaviour of the horizons is illustrated in figure 4.2.

Due to the presence of rotation, there are three degrees of freedom that are relevant for the description of the vortex in this background, namely X, P_ϕ and P_t.

The equations for these fields become

$$\begin{aligned} 0 &= \Delta X_{,rr} + \Delta' X_{,r} + S X_{,\theta\theta} + \cot\theta\Big(S + \frac{2a^2}{\ell^2}\sin^2\theta\Big) X_{,\theta} \\ &\quad + \Sigma P_\mu^2 X - \frac{\Sigma}{2} X(X^2-1)\,, \end{aligned} \tag{4.2.8}$$

$$\begin{aligned} \frac{X^2}{\beta} P_t &= \frac{\triangle}{\Sigma} P_{t,rr} + \frac{S}{\Sigma} P_{t,\theta\theta} + \frac{2a\Xi\cot\theta}{\Sigma^3}\Big(\rho^2 S - \Delta + \frac{a^2}{\ell^2}\Sigma\sin^2\theta\Big) P_{\phi,\theta} \\ &\quad - \frac{a\Xi}{\Sigma^3}\Big(2r(Sa^2\sin^2\theta - \Delta) + \Sigma\Delta'\Big) P_{\phi,r} \\ &\quad + \frac{\cot\theta}{\Sigma^3}\left(S\big(\rho^4 + a^4\sin^4\theta\big) - 2a^2\sin^2\theta\Big(\Delta - \frac{\rho^2\Sigma}{\ell^2}\Big)\right) P_{t,\theta} \\ &\quad - \frac{\sin^2\theta}{\Sigma^3}\Big(a^2\big(2r\rho^2 S + \Sigma\Delta'\big) - \frac{2r\rho^2\Delta}{\sin^2\theta}\Big) P_{t,r}\,, \end{aligned} \tag{4.2.9}$$

$$\begin{aligned} \frac{X^2}{\beta} P_\phi &= \frac{\Delta}{\Sigma} P_{\phi,rr} + \frac{S}{\Sigma} P_{\phi,\theta\theta} + \frac{\rho^2}{\Sigma^3}\big(2rSa^2\sin^2\theta + \Sigma\Delta' - 2r\Delta\big) P_{\phi,r} \\ &\quad + \frac{\cot\theta}{\Sigma^3}\left(2a^2\sin^2\theta\Big(\Delta - \frac{a^2}{\ell^2}\Sigma\sin^2\theta\Big) - S\Big(a^2\sin^2\theta(\rho^2-\Sigma) + \rho^4\Big)\right) P_{\phi,\theta} \\ &\quad + \frac{2\cot\theta a^3\sin^4\theta}{\Xi\Sigma^3}\left(\Delta - \rho^2\Big(1 + \frac{r^2}{\ell^2}\Big)\right) P_{t,\theta} \\ &\quad + \frac{a\sin^2\theta}{\Xi\Sigma^3}\Big(2r\big(\rho^4 S - \Delta(\Sigma+\rho^2)\big) + \rho^2\Sigma\Delta'\Big) P_{t,r}\,, \end{aligned} \tag{4.2.10}$$

where $\rho^2 = r^2 + a^2$ has been introduced for visual clarity, $\Delta' = d\Delta/dr$, and

$$P_\mu^2 = \frac{(\rho^2 P_t + a\Xi P_\phi)^2}{\Sigma\Delta} - \frac{(\Xi P_\phi + a\sin^2\theta P_t)^2}{\Sigma S\sin^2\theta}\,. \tag{4.2.11}$$

4.2.1 Approximate solution

As with the asymptotically flat black hole spacetimes, at small enough scales the effects of curvature are expected to be irrelevant for the vortex. In this thin string limit, one can find an appropriate combination of r and θ that acts as a radial distance from the core of the vortex in cylindrical coordinates, such that the vortex equations may be written as ordinary differential equations at leading order.

For the AdS black hole background, consider the function

$$R \equiv \frac{\rho}{\sqrt{\Xi}}\sin\theta\,, \tag{4.2.12}$$

which tends to the Kerr expression $\rho\sin\theta$ as $\ell \to \infty$. Then, assuming that the vortex is much thinner than the black hole horizon radius implies that $\rho \gg 1$,

and restricting attention to the core region of the vortex [$R < \mathcal{O}(10)$] implies that $\sin\theta \ll 1$. The metric functions may then be expanded as

$$\Sigma = \rho^2\left(1 - \frac{a^2R^2\Xi}{\rho^4}\right) \simeq \rho^2\,, \quad S = \Xi\left(1 + \frac{a^2R^2}{\ell^2\rho^2}\right) \simeq \Xi\,, \tag{4.2.13}$$

and derivatives as

$$\begin{aligned} \frac{\partial}{\partial r} &= \frac{Rr}{\rho^2}\frac{d}{dR}\,, \qquad \frac{\partial}{\partial\theta} = \frac{\rho}{\sqrt{\Xi}}\left(1 - \frac{\Xi R^2}{\rho^2}\right)^{1/2}\frac{d}{dR} \simeq \frac{\rho}{\sqrt{\Xi}}\frac{d}{dR}\,, \\ \Delta\frac{\partial^2}{\partial r^2} + S\frac{\partial^2}{\partial\theta^2} &= \left[S\Big(\frac{\rho^2}{\Xi} - R^2\Big) + \frac{\Delta R^2r^2}{\rho^4}\right]\frac{d^2}{dR^2} + \Big(\frac{\Delta a^2}{\rho^4} - S\Big)R\frac{d}{dR} \\ &\simeq \rho^2\Big(1 + \frac{\Delta R^2}{\rho^4}\Big)\frac{d^2}{dR^2}\,. \end{aligned} \tag{4.2.14}$$

Following the same procedure as for the Kerr case in Section 3.1.1, one can then extract approximate analytic forms for the fields by expanding the vortex equations out to order $\mathcal{O}(\rho^{-2})$. This procedure suggests the following forms for the approximate analytic solution:

$$X \simeq X_0(R)\,, \quad P_\phi \simeq P_0(R)\,, \quad P_t \simeq \frac{a}{\rho^2}\Big(\frac{\Delta}{\rho^2} - \Xi\Big)P_0(R)\,, \tag{4.2.15}$$

which to leading order give the approximate equations:

$$\begin{aligned} 0 &= \left(1 + \frac{\Delta R^2}{\rho^4}\right)X_0'' + \left(1 + \frac{4R^2}{\ell^2}\right)\frac{X_0'}{R} - \frac{P_0^2X_0}{R^2} - \frac{X_0}{2}(X_0^2 - 1)\,, \\ \frac{X_0^2}{\beta}P_0 &= \left(1 + \frac{\Delta R^2}{\rho^4}\right)P_0'' - \left(1 + \frac{(2\Delta - r\Delta')\,R^2}{\rho^4}\right)\frac{P_0'}{R}\,. \end{aligned} \tag{4.2.16}$$

There are several things to notice about the forms of the corrections in these equations. For the Kerr case, the metric function $\Delta = \mathcal{O}(\rho^2)$ to leading order, therefore we did not retain the terms that were proportional to Δ, and we recovered the Nielsen–Olesen vortex equations (2.4.15) at leading order. However, in the presence of a negative cosmological constant, we instead find that away from the horizon, $\Delta \sim \rho^4/\ell^2$ to leading order. Retaining the terms proportional to Δ, we then recover the AdS Nielsen-Olesen equations (4.1.2) at leading order. On the other hand, bearing in mind that the horizon radius shrinks rapidly for low values of ℓ, we see that retaining terms proportional to R^2/ℓ^2, which only makes sense if $\ell \lesssim R$, could take us outside of the realm of validity of the thin string limit, which relies on the string being much smaller than the black hole horizon. To remain safely within the approximation, we require $\ell > \mathcal{O}(10)$, which allows us to drop these correction terms.

Finally, we also see that on (or near) the horizon, the $\mathcal{O}(R^2/\ell^2)$ corrections to the Nielsen-Olesen equations fail to have the precise AdS form. As a consequence, while the approximate analytic solution is reliable to good precision away from the horizon of the black hole, near the horizon we would expect corrections to this solution at order $\mathcal{O}(\ell^{-2})$.

Note that asymptotically, P_t in (4.2.15) becomes proportional to P_ϕ and the gauge potential becomes

$$\boldsymbol{P} = P_\phi d\phi + P_t dt \sim P_0(R)\left(d\phi + \frac{a}{\ell^2}dt\right), \tag{4.2.17}$$

implying the presence of an electric field at large r along the string. This is in fact an artifact of the Boyer-Lindquist style coordinates we have used in (4.2.3), which asymptote to AdS_4 in a rotating frame with angular momentum $\Omega_\infty = a/\ell^2$ [115]. Employing new variables,

$$\varphi = \phi + \frac{a}{l^2}t\,, \quad T = t\,, \tag{4.2.18}$$

the asymptotic rotation is removed, and $\boldsymbol{P}$ becomes

$$\boldsymbol{P} = P_0(R)\Big(d\varphi - \frac{a(2mr - q^2)}{\rho^4}dT\Big)\,, \tag{4.2.19}$$

which exhibits the appropriate fall-off at large r.

Figure 4.2.1 shows a comparison of this pseudo-analytic approximation with a numerically obtained solution for an extremal low mass lowish ℓ black hole. We take the values $m = 3, \ell = 20, q = 0$, and with $a \simeq 2.939$ at its extremal value in order to draw a parallel with the plot in [98]. What is clearly shown is that the approximation is extremely good almost everywhere, the only slight discrepancy appearing near the event horizon – as expected given the structure of the corrections to the approximation there.

4.2.2 Extremal black holes

We have seen that in the presence of an axisymmetric cosmic string, small black holes with extremal horizons are able to exhibit a Meissner effect and expel the magnetic flux of the string from their interiors. For the Reissner-Nordstrom case, we saw immediately that the vortex equations on the horizon decouple from the bulk, and

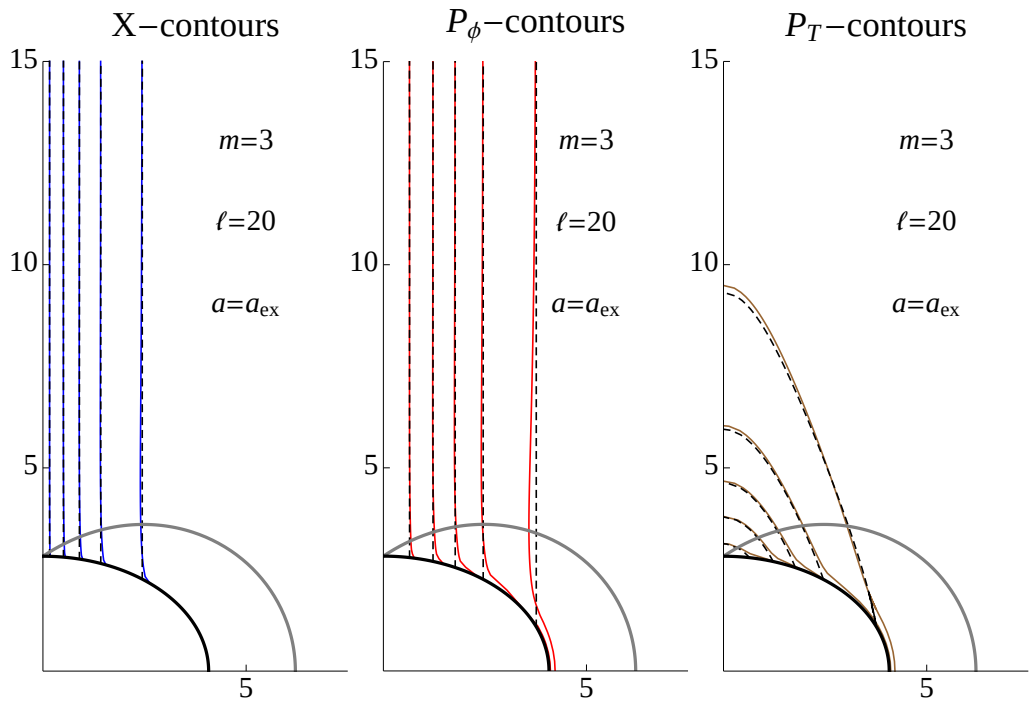

Figure 4.3: **Approximate vs. numerical solution:** In each case the numerical solution is shown in solid colour, and the approximation in dashed black. Contours of $0.1 - 0.9$ (in steps of 0.2) of the range of each field are shown. From left to right: The Higgs field in blue, the P_ϕ field in red, and P_T (the component with respect to the nonrotating frame at infinity) in brown. For P_T, we show contours of $0.1 - 0.9$ of the maximal negative value, which is attained on the poles of the horizon. The outer grey curve represents the boundary of the ergosphere.

admit a flux expelled solution, where the fields remain in the false vacuum uniformly across the horizon. In the case of Kerr, the two components of the gauge field can be written into linear combinations P and Q, where finiteness on the horizon imposes $Q(r_+) = 0$. The horizon equations do not decouple in general, however in the special case of flux expulsion, namely $X(r_+) = 0$, $P(r_+) = 1$, the decoupling takes place. These flux expelled solutions were shown to be extendable into the bulk for both Reissner-Nordstrom [95] and Kerr [98] black holes.

In the case of Kerr, one finds that the field Q is discontinuous between piercing and expulsion. This leads to a first order phase transition, whereas for Reissner-Nordstrom, the phase transition is second order, where the order parameter for the transition is the magnitude of the Higgs field X measured at the equator.

We will now investigate the possible existence of a Meissner effect in the case of AdS-Kerr-Newman black holes. Given that these black holes have extremal limits, and are extensions of the Kerr-Newman family to one more parameter ℓ, it is to be expected that they too will exhibit a flux-expelling phase. We begin by defining new variables P and Q, where finiteness implies $Q(r_+) = 0$:

$$SP = \Xi P_\phi + a\sin^2\theta P_t\,, \quad Q = \rho^2 P_t + a\Xi P_\phi\,. \tag{4.2.20}$$

The field equations (4.2.8)-(4.2.9) become

$$\begin{aligned} 0 &= \frac{\Delta}{\Sigma}X_{,rr} + \frac{\Delta'}{\Sigma}X_{,r} + \frac{1}{\Sigma\sin\theta}\Big(S\sin\theta X_{,\theta}\Big)_{,\theta} \\ &\quad + \left(\frac{Q^2}{\Sigma\,\Delta} - \frac{P^2}{\Sigma\,S\,\sin^2\theta}\right)X - \frac{X}{2}(X^2-1), \end{aligned} \tag{4.2.21}$$

$$\begin{aligned} \frac{X^2 P}{\beta} &= \frac{\Delta}{\Sigma}P_{,rr} + \frac{S}{\Sigma}P_{,\theta\theta} + \frac{\Sigma\Delta' - 2r\Delta}{\Sigma^2}P_{,r} + \frac{\cot\theta}{\Sigma}\Big(4\frac{a^2}{l^2}\sin^2\theta - \frac{S}{\Sigma}\big(\Sigma - 2a^2\sin^2\theta\big)\Big)P_{,\theta} \\ &\quad + \frac{2a\sin^2\theta}{\Sigma^2}\left((rQ_{,r} - \cot\theta\,Q_{,\theta} - Q) + aP\Big(1 - \frac{r^2}{l^2}\Big) + rQ\right), \end{aligned} \tag{4.2.22}$$

$$\begin{aligned} \frac{X^2 Q}{\beta} &= \frac{\Delta}{\Sigma}Q_{,rr} + \frac{S}{\Sigma}Q_{,\theta\theta} + \frac{\cot\theta}{\Sigma^2}(2a^2\sin^2\theta(1+\frac{r^2}{\ell^2}) + S\,\Sigma)Q_{,\theta} \\ &\quad + \frac{2\Delta}{\Sigma^2}\Big(a(rSP_{,r} - S\cot\theta P_{,\theta} - (2-S)P) - rQ_{,r} + Q\Big)\,. \end{aligned} \tag{4.2.23}$$

Expanding these equations using the expansions

$$\begin{aligned} X &= \xi_0(\theta) + (r - r_+)\xi_1(\theta) + \dots , \\ P &= \pi_0(\theta) + (r - r_+)\pi_1(\theta) + \dots , \\ Q &= \psi_0(\theta) + (r - r_+)\psi_1(\theta) + \dots , \end{aligned} \tag{4.2.24}$$

as for the Kerr case, in the extremal limit and on the horizon they reduce to

$$(S\sin\theta\xi_0')' = \xi_0\sin\theta\left[\frac{S\pi_0^2}{\sin^2\theta} - \psi_1^2 - \frac{\Sigma_+}{2}(1-\xi_0^2)\right], \tag{4.2.25}$$

$$\begin{aligned} \left(\frac{S^2\pi_0'}{\Sigma_+\sin\theta}\right)' &= \pi_0 S\sin\theta\left[\frac{\xi_0^2}{\beta\sin^2\theta} - \frac{2a^2}{\Sigma_+^2}\left(1 - \frac{r_+^2}{\ell^2}\right)\right] \\ &\quad - \frac{2ar_+S\psi_1\sin\theta}{\Sigma_+^2}, \end{aligned} \tag{4.2.26}$$

$$\left(\frac{S\sin\theta\psi_1'}{\Sigma_+}\right)' = \frac{\xi_0^2\psi_1}{\beta}\sin\theta, \tag{4.2.27}$$

Note that these equations feature two extra parameters compared to the Kerr case in (3.2.30)-(3.2.32), namely ℓ and a. This is due to the fact that for extremal Kerr we have $r_+ = a$, which also leads to a particularly simple factorization of Σ_+, that is no longer possible in the present case. However, we see that setting $a = 0$, $\psi_1 \equiv 0$, and $S \equiv 1$, these equations reduce to the Reissner-Nordstrom horizon equations studied in [95], or setting $a \equiv r_+$ and $S \equiv 1$, they reduce to the Kerr case. Therefore we expect essentially the same analytic arguments for the existence of expulsion to hold here.

Let us look first at the behaviour of the function ψ_1, as this will give us the order of the phase transition. For the case of Kerr, we saw that $\psi_1 = 0$ if $\xi_0 \neq 0$. We will now show succintly that the same applies in the presence of ℓ. For a piercing solution, ξ_0 is nontrivial on the horizon, hence

$$S\beta\sin\theta\psi_1'(\theta) = \Sigma_+\int_0^\theta \xi_0^2\psi_1\sin\theta d\theta, \tag{4.2.28}$$

upon integrating (4.2.27). However, this cannot be true unless $\psi_1 = 0$. Indeed, evaluating (4.2.28) at the first point at which $\psi_1' = 0$ tells us that $\int_0^\theta \xi_0^2\psi_1\sin\theta = 0$. But just as we argued for the Kerr case, ψ_1 is either positive and increasing on this range, or negative and decreasing. Either way, the integrand is positive or negative definite, thus cannot be zero. Therefore $\psi_1 \equiv 0$ for a piercing solution

$\xi_0 \neq 0$. On the other hand, an expelling solution has $\xi_0 \equiv 0$, with $P_\phi(r_+) = 1$ and $P_t(r_+) = -a\Xi/\rho_+^2$, hence

$$P(r_+) \equiv \pi_0 = \frac{\Xi\Sigma_+}{\rho_+^2 S}\,, \qquad Q'(r_+) \equiv \psi_1 = -\frac{2ar_+\Xi}{\rho_+^2}\,, \tag{4.2.29}$$

where we use (4.2.26) to determine ψ_1 in the above. Thus we see that ψ_1 is discontinuous between expulsion and penetration, giving rise to a first order phase transition.

Having demonstrated that an expelling solution exists on the horizon, we must now extend this to the bulk. Namely, if the flux is expelled such that $X(r_+) \equiv 0$ and $P(r_+) \equiv 1$, then near r_+ where $X > 0$, $P < 1$ and $X^2 \ll 1$, both $\partial_r(\Delta\partial_r X) > 0$ and $(Q^2/\Delta\Sigma - X^2/2) > 0$. Referring to (4.2.21), this implies

$$(S\sin\theta X_{,\theta})_{,\theta} + \frac{(r_+^2 + a^2\cos^2\theta)X}{2}\sin\theta < \frac{SP^2}{\sin\theta}X < \frac{SX}{\sin\theta}\,, \tag{4.2.30}$$

which we take as a condition for a flux expelling solution to exist. Integrating on $[\theta_0, \pi/2]$ then yields

$$S\sin\theta_0 X_{,\theta_0} > \int_{\theta_0}^{\pi/2}\left(\frac{(r_+^2 + a^2\cos^2\theta)\sin\theta}{2} - \frac{S}{\sin\theta}\right)X d\theta\,. \tag{4.2.31}$$

Defining α so that $\Sigma_+\sin^2\alpha/S = 2$, by taking $\theta_0 > \alpha$ we can bound this integral from below using $X(\theta) > X(\theta_0)$. We can also bound the derivative of X by $X_{,\theta_0} < \frac{X(\theta_0)-X(\alpha)}{\theta_0-\alpha} < \frac{X(\theta_0)}{\theta_0-\alpha}$, leading to

$$S\sin\theta_0\frac{X(\theta_0)}{\theta_0-\alpha} > S\sin\theta_0 X_{,\theta_0} > X(\theta_0)\int_{\theta_0}^{\pi/2}\left(\frac{(r_+^2 + a^2\cos^2\theta)\sin\theta}{2} - \frac{S}{\sin\theta}\right)d\theta\,, \tag{4.2.32}$$

which implies

$$\frac{(\theta_0-\alpha)}{S(\theta_0)\sin\theta_0}\left(\frac{r_+^2\cos\theta_0}{2} + \frac{a^2\cos^3\theta_0}{6} + \Xi\log\tan\Big(\frac{\theta_0}{2}\Big) - \frac{a^2}{l^2}\cos\theta_0\right) < 1 \tag{4.2.33}$$

on the interval $[\alpha, \pi/2]$. If this inequality is violated, then we cannot have flux expulsion, and the vortex *must* pierce the black hole. Note, if $a = 0$, then (4.2.33) is independent of ℓ, and reduces to the previously explored Reissner-Nordstrom relation [95], giving the same upper bound on the horizon radius for flux expulsion of $\sqrt{8.5}$. For $a \neq 0$, we must explore the $\{a, \ell\}$ phase plane (having ensured that a solution α exists) to determine the upper bound on the horizon radius. Clearly if ℓ

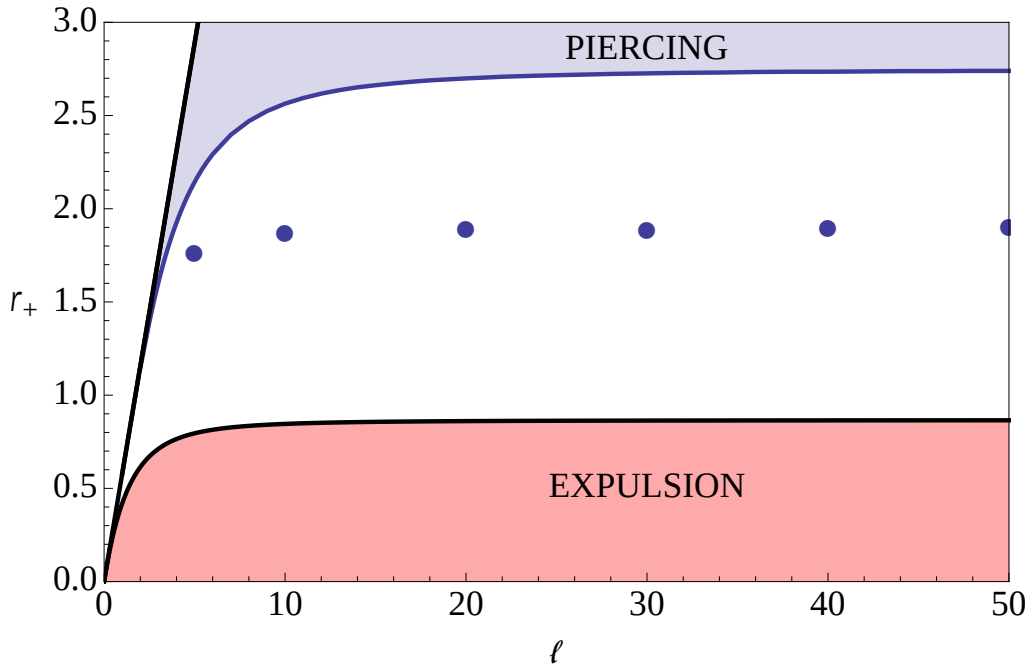

Figure 4.4: **Meissner effect:** An illustration of the analytic bounds on the critical horizon radius for the Meissner effect for $q = 0$. In the shaded regions, the vortex should either pierce the horizon, or be expelled as indicated. The critical radius therefore lies between these two bounds. For sufficiently low ℓ, flux is always expelled. Numerically obtained transition radii are indicated. The solid $r_+ = \ell/\sqrt{3}$ line on the left indicates the $a = \ell$ singular limit.

drops too low, we require a large charge to allow for a solution to α. Hence for a given q, we expect a minimal value of ℓ for this upper bound to exist. This is shown most clearly for $q = 0$, in figure 4.4.

To argue that a Meissner effect should exist for sufficiently low horizon scales, we assume a piercing solution to (4.2.25)-(4.2.27) exists, in which X and P will have nontrivial profiles symmetric around $\theta = \pi/2$, with X maximised and P minimised (at least for large ℓ or small $a < q$) at $\pi/2$. If $a = 0$, the argument of [95] can be used to deduce that for $r_+ \lesssim 0.7$ the flux must be expelled, and this argument can be extended to include small a.

Following [95], assume a piercing solution exists, then (4.2.25) and (4.2.26) have smooth solutions for ξ_0 and π_0 in which ξ_0 increases from zero at the poles to a

maximum at the equator, and π_0 decreases from unity at the poles to a minimum at the equator. Evaluating (4.2.25) and (4.2.26) at the equator gives the relations:

$$\xi_0''\left(\frac{\pi}{2}\right) = \xi_0\left[\pi_0^2 + \tfrac{r_+^2}{2}\left(\xi_0^2-1\right)\right] \leq 0 \quad \Rightarrow \pi_0^2 \leq \frac{r_+^2}{2}\left(1-\xi_0^2\right) \leq \frac{r_+^2}{2}\,, \tag{4.2.34}$$

$$\pi_0''\left(\frac{\pi}{2}\right) = \pi_0\left[\tfrac{\xi_0^2 r_+^2}{\beta} - \tfrac{2a^2}{r_+^2}\left(1-\tfrac{r_+^2}{\ell^2}\right)\right] \geq 0 \quad \Rightarrow\ r_+^4 \geq \xi_0^2 r_+^4 \geq 2a^2\beta\Big(1-\frac{r_+^2}{\ell^2}\Big) \tag{4.2.35}$$

Since $\pi_0 \leq 1$, the first relation gives no new information unless $r_+ < \sqrt{2}$, so we will assume this from now on. The second relation clearly gives no information if $a = 0$. For $a \neq 0$, we know that the size of the horizon cannot exceed the size of the Kerr-Newman horizon,

$$r_+^2 \leq a^2 + q^2\,, \tag{4.2.36}$$

therefore we see that

$$4a^4 > (a^2+q^2)^2 \geq 2a^2\beta \Rightarrow a > \sqrt{\beta/2}\,, \tag{4.2.37}$$

thus for $\sqrt{\beta} = \mathcal{O}(1)$, the bound (4.2.35) is violated at all ℓ for $q < a \lesssim 0.6$. On the other hand, finiteness of the metric requires that at all times we must have $a < \ell$, therefore for small ℓ we have from (4.2.7)

$$r_+^2 \simeq q\ell\,, \tag{4.2.38}$$

so the bound is violated for sufficiently small ℓ and q.

We will now generalise the argument for the Reissner-Nordstrom case in Section 2.5.2 to find a lower bound on r_+, given that a is too small to give any useful information in (4.2.35). We begin by assuming a piercing solution. Using (4.2.34), at $\theta = \pi/2$ (4.2.35) becomes

$$\pi_0''\left(\frac{\pi}{2}\right) \leq \frac{r_+}{\sqrt{2}}\left[\frac{\xi_0^2 r_+^2}{\beta} - \frac{2a^2}{r_+^2}\Big(1-\frac{r_+^2}{\ell^2}\Big)\right]\sqrt{1-\xi_0^2} \leq \frac{\sqrt{2}r_+^3}{3\sqrt{3}\beta}\left(1-\frac{2a^2\beta}{r_+^4}\Big(1-\frac{r_+^2}{\ell^2}\Big)\right)^{3/2}, \tag{4.2.39}$$

where we maximise over ξ_0 in the second inequality. We now have an upper bound on π_0'' at the equator. To obtain a lower bound, we use the fact that at some $\theta \in (\theta_0, \pi/2)$, we must have $\pi_0''(\theta_0) = 0$, which is where π_0' will be maximally negative. Using that $\pi_0''(\pi/2) \geq -\pi_0'(\theta_0), /(\pi/2-\theta_0)$ (4.2.26), yields

$$\pi_0'(\theta_0) = -\frac{\pi_0 \tan\theta}{\beta}\frac{\Sigma_+^2\xi_0^2 - 2a^2\beta\sin^2\theta\left(1-r_+^2/\ell^2\right)}{S(\Sigma_+ - 2a^2\sin^2\theta) - 4\Sigma_+(a^2/\ell^2)\sin^2\theta}\bigg|_{\theta=\theta_0}. \tag{4.2.40}$$

Therefore we can write

$$|\pi_0'(\theta_0)| \leq \frac{\pi_0(\theta_0)\tan\theta_0}{\beta}\frac{\Sigma_+^2(\theta_0)-2a^2\beta\sin^2\theta_0\left(1-r_+^2/\ell^2\right)}{S(\theta_0)(\Sigma_+(\theta_0)-2a^2\sin^2\theta_0)-4\Sigma_+(\theta_0)(a^2/\ell^2)\sin^2\theta_0}$$
$$\leq \frac{\left(r_+^4-2a^2\beta\left(1-r_+^2/\ell^2\right)\right)\tan\theta_0}{\left(r_+^2(1-4a^2/\ell^2)-2a^2\right)\beta}\,. \tag{4.2.41}$$

We see that this bound is only meaningful in the case that $r_+^2(1-4a^2/\ell^2) > 2a^2$, so we will assume this holds. Thus we find

$$\frac{\pi}{2}-\theta_0 < \cot\theta_0 \leq \frac{r_+^4-2a^2\beta\left(1-r_+^2/\ell^2\right)}{\left(r_+^2(1-4a^2/\ell^2)-2a^2\right)\beta\,|\pi_0(\theta_0)'|}\,. \tag{4.2.42}$$

On the other hand, the value of π_0 at its minimum must be larger than it would have been if π_0 had decreased linearly from the poles with slope $|\pi_0'(\theta_0)|$, which is the largest possible slope. This allows us to write

$$1-\frac{\pi}{2}|\pi_0'(\theta_0)| < \pi_0(\pi/2) < \frac{r_+}{\sqrt{2}} \qquad \Rightarrow \qquad |\pi_0'(\theta_0)| > \frac{2}{\pi}\Big(1-\frac{r_+}{\sqrt{2}}\Big)\,, \tag{4.2.43}$$

leading to

$$\pi_0''\left(\frac{\pi}{2}\right) \geq \frac{|\pi_0'(\theta_0)|}{\pi/2-\theta_0} \geq \beta|\pi_0'(\theta_0)|^2\frac{r_+^2(1-4a^2/\ell^2)-2a^2}{r_+^4-2a^2\beta\left(1-r_+^2/\ell^2\right)}\,. \tag{4.2.44}$$

Combining the upper and lower bounds, we see that for a piercing solution to exist we must have

$$\frac{6\sqrt{6}\beta^2}{\pi^2}\Big(1-\frac{r_+}{\sqrt{2}}\Big)^2\left(1-\frac{2a^2\beta}{r_+^4}\Big(1-\frac{r_+^2}{\ell^2}\Big)\right)^{-5/2}\frac{r_+^2(1-4a^2/\ell^2)-2a^2}{r_+^7} < 1\,, \tag{4.2.45}$$

with $2 > r_+^2 > 2a^2/(1-4a^2/\ell^2)$ and $r_+^4+2a^2r_+^2/\ell^2 > 2a^2\beta$. The running of the lower bound (4.2.45) with a is depicted in figure 4.2.2.

For low ℓ and q, an alternate argument must be used, as we can no longer show that π_0 is minimised at $\pi/2$. This argument is detailed in Ref. [116].

All of the various features of the phase transition are depicted in figure 4.4, which shows the numerically obtained critical horizon radius as a function of ℓ for $q = 0$ together with the analytic lower and upper bounds on $r_{+,crit}$.

4.2.3 Numerical solution

The full solutions to the vortex equations (4.2.8)-(4.2.10) must be solved numerically. The numerical method employed is the gradient flow technique, just as for the vacuum Kerr case.

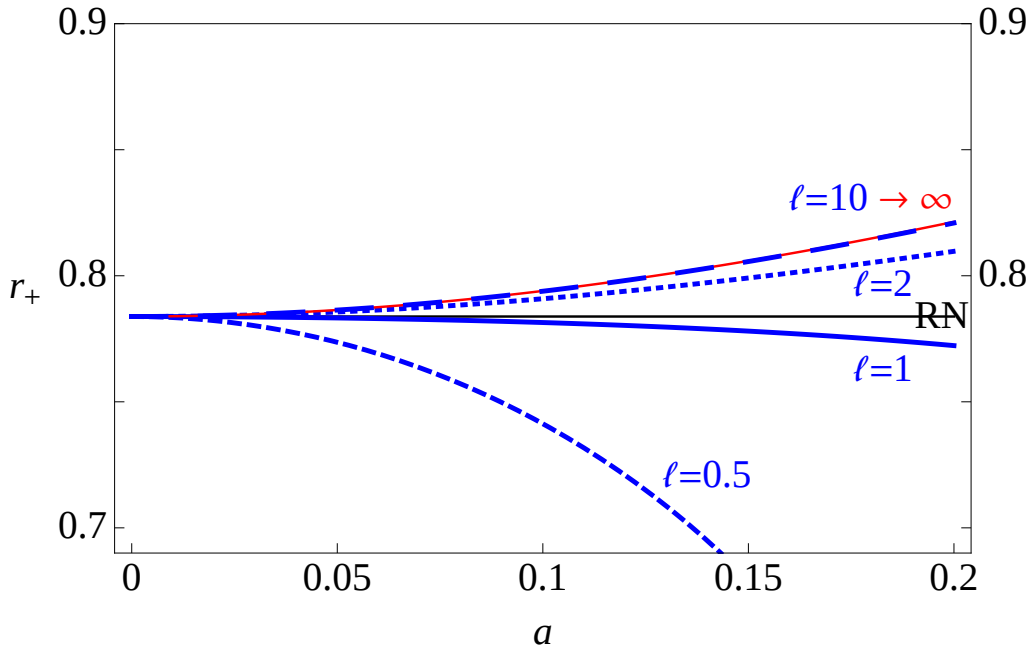

Figure 4.5: **Expulsion bound:** An illustration of the running of the lower bound with a. The bound is plotted for $\ell = 0.5, 1, 2, 10, \infty$ as labeled. For $\ell > 5$, the curve changes very little, as can be seen by the infinite ℓ curve depicted by a thin red line. The value at $a = 0$ is the RN value obtained in [95], and is shown as the horizontal solid black line.

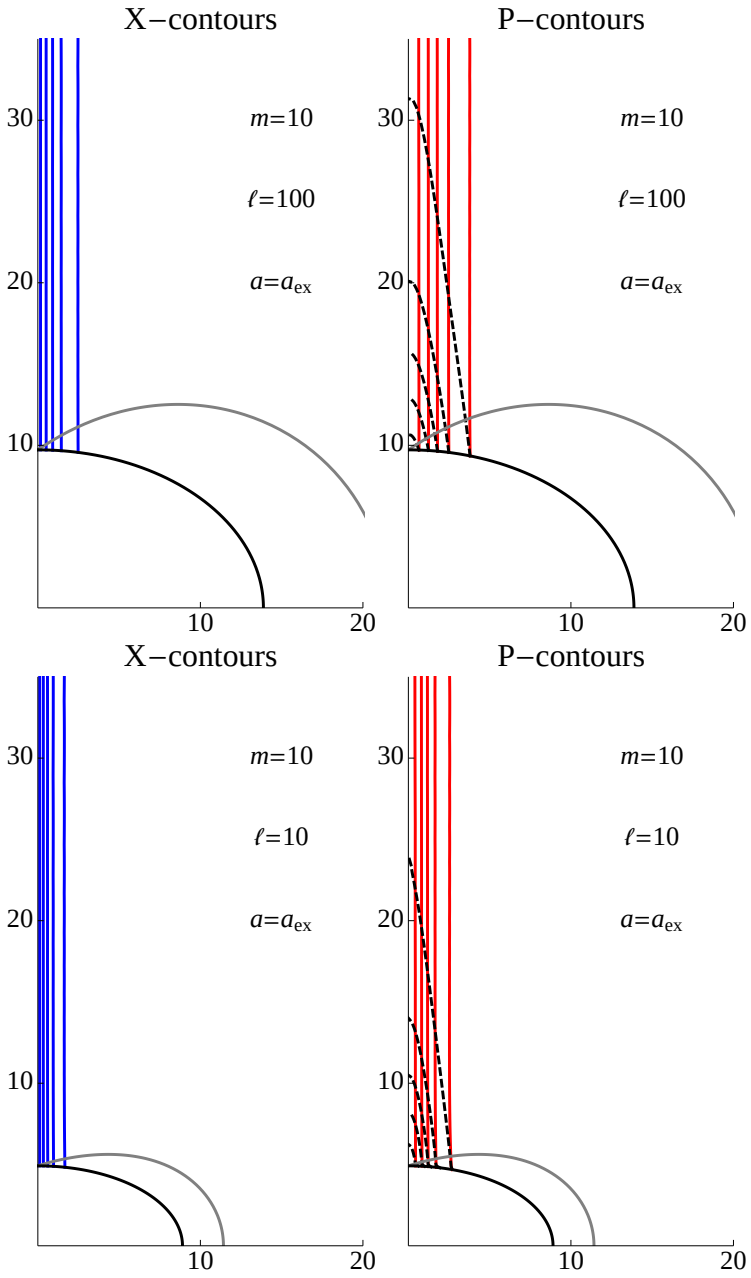

Figure 4.6: **AdS-Kerr vortex:** A depiction of the numerical solution for the AdS-Kerr vortex for an extremal uncharged rotating black hole. The upper plots have $\ell = 100$, the lower plots $\ell = 10$. In each case, the contours of the Higgs field are shown on the left in blue ($X = 0.1 - 0.9$ in steps of 0.2), and on the right, the angular component of the gauge field, P_φ in red (with the same contour steps as for X), and P_T in dashed black with contours of $0.1 - 0.9$ of $P_{T,min} = -0.0519, -0.116$ for the $\ell = 100$ and $\ell = 10$ cases respectively.

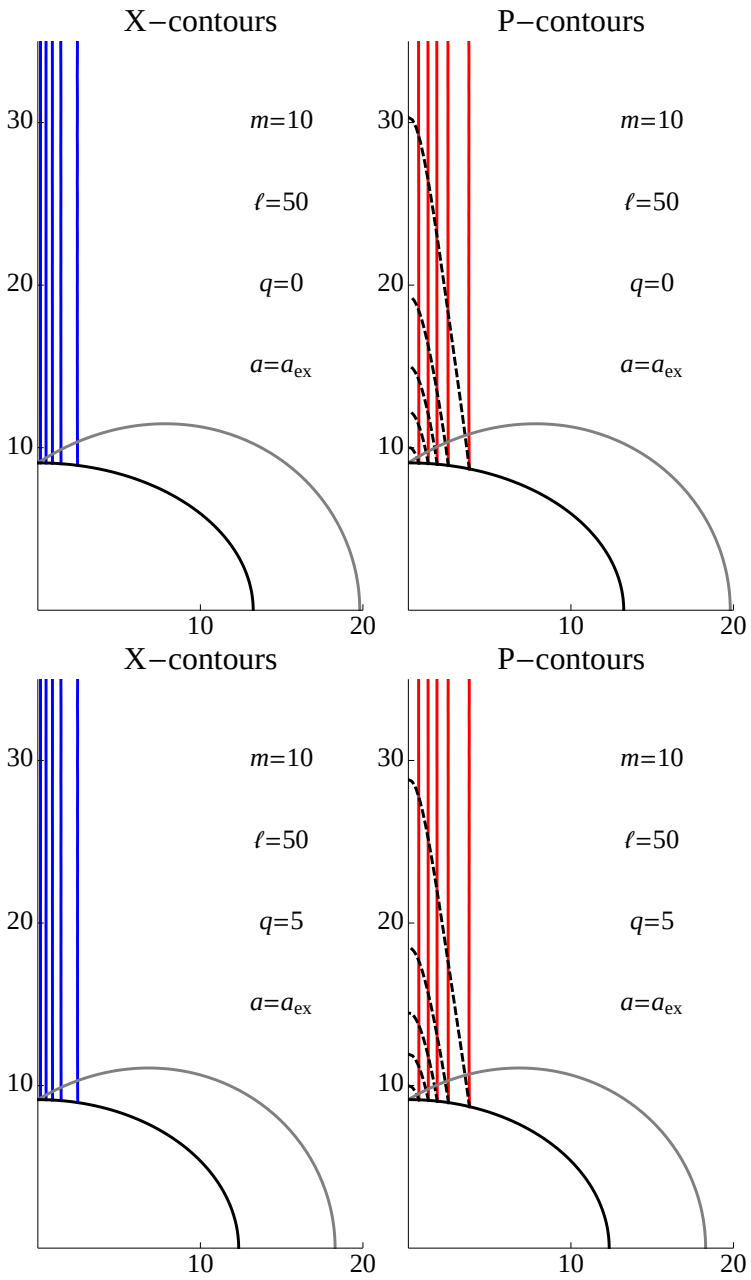

Figure 4.7: **AdS-Kerr-Newman vortex:** Numerical solutions for the AdS-Kerr-Newman vortex with $\ell = 50$ and $q = 0$, (upper) and $q = 5$ (lower) with the same contour conventions as for figure 4.2.3, with $P_{T,min} = -0.0569$ for $q = 0$, and $P_{T,min} = -0.0563$ for $q = 5$.

Figures 4.2.3 and 4.2.3 show a selection of the solutions obtained from the integration method above which highlight the effects of the parameters ℓ and q on the rotating black hole vortex. In all plots, we have chosen to illustrate the solution by plotting contour lines for each field of $0.1 - 0.9$ of the full range of the field in steps of 0.2. Thus, for the X and P_ϕ fields, we have shown the $0.1, 0.3, 0.5, 0.7$, and 0.9 contours, but for the P_T field (note – this is the gauge field component with respect to a *non-rotating* frame at infinity) the maximally negative value of P_T is attained on the horizon at the poles. The numerical values of these contours therefore vary from plot to plot. The actual value of $P_{T,min}$ is given in the captions.

Figure 4.2.3 shows the vortex solution for the case of $\ell = 100$ and $\ell = 10$ respectively, at the extremal limit with the charge parameter q set to zero. The solution away from the extremal limit is similar (see [98]), the main difference being that the actual numerical values of the P_T contours are lower. For $\ell = 100$, the plots are almost indistinguishable from the vacuum Kerr vortex solution analysed in [98], however, for $\ell = 10$, the effect of the cosmological constant can be easily seen. Comparing the figures, one notes that dropping the value of ℓ strongly impacts the size of both the black hole horizon as well as the vortex, causing the vortex width to tighten, the P_T fields to shrink closer to the horizon, which itself shrinks significantly.

Figure 4.2.3 then demonstrates the effect of adding a non-zero charge to the AdS-Kerr vortex. As can be seen, this does not significantly impact the vortex, and appears to merely shift the horizon and ergosphere inwards, while slightly causing the P_T contour lines to creep closer to the horizon, as is expected since the rotation parameter $a = a_{ex}$ will be lower with the charged black hole at the same mass.

4.3 Discussion

In this chapter we have explored the behaviour of the probe Abelian Higgs vortex in the background of an asymptotically AdS charged and rotating black hole.

We first obtained solutions for the vortex profiles in a pure AdS background. Compared to the flat-space case for which $\ell \to \infty$, we found that the effects of the negative cosmological constant are to tighten the vortex fields inwards near the core,

while asymptotically they fall towards the vacuum more gradually. Profiles for the AdS vortex fields over a range of ℓ are given in figure 4.1.

We then examined the vortex equations in the presence of the black hole. In the thin string limit, we were able to extract a very good approximate analytic solution to these equations, which we implemented as an initial condition for the numerical solution. A comparison between the approximate solution and the numerical solution is given in figure 4.2.1, for a low mass black hole with $GM = 3$. Given that the approximation is valid up to $\mathcal{O}(GM^{-2})$, at this mass range one would expect the deviations to be apparent. Nevertheless, the solutions are in very good agreement, with the discrepancies only starting to show very close to the horizon.

Finally, we investigated the extremal behaviour of the vortex and black hole system. As with the Kerr and Reissner-Nordstrom cases, the asymptotically AdS black hole has an extremal limit, therefore as can be expected, the Meissner effect arises in this context. To expel the flux, the black hole must be small enough such that it effectively sees only a massless gauge boson. For the AdS black hole, the shrinking of the horizon does not only occur for low mass black holes, but also for low values of the AdS length ℓ. However, in the latter case, the width of the vortex is also contracted, essentially making the mass of the gauge boson appear larger. To determine the implications of ℓ we explored the phase transition analytically and then confirmed the results numerically. The results are detailed in figure 4.8, which displays the numerical results for the phase transition at several values of ℓ and β. Firstly, we demonstrated that in the presence of rotation and hence a second gauge field component, the transition is first order, as with the pure Kerr case. Next, we found that the effect of ℓ is to lower the critical value of r_+ at which the transition occurs, as well as to lower the bounds for the transition.

Figure 4.8 shows the order parameter, namely the value of the Higgs field at the equator, plotted against the horizon radius r_+. We see in the right figure that the order parameter increases as ℓ decreases. The left figure displays the effects of varying the Bogomolnyi parameter β for $\ell = 10$. As with the Kerr case, increasing β has the effect of increasing the critical value of r_+ at which the transition occurs.

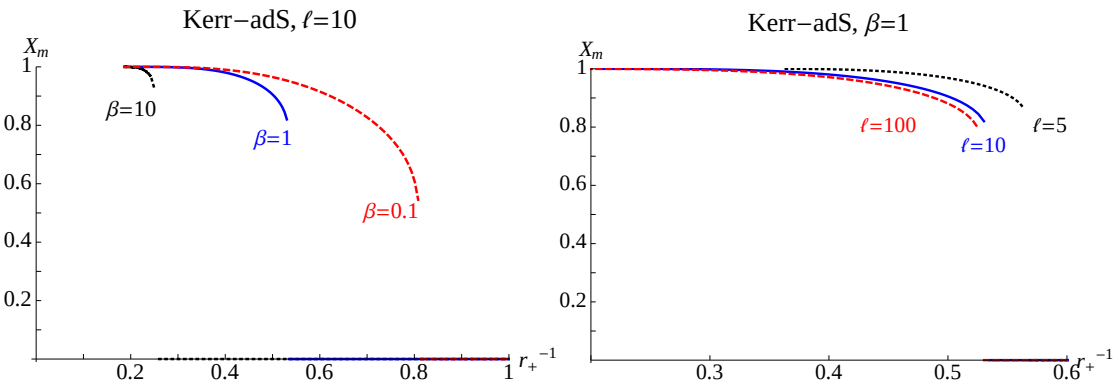

Figure 4.8: **Flux expulsion behavior:** Plots illustrating features of the flux expulsion phase transition on the event horizon of the black hole. The maximal value of the Higgs field $X_m = X(\pi/2)$ is shown as a function of r_+^{-1} for varying β (left) and ℓ (right).

Chapter 5

Dark D-brane Cosmology

The cosmological dark sector, as we have seen, does not appear to interact directly with standard model particles, but instead makes its presence known only gravitationally. In addition, we have seen that fundamental theories such as string theory posit the existence of extra dimensions which can contain all kinds of fundamental matter fields, which may coexist with our world of standard model particles in four dimensions, but yet be spatially separated from visible matter in higher dimensions.

In the light of these theories, in this Chapter we will examine the hypothesis that the dark fluids in the universe may be due to the presence of another four-dimensional "world", which is separated from our own by additional dimensions of space.

In addition to the dark fluids themselves, there is the question of the possible interactions between them. It is often simply assumed that the components of the dark sector are independent and do not interact directly with one another, however there is no fundamental principle nor convincing observational evidence which forbids or suppresses such an interaction. Indeed, whereas interactions between dark energy and visible matter particles are heavily constrained by observations (*e.g.* by solar system tests as well as gravitational experiments on Earth), this is not the case for dark matter particles. In other words, it is possible that the dark components interact with each other, while not being coupled to standard model particles. Several phenomenological interacting dark sector models have been proposed in the literature (see *e.g.* [20] for a recent review with several references therein), however, these

models typically lack a compelling fundamental origin for the form of the proposed couplings.

In what follows we will propose a unified picture of the dark phenomena in the universe in which dark matter and dark energy are naturally interacting. Specifically, we will suggest that the cosmological dark sector, namely dark energy, dark matter and any possible dark radiation, may be naturally unified as distinct phenomena arising from a single object, which we call the *Dark D-brane*, moving in a higher dimensional space-time.

The Dark D-brane world scenario we propose can arise from "hidden sector branes", which are ubiquitous in string theoretic D-brane constructions. Hidden sector D-branes are those branes which have no intersection with the stack of D-branes responsible for the visible sector, and therefore they interact with the visible sector only gravitationally or via very massive states that do not play a role in the low energy theory. Thus the matter fields on these branes are *dark* by construction. For a single D-brane, the matter fields are U(1) gauge fields which may be massive or massless. Hence they can simultaneously provide candidates for a dark matter species and a dark radiation species in the universe. Then, if these hidden branes are currently moving in the warped extra dimensions, their motion can cause other degrees of freedom to appear in our world, which could act as dark energy and thus complete the dark spectrum in four dimensions.

As a geometrical framework for describing the dark sector, it is compelling that the dark fluids in this scenario turn out to be non-minimally coupled in a very particular way: the coupling is precisely a realisation of the disformal transformation (1.3.88) which we discussed in Section 1.3 in the context of scalar-tensor theories of gravity, repeated here:

$$\bar{g}_{\mu\nu} = C(\phi, X) g_{\mu\nu} + D(\phi, X) \partial_\mu \phi \, \partial_\nu \phi \,. \tag{5.0.1}$$

Therefore, this picture creates a direct link between fundamental theory and phenomenological theories of modified gravity, and provides a robust motivation for the disformal coupling. As we will see, in the present context the general relation in Eq. (5.0.1) has a concrete interpretation as the induced metric on a probe D-

brane moving in a warped higher dimensional spacetime[1], such that ϕ is the scalar field associated with the position of the brane, and C and D are both functions of the warp factor h. In addition, the matter fields which are disformally coupled are precisely those fields which are localised on the moving D-brane. In our scenario we will associate ϕ with dark energy, and the disformally coupled matter with dark matter.

In the context of string phenomenology, Eq. (5.0.1) has been widely exploited in cosmological applications. Indeed the so-called Dirac-Born-Infeld (DBI) inflationary scenarios [37,38] are based on this relation[2], where the scalar field ϕ plays the role of the inflaton. As we described briefly in Section 1.2.2, DBI inflation can arise when a D-brane is moving relativistically in a strongly warped region of the compact space. The vast majority of D-brane inflation models deal exclusively with scalar fields, while any other open string fields localised on the brane are usually not considered: apart from the inflaton, the branes are "empty", despite the fact that these additional fields are naturally present, and can indeed give rise to interesting cosmology[3]. In the current work we will instead consider DBI quintessence [130,131], where matter fields on the brane are taken into account. To study the homogenous cosmology, we will use the method of dynamical system analysis and numerical integration[4].

A primary reason for considering an interacting dark sector scenario is that it allows for a possible alleviation of the cosmic coincidence problem, due to the energy

[1]Our proposal does not need to be restricted to string theory, but could be in principle realised in a 'pure' brane world scenario [118–121].

[2]More specifically, single field models in which the brane moves along a single compact direction are based on Eq. (5.0.1). While in the standard scenarios the D-brane moves only radially in a warped region, the generalisation to allow motion in all six of the compact directions has been studied, and there it was found that motion in all directions other than the radial is rapidly damped by the cosmological expansion [122–124]

[3]In the early universe context, it has been shown that such matter fields may play the role of Wilson-line inflatons in both the warped and unwarped cases [126,127], and that they may act as vector curvatons on both stationary as well as moving branes [128,129].

[4]Previously these methods have been applied for DBI scalar field cosmologies in Refs. [130,131, 159–162]. For some other works on DBI dark energy see Refs. [150–158].

exchange between the dark components. This exchange can lead to so-called "scaling solutions" [17–19] discussed in Section 1.1.3, where the effective equations of state for dark matter and dark energy take on the same value, allowing the two fluids to dilute at the same rate across several efolds of the cosmological evolution. We will show in what follows that these scaling solutions do indeed arise in our disformal Dark D-brane scenario.

Thus our Dark D-brane world scenario, a realisation of coupled quintessence cosmology, is a naturally unified picture of the cosmological dark sector in which dark energy arises from the motion of a hidden sector brane in the warped internal space and is disformally coupled to the dark matter fields on its world-volume[5]. The scalar and matter fields appearing in our scenario then have clear geometric interpretation and their properties and interactions can be explicitly derived from the higher dimensional fundamental theory[6].

This Chapter is based on the work done in Ref. [117].

5.1 The general set-up

In this Section we will first discuss how the disformal coupling arises from D-branes in the context of Type IIB string theory warped compactifications [166–168]. This comprises Section 5.1.1. Then in Section 5.1.2 we will present the set-up for disformally interacting massive particles (DIMPs) on the moving brane and discuss some general physical implications of the disformal coupling.

[5]Extra dimensional dark matter has also been proposed in the brane world context where the fluctuations of our brane give rise to "branon" particles [141–143]. In addition, Kaluza-Klein modes in universal extra dimensions have been widely studied as viable candidates for dark matter [144–146], see [147, 148] for reviews.

[6]A string inspired coupled quintessence model was presented in [149] in terms of closed string moduli.

5.1.1 Disformal coupling from moving D-branes

Consider a warped flux compactification of Type IIB string theory , where the higher dimensional generalisations of gauge fields, the RR-forms, $F_{n+1} = dC_n$ for $n = 0, 2, 4$ and their duals $n = 6, 8$, as well as the NSNS-form $H_3 = dB_2$ are turned on in the internal six dimensional space. These fluxes back-react on the geometry, warping it. In addition, it has been shown that they generate a potential for most of the geometric moduli present in the compactification, which allows these moduli to be stabilised [166].

Assigning the coordinates x^μ to the noncompact dimensions, where $\mu = (0, ..., 3)$, and the coordinates y^A to the compact dimensions, with $A = (4, ..., 9)$, the ten dimensional metric takes the form

$$G_{MN}dx^M dx^N = h^{-1/2}(y^A)g_{\mu\nu}dx^\mu dx^\nu + h^{1/2}(y^A)g_{AB}dy^A dy^B, \tag{5.1.2}$$

where g_{AB} is the metric of the internal six dimensional Calabi-Yau manifold, and in order to preserve Lorentz symmetry in the noncompact four dimensions, the warp factor h is a function of only the internal coordinates, $h = h(y^A)$.

We now want to consider probe Dp-branes embedded in this background. Defining the coordinates ξ^a on the world-volumes of the D-branes, where $a = (0, ..., p)$, we can embed them into the spacetime by the mapping $x^M(\xi^a)$. This is simply a higher dimensional generalisation of the familiar point-particle worldline in four dimensions, $x^\mu(\tau)$, where τ is usually taken to be the proper time. As spatially extended objects, D-branes will also break Lorentz symmetry, and thus should be space-filling in the noncompact dimensions. We are then free to align the four-dimensional world-volume coordinates with the four-dimensional spacetime coordinates, by choosing the static gauge $\xi^\mu = x^\mu$. In the compact dimensions on the other hand, the D-branes will naturally tend to move about as they search for the minima of their potentials, and thus the embedding functions are kept general, $y^A(\xi^a)$.

The matter fields that live on the world-volume of a D-brane will naturally follow geodesics of the induced metric, which we denote as $\bar{g}_{\mu\nu}$. For a D3-brane that is moving along a single compact direction r for example, this is given by

$$\bar{g}_{\mu\nu} = G_{MN}\partial_\mu x^M \partial_\nu x^N = h^{-1/2}(r)g_{\mu\nu} + h^{1/2}(r)\partial_\mu r \partial_\nu r\,, \tag{5.1.3}$$

where the first term arises because we are in the static gauge, and $r(x^\mu)$ is proportional to the scalar field associated to the brane's position parameterising its motion in the r direction. We see then that the induced metric on a D-brane moving along a single direction in the compact space is precisely a realisation of the disformal relation, Eq. (5.0.1), where we can readily identify the form of the couplings in terms of the warp factor $C(r)^{-1} = D(r) = h(r)^{1/2}$ and the scalar field with the brane's position $\phi \propto r$. On the other hand, the metric $g_{\mu\nu}$ describes the geometry of the bulk spacetime.

In order to see how the disformal coupling arises from the Dp-brane action, we will now look in more detail at the full action describing its dynamics. In the Einstein frame[7], the DBI action of a Dp-brane is given by[8]

$$S_{\rm DBI} = -\mu_p \int d^{p+1}\xi e^{\frac{(p-3)}{4}\varphi}\sqrt{-\det(\bar{g}_{ab} + e^{-\frac{\varphi}{2}}\mathcal{F}_{ab})} \tag{5.1.4}$$

where

$$\mu_p = (2\pi)^{-p}(\alpha')^{-\frac{(p+1)}{2}}, \qquad T_p = \mu_p e^{\frac{(p-3)}{4}\varphi}, \tag{5.1.5}$$

with T_p being the tension of the brane, where $\alpha' = \ell_s^2$ with ℓ_s the string scale and the vacuum expectation value of the dilaton field φ gives the string coupling as $e^{\varphi_0} = g_s$. The pullback of the ten dimensional metric onto the Dp-brane world-volume takes the form (5.1.3)

$$\bar{g}_{\mu\nu} = G_{\mu\nu} + \frac{\partial y^i}{\partial \xi^\mu}\frac{\partial y^j}{\partial \xi^v}G_{ij} = h^{-1/2}g_{\mu\nu} + h^{1/2}\partial_\mu y^i \partial_\nu y^j g_{ij}, \tag{5.1.6}$$

for the four dimensional components, whereas

$$\bar{g}_{mn} = \frac{\partial y^l}{\partial \xi^m}\frac{\partial y^r}{\partial \xi^n}G_{lr}. \tag{5.1.7}$$

[7]In D dimensions the Einstein frame and string frame are related by $G^E_{MN} = e^{-\frac{4}{D-2}\varphi}G^s_{MN}$ where φ is the dilaton.

[8]We use the following indices for the various coordinates:

$M, N = 0, ..., 9$	for 10D coordinates
$\mu, \nu = 0, ..., 3$	for 4D coordinates
$A, B = 4, ..., 9$	for 6D coordinates
$a, b = 0, ..., p$	for world-volume coordinates
$m, n = 4, ..., p$	internal (p - 3) world-volume coordinates
$i, j = p+1, ..., 9$	internal transverse to brane coordinates

for the internal ones. Moreover, $\mathcal{F}_{ab} = \mathcal{B}_{ab} + 2\pi\alpha' F_{ab}$ is the gauge invariant combination of the pullback of the NSNS 2-form $\mathcal{B}_2$ and the field strength of the world-volume $U(1)$ gauge field.

The coupling of the brane and its world-volume fields to the bulk RR-fields is described by the Wess-Zumino (WZ) action, which is given by

$$S_{WZ} = \mu_p \int_{\mathcal{W}_{p+1}} \sum_n \mathcal{C}_n \wedge e^{\mathcal{F}} \tag{5.1.8}$$

where $\mathcal{W}_{p+1}$ is the world-volume of the brane, and $\mathcal{C}_n$ are the pullbacks of the bulk RR-C_n forms to which the brane couples. In this expression, the wedge product picks out the relevant terms in the exponential. The total action for a Dp-brane is then given by the sum of the DBI and WZ actions, namely

$$S_{D_p} = S_{\text{DBI}} + S_{\text{WZ}}. \tag{5.1.9}$$

The scalar sector

The four-dimensional induced metric in Eq. (5.1.6), which gives the kinetic terms for the brane's position fields in the DBI action (5.1.4), is precisely of the disformal type. We will from now on consider the simplest case of a D3-brane. For such a brane, there are no compact coordinates, and we may define the canonically normalised position field $\phi \equiv \sqrt{T_3} r$ with corresponding warp factor $h(\phi) \equiv T_3^{-1} h(r)$, for the radial direction r in a warped throat region of the compactification. The brane acquires a potential which is Coulomb-like in the vicinity of an anti-brane, but more generally receives a variety of contributions from "compactification effects" such as fluxes and other objects present in the bulk. For the case of the D3-brane in a warped throat, these effects have been explicitly computed in [169].

Finally, the D3-brane is charged under the four-form C_4, which appears as the first term in (5.1.8) for the case of the D3-brane. We may write this charge as $C_4 = h^{-1}\sqrt{-g}\, dx^0 \wedge dx^1 \wedge dx^2 \wedge dx^3$, and thus it is given in terms of the warp factor. Ignoring for the moment the brane gauge field, after computing the determinant in the DBI action, the scalar action for a D3-brane then takes the form

$$S_\phi = -\int d^4x \sqrt{-g} \left[h^{-1}(\phi) \left(\sqrt{1 + h(\phi) \partial_\mu \phi \partial^\mu \phi} - 1 \right) + V(\phi) \right] . \tag{5.1.10}$$

This action then gives us the scalar part of the action. We now take into account the matter fields living on the brane.

The matter sector

Let us now focus on the kinetic terms for matter on the brane, namely the U(1) gauge field, which is encoded in the DBI action (5.1.4) above. Matter fields that live on D-branes naturally feel the induced metric $\bar{g}_{\mu\nu}$. Indeed, we will see in Section 5.1.2 that their associated particles follow geodesics of $\bar{g}_{\mu\nu}$. Thus, these fields see a disformal metric. To see this concretely, we can rewrite the determinant in Eq. (5.1.4) as follows ($p = 3$)

$$-\det[\bar{g}_{\mu\nu} + e^{-\frac{\varphi}{2}}\mathcal{F}_{\mu\nu}] = -\det[\bar{g}_{\mu\beta}]\det[\delta^{\beta}_{\nu} + e^{-\varphi/2}\bar{\mathcal{F}}^{\beta}_{\nu}], \tag{5.1.11}$$

leading to

$$S_{\rm DBI} = -T_3\int d^4x\sqrt{-\bar{g}}\sqrt{\det(\delta^{\beta}_{\nu} + e^{-\varphi/2}\bar{\mathcal{F}}^{\beta}_{\nu})}. \tag{5.1.12}$$

Here we have denoted $\bar{\mathcal{F}}$ to make it clear that here $\mathcal{F}$ is contracted with $\bar{g}_{\mu\nu}$ and not with $g_{\mu\nu}$. On the other hand, from the point of view of $g_{\mu\nu}$, the DBI action takes the form

$$S_{\rm DBI} = -T_3\int d^4x\sqrt{-g}\,h^{-1}\sqrt{\det(\delta^{\beta}_{\nu} + h\,\partial^{\beta}y^{A}\partial_{\nu}y^{B}g_{AB} + e^{-\varphi/2}h^{1/2}\mathcal{F}^{\beta}_{\nu})}. \tag{5.1.13}$$

Therefore, observers living in the background spacetime see the world-volume fields following geodesics of $g_{\mu\nu}$ but new scalar fields have appeared, namely the fields associated with the position of the brane in the compact space. In addition, the warp factor now appears in the action as the function which gives both the conformal and disformal factors, $C(\phi) \equiv (T_3\,h(\phi))^{-1/2}$ and $D(\phi) \equiv (h(\phi)/T_3)^{1/2}$ respectively, when restricted to motion in a single direction $\phi = \sqrt{T_3}\,r$.

Expanding the square root in the DBI action we can rewrite (5.1.13) as

$$S_{\rm DBI} = -T_3\int d^4x\sqrt{-\bar{g}}\left(1 + \frac{e^{-\varphi/2}}{4}\bar{\mathcal{F}}^2 + \cdots\right), \tag{5.1.14}$$

where the first term corresponds to the kinetic term for the scalar, which appeared in (5.1.10), above and the dots correspond to higher order terms in $\bar{\mathcal{F}}$.

In Type IIB string theory, vector fields can acquire masses via the familiar Higgs mechanism or via a stringy Stückelberg mechanism (see appendix of [128] for a

detailed discussion). This stringy mechanism takes place whenever the vector field couples to a two-form field in the 4D theory. Therefore if the coupling is present, the vector will acquire a mass. Depending upon the details of the compactification, the various two-forms which give rise to vector masses may be projected out of the spectrum: this is due to the action of objects known as orientifold planes: O-planes. In compactifications with O3/O7 planes, the coupling for a D3-brane vector field vanishes because the associated 2-form field is projected out of the spectrum. This entails that D3-brane vector fields remain massless or acquire a Higgs mass for these compactifications. On the other hand, vector fields on branes of lower codimension, such as wrapped D5 and D7-branes, can acquire Stückelberg masses in these compactifications, because the 4D two-form to which they couple remains in the spectrum. In what follows we consider D3-branes with pressureless, *i.e.* massive particles on their world-volumes, as the simplest scenario one can build. It should be clear that our study can readily be generalised to include matter fields with pressure, or branes of lower codimension.

For a D3-brane we can then collect the vector terms into a general action of the form

$$S_{U(1)} = \int d^4x \sqrt{-\bar{g}}\, \mathcal{L}_{U(1)}\,(\bar{g}_{\mu\nu}), \tag{5.1.15}$$

where we have chosen to write the action in the disformal frame to highlight that the matter field couples to the induced metric $\bar{g}_{\mu\nu}$. Above we have illustrated explicitly the case where the matter living on the brane is a vector field. However, the coupling of the induced metric will be also there for more general matter fields living on the brane. Therefore below we model a generic type of Dark D-brane matter in terms of a coupled gas of particles, our DIMPs, which will serve to illustrate the effects of the "disformal" coupling.

The geometry

The prototype warped compactification, which is smooth all the way to the tip of the throat, is given by the compact version of the Klebanov-Strassler geometry [166,170]. It arises due to the presence of fluxes sourced by wrapped D3 and D5-branes, and is an exact non-singular supergravity solution. Such a geometry is rather complicated,

however it features an interior region which may be approximated by the simpler $AdS_5 \times S^5$ geometry, which corresponds to the near horizon limit of a stack of N D3-branes. This is cut off in the infra-red which corresponds to the tip of the throat. The warp factor in this case is given by

$$h = \frac{\lambda_{AdS}}{r^4}, \qquad \lambda_{adS} = 4\pi\alpha'^2 g_s N, \tag{5.1.16}$$

where $g_s N \gg 1$ for the supergravity approximation to be valid, while $g_s < 1$ for string perturbation theory approximation to hold, so that the t'Hooft coupling, $\lambda_{AdS} \gg 1$. For the Klebanov-Srassler (KS) geometry, the AdS_5 approximation breaks down near the tip of the throat. Very near the tip of the KS throat the warp factor approaches a constant value $h \to \text{const.}(\mathcal{O}(1))$ with corrections of order $\mathcal{O}(r^2)$.

In what follows we study the D-brane dynamics in the mid-throat region as well as near the tip. For the former we use the AdS_5 approximation with the warp factor given in (5.1.16) above, and for the latter, we will simply take h to be a constant. This should capture the predominant behaviour of the system in the regions of interest. Furthermore, in large-volume scenarios [171] the effect of the warping is washed away and thus these type of compactifications are also explored when $h \to const.$

5.1.2 Disformally Interacting Massive Particles (DIMPs)

To outline the essential implications of the disformal coupling for particles on a moving brane, we will now adopt a classical point-particle description in place of the usual field theory description. This approach can also be justified as we would eventually want to describe a fluid comprised of galaxies, which can be viewed as point particles moving in the universe.

Consider the effective action for massive particles evolving in a $p+1$-dimensional disformal geometry $\bar{g}_{\mu\nu}$. For a D3-brane ($p = 3$) as we are considering, the brane

actions is entirely four-dimensional and it is simply given by[9]

$$S_{\rm DDM} = -\sum_{i=1}^{N} \int d^4x \; m_i \sqrt{-\bar{g}_{\mu\nu}\dot{x}_i^\mu \dot{x}_i^\nu} \; \delta^{(4)}(x_i(\tau) - x_i), \tag{5.1.17}$$

where we have used that $d\tau = d^4x\, \delta^{(4)}(x_i(\tau) - x_i)$ and the dot denotes the derivative with respect to the affine parameter τ. Moreover, the disformal metric $\bar{g}_{\mu\nu}$ is the induced metric on the brane in Eq. (5.1.3).

Causality

Let us discuss how causality arises in this context. Firstly, motion in the higher dimensional spacetime must also obey causality, and as objects with tension or mass per unit volume, D-branes follow timelike trajectories. In particular, for a scalar field which parameterises the motion of a brane in a single compact direction, we may define a Lorentz factor

$$\gamma \equiv \frac{1}{\sqrt{1 + h(\phi) g^{\mu\nu} \partial_\mu \phi \partial_\nu \phi}} \tag{5.1.18}$$

which must always be real. In the four dimensional disformal spacetime, a necessary condition for causality is that the metric $g_{\mu\nu}$ preserves Lorentzian signature for all values of the scalar field and its derivatives; and then physical particles must follow trajectories for which $d\bar{s}^2 \leq 0$. Note that in four dimensions, there are now *two* invariant speeds and indeed *two* copies of the Lorentz group, one associated with the background spacetime and the other with the disformal spacetime. Writing the disformal metric as

$$\bar{g}_{\mu\nu} = \frac{g_{\mu\beta}}{\sqrt{T_3 h(\phi)}} [\delta^\beta_\nu + h(\phi)\, \partial^\beta \phi\, \partial_\nu \phi], \tag{5.1.19}$$

we see that for a time-dependent scalar field in a cosmological background, the components are just

$$\bar{g}_{00} = \frac{g_{00}}{\sqrt{T_3 h(\phi)}} [1 + h(\phi)\, \partial^0 \phi\, \partial_0 \phi] \equiv \frac{g_{00}}{\sqrt{T_3 h(\phi)}}\, \gamma^{-2}, \qquad \bar{g}_{ij} = \frac{g_{ij}}{\sqrt{T_3 h(\phi)}}. \tag{5.1.20}$$

[9]For branes of lower codimension we extra factors arise from the integration over the compact directions.

The warp factor $h > 0$ always and due to causality in the higher dimensions, $\gamma^{-2} > 0$ always. Therefore the signature of the disformal metric is simply given by that of the four dimensional metric $g_{\mu\nu}$, and so causality is never violated.[10]

Geodesics

Extremising the action (5.1.17), we see that particles on the D-brane naturally follow geodesics of the disformal metric and thus the geodesic equation becomes

$$\ddot{x}^\mu + \bar{\Gamma}^\mu_{\alpha\beta}\dot{x}^\alpha\dot{x}^\beta = 0, \tag{5.1.22}$$

where the disformal Levi-Civita connection $\bar{\Gamma}^\mu_{\alpha\beta}$ is torsion-free, and can be expressed in terms of the usual connection $\Gamma^\mu_{\alpha\beta}$ associated with $g_{\mu\nu}$ as follows:

$$\bar{\Gamma}^\mu_{\alpha\beta} = \Gamma^\mu_{\alpha\beta} - \frac{h'}{2h}\delta^\mu_{(\alpha}\partial_{\beta)}\phi + \frac{\gamma^2}{4}\partial^\mu\phi\left(\frac{h'}{h}g_{\alpha\beta} + 4h\nabla_\alpha\nabla_\beta\phi + 3h'\,\partial_\alpha\phi\partial_\beta\phi\right). \tag{5.1.23}$$

The connection $\bar{\Gamma}^\mu_{\alpha\beta}$ is the unique connection that is metric-compatible with the induced metric $\bar{g}_{\mu\nu}$ on the moving brane.

Note that while the extra terms in Eq. (5.1.23) could in principle lead to dangerous fifth forces if visible matter follows geodesics of $\bar{g}_{\mu\nu}$, in the present construction only dark matter lives on the moving brane and therefore such forces, if they arise, would not impact the visible sector directly, and are not a problem for local gravity tests.

[10] Note that this coincides with the standard constraints given in [172] for a general disformal metric as in (5.0.1), namely

$$C(\phi, X) > 0, \qquad C(\phi, X) + D(\phi, X)X > 0, \tag{5.1.21}$$

where $X \equiv g^{\mu\nu}\partial_\mu\phi\partial_\nu\phi$, and for our case the first condition amounts to $h > 0$ and the second to $\gamma^{-2} > 0$, where $C(r) = D(r)^{-1} = h(r)^{-1/2}$. In [172] it is argued that if C does not depend on X, then the second constraint can only be met if D depends on X. In our case, neither C nor D depend on X, and yet the second constraint is ensured *dynamically* as outlined above.

Stress energy tensor

Let us consider now the energy density on the brane which will be important for cosmology. The stress-energy tensor for disformally coupled matter is defined in the usual manner by

$$T_{\mu\nu} = -\frac{2}{\sqrt{-g}}\frac{\delta\left(\sqrt{-\bar{g}}\,\mathcal{L}_{DDM}\right)}{\delta g^{\mu\nu}}. \tag{5.1.24}$$

For the point particle action (5.1.17), the stress-energy tensor is found to be

$$T_{\mu\nu} = \rho\, u_\mu u_\nu\,, \tag{5.1.25}$$

where the four velocity, normalized as $u^2 = -1$, is

$$u_\mu = \frac{\dot{x}_\mu}{\sqrt{-\dot{x}^2}}\,, \tag{5.1.26}$$

and the energy density is given as

$$\rho = \sum_i m_i \delta^{(4)}(x^i - x^i(\tau))\,\left(\frac{1}{T_3\,h(\phi)}\right)^{\frac{1}{4}}\sqrt{\frac{\dot{x}^2}{g}}\left[1 - h(\phi)\,(u^\mu\partial_\mu\phi)^2\right]^{-\frac{1}{2}}\,. \tag{5.1.27}$$

Comparing Eq. (5.1.27) with the standard expression for the energy density of pressureless matter, the "bare" energy density,

$$\rho_b = \sum_i m_i \delta^{(4)}(x^i - x^i(\tau))\,\sqrt{\frac{\dot{x}^2}{g}}, \tag{5.1.28}$$

we might indeed expect that the disformally coupled fluid behaves quite unlike a standard pressureless fluid. We will see in what follows that this is certainly the case. In particular, the inherent coupling of dark matter to dark energy in (5.1.27) leads to a non-conservation of the dark matter energy density, which modifies its time evolution as the universe expands.

5.2 Disformal Dark D-brane Cosmology

We will now study the cosmology of the Dark D-brane system in detail. We will begin by deriving the relevant equations, then we will obtain solutions numerically as well as by way of a dynamical systems analysis technique, which will be reviewed briefly in what follows.

5.2.1 Field equations

Since we are interested in cosmology, we will now follow the usual effective field theoretic approach and couple our probe Dark D-brane as described in Section 5.1 to four dimensional gravity. The total action we consider, collecting together the pieces derived Section 5.1.1, is thus

$$S = \frac{1}{2\kappa}\int d^4x\sqrt{-g}\,R - \int d^4x\sqrt{-g}\left[h^{-1}(\phi)\left(\sqrt{1+h(\phi)\partial_\mu\phi\partial^\mu\phi}-1\right)+V(\phi)\right] + \int d^4x\sqrt{-\bar{g}}\,\mathcal{L}_{DDM}(\bar{g}_{\mu\nu})\,, \quad (5.2.29)$$

where the first term is the ordinary four-dimensional Einstein-Hilbert action, which arises from dimensional reduction of the ten dimensional closed string sector action, $\kappa = M_P^{-2} = 8\pi G$ is the reduced Planck mass in four dimensions, which is related to the internal volume as $M_P^2 = 2V_6^{(w)}/((2\pi)^7\alpha'^4) = M_s^2\,\mathcal{V}_6/((2\pi)^6\pi g_s^2)$, where $V_6^{(w)} = \int d^6y\sqrt{g_6}\,h$, $\mathcal{V}_6 = V_6^w/\ell_s^6$ and $M_s = \ell_s^{-1}$.

The Einstein equations derived from (5.2.29) are

$$R_{\mu\nu} - \frac{1}{2}g_{\mu\nu}R = \kappa\left(T^\phi_{\mu\nu} + T^m_{\mu\nu}\right)\,, \quad (5.2.30)$$

where the energy momentum tensors are defined as:

$$T^{(\phi)}_{\mu\nu} = -\frac{2}{\sqrt{-g}}\frac{\delta S_\phi}{\delta g^{\mu\nu}}\,, \quad T_{\mu\nu} = -\frac{2}{\sqrt{-g}}\frac{\delta\left(\sqrt{-\bar{g}}\,\mathcal{L}_{DDM}\right)}{\delta g^{\mu\nu}}\,. \quad (5.2.31)$$

Furthermore, the equation of motion for the scalar field becomes

$$\nabla_\mu\left[\gamma\,\partial^\mu\phi\right] - V' + \frac{\gamma}{2}\frac{h'}{h^2}\left(\gamma^{-1}-1\right)^2 = \nabla_\mu\left[h\,T^{\mu\nu}\partial_\nu\phi\right] + \frac{T^{\mu\nu}}{2}\left[\frac{h'}{2\,h}g_{\mu\nu} - \frac{h'}{2}\partial_\mu\phi\partial_\nu\phi\right]\,. \quad (5.2.32)$$

The energy momentum tensor for pressureless matter on the brane takes the form

$$T_{\mu\nu} = \rho\,u_\mu u_\nu, \quad (5.2.33)$$

where for the point particle action in (5.1.17), u_μ is given by (5.1.26) and the energy density ρ by (5.1.27). For the scalar field the energy momentum tensor turns out to be:

$$T^\phi_{\mu\nu} = P_\phi\,g_{\mu\nu} + (\rho_\phi + P_\phi)u^\phi_\mu u^\phi_\nu\,, \quad (5.2.34)$$

where

$$u_\mu^\phi = \frac{\partial_\mu \phi}{\sqrt{-\partial_\mu \phi \, , \partial^\mu \phi}} \tag{5.2.35}$$

and we have defined

$$\rho_\phi = \frac{\gamma - 1}{h} + V \, , \qquad P_\phi = \frac{1 - \gamma^{-1}}{h} - V \, , \tag{5.2.36}$$

with γ being the Lorentz factor for the brane's motion, given in (5.1.18).

Due to the non-minimal coupling, the individual conservation equations for the two energy momentum tensors are modified. The conservation equation for the full system is given in the usual fashion as $\nabla_\mu (T_\phi^{\mu\nu} + T^{\mu\nu}) = 0$, and we have

$$\nabla_\mu T_\phi^{\mu\nu} = \left[\nabla_\mu \left(\gamma \, \partial^\mu \phi \right) - V' + \frac{\gamma h'}{4h^2} \left(\gamma^{-1} - 1 \right)^2 \right] \partial^\nu \phi = Q \, \partial^\nu \phi \tag{5.2.37}$$

where we use (5.2.32) to define the non-conservation coupling,

$$Q \equiv \nabla_\mu \left[h \, T^{\mu\nu} \partial_\nu \phi \right] + \frac{h'}{4h} T^{\mu\nu} \left[g_{\mu\nu} - h \partial_\mu \phi \partial_\nu \phi \right] . \tag{5.2.38}$$

Cosmological equations

In order to study cosmology we will now consider a flat Friedmann-Lamaître-Robertson-Walker (FLRW) spacetime, with metric

$$ds^2 = -dt^2 + a^2(t) \left(dx^2 + dy^2 + dz^2 \right) . \tag{5.2.39}$$

Since the field must be homogeneous in this background, the Lorentz γ-factor becomes

$$\gamma = \frac{1}{\sqrt{1 - h \, \dot{\phi}^2}} \, . \tag{5.2.40}$$

The Friedmann equations and the Klein-Gordon equation for the scalar field become, respectively

$$H^2 = \frac{\kappa^2}{3} \left[\rho_\phi + \rho \right] , \tag{5.2.41}$$

$$\dot{H} + H^2 = -\frac{\kappa^2}{6} \left[\rho_\phi + 3P_\phi + \rho \right] , \tag{5.2.42}$$

$$\ddot{\phi} + \frac{h'}{2h^2} (1 - 3\gamma^{-2} + 2\gamma^{-3}) + \gamma^{-3} (V' + Q_0) + 3H\gamma^{-2} \dot{\phi} = 0 \, . \tag{5.2.43}$$

We further have the continuity equation for the scalar field and matter

$$\dot{\rho}_\phi + 3H(\rho_\phi + P_\phi) = -Q_0\dot{\phi}\,, \qquad \dot{\rho} + 3H\rho = Q_0\dot{\phi}\,. \tag{5.2.44}$$

Finally, the non-conservation coupling for the background, Q_0, is given by

$$Q_0 = h\rho\left[\frac{3h'}{4h}\dot{\phi}^2 - \frac{h'}{4h^2} + \dot{\phi}\left(3H + \frac{\dot{\rho}}{\rho}\right) + \ddot{\phi}\right]. \tag{5.2.45}$$

Solving away the leading derivative terms for ϕ and ρ using Eqs. (5.2.43), (5.2.44), this becomes

$$Q_0 = -\left[\frac{h\left(V' + 3\gamma H\dot{\phi}\right) + \frac{h'}{h}\left(1 - \frac{3}{4}\gamma\right)}{\gamma + h\rho}\right]\rho\,. \tag{5.2.46}$$

Let us now consider some implications of this coupling.

The effects of the coupling

In order to gain some intuition regarding the interaction between dark matter and dark energy in this picture, we can compute Q_0 in an alternative way. In an FRW background, the energy density for pressureless particles on the brane given in (5.1.27) is:

$$\rho = (T_3 h)^{-1/4}\,\rho_b\,\gamma\,, \tag{5.2.47}$$

where the bare energy density ρ_b solves the standard continuity equation for uncoupled matter yielding

$$\rho_b = \rho_0\, a^{-3}. \tag{5.2.48}$$

Taking the first derivative of (5.2.47) using (5.2.48), we obtain the equation

$$\frac{\dot{\rho}}{\rho} + 3H = \frac{\dot{\gamma}}{\gamma} - \frac{h'}{4h}\dot{\phi}\,, \tag{5.2.49}$$

which exactly matches the second of Eqs. (5.2.44) with Q_0 defined by (5.2.45). This also allows us to write Q_0 in a particularly compact form

$$\frac{Q_0}{\rho}\,\dot{\phi} = \frac{d}{dt}\log\left(\frac{\gamma}{h^{1/4}}\right). \tag{5.2.50}$$

In conformally coupled theories, the bare energy density is modified by a field dependent conformal factor [22]: we see quite neatly here that new disformal effect is

simply to modulate the bare energy density by an additional factor γ that involves the kinetic term of field as well.

We can gain some additional useful insight into the dynamics of the system by rewriting (5.2.49) in terms of an effective equation of state for the *disformal dark matter* (DDM),

$$\frac{\dot{\rho}}{\rho} + 3H(1 + w^{eff}_{DDM}) = 0, \qquad w^{eff}_{DDM} \equiv -\frac{1}{3H}\left(\frac{\dot{\gamma}}{\gamma} - \frac{h'}{4h}\dot{\phi}\right) = -\frac{1}{3H}\frac{Q_0\dot{\phi}}{\rho}\,. \quad (5.2.51)$$

The effective equation of state simply quantifies how the dark matter dilutes with the expansion. In particular we see clearly that if $w^{eff}_{DDM} < 0$, the dark matter will redshift slower than a^{-3}, and faster in the opposite case, $w^{eff}_{DDM} > 0$.

In a completely analogous way, we can consider an effective equation of state for the DBI field,

$$\frac{\dot{\rho}_\phi}{\rho_\phi} + 3H(1 + w^{eff}_\phi) = 0, \qquad w^{eff}_\phi \equiv w_\phi - \frac{\rho}{\rho_\phi}w^{eff}_{DDM}, \qquad w_\phi \equiv \frac{P_\phi}{\rho_\phi}\,. \quad (5.2.52)$$

If the energy in dark matter is boosted such that $w^{eff}_{DDM} < 0$, w^{eff}_ϕ will correspondingly receive a positive contribution from the coupling term, having then less accelerating power. On the other hand, if $w^{eff}_{DDM} > 0$, then dark energy is draining energy from dark matter and thus w^{eff}_ϕ receives a negative contribution from the coupling term, having thus more accelerating power.

As can be seen from (5.2.51), the sign of the effective equation of state parameter depends on the behaviour of $\dot{\gamma}$, h' and $\dot{\phi}$. Note that $\dot{\gamma}$ will always start off as positive as the brane starts moving down the throat. In the case of a smooth throat such as the Klebanov-Strassler one, the brane will eventually start slowing down till $\gamma \to 0$. Now, the warp factor is always positive and it grows as we reach the tip of the throat at $\phi = 0$, therefore the contribution from the warp factor is always negative. On the other hand, the sign of $\dot{\phi}$ depends on whether the brane is moving down or up the throat.

Let us consider more explicitly the case we will be mostly interested in, an AdS-like throat, such that $h \propto \phi^{-4}$. In this case the time-dependent combination $h^{-1/4}\gamma$ which appears in (5.2.50) is simply $\phi\gamma$. The general solution to the continuity equation in Eq. (5.2.51) is then $\rho \propto a^{-3(1+w^{eff}_{DDM})}$. Due to the fact that $\rho_b \propto a^{-3}$,

we see that $\phi\gamma \propto a^{-3w^{eff}_{DDM}}$ in Eq. (5.2.47). Thus the disformal coupling may either quicken or slow the dilution of dark matter, depending on whether w^{eff}_{DDM} is positive or negative, as explained above. Now, despite the fact that $\phi \to 0$ as the brane moves towards the tip of the throat, the Lorentz factor may in fact grow rapidly enough such that the overall effect is that $\phi\gamma$ is growing with time. This would imply that w^{eff}_{DDM} in Eq. (5.2.51) becomes *negative* due to the presence of the coupling term, so that the dark matter energy density dilutes slower with the expansion due to its energy interchange with dark energy. So, interestingly, while the the conformal contribution $\sim d\log\phi/dt$ in Eq. (5.2.51) tends to quicken the dilution of dark matter particles, the disformal effect $\sim d\log\gamma/dt$ can act against the dilution and could, if it dominates, serve to boost the energy density residing in dark matter.

In the following it will be useful to define the total equation of state parameter w which characterises the expansion rate as

$$w_T \equiv -\frac{2\dot{H}}{3H^2} - 1 = \frac{P_\phi}{\rho_\phi + \rho}. \tag{5.2.53}$$

This is the quantity that is relevant for observations. It is the ratio between the total pressure content of the universe and its total energy density.

In a so-called *scaling solution*, where $w^{eff}_\phi = w^{eff}_{DDM}$, the scaling components dilute at the same rate and their fractional energy densities maintain a constant ratio. In this case, $w^{eff}_{\phi/DDM} = P_\phi/(\rho_\phi + \rho) = w_T$ as we see from the second equation in (5.2.52). *Accelerating* scaling solutions then occur when $w^{eff}_\phi = w^{eff}_{DDM} < -1/3$. In the following we will show, using the method of dynamical system analysis, that such solutions arise for the model at hand due to the presence of the disformal coupling. Obviously, in the absence of the coupling, there can be no accelerating scaling solutions, since then $w^{eff}_{DDM} = w_{CDM} = 0$ as seen in Eq. (5.2.51).

In a DBI scenario where matter on the brane is not taken into account, $w_T \equiv w_\phi$ becomes negative when the brane is relativistic and warping is strong, because in that case the pressure $p_\phi \to -V$ in (5.2.36), and acceleration is attained when $w_\phi < -1/3$. Expansion is of the power law type, while quasi de Sitter expansion, for which $w \sim -1$, can usually only arise in the slow-roll limit of DBI, for then $\gamma \sim 1$ and so $\rho_\phi \sim V \sim -P_\phi$ in Eqs. (5.2.36). In this case the DBI dark energy field is almost constant as the universe expands.

On the other hand, in the present case where matter on the brane is taken into account, w_T is given by Eq. (5.2.53), which reduces to w_ϕ only when matter is diluted away and thus $\rho \to 0$. One consequence of this is that if w_{DDM}^{eff} is positive, w_ϕ^{eff} can be pushed to -1 even when $w_\phi > -1$, *i.e.*, dark energy can be constant as the universe expands. This occurs if the purely conformal contribution $\sim d\log\phi/dt$ in Eq. (5.2.51) is dominating over the disformal contribution $\sim d\log\gamma/dt$. As mentioned above, the other possibility is if the growth of the Lorentz factor is rapid enough, the disformal effect can dominate and thus the energy density in matter can be boosted, resulting in w_{DDM}^{eff} becoming negative. For a brane moving towards the tip of a warped throat, we expect that the Lorentz factor will grow very rapidly at first. This could result in $w_{DDM}^{eff} < -1/3$, *i.e.* the disformally coupled matter could contribute to driving the expansion of the universe: this is the emergence of a scaling solution. Then, once the strong warping forces the growth of γ to become less rapid, the disformal dark matter will be less boosted and might be diluted away, eventually giving rise to a standard DBI epoch.

So here we see the emergence of a new aspect to the usual DBI scenarios: the Lorentz factor acts on ρ_b to slow down its usual dilution by a^{-3}, allowing for the possibility of a new epoch of accelerated expansion that is driven in part by the disformally coupled dark matter on the brane. This could eventually evolve into the standard scenario in which matter does not contribute to the expansion. In this way, the accelerated expansion of the current universe can begin in a matter dominated era, during which the disformally coupled dark matter fluid is active in initiating the acceleration of the expansion, due to its non-minimal coupling to dark energy. This early accelerating era featuring an interplay between dark matter and dark energy eventually gives way to a fully dark energy dominated era. In what follows, these various regimes will be explored using both dynamical systems analysis as well as numerical examples.

5.2.2 Phase space analysis

In this section we make use of a dynamical system approach to solve the equations of motion. In this approach one considers a system of coupled differential equations

in first order form:

$$\dot{\mathbf{x}} = \mathbf{f}(\mathbf{x})\,. \tag{5.2.54}$$

The vector $\mathbf{x}$ may have any integer dimension and its components span the phase space of the same dimension. The evolution of the system is described by trajectories in this phase space. The fixed points (or equilibrium points or critical points as they are sometimes called), are those points in the phase space where the trajectories may stay constant. At a fixed point $\mathbf{x} = \mathbf{x}_c$ then,

$$\dot{\mathbf{x}}_c = \mathbf{f}(\mathbf{x}_c) = 0\,. \tag{5.2.55}$$

For example, if one of the components of $\mathbf{x}$ was H, all the fixed points would correspond to de Sitter solutions with different constants $H = H_c$. This illustrates two basic points: the fixed points do not need to describe static situations (in the de Sitter example the scale factor is evolving with time), and secondly how one sets up the phase space, *i.e.* chooses the variable combinations that define $\mathbf{x}$, determines very crucially whether the fixed points correspond to interesting situations of the system at hand or not (if one would have chosen aH as the variable instead of H, the fixed points would correspond to turnarounds or trivial solutions instead of de Sitter ones). The linear stability of each fixed point with respect to small perturbations defined by $\mathbf{x} = \mathbf{x}_c + \delta\mathbf{x}$, can be studied from the first order perturbed equations:

$$\dot{\mathbf{x}} = \mathbf{f}(\mathbf{x}_c + \delta\mathbf{x}) = \mathbf{f}(\mathbf{x}_c) + \mathbf{F}\cdot\delta\mathbf{x} + \cdots \Rightarrow \dot{\delta\mathbf{x}} = \mathbf{F}\cdot\delta\mathbf{x}\,, \tag{5.2.56}$$

where $\mathbf{F}$ is a matrix with the components $F_{MN} = \partial f_M/\partial x_N$ and the equality holds up to the linear order. Now, in an orthogonal basis, $\mathbf{F}^{(o)}$ is just a diagonal matrix consisting of the eigenvalues, and the above equation has the solution $\delta x_N^{(o)} \sim \exp(\lambda_N)$, where λ_N is the eigenvalue corresponding to the orthogonal basis vector $\delta x_N^{(o)}$. Since the eigenvalues are independent of the basis, we can compute them directly from $\mathbf{F}$. Stability is then determined from the eigenvalues as follows: a) if all the $\lambda_N < 0$ are negative, all the perturbations decay, that is the fixed point is stable and we call it an *attractor*. b) If all $\lambda_N > 0$ are positive, any fluctuation away from the fixed point will grow and take the system away from the solution $\mathbf{x} = \mathbf{x}_c$. This point is thus unstable and can be called a *repellor*. c) Finally, if some of the eigenvalues are

positive and at least one negative, the system is unstable when disturbed in some direction in the phase space, while stable to disturbances in some other directions. Such a solution is called a *saddle point*.

Let us then consider our specific system of cosmological equations in Section 5.2.1. The phase space is then two-dimensional: we can formulate the equations as three coupled first order differential equations (for the dark energy scalar field, its derivative, and the matter density), subject to one constraint (given by the Friedmann equation). A convenient choice of variables turns out to be

$$x \equiv \frac{\kappa\gamma}{\sqrt{3\,(\gamma+1)}}\frac{\dot{\phi}}{H}\,, \quad z \equiv \frac{\kappa\sqrt{V}}{\sqrt{3}H}\,, \quad \Omega \equiv \frac{\kappa^2\rho}{3H^2}\,. \tag{5.2.57}$$

The Friedmann constraint (5.2.41) allows us to then to eliminate Ω as

$$\Omega = 1 - x^2 - z^2\,, \tag{5.2.58}$$

leaving us with physical space spanned by[11] $-1 \leq x \leq 1$, $0 \leq z \leq 1$. Furthermore, it is convenient to use, instead of γ, the variable

$$\tilde{\gamma} \equiv \frac{1}{\gamma}\,, \quad 0 \leq \tilde{\gamma} \leq 1\,. \tag{5.2.59}$$

The expansion rate corresponding to each parameter value is described then by the total equation of state defined in (5.2.53),

$$w_T = \tilde{\gamma}x^2 - z^2\,. \tag{5.2.60}$$

In fact, to close the system of equations, we will also need to specify $\tilde{\gamma}$, and in this sense we have a three-dimensional phase space. However, as seen from (5.2.58), it is only x (roughly speaking, the kinetic energy contribution) and z (the potential energy contribution), that determine the expansion rate. For this reason, it is useful to view the phase space in terms of these variables, considering $\tilde{\gamma}$ as a parameter. This kind of approach was also implemented in Refs. [160, 161].

After some algebra, using the equations of the previous section together with the definitions above, the evolution equations for the three dimensionless variables, in

[11] We assume positive potential energies for the field in the following. However, the formulas would apply also for negative potentials when extended to imaginary z.

terms of the e-folding time $N = \log a$, can be brought into the following form:

$$\frac{dx}{dN} = \frac{3x}{2}\left(\frac{(\tilde{\gamma}+1)(2\tilde{\gamma}-1)x^2}{\tilde{\gamma}\,(x^2+z^2-1)-z^2+1} + \tilde{\gamma}x^2 - z^2 + 1\right) \tag{5.2.61}$$
$$+\frac{\sqrt{3\tilde{\gamma}(\tilde{\gamma}+1)}x^2\left[\mu\left((10\tilde{\gamma}-3)x^2-2\tilde{\gamma}+3\right)+z^2((4-8\tilde{\gamma})\lambda+(2\tilde{\gamma}-3)\mu)\right]}{8\left(\tilde{\gamma}\,(x^2+z^2-1)-z^2+1\right)},$$

$$\frac{dz}{dN} = \frac{z}{2}\left(3+3\tilde{\gamma}x^2-3z^2-\sqrt{3\tilde{\gamma}(\tilde{\gamma}+1)}\lambda\,x\right), \tag{5.2.62}$$

$$\frac{d\tilde{\gamma}}{dN} = \frac{3\tilde{\gamma}\,(1-\tilde{\gamma}^2)\,x^2}{\tilde{\gamma}\,(x^2+z^2-1)-z^2+1}$$
$$+\frac{\sqrt{3\tilde{\gamma}(\tilde{\gamma}+1)}(1-\tilde{\gamma})\tilde{\gamma}x\,(\mu+3\mu x^2-z^2(4\lambda+\mu))}{4\left(\tilde{\gamma}\,(x^2+z^2-1)-z^2+1\right)}. \tag{5.2.63}$$

To close the system, we define the following quantities:

$$\mu \equiv -\frac{h'}{\kappa h}, \quad \lambda \equiv -\frac{V'}{\kappa V}. \tag{5.2.64}$$

In general, their evolution equations are

$$\frac{d\mu}{dN} = \Gamma_\mu\sqrt{3\tilde{\gamma}(1+\tilde{\gamma})}, \quad \Gamma_\mu = \frac{h'^2-h''h}{\kappa^2h^2}, \tag{5.2.65}$$

$$\frac{d\lambda}{dN} = \Gamma_\lambda\sqrt{3\tilde{\gamma}(1+\tilde{\gamma})}, \quad \Gamma_\lambda = \frac{V'^2-V''V}{\kappa^2V^2}. \tag{5.2.66}$$

Our system can be closed, *i.e.* put into an autonomous form when the factors Γ_μ and Γ_λ can be expressed in terms of the other quantities. If the functions h and V were exponential, these factors would vanish and thus both μ and λ would be constants. However, this simplification is not motivated by the geometries discussed above in Section 5.1.1, though it might arise in some suitable brane-world scenario. In the following we study the case in which the warp factor and the potential both have a power-law form. We will then focus specifically on the cases in which the powers are those corresponding to an adS_5 and constant-warped geometries.

Power-law evolution

In this section, we take power law forms for the warp factor and the potential, which include adS_5 and a mass term potential:

$$h(\phi) = h_0\frac{\kappa^{4-m}}{\phi^m}, \quad V(\phi) = V_0\kappa^{n-4}\phi^n. \tag{5.2.67}$$

The parameters V_0 and h_0 are dimensionless numbers and n and m are constants. A restriction we need to impose is that $n \neq m$; then we can solve for μ and λ in terms of the other variables as

$$\mu = m\left(\frac{(1-\tilde{\gamma})z^2}{\tilde{\gamma}\Gamma_0 x^2}\right)^{\frac{1}{m-n}}\,, \quad \lambda = -n\left(\frac{(1-\tilde{\gamma})z^2}{\tilde{\gamma}\Gamma_0 x^2}\right)^{\frac{1}{m-n}}\,, \tag{5.2.68}$$

where we have defined

$$\Gamma_0 \equiv h_0 V_0\,, \tag{5.2.69}$$

which turns out to be a very useful parameter. Here and in the following we take $\phi \geq 0$, since the field corresponds to the brane's position in the internal space.

Using the equations (5.2.62)-(5.2.63) above, together with the definitions (5.2.67, 5.2.69), the evolution equations for the three dimensionless phase space variables, in terms of the e-folding time $N = \log a$, turn out to be

$$\frac{dx}{dN} = \frac{x}{8\left(\tilde{\gamma}\left(x^2+z^2-1\right)-z^2+1\right)}\Bigg[12\Big(\tilde{\gamma}^2x^4+\tilde{\gamma}x^2\big((\tilde{\gamma}-2)z^2+\tilde{\gamma}+3\big)-(\tilde{\gamma}-1)\big(z^2-1\big)^2-x^2\Big)$$
$$+\sqrt{3\tilde{\gamma}(\tilde{\gamma}+1)}\,x\big(z^2(2\tilde{\gamma}m+8\tilde{\gamma}n-3m-4n)+m\big((10\tilde{\gamma}-3)x^2-2\tilde{\gamma}+3\big)\big)\left(\frac{\Gamma_0\tilde{\gamma}x^2}{(1-\tilde{\gamma})z^2}\right)^{\frac{1}{n-m}}\Bigg]\,, \tag{5.2.70}$$

$$\frac{dz}{dN} = \frac{z}{2}\left[\sqrt{3\tilde{\gamma}\left(\tilde{\gamma}+1\right)}\,n\,x\left(\frac{\tilde{\gamma}\Gamma_0 x^2}{(1-\tilde{\gamma})z^2}\right)^{\frac{1}{n-m}} + 3\,\tilde{\gamma}\,x^2 - 3z^2 + 3\right]\,, \tag{5.2.71}$$

$$\frac{d\tilde{\gamma}}{dN} = \frac{\tilde{\gamma}(1-\tilde{\gamma})\,x\left[\sqrt{3\tilde{\gamma}\left(\tilde{\gamma}+1\right)}\left(3\,m\,x^2-m\,z^2+m+4nz^2\right)\left(\frac{\tilde{\gamma}\Gamma_0 x^2}{(1-\tilde{\gamma})z^2}\right)^{\frac{1}{n-m}}+12(\tilde{\gamma}+1)x\right]}{4\left(\tilde{\gamma}\left(x^2+z^2-1\right)-z^2+1\right)}. \tag{5.2.72}$$

Interestingly, the structure of the phase space depends solely upon the product of the parameters defined in (5.2.67) which quantifies the energy scales of the potential and the warp factor, Γ_0 defined in equation (5.2.69).

General behaviour

Before considering particular values for the exponents in the warp factor and potential, we can make some general statements about the possible fixed points of the system (5.2.70)-(5.2.72). Indeed, the equations (5.2.70)=(5.2.71)=(5.2.72)=0, can be solved in various ways:

(A) *Standard matter dominated solution*: in this case $x_{MD} = z_{MD} = 0 \Rightarrow \omega_{MD} = 0$ and $\Omega_{MD} = 1$. This is valid for all values of n, m and γ. The eigenvalues corresponding to small perturbations around this solution are $(\frac{3}{2}, \frac{3}{2})$. Therefore this solution is always unstable.

(B) *Potential dominated de Sitter solution*: in this case $x_{dS} = \Omega_{dS} = 0$ so that $z_{dS} = 1$ and thus $\omega_{dS} = -1$. From (5.2.70) and (5.2.71) one can check that in order for it to be a solution, n and m must satisfy:

$$n - m \leq -2\,, \tag{5.2.73}$$

and the solutions have $\tilde{\gamma}_{dS} = 1$. The eigenvalues corresponding to this solution are $(-3, 3)$, and therefore the solution is always a saddle point.

(C) *Kinetic dominated solution*: in this case $x_{kin} = \pm 1$, $z_{kin} = \Omega_{kin} = 0$. From (5.2.70) and (5.2.71) we see that in order for this to be a solution to these equations we need

$$n - m < 0 \tag{5.2.74}$$

and therefore the only solutions have $\tilde{\gamma} = \omega_{kin} = 0$. The eigenvalues corresponding to this solution are $3(\frac{1}{2}, -1)$, thus this solution is a saddle point.

(D) For more general solutions with $0 < z < 1$, which will be the most interesting ones, we can make some general statements and will look into two concrete examples below. Solving (5.2.71) =0 gives rise to the following equation:

$$3(1+\tilde{\gamma}\,x^2)\,z^{\frac{2}{n-m}} - 3\,z^{2\left(1+\frac{1}{n-m}\right)} + n\,\Gamma_0^{\frac{1}{n-m}}\sqrt{3(\tilde{\gamma}+1)\,\tilde{\gamma}}\;\frac{x\,(\tilde{\gamma}\,x^2)^{\frac{1}{n-m}}}{(1-\tilde{\gamma})^{\frac{1}{n-m}}} = 0\,. \tag{5.2.75}$$

One can check that if the last term in this equation vanishes, then we are back at one of the previous solutions. Therefore, non-trivial solutions arise when the last term does not vanish. We can then have the following situations

(i) $x = 0$ or $\tilde{\gamma} = 0$. This case requires that

$$n - m = -2 \tag{5.2.76}$$

and the solution to (5.2.75) can be easily found (see below).

(ii) For general values of x and $\tilde{\gamma}$, the solution to (5.2.75) is more complicated depending on the precise values of n and m.

In what follows we consider two explicit examples of the classes of solutions above, corresponding to a brane moving down an AdS_5 throat along a mass term potential, and a constant warp factor with an inverse law potential, where the brane moves towards the bulk geometry. This latter case can be seen as an example of a moving brane in a large volume scenario.

The AdS_5 warp factor

Let us consider first the AdS case where the warp factor goes like $h \sim \phi^{-4}$. For the potential we consider a mass term, that is we set $m = 4$, $n = 2$, so $n - m = -2$. From the general discussion above we see that the system contains classes (a), (b), (c) of fixed points. Furthermore, within class (d) we have the following fixed points:

Class (d): $0 < z < 1$**.** In this example, the condition $dz/dN = 0$ from Eq. (5.2.75) reduces to

$$3\left(1 + \tilde{\gamma}x^2 - z^2\right) + 2\,z\,\sqrt{\frac{3(1-\tilde{\gamma}^2)}{\Gamma_0}}S(x) = 0\,, \tag{5.2.77}$$

where $S(x) = \text{sign}(x)$. The solutions to this equation are

$$z_\pm \;=\; \frac{1}{\sqrt{3\Gamma_0}}\left[S(x)\sqrt{1-\tilde{\gamma}^2} \pm \sqrt{1-\tilde{\gamma}^2 + 3\Gamma_0\,(1+\tilde{\gamma}x^2)}\right]\,. \tag{5.2.78}$$

Thus we see that physical solutions exist only when the field is rolling down the throat, $S(x) = -1$, for the positive branch, since otherwise either $z < 0$ or the matter energy density is negative, since $z > 1$. It is difficult to find the most general solution for x. However, we can focus on the special case $\tilde{\gamma} = 0$, corresponding to an ultra relativistic regime, (d)(i) above. In this case we obtain the following fixed points:

- Matter scaling solution with $x_{DDM} = 0$. For this solution we have

$$x_{DDM} = 0\,, \quad z_{DDM} = \frac{-1+\sqrt{1+3\Gamma_0}}{\sqrt{3\Gamma_0}}\,, \quad \Omega_{DDM} = \frac{2}{1+\sqrt{1+3\Gamma_0}}\,. \tag{5.2.79}$$

The total equation of state parameter approaches minus unity as one increases Γ_0,

$$w_{DDM} = -\frac{\left(1-\sqrt{1+3\Gamma_0}\right)^2}{3\Gamma_0}\,. \tag{5.2.80}$$

The eigenvalues for this fixed points are

$$\left(-\frac{1+3\Gamma_0-\sqrt{1+3\Gamma_0}}{\Gamma_0}\,,\frac{3\left(1+\Gamma_0-\sqrt{1+3\Gamma_0}\right)}{2\Gamma_0}\right)\,. \tag{5.2.81}$$

Requiring these to be negative, we find that this solution is stable for $0<\Gamma_0<1$. Otherwise it is a saddle point. Moreover, we are interested in accelerating solutions, which means that the total effective equation of state parameter (5.2.80) for this solution should satisfy $w_{DDM}<-1/3$. This requires $\Gamma_0>1$. Therefore we see that the solution is not an accelerating attractor for $0<\Gamma_0<1$, however it could be a viable matter scaling attractor when Γ_0 is small enough, such that $w\sim 0$. The reason this needs to be small is that large-scale structure would be too different from the ΛCDM case if dark matter was not effectively nearly pressureless during the structure formation era. As we will see in the numerical study below, this fixed point is typically reached as an intermediate stage for a cosmological evolution which is close to ΛCDM cosmology.

- Kinetic solution with $\Omega_{DBI}=0$. For this ultra-relativistic solution the matter contribution vanishes and

$$x_{DBI} = -\sqrt{\frac{2}{1+\sqrt{1+3\Gamma_0}}}\,,\quad z_{DBI}=\frac{-1+\sqrt{1+3\Gamma_0}}{\sqrt{3\Gamma_0}}\,,\quad \Omega_{DBI}=0\,. \tag{5.2.82}$$

The total equation of state is the same as for the matter-scaling solution above,

$$w_{DBI} = -\frac{\left(1-\sqrt{1+3\Gamma_0}\right)^2}{3\Gamma_0}\,. \tag{5.2.83}$$

Now we obtain for the eigenvalues of this fixed points:

$$\left(-\frac{1+3\Gamma_0-\sqrt{1+3\Gamma_0}}{\Gamma_0}\,,\frac{3\left(2-\sqrt{1+3\Gamma_0}\right)}{1+\sqrt{1+3\Gamma_0}}\right)\,. \tag{5.2.84}$$

From this we see that this solution is a saddle point when the previous one is an attractor, that is when $0<\Gamma_0<1$. Moreover, when $\Gamma_0>1$, the solution

is an accelerating attractor with $w_{DBI} < -1/3$, while the previous one is a saddle point for these values of Γ_0.

In summary, for the AdS case with a mass term potential we have found two accelerating attractors for the system: a nonrelativistic potential-dominated de Sitter solution (class (c)), and an ultra-relativistic DBI solution (class (d)-(i)).

Constant warp factor

In regions both asymptotically far into the bulk and very near to the tip of a Klebanov-Strassler throat, the warp factor can be approximated by a constant. This provides the simplest example of a nontrivial disformal relation, where both C and D are constants. In this case $m = 0$. Following the general discussion above, we know that this case has class (a) of fixed points. Furthermore, it possesses an accelerated saddle point, class (b) of solutions, only for $n = -2$, that is, an inverse power law potential. Moreover, for all $n < 0$ it possesses class (c) of fixed points as well. Regarding class (d), we have the following fixed points:

Class (d): $0 < z < 1$**.** Focusing again in class (d)-(i), we need $n = -2$. Then Eq. (5.2.75) yields for z

$$z_{\pm} = \frac{1}{\sqrt{3\Gamma_0}}\left[-S(x)\sqrt{1-\tilde{\gamma}^2} \pm \sqrt{1-\tilde{\gamma}^2+3\Gamma_0\left(1+\tilde{\gamma}x^2\right)}\right] . \quad (5.2.85)$$

From here we can see that now the physical solutions correspond to a brane moving towards the bulk geometry, that is $S(x) = +1$, and furthermore, we should pick the $+$-branch of the solution such that $z > 0$. Focusing again in the ultra-relativistic limit $\tilde{\gamma} = 0$ we consider the cases when either the matter contribution or the kinetic contribution to the expansion are negligible.

- Matter scaling solution $x_{DDM} = 0$. This fixed point and its total equation of state are given by the expressions (5.2.79) and (5.2.80). However, now the eigenvalues of the perturbation matrix turn out to be

$$\left(\frac{-1-3\Gamma_0+\sqrt{1+3\Gamma_0}}{\Gamma_0}, \frac{3}{2}\right) , \quad (5.2.86)$$

thus this solution is never an attractor when Γ_0 is positive, but always a saddle point.

Fixed point	Stability when $m = 4, n = 2$	Stability for $m = 0, n = -2$	w
(a) Matter domination	Unstable	Unstable	0
(b) de Sitter solution	Saddle	Saddle	-1
(c) Kinetic domination	Saddle	Saddle	1
(d) Matter scaling solution	Attractor iff $0 < \Gamma_0 < 1$	Saddle	$-\frac{\left(1-\sqrt{1+3\Gamma_0}\right)^2}{3\Gamma_0}$
(d) Kinetic scaling solution	Attractor iff $\Gamma_0 > 1$	Attractor	$-\frac{\left(1-\sqrt{1+3\Gamma_0}\right)^2}{3\Gamma_0}$

Table 5.1: Summary of the fixed points in the two examples considered.

- Kinetic scaling solution with $\Omega_{DBI} = 0$. In analogy with the above, this fixed point and its total equation of state are given by the expressions (5.2.79) and (5.2.80), but now the stability properties differ because of the different warp factor and potential. From the eigenvalues

$$\left(-\frac{1+3\Gamma_0-\sqrt{1+3\Gamma_0}}{\Gamma_0}\,,-3\right)\,, \tag{5.2.87}$$

  we see that this solution is always an attractor. The difference with the $m = 4$, $n = 2$ case is that in that case, the matter scaling solution is a saddle point and the kinetic solution an attractor in the accelerating case $\Gamma_0 > 1$, while in the present case, we find that for all $\Gamma_0 > 0$ the matter scaling solution is a saddle point, while the kinetic scaling solution is an attractor.

The fixed points and their stability properties in the two examples considered above are summarised in Table 5.1.

In the dynamical system analyses of DBI cosmologies, scaling solutions have been found in the literature [130, 131, 159–162]. However these solutions described non-accelerating expansion with $w_T = 0$. The possibility of scaling with $w_T \neq 0$ appears only when a coupling is taken into account (recall our discussion in Section 5.2.1).

5.2.3 Numerical solutions

In this section we will investigate the system of equations (5.2.70)-(5.2.72) numerically, in order to confirm the expectations from the analytic arguements in Section 5.2.1, and from the dynamical system analysis in Section 5.2.2 above. In addition, this will enable us to uncover some of the typical details of the evolution as the system converges to its asymptotic state described by the attracting fixed points. Our aim is to construct realistic cosmological scenarios which start from a standard matter dominated era and end in an accelerating era, where as we are only interested in late-time cosmology, we have omitted any contribution from radiation to the expansion. For purposes of illustration we consider an AdS geometry for the warp factor and a quadratic potential for the scalar field. Thus we set $m = 4$ and $n = 2$ in what follows.

Let us describe the generic behaviour. Upon integration of the equations of motion with matter dominated initial conditions, the system is naturally ends up in a regime where the DBI field has a significant impact on the dynamics. This is indeed expected given that the matter dominated solution is a repeller. We also find that the universe quickly enters an accelerating phase described by the DBI scaling fixed points when $\Gamma_0 > 1$. Specifically, for the quadratic AdS model at hand, a typical evolution is such that the universe evolves via the matter scaling saddle point (5.2.79) into the kinetic scaling attractor (5.2.82). Examples are shown in figure 5.1, for two values of the parameter Γ_0. Since the universe typically spends a few e-folds in the saddle point stage and in a realistic case the acceleration has begun only recently, the prediction is that our universe is currently entering the accelerating scaling saddle point. Interestingly, the equations of state (5.2.80) and (5.2.83) for these two physically distinct fixed points coincide, which means that judging from the expansion of the universe alone, they cannot be observationally distinguished. For the fixed point (5.2.79) there is a non-negligible contribution from the disformally coupled dark matter, and for the fixed point (5.2.82) a non-negligible contribution from the kinetic energy of the scalar field[12].

[12]The reason that they still can have identical expansion rates is that from Eq. (5.2.60) one sees that for relativistic motion of the brane, neither kinetic energy nor dark matter density but only

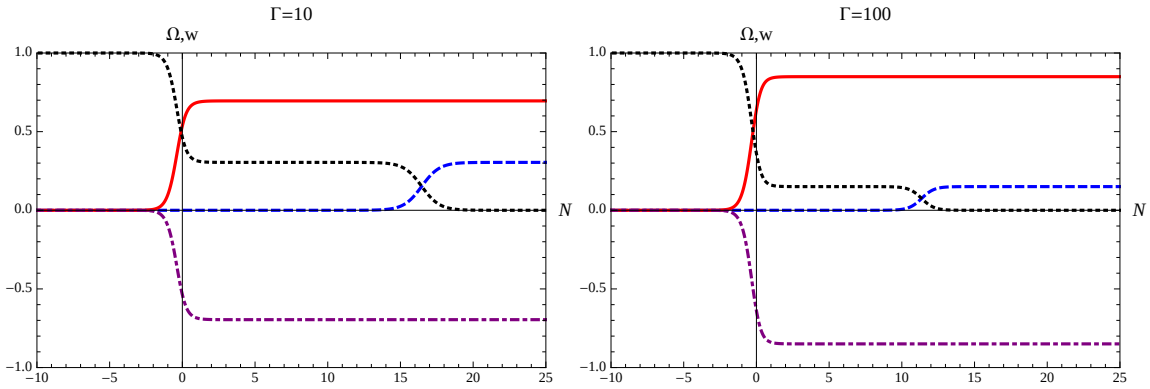

Figure 5.1: The evolution of the fractional energy densities and the total equation of state as functions of the e-folding time $N = \log a$ for $\Gamma_0 = 10$ (left panel) and $\Gamma_0 = 100$ (right panel). The equation of state is the dash-dotted purple line that settles to its attractor value given by Eq. (5.2.80). The black dotted line is the matter contribution Ω, that drops first from the matter-dominated value $\Omega = 1$ to the saddle point solution value given by Eq. (5.2.79), and then to zero as the universe eventually reaches the attractor described by Eq. (5.2.82). At the latter transition, the kinetic energy contribution of the field, x^2, plotted as the blue dashed line, becomes important. The potential energy contribution z^2, plotted as the red solid line, retains its value through the two latter stages.

The various equations of state defined in Section 5.2.1 provide another perspective from which to explore the workings of the disformal coupling. In addition to the total equation of state in (5.2.60), one has the usual definitions for the equations of state of the individual fluids, given in terms of our phase space variables as

$$w_{DDM} = 0\,, \quad w_\phi = \frac{\tilde{\gamma}x^2 - z^2}{x^2 + z^2}\,. \tag{5.2.88}$$

In the presence of the non-minimal coupling however, the scaling of the energy components is defined by the effective equations of state which may now be written as

$$w_{DDM}^{eff} = \frac{1}{3}\left[\frac{1}{\tilde{\gamma}}\frac{d\tilde{\gamma}}{dN} \pm \sqrt{\frac{3(1-\tilde{\gamma}^2)}{\Gamma_0}}\,z\right]\,, \quad w_\phi^{eff} = w_\phi - \frac{1-x^2-z^2}{x^2+z^2}w_{DDM}^{eff}\,, \tag{5.2.89}$$

where the positive sign should be chosen in the former equation, and the derivative of $\tilde{\gamma}$ is given by Eq. (5.2.72). The time evolution for these quantities is shown in figure 5.2. Because $\gamma\phi$ grows with time, there is energy transfer from the scalar field to dark matter that makes the latter dilute slower, as is discussed in Section 5.2.1. During the scaling era, by definition, $w_T = w_{DDM}^{eff} = w_\phi^{eff}$. Even when this era ends, the coupling continues to slow down the dilution of the dark matter energy density, such that w_{DDM}^{eff} remains at a constant negative value. In the right panel of figure 5.2, we display an example of a case wherein initially the energy density of the field is not potential-dominated. In that case the kinetic scaling era begins shortly after the coupling becomes important, and the scaling behaviour never quite takes place. Such initial conditions require the coupling and the kinetic contribution to both become significant around the present epoch, and are thus less generic than the initial conditions that allow some e-folds of scaling. An interesting detail to observe is that due to the fact that we have set the scalar field evolving as an initial condition, the coupling is effective from early on: in particular, as suggested in Section 5.2.1, it forces the energy density of the DBI field to remain constant, *i.e.* $w_\phi^{eff} = -1$ even though $w_\phi > -1$. This is because the effect of the coupling is to produce an energy flow from dark matter to dark energy, which contributes a very tiny positive w_{DDM}^{eff}: when $w_\phi^{eff} = -1$, $w_{DDM}^{eff} = (1+w_\phi)\rho_\phi/\rho$ as seen from (5.2.52).

---

the scalar potential energy determines the total equation of state.

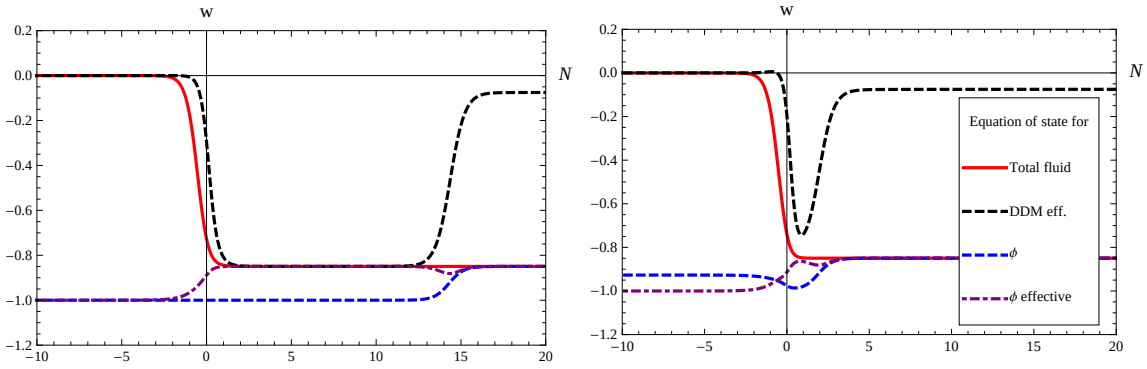

Figure 5.2: The time evolution for the various equations of state as functions of the e-folding time $N = \log a$ when $\Gamma_0 = 50$. In the left panel the kinetic energy x is initially small and the equation of state $w_\phi = p_\phi/\rho_\phi$ (purple dash-dotted line), as well as the effective equation of state for the field w_ϕ^{eff} (blue dashed line), are essentially $w_\phi = -1$ until the coupling begins to modify the dynamics. The effect of the coupling is to increase w_ϕ^{eff} and to lower the effective equation of state for dark matter w_{DDM}^{eff} (black dotted line), so that they both track the total equation of state w (red thick line) during the scaling epoch. When this epoch ends, the dark matter dilutes faster than dark energy, but as seen from the plot, the coupling continues to have an effect on the DDM-component. In the right panel, initial conditions are set such that the kinetic energy x is significant and thus $w_\phi > -1$. In such a case the universe evolves to the kinetic attractor soon after the coupling kicks in, before the scaling solution is reached.

To gain a better understanding of the dynamics behind this evolution and the role of initial conditions, we plot the variable x and the Lorenz factor γ as functions of the scale factor in figure 5.3 for different initial values of γ. We start with a small x and z: for a fixed γ, the initial value of z determines when we enter into the saddle point, and the initial value of x, into the attractor. We see that the transition from the accelerating fixed point to another point occurs when x reaches its critical value given by Eq. (5.2.82). The more nonrelativistic γ is, the longer this will take. If the brane starts moving very slowly from a virtually non-warped region in the early universe, after reaching the matter scaling fixed point the universe can stay there for, in principle, an arbitrary number of e-folds before the brane has moved close enough to the tip of the throat to end the matter scaling behaviour. On the other hand, if the initial conditions are relativistic enough, the x-variable also grows with a "saturated" rate during the matter dominated epoch, and there is no difference in the observational predictions. In the right panel of figure 5.3 we see that the scaling of the γ-factor, which is identical for all initial values during the matter epochs, changes only when the attractor is reached. The scaling is such that $\gamma\phi \sim a^{-3w_T}$, as expected already from the considerations in Section 5.2.1.

Finally we check how the cosmology depends upon the parameter Γ_0, which is the sole theoretical quantity that controls the evolution. We illustrate this in figure 5.4 by plotting x and Ω as functions of the scale factor for a few different values of Γ_0. In complete agreement with the results of the analytic study in Section 5.2.2, we find that $\Gamma_0 = 1$ is the dividing value above which the universe accelerates and eventually ends with $\Omega = 0$, and below which the universe decelerates forever and Ω retains a constant finite value.

5.3 Discussion

In this Chapter we have proposed an inherently unified and fundamental origin for the observed cosmological dark sector in four dimensions. Specifically, we have suggested that the dark fluids in the universe may be due to the presence of a hidden sector D-brane moving in the warped extra dimensions. We have named this object

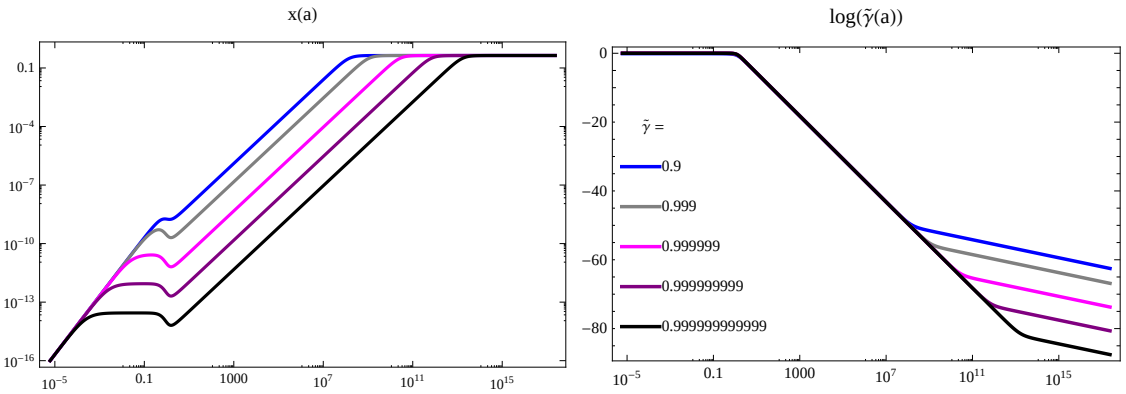

Figure 5.3: The evolution of the "kinetic term" x (left panel) and the brane Lorenz factor in the form of $\log\tilde{\gamma}$ (right panel) as functions of the scale factor a when $\Gamma_0 = 30$. The results are presented for five different initial conditions (set at $a = 10^{-12}$) as given in the legend of the right panel. We see that x, initially set to a small value, grows until it reaches the attractor value given by Eq. (5.2.82). For sufficiently non-relativistic initial conditions ($\tilde{\gamma}$ very close to unity), x can be frozen during the matter dominated era but starts growing as the universe enters into the accelerating scaling saddle point solution Eq. (5.2.79). For sufficiently relativistic initial conditions ($\tilde{\gamma}$ very close to zero) this does not occur. During the matter dominated era γ is constant, but begins to evolve at a constant rate towards relativistic values $\gamma \to \infty$ as the accelerating era begins. When the attractor is reached, this rate changes. The rate is given by Γ_0 in such a way that $\gamma\phi \sim a^{-3w}$ where w is the equation of state parameter in Eq. (5.2.80), as expected from considerations in Section 5.2.1.

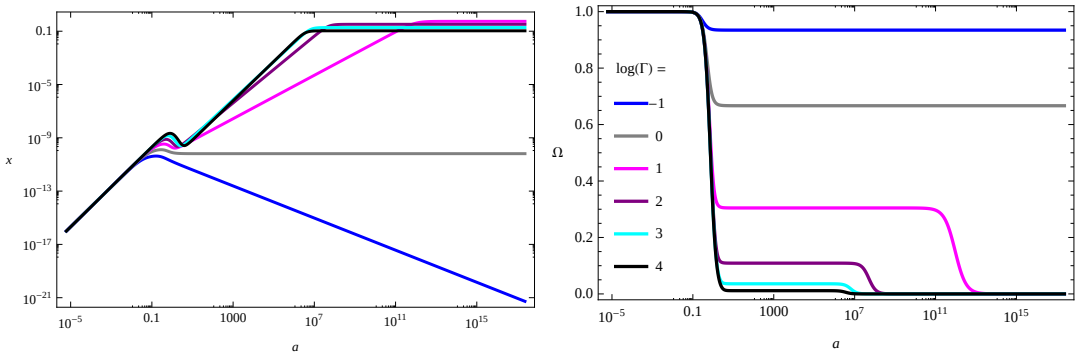

Figure 5.4: The evolution of the "kinetic term" x (left panel) and Ω (right panel) as functions of the scale factor a for different values of Γ_0 (as given in the legend of the right panel). For Γ_0 larger than unity, the evolution of x is similar to that which is depicted in figure 5.3, and Ω behaves as depicted in figure 5.1. For the limiting value $\Gamma_0 = 1$, for which the attractor value of the equation of state is $w = -1/3$, the x-term freezes, while the matter scaling persists. When $\Gamma_0 < 1$, the attractor value of the equation of state parameter is non-accelerating, $w > -1/3$, and instead of growing the x-term begins to decay when the matter scaling solution is reached. The solution is now an attractor and Ω remains as the constant given in Eq. (5.2.79).

the "Dark D-brane".

In this scenario, dark energy descends from the brane's motion in the compact space, which manifests in the four-dimensional theory as a scalar field with non-standard (DBI) kinetic terms. In addition, dark matter, and possibly dark radiation, are associated with the matter fields which are localised on this brane. Due to the form of the induced metric on the brane, the dark fluids interact with one another via a disformal coupling, which then provides an explicit realisation of this coupling within a fundamental theory.

Due to the particular form of the energy exchange between the dark fluids, we have demonstrated that the Dark D-brane scenario proposed herein exhibits scaling solutions, and thus can alleviate the "cosmic coincidence" problem by allowing the energy densities in dark energy and dark matter to be proportional across several efolds of the cosmological evolution. Furthermore, since the Dark D-brane is a hidden brane, this scenario can naturally account for the observational fact that the coupling between dark matter and standard model fields is strongly suppressed.

For the purpose of illustration we have herein considered the simplest Dark D-brane model, which features a probe D3-brane moving in a warped region of a Type IIB flux compactification, and have explored the resulting homogeneous cosmological evolution.

To study the dynamics we have implemented a dynamical systems analysis, in which we focused on a power law form for the warp factor h as well as for the brane's potential V. We derived four classes of fixed points, which correspond to matter domination, a de Sitter solution, kinetic domination, and the scaling solutions respectively. Among these, only the matter dominated fixed point is independent of the values of the parameters, while the other fixed points depend upon the values of the exponents in the power law expressions for h and V.

The most interesting class of fixed points are the scaling accelerating solutions, as these can resolve the coincidence problem. Within this class of fixed points, we have studied explicitly two representative cases. Firstly, we considered a Dark D-brane moving in an AdS_5 geometry, which can be seen as an approximation to the mid-region of a realistic Klebnov-Strassler geometry, along a quadratic potential.

Secondly, we considered a constant warp factor, which can arise in a very near-tip Klebanov-Strassler region, or simply as an unwarped region in a large volume scenario, with an inverse power law potential. In the ultra-relativistic limit, we found two different types of disformal scaling fixed points for the two cases, namely a matter scaling and a kinetic scaling fixed point. At the matter scaling point, the disformally coupled dark matter contributes a constant fraction to the expansion rate. At the kinetic scaling point on the other hand, the matter sources contribute negligibly to the energy density, and yet this fixed point exhibits precisely the same total equation of state as the matter scaling fixed point.

Finally, we numerically confirmed all of the results for the AdS_5 case which were expected from analytic considerations as well as from the dynamical system analysis. While we focussed more on this case, it is worth mentioning that inverse power law potentials of precisely the type considered in our second case, namely for which $n = -2$, can alleviate the fine-tuning problem of the scale of dark energy [174, 175]. However, it remains to be seen whether such potentials can be realised robustly in Type IIB flux compactifications. Therefore, while our scenario is able to address one of the two long-standing problems of dark energy, there is much that still needs to be understood in relation to how this scenario might address the remaining problem. Furthermore, in the current work we considered only the background expansion. In order to fully access the viability of this model, an obvious next step is to study the perturbations.

In summary, we found that the expansion can generically begin with an accelerating scaling regime which eventually gives way to a purely dark energy dominated regime with the same expansion rate. Therefore, the simplest Dark D-brane scenario can give rise to very viable late-time cosmology, which motivates the study of more realistic and concrete models within this framework, as well as the search for observational signatures that could distinguish the presence of a Dark D-brane world from other dark sector scenarios.

Chapter 6

Concluding Remarks

In this thesis we have explored a variety of exotic cosmological phenomena in the late-time universe, when structures such as black holes and galaxy clusters have formed. In particular, we have focussed on the interactions between the theoretically well-motivated but physically mysterious entities that may populate the cosmological landscape today.

Cosmic strings are objects which are believed to be formed in the early universe during the symmetry breaking processes that allow the particle spectrum to evolve into its present form, namely the standard model of particle physics. In addition, they can be formed at the end of D-brane inflation scenarios in string theoretic descriptions of the early universe. In this way, their existence is motivated by and expected from both pure field theory models as well as fundamental high-energy models of cosmology. Furthermore, while their existence remains hypothetical in cosmology, there are in fact strong indications from observations of other natural systems that they may indeed be someday glimpsed in the cosmos. Namely, string-like defects have indeed been observed to arise in condensed matter systems such as liquid crystals. The physics underpinning the formation of these objects is precisely the same as that which predicts defects in the cosmological fluid.

While most studies of the cosmological journey of these objects have focussed on their formation and evolution into networks of strings and loops, in the present study we have instead addressed the question of their ultimate fate in the universe. The evolution of cosmic strings is such that once they have formed in the early

universe, the individual strings are stretched by the expanding background, while at the same time loops are formed during the intercommutation process, which dilutes the initial density of the strings. Eventually however the string network enters a regime during which the density of the network becomes scale-invariant. The overall result is that a small number of strings are expected to be present today, amid a gas of oscillating loops.

So, what happens to these strings? This is a very pertinent question as its answer determines whether or not, and where or where not, we might actually concretely observe them. As the strings drift through the universe, we can expect that they will naturally move into gravitationally dense regions much like all other physical objects which traverse the cosmos. Therefore, along with other forms of visible matter, they will trace the dark matter density, and collect in dark haloes along side galaxies and clusters, eventually journeying towards the dense cores of these regions, which are strongly believed to harbour supermassive black holes. Thus the question of what happens to the strings may ultimately be the question of how the strings might interact with black holes. Can a black hole "catch" a cosmic string? Or are strings somehow repelled by black holes, such that they must avoid regions of dense matter entirely, and thus can be expected to end up collecting in voids?

In order to address this, in Chapter 3 we have considered the interaction between an astrophysical black hole, namely a black hole that is *rotating*, and a single cosmic string. We focussed on the end state of the interaction, namely the intersection or composite configuration of the two objects that could form once the objects meet. Employing the abelian Higgs vortex model for the string, we solved the vortex equations in the Kerr background, treating the string as a probe in the spacetime of the black hole, and aligning it in such a way as to respect the symmetries of the spacetime. From this probe analysis, we found that it is quite possible to form a stable, composite state consisting of a cosmic string piercing through the poles of a rotating black hole. Indeed, due to the fact that the energy and tension balance one another in the core of the string, the string does not feel a gravitational force through its interior and thus does not become swallowed by the black hole, but instead threads through it.

Having verified that such a configuration can exist, we went on the explore its phenomenology, which turns out to be diverse and abundant. Firstly, in the presence of rotation, the constant axial magnetic flux lines of the string become accompanied by electric flux lines which emerge in the close vicinity of the event horizon. Thus the gauge field of the string naturally picks up a time component, which is in fact generated by the rotating background due to the non-trivial mixing between the time and azimuthal directions, and so the standard duet of string degrees of freedom becomes a trio, $\{X, P_\phi, P_t\}$.

Secondly, upon examination of the extremal limit of the system for a variety of black hole masses, we found that the Kerr string system exhibits a Meissner effect, in which the flux lines of the string become expelled from the black hole and thus the fields remain in their vacuum states across the entirety of the horizon. This flux-expelling behaviour occurs for extremal black holes of lower mass relative to the width of the string. Specifically, as one lowers the mass of the extremal black hole, a first-order phase transition takes place during which the piercing fields become expelled, such that the black hole essentially sits within the core of the string, enveloped by the scalar condensate and gauge flux lines.

Thirdly, taking into account the gravitational effects of the string on the Kerr spacetime, we uncovered another striking consequence of the non-trivial mixing between the time and azimuthal directions in this spacetime. Whereas in a static or flat background, the gravitational effect of the string is to induce an azimuthal conical deficit at spatial infinity, in a stationary background, we verified herein that the deficit is blended in with the time direction. Another way to phrase this is that the purely conical effect is with respect to a local co-rotating frame, rather than with respect to an observer at infinity, thus an asymptotic observer sees a conical effect in the intersection of the time and azimuthal directions. The physical consequences of this rotationally blended deficit are that the ergosphere and possibly the innermost stable circular orbits of objects near to the black hole are shifted by the presence of the string. While this avenue remains to be explored, it provides a potential direct signal for the composite string and black hole system through studies of the perturbations of geodesic motion in the close vicinity of galactic black holes.

In Chapter 4, we then took this line of research into a more theoretical direction, and examined the effects of a negative cosmological constant on the Kerr vortex system. Such a system is not realised in nature, at least not in our four-dimensional universe, however derives its motivation from holography and higher dimensional theories such as string theory.

For the purposes of this study, we considered the vortex to be a probe in the AdS black hole spacetime. We began by exploring the effect of the cosmological constant on the string fields in a purely AdS background, and found that shortening the AdS length ℓ tends to tighten the core of the string while at the same time causes the fields to fall off more gradually towards their vacuum values. We then addressed the physics of the full vortex and black hole system, including a black hole charge for completeness. In this way, we were able to extract a detailed picture of the roles played by all the various parameters which can be contained in such a system.

As with the pure Kerr case, the rotation generated a time component for the gauge field, and thus electric flux lines near the horizon. In addition, small mass black holes exhibited a Meissner effect, once again governed by a first-order phase transition. The effect of decreasing ℓ on the transition is to lower to ciritical radius of the horizon at which the transition takes place. On the other hand, the charge of the black hole does not appear to impact the physics of the composite system studied herein.

Thus the work in Chapters 3 and 4 provides an insight into the interactions between two notable classical objects in cosmology, namely cosmic strings and rotating black holes, with the studies in Chapter 3 being of interest for physical cosmology while those in Chapter 4 being instead relevant for purely theoretical constructions.

These objects form part of the visible sector of the cosmological phenomena, in that they are made from standard model particles, with a black hole originating from a collapsed star composed of baryonic material, and a cosmic string consisting of a Higgs condensate core threaded with magnetic flux.

However, as we have reviewed in detail, the late-time universe is in fact dominated by some kind of invisible or dark sector, with dark matter and dark energy in fact completely governing the cosmological behaviour of visible matter. Dark energy

is the elusive fluid which is currently causing visible galaxies and clusters to fly apart from one another, while dark matter dominates the gravity inside the galaxies and clusters, and thus determines their internal structural and dynamical properties.

In Chapter 5, we trace the possible origins for the observed cosmological dark sector into higher dimensions of spacetime, and propose a unified model for this sector as a "Dark D-brane world" moving in these higher dimensions. In this sense, what we observe as dark phenomenology in four dimensions descends in fact from the dynamics of fundamental objects in the higher dimensional geometry. Compellingly, while the Dark D-brane world is constructed purely from the point of view of string theory, it turns out that the dark fluids associated with this object are exchanging energy with one another via a disformal coupling, which has been widely studied in the context of phenomenological theories of modified gravity. Thus our scenario forms a connection point between phenomenological and fundamental approaches to cosmology.

The Dark D-brane matter fields, which we associate with dark matter, are naturally and *necessarily* distinct from the visible sector, providing at once a concrete explanation for why these sectors are observed to be non-interacting. Furthermore, a study of the cosmological evolution in the Dark D-brane scenario, where the motion of the brane is associated with dark energy, revealed the presence of accelerating scaling solutions which can then address the cosmic coincidence problem. It remains to be seen however whether or not the observed scale of the vacuum energy can be robustly derived from this picture, and this might involve constructing the Dark D-brane from branes of lower codimension.

Therefore, at the level of the homogenous background studied herein, it seems at least plausible that the dark fluids could in fact be telling us something about what is going on in the higher dimensional spacetime. If so, then these fields provide a tantalising means for us to glimpse into worlds beyond our own.

Figure 6.1: Tibetan Cosmology: The "Wheel of Life", containing the six realms into which beings are reborn, held in the claws of Mara, who represents death and impermanence. In the centre are the three poisons, and an individual's response to these poisons determines the realm into which he or she will be reborn.

You are the formless within all forms, the silence and stillness inside all movements of time and manifestation.
Arise into the fullness of your real nature, as the unchanging self, the goal and source of all being.
–Mooji

Bibliography

[1] P. T. Chrusciel, *'No hair' theorems: Folklore, conjectures, results,* Contemp. Math. **170**, 23 (1994) [gr-qc/9402032].

[2] J. D. Bekenstein, *Black hole hair: 25 - years after,* In *Moscow 1996, 2nd International A.D. Sakharov Conference on physics* 216-219 [gr-qc/9605059].

[3] J. E. Chase, *Event Horizons in Static Scalar-Vacuum Space-Times,* Com. Math. Phys. **19** 276–288 (1970).

[4] S. L. Adler and R. B. Pearson, *'No Hair' Theorems for the Abelian Higgs and Goldstone Models,* Phys. Rev. **D18**, 2798 (1978).

[5] S. Perlmutter *et al.* [Supernova Cosmology Project Collaboration], *Measurements of Omega and Lambda from 42 high redshift supernovae*, Astrophys. J. **517**, 565 (1999) [astro-ph/9812133].

[6] A. G. Riess *et al.* [Supernova Search Team Collaboration], *Observational evidence from supernovae for an accelerating universe and a cosmological constant*, Astron. J. **116**, 1009 (1998) [astro-ph/9805201].

[7] D. N. Spergel *et al.* [WMAP Collaboration], *Wilkinson Microwave Anisotropy Probe (WMAP) three year results: implications for cosmology*, Astrophys. J. Suppl. **170**, 377 (2007) [astro-ph/0603449].

[8] M. Tegmark *et al.* [SDSS Collaboration], *Cosmological parameters from SDSS and WMAP*, Phys. Rev. D **69**, 103501 (2004) [astro-ph/0310723].

[9] N. Mustapha, C. Hellaby and G. F. R. Ellis, *Large scale inhomogeneity versus source evolution: Can we distinguish them observationally?*, Mon. Not. Roy. Astron. Soc. **292**, 817 (1997) [gr-qc/9808079].

[10] E. J. Copeland, M. Sami and S. Tsujikawa, *Dynamics of dark energy*, Int. J. Mod. Phys. D **15**, 1753 (2006) [hep-th/0603057].

[11] P. A. R. Ade *et al.* [Planck Collaboration], *Planck 2015 results. XIII. Cosmological parameters*, arXiv:1502.01589 [astro-ph.CO].

[12] M. Milgrom, *A Modification of the Newtonian dynamics as a possible alternative to the hidden mass hypothesis*, Astrophys. J. **270**, 365 (1983).

[13] J. D. Bekenstein, *Relativistic gravitation theory for the MOND paradigm*, Phys. Rev. D **70**, 083509 (2004) [Erratum-ibid. D **71**, 069901 (2005)] [astro-ph/0403694].

[14] D. Clowe, M. Bradac, A. H. Gonzalez, M. Markevitch, S. W. Randall, C. Jones and D. Zaritsky, *A direct empirical proof of the existence of dark matter*, Astrophys. J. **648**, L109 (2006) [astro-ph/0608407].

[15] B. Ratra and P. J. E. Peebles, *Cosmological Consequences of a Rolling Homogeneous Scalar Field*, Phys. Rev. D **37**, 3406 (1988).

[16] R. R. Caldwell, R. Dave and P. J. Steinhardt, *Cosmological imprint of an energy component with general equation of state*, Phys. Rev. Lett. **80**, 1582 (1998) [astro-ph/9708069].

[17] E. J. Copeland, A. R. Liddle, and D. Wands, *Exponential potentials and cosmological scaling solutions*, *Phys.Rev.* **D57** (1998) 4686–4690, `gr-qc/9711068`.

[18] P. G. Ferreira and M. Joyce, *Cosmology with a primordial scaling field*, *Phys.Rev.* **D58** (1998) 023503, `astro-ph/9711102`.

[19] L. Amendola, *Scaling solutions in general nonminimal coupling theories*, *Phys.Rev.* **D60** (1999) 043501, `astro-ph/9904120`.

[20] Y. L. Bolotin, A. Kostenko, O. A. Lemets and D. A. Yerokhin, *Cosmological Evolution With Interaction Between Dark Energy And Dark Matter*, 1310.0085.

[21] C. Wetterich, *The Cosmon model for an asymptotically vanishing time dependent cosmological 'constant'*, *Astron.Astrophys.* **301** (1995) 321–328, hep-th/9408025.

[22] L. Amendola, *Coupled quintessence*, *Phys.Rev.* **D62** (2000) 043511, astro-ph/9908023.

[23] L. Amendola, M. Quartin, S. Tsujikawa, and I. Waga, *Challenges for scaling cosmologies*, *Phys.Rev.* **D74** (2006) 023525, astro-ph/0605488.

[24] C. G. Boehmer, G. Caldera-Cabral, R. Lazkoz, and R. Maartens, *Dynamics of dark energy with a coupling to dark matter*, *Phys.Rev.* **D78** (2008) 023505, 0801.1565.

[25] B. Li and H. Zhao, *Structure Formation by Fifth Force I: N-Body vs. Linear Simulations*, *Phys.Rev.* **D80** (2009) 044027, 0906.3880.

[26] L. L. Honorez, B. A. Reid, O. Mena, L. Verde, and R. Jimenez, *Coupled dark matter-dark energy in light of near Universe observations*, *JCAP* **1009** (2010) 029, 1006.0877.

[27] T. Clemson, K. Koyama, G.-B. Zhao, R. Maartens, and J. Valiviita, *Interacting Dark Energy – constraints and degeneracies*, *Phys.Rev.* **D85** (2012) 043007, 1109.6234.

[28] A. Pourtsidou, C. Skordis, and E. Copeland, *Models of coupled dark matter to dark energy*, 1307.0458.

[29] T. Kaluza, *On the Problem of Unity in Physics*, Sitzungsber. Preuss. Akad. Wiss. Berlin (Math. Phys.) **1921**, 966 (1921).

[30] O. Klein, *Quantum Theory and Five-Dimensional Theory of Relativity. (In German and English)*, Z. Phys. **37**, 895 (1926) [Surveys High Energ. Phys. **5**, 241 (1986)].

[31] W. Nahm, *Supersymmetries and their Representations*, Nucl. Phys. B **135**, 149 (1978).

[32] E. Witten, *Search for a Realistic Kaluza-Klein Theory*, Nucl. Phys. B **186**, 412 (1981).

[33] P. G. O. Freund and M. A. Rubin, *Dynamics of Dimensional Reduction*, Phys. Lett. B **97**, 233 (1980).

[34] M. B. Green and J. H. Schwarz, *Anomaly Cancellation in Supersymmetric D=10 Gauge Theory and Superstring Theory*, Phys. Lett. B **149**, 117 (1984).

[35] S. W. Hawking, *Virtual black holes*, Phys. Rev. D **53**, 3099 (1996) [hep-th/9510029].

[36] J. A. Wheeler, *On the Nature of quantum geometrodynamics*, Annals Phys. **2**, 604 (1957).

[37] E. Silverstein and D. Tong, *Scalar speed limits and cosmology: Acceleration from D-cceleration*, *Phys.Rev.* **D70** (2004) 103505, `hep-th/0310221`.

[38] M. Alishahiha, E. Silverstein, and D. Tong, *DBI in the sky*, *Phys.Rev.* **D70** (2004) 123505, `hep-th/0404084`.

[39] R. Kallosh, *On inflation in string theory*, *Lect.Notes Phys.* **738** (2008) 119–156, `hep-th/0702059`.

[40] C. Burgess, *Lectures on Cosmic Inflation and its Potential Stringy Realizations*, *Class.Quant.Grav.* **24** (2007) S795, `0708.2865`.

[41] C. Burgess and L. McAllister, *Challenges for String Cosmology*, *Class.Quant.Grav.* **28** (2011) 204002, `1108.2660`.

[42] D. Baumann and L. McAllister, *Advances in Inflation in String Theory*, *Ann.Rev.Nucl.Part.Sci.* **59** (2009) 67–94, 0901.0265.

[43] L. McAllister and E. Silverstein, *String Cosmology: A Review*, *Gen.Rel.Grav.* **40** (2008) 565–605, 0710.2951.

[44] A.-C. Davis and T. W. B. Kibble, *Fundamental cosmic strings*, Contemp. Phys. **46**, 313 (2005) [hep-th/0505050].

[45] E. J. Copeland, R. C. Myers and J. Polchinski, *Cosmic F and D strings*, JHEP **0406**, 013 (2004) [hep-th/0312067].

[46] L. Pogosian, S. H. H. Tye, I. Wasserman and M. Wyman, *Observational constraints on cosmic string production during brane inflation*, Phys. Rev. D **68** (2003) 023506 [Erratum-ibid. D **73** (2006) 089904] [hep-th/0304188].

[47] J. J. Noller, *Disformal Gravity*, Ph.D thesis, Oxford University (2012)

[48] M. Ostrogradski, Memoires de l'Academie Imperiale des Science de Saint-Petersbourg, 4:385 (1850)

[49] J. D. Bekenstein, *The Relation between physical and gravitational geometry*, Phys. Rev. D **48**, 3641 (1993) [gr-qc/9211017].

[50] V. Faraoni, E. Gunzig, and P. Nardone, *Conformal transformations in classical gravitational theories and in cosmology*, *Fund.Cosmic Phys.* **20** (1999) 121, gr-qc/9811047.

[51] A. De Felice and S. Tsujikawa, *f(R) theories*, *Living Rev.Rel.* **13** (2010) 3, 1002.4928.

[52] M. Zumalacarregui, T. S. Koivisto, and D. F. Mota, *DBI Galileons in the Einstein Frame: Local Gravity and Cosmology*, *Phys.Rev.* **D87** (2013) 083010, 1210.8016.

[53] D. Bettoni and S. Liberati, *Disformal invariance of second order tensor-scalar theories: framing the Horndeski action*, 1306.6724.

[54] M. Zumalacárregui and J. García-Bellido, *Transforming gravity: from derivative couplings to matter to second-order scalar-tensor theories beyond the Horndeski Lagrangian*, 1308.4685.

[55] C. de Rham, G. Gabadadze, and A. J. Tolley, *Resummation of Massive Gravity*, *Phys.Rev.Lett.* **106** (2011) 231101, 1011.1232.

[56] C. de Rham and G. Gabadadze, *Generalization of the Fierz-Pauli Action*, *Phys.Rev.* **D82** (2010) 044020, 1007.0443.

[57] R. Sanders, *A Stratified framework for scalar - tensor theories of modified dynamics*, *Astrophys.J.* **480** (1997) 492–502, astro-ph/9612099.

[58] C. Skordis, D. Mota, P. Ferreira, and C. Boehm, *Large Scale Structure in Bekenstein's theory of relativistic Modified Newtonian Dynamics*, *Phys.Rev.Lett.* **96** (2006) 011301, astro-ph/0505519.

[59] J.-P. Bruneton, *On causality and superluminal behavior in classical field theories: Applications to k-essence theories and MOND-like theories of gravity*, *Phys.Rev.* **D75** (2007) 085013, gr-qc/0607055.

[60] C. Skordis, *The Tensor-Vector-Scalar theory and its cosmology*, *Class.Quant.Grav.* **26** (2009) 143001, 0903.3602.

[61] J. Magueijo, *New varying speed of light theories*, *Rept.Prog.Phys.* **66** (2003) 2025, astro-ph/0305457.

[62] M. Clayton and J. Moffat, *A Scalar - tensor cosmological model with dynamical light velocity*, *Phys.Lett.* **B506** (2001) 177–186, gr-qc/0101126.

[63] J. Magueijo, *Bimetric varying speed of light theories and primordial fluctuations Phys.Rev.* **D79** (2009) 043525, 0807.1689.

[64] P. Brax, C. Burrage, and A.-C. Davis, *Shining Light on Modifications of Gravity*, *JCAP* **1210** (2012) 016, 1206.1809.

[65] C. van de Bruck, J. Morrice, and S. Vu, *Constraints on Disformal Couplings from the CMB Temperature Evolution*, 1303.1773.

[66] P. Brax, C. Burrage, A.-C. Davis, and G. Gubitosi, *Cosmological Tests of the Disformal Coupling to Radiation*, 1306.4168.

[67] C. van de Bruck and G. Sculthorpe, *Modified Gravity and the Radiation Dominated Epoch*, *Phys.Rev.* **D87** (2013) 044004, 1210.2168.

[68] J. Sakstein, *Disformal Theories of Gravity: From the Solar System to Cosmology*, JCAP **1412**, no. 12, 012 (2014) [arXiv:1409.1734 [astro-ph.CO]].

[69] J. Sakstein, *Towards Viable Cosmological Models of Disformal Theories of Gravity*, Phys. Rev. D **91**, no. 2, 024036 (2015) [arXiv:1409.7296 [astro-ph.CO]].

[70] N. Kaloper, *Disformal inflation*, *Phys. Lett. B* **583** (2004) 1, hep-ph/0312002.

[71] P. Brax and C. Burrage, *Constraining Disformally Coupled Scalar Fields*, Phys. Rev. D **90** (2014) 10, 104009 [arXiv:1407.1861 [astro-ph.CO]].

[72] A. Vilenkin, *Cosmic Strings and Domain Walls,* Phys. Rept. **121**, 263 (1985).

[73] A. Vilenkin and E. P. S. Shellard, *Cosmic Strings and other Topological Defects*. Cambridge University Press, Cambridge, England, 1994.

[74] T. W. B. Kibble, *Topology of Cosmic Domains and Strings*, J. Phys. A **9**, 1387 (1976).

[75] J. Ipser and P. Sikivie, *The Gravitationally Repulsive Domain Wall,* Phys. Rev. **D30**, 712 (1984).

[76] G. W. Gibbons, *Global structure of supergravity domain wall space-times,* Nucl. Phys. B **394**, 3 (1993).

[77] H. B. Nielsen and P. Olesen, *Vortex Line Models for Dual Strings*, *Nucl.Phys.* **B61** (1973) 45–61.

[78] A. Vilenkin, *Gravitational Field of Vacuum Domain Walls and Strings,* Phys. Rev. **D23**, 852 (1981).

[79] D. Garfinkle, *General relativistic strings*, *Phys. Rev. D* **32** (1985) 1323.

[80] M. Aryal, L. Ford, and A. Vilenkin, *Cosmic strings and black holes*, *Phys.Rev.* **D34** (1986) 2263.

[81] R. Gregory, *Gravitational stability of local strings*, *Phys.Rev.Lett.* **59** (1987) 740.

[82] R. Emparan, R. Gregory and C. Santos, *Black holes on thick branes,* Phys. Rev. **D63**, 104022 (2001) [hep-th/0012100].

[83] A. Achucarro, R. Gregory, and K. Kuijken, *Abelian Higgs hair for black holes*, Phys. Rev. **D52** (1995) 5729–5742, [gr-qc/9505039].

[84] R. Gregory and M. Hindmarsh, *Smooth metrics for snapping strings*, Phys. Rev. **D52** (1995) 5598–5605, [gr-qc/9506054].

[85] D. M. Eardley, G. T. Horowitz, D. A. Kastor and J. H. Traschen, *Breaking cosmic strings without monopoles,* Phys. Rev. Lett. **75**, 3390 (1995) [gr-qc/9506041].

[86] S. W. Hawking and S. F. Ross, *Pair production of black holes on cosmic strings,* Phys. Rev. Lett. **75**, 3382 (1995) [gr-qc/9506020].

[87] R. Emparan, *Pair creation of black holes joined by cosmic strings,* Phys. Rev. Lett. **75**, 3386 (1995) [gr-qc/9506025].

[88] A. Achucarro and R. Gregory, *Selection rules for splitting strings,* Phys. Rev. Lett. **79**, 1972 (1997) [hep-th/9705001].

[89] M. Dehghani, A. Ghezelbash, and R. B. Mann, *Abelian Higgs hair for AdS-Schwarzschild black hole*, Phys. Rev. **D65** (2002) 044010, [hep-th/0107224].

[90] A. Ghezelbash and R. Mann, *Vortices in de Sitter space-times*, *Phys.Lett.* **B537** (2002) 329–339, [hep-th/0203003].

[91] M. H. Dehghani, A. M. Ghezelbash and R. B. Mann, *Vortex holography,* Nucl. Phys. **B625**, 389 (2002) [hep-th/0105134].

[92] A. Chamblin, J. Ashbourn-Chamblin, R. Emparan, and A. Sornborger, *Can extreme black holes have (long) Abelian Higgs hair?*, Phys. Rev. **D58** (1998) 124014, [gr-qc/9706004].

[93] A. Chamblin, J. Ashbourn-Chamblin, R. Emparan, and A. Sornborger, *Abelian Higgs hair for extreme black holes and selection rules for snapping strings*, Phys. Rev. Lett. **80** (1998) 4378–4381, [gr-qc/9706032].

[94] F. Bonjour and R. Gregory, *Comment on 'Abelian Higgs hair for extremal black holes and selection rules for snapping strings'*, Phys. Rev. Lett. **81** (1998) 5034,

[95] F. Bonjour, R. Emparan, and R. Gregory, *Vortices and extreme black holes: The Question of flux expulsion*, Phys. Rev. **D59** (1999) 084022,

[96] A. Ghezelbash and R. B. Mann, *Abelian Higgs hair for rotating and charged black holes*, Phys. Rev. **D65** (2002) 124022, [hep-th/0110001].

[97] A. N. Aliev and D. V. Galtsov, *Gravitational Effects in the Field of a Central Body Threaded by a Cosmic String, Sov. Astron. Lett.* **14**, 48 (1988).

[98] R. Gregory, D. Kubiznak and D. Wills, *Rotating black hole hair,* JHEP **1306**, 023 (2013) [arXiv:1303.0519 [gr-qc]].

[99] P. Bizon, *Colored black holes,* Phys. Rev. Lett. **64**, 2844 (1990).

[100] H. Luckock and I. Moss, *Black Holes Have Skyrmion Hair,* Phys. Lett. **B176**, 341 (1986).

[101] K. -M. Lee, V. P. Nair and E. J. Weinberg, *Black holes in magnetic monopoles,* Phys. Rev. **D45**, 2751 (1992) [hep-th/9112008].

[102] T. Jacobson, *Primordial black hole evolution in tensor scalar cosmology,* Phys. Rev. Lett. **83**, 2699 (1999) [astro-ph/9905303].

[103] S. Chadburn and R. Gregory, *Time dependent black holes and scalar hair,* [arXiv:1304.6287 [gr-qc]].

[104] E. Abdalla, N. Afshordi, M. Fontanini, D. C. Guariento and E. Papantonopoulos, *Cosmological black holes from self-gravitating fields,* [arXiv:1312.3682 [gr-qc]].

[105] S. Hod, *Stationary Scalar Clouds Around Rotating Black Holes, Phys. Rev. D* **86**, 104026 (2012) [Erratum-ibid. D **86**, 129902 (2012)] [arXiv:1211.3202 [gr-qc]].
C. A. R. Herdeiro and E. Radu, *Kerr black holes with scalar hair, Phys. Rev. Lett.* **112**, 221101 (2014) [arXiv:1403.2757 [gr-qc]].

[106] V. Cardoso, O. J. C. Dias, J. P. S. Lemos and S. Yoshida, *The Black hole bomb and superradiant instabilities,* Phys. Rev. D **70**, 044039 (2004) [Erratum-ibid. D **70**, 049903 (2004)] [hep-th/0404096].

[107] V. Cardoso and O. J. C. Dias, *Small Kerr-anti-de Sitter black holes are unstable,* Phys. Rev. D **70**, 084011 (2004) [hep-th/0405006].

[108] E. B. Bogomolnyi, *The stability of classical solutions*, *Sov. J. Nucl. Phys.* **24** (1976) 449.

[109] R. Wald, *Black hole in a uniform magnetic field*, *Phys.Rev.* **D10** (1974) 1680–1685.

[110] D. V. Galtsov and E. Masar, *Geodesics In Space-times Containing Cosmic Strings,* Class. Quant. Grav. **6**, 1313 (1989).

[111] C. Charmousis, D. Langlois, D. A. Steer and R. Zegers, *Rotating spacetimes with a cosmological constant,* JHEP **0702**, 064 (2007)

[112] O. J. C. Dias, G. T. Horowitz, N. Iqbal and J. E. Santos, *Vortices in holographic superfluids and superconductors as conformal defects* [arXiv:1311.3673 [hep-th]].

[113] P. Breitenlohner and D. Z. Freedman, *Stability in Gauged Extended Supergravity,* Annals Phys. **144**, 249 (1982).

[114] B. Carter, *Hamilton-Jacobi and Schrodinger separable solutions of Einstein's equations,* Commun. Math. Phys. **10**, 280 (1968).

[115] G. W. Gibbons, M. J. Perry and C. N. Pope, *The First law of thermodynamics for Kerr-anti-de Sitter black holes,* Class. Quant. Grav. **22**, 1503 (2005) [hep-th/0408217].

[116] R. Gregory, P. C. Gustainis, D. Kubizk, R. B. Mann and D. Wills, *Vortex hair on AdS black holes*, JHEP **1411**, 010 (2014) [arXiv:1405.6507 [hep-th]].

[117] T. Koivisto, D. Wills and I. Zavala, *Dark D-brane Cosmology*, JCAP **1406**, 036 (2014) [arXiv:1312.2597 [hep-th]].

[118] K. Akama, *An Early Proposal of 'Brane World'*, *Lect.Notes Phys.* **176** (1982) 267–271, hep-th/0001113.

[119] V. Rubakov and M. Shaposhnikov, *Do We Live Inside a Domain Wall?*, *Phys.Lett.* **B125** (1983) 136–138.

[120] M. Visser, *An Exotic Class of Kaluza-Klein Models*, *Phys.Lett.* **B159** (1985) 22, hep-th/9910093.

[121] G. Gibbons and D. Wiltshire, *Space-Time as a Membrane in Higher Dimensions*, *Nucl.Phys.* **B287** (1987) 717, hep-th/0109093.

[122] D. A. Easson, R. Gregory, G. Tasinato, and I. Zavala, *Cycling in the Throat*, *JHEP* **0704** (2007) 026, hep-th/0701252.

[123] D. A. Easson, R. Gregory, D. F. Mota, G. Tasinato, and I. Zavala, *Spinflation*, *JCAP* **0802** (2008) 010, 0709.2666.

[124] R. Gregory and D. Kaviani, *Spinflation with Angular Potentials*, *JHEP* **1201** (2012) 037, 1107.5522.

[125] C. Burgess, F. Quevedo, R. Rabadan, G. Tasinato, and I. Zavala, *On bouncing brane worlds, S-branes and branonium cosmology*, *JCAP* **0402** (2004) 008, hep-th/0310122.

[126] A. Avgoustidis, D. Cremades, and F. Quevedo, *Wilson line inflation*, *Gen.Rel.Grav.* **39** (2007) 1203–1234, hep-th/0606031.

[127] A. Avgoustidis and I. Zavala, *Warped Wilson Line DBI Inflation*, *JCAP* **0901** (2009) 045, 0810.5001.

[128] K. Dimopoulos, D. Wills, and I. Zavala, *Statistical Anisotropy from Vector Curvaton in D-brane Inflation*, *Nucl.Phys.* **B868** (2013) 120–155, 1108.4424.

[129] D. Wills, K. Dimopoulos, and I. Zavala, *D-branes and cosmic structure*, 1303.5581.

[130] J. Martin and M. Yamaguchi, *DBI-essence*, *Phys.Rev.* **D77** (2008) 123508, 0801.3375.

[131] B. Gumjudpai and J. Ward, *Generalised DBI-Quintessence*, *Phys.Rev.* **D80** (2009) 023528, 0904.0472.

[132] E. Pajer, *JCAP* **0804** (2008) 031, 0802.2916.

[133] D. Baumann, A. Dymarsky, I. R. Klebanov, and L. McAllister, *JCAP* **0801** (2008) 024, 0706.0360.

[134] P. Brax, A.-C. Davis, B. Li, and H. A. Winther, *Phys.Rev.* **D86** (2012) 044015, 1203.4812.

[135] J. Noller, *JCAP* **1207** (2012) 013, 1203.6639.

[136] T. S. Koivisto, D. F. Mota, and M. Zumalacarregui, *Phys.Rev.Lett.* **109** (2012) 241102, 1205.3167.

[137] T. Koivisto, *Phys.Rev.* **D72** (2005) 043516, astro-ph/0504571.

[138] D. Mota, V. Pettorino, G. Robbers, and C. Wetterich, *Phys.Lett.* **B663** (2008) 160–164, 0802.1515.

[139] R. Bean, E. E. Flanagan, I. Laszlo, and M. Trodden, *Phys.Rev.* **D78** (2008) 123514, 0808.1105.

[140] A. L. Erickcek, N. Barnaby, C. Burrage, and Z. Huang, *Catastrophic Consequences of Kicking the Chameleon*, 1304.0009.

[141] J. Cembranos, A. Dobado, and A. L. Maroto, *Brane world dark matter*, *Phys.Rev.Lett.* **90** (2003) 241301, hep-ph/0302041.

[142] J. Cembranos, A. Dobado, and A. L. Maroto, *Cosmological and astrophysical limits on brane fluctuations*, *Phys.Rev.* **D68** (2003) 103505, hep-ph/0307062.

[143] J. Cembranos, A. Dobado, and A. L. Maroto, *Dark geometry*, *Int.J.Mod.Phys.* **D13** (2004) 2275–2280, hep-ph/0405165.

[144] G. Servant and T. M. Tait, *Is the lightest Kaluza-Klein particle a viable dark matter candidate?*, *Nucl.Phys.* **B650** (2003) 391–419, hep-ph/0206071.

[145] H.-C. Cheng, J. L. Feng, and K. T. Matchev, *Kaluza-Klein dark matter*, *Phys.Rev.Lett.* **89** (2002) 211301, hep-ph/0207125.

[146] D. Chialva, P. B. Dev, and A. Mazumdar, *Multiple dark matter scenarios from ubiquitous stringy throats*, *Phys.Rev.* **D87** (2013) 063522, 1211.0250.

[147] L. Bergstrom, *Dark Matter Candidates*, *New J.Phys.* **11** (2009) 105006, 0903.4849.

[148] D. Hooper and S. Profumo, *Dark matter and collider phenomenology of universal extra dimensions*, *Phys.Rept.* **453** (2007) 29–115, hep-ph/0701197.

[149] M. Cicoli, F. G. Pedro and G. Tasinato, *Natural Quintessence in String Theory*, JCAP **1207** (2012) 044, 1203.6655.

[150] L. R. Abramo, F. Finelli, and T. S. Pereira, *Constraining Born-Infeld models of dark energy with CMB anisotropies*, *Phys.Rev.* **D70** (2004) 063517, astro-ph/0405041.

[151] M. R. Garousi, M. Sami, and S. Tsujikawa, *Constraints on Dirac-Born-Infeld type dark energy models from varying alpha*, *Phys.Rev.* **D71** (2005) 083005, hep-th/0412002.

[152] S. Panda, M. Sami, and S. Tsujikawa, *Inflation and dark energy arising from geometrical tachyons*, *Phys.Rev.* **D73** (2006) 023515, hep-th/0510112.

[153] L. P. Chimento and R. Lazkoz, *Bridging geometries and potentials in DBI cosmologies*, *Gen.Rel.Grav.* **40** (2008) 2543–2555, 0711.0712.

[154] H. Wei, *Varying Alpha Driven by the Dirac-Born-Infeld Scalar Field*, *Phys.Lett.* **B682** (2009) 98–104, 0907.2749.

[155] L. P. Chimento, R. Lazkoz, and I. Sendra, *DBI models for the unification of dark matter and dark energy*, *Gen.Rel.Grav.* **42** (2010) 1189–1209, 0904.1114.

[156] J. Bhadra and U. Debnath, *Dynamical Study of DBI-essence in Loop Quantum Cosmology and Braneworld*, *Eur.Phys.J.* **C72** (2012) 2087, 1207.2144.

[157] P. Brax, C. Burrage, and A.-C. Davis, *Screening fifth forces in k-essence and DBI models JCAP* **1301** (2013) 020, 1209.1293.

[158] D. Bessada, *DBI analog of a decaying vacuum cosmology*, 1307.1099.

[159] Z.-K. Guo and N. Ohta, *Cosmological Evolution of Dirac-Born-Infeld Field*, *JCAP* **0804** (2008) 035, 0803.1013.

[160] C. Ahn, C. Kim, and E. V. Linder, *Cosmological Constant Behavior in DBI Theory Phys.Lett.* **B684** (2010) 181–184, 0904.3328.

[161] C. Ahn, C. Kim, and E. V. Linder, *Dark Energy Properties in DBI Theory*, *Phys.Rev.* **D80** (2009) 123016, 0909.2637.

[162] E. J. Copeland, S. Mizuno, and M. Shaeri, *Cosmological Dynamics of a Dirac-Born-Infeld field*, *Phys.Rev.* **D81** (2010) 123501, 1003.2881.

[163] J. Valiviita, E. Majerotto, and R. Maartens, *Instability in interacting dark energy and dark matter fluids*, *JCAP* **0807** (2008) 020, 0804.0232.

[164] M. Gavela, D. Hernandez, L. Lopez Honorez, O. Mena, and S. Rigolin, *Dark coupling*, *JCAP* **0907** (2009) 034, 0901.1611.

[165] C. Kaeonikhom, D. Singleton, S. V. Sushkov, and N. Yongram, *Dynamics of Dirac-Born-Infeld dark energy interacting with dark matter*, *Phys.Rev.* **D86** (2012) 124049, 1209.5219.

[166] S. B. Giddings, S. Kachru, and J. Polchinski, *Hierarchies from fluxes in string compactifications*, *Phys.Rev.* **D66** (2002) 106006, hep-th/0105097.

[167] F. Denef and M. R. Douglas, *Distributions of flux vacua*, *JHEP* **0405** (2004) 072, hep-th/0404116.

[168] A. Hebecker and J. March-Russell, *The Ubiquitous throat*, *Nucl.Phys.* **B781** (2007) 99–111, hep-th/0607120.

[169] D. Baumann, A. Dymarsky, S. Kachru, I. R. Klebanov and L. McAllister, *JHEP* **1006** (2010) 072, 1001.5028.

[170] I. R. Klebanov and M. J. Strassler, *Supergravity and a confining gauge theory: Duality cascades and chi SB resolution of naked singularities*, *JHEP* **0008** (2000) 052, hep-th/0007191.

[171] V. Balasubramanian, P. Berglund, J. P. Conlon, and F. Quevedo, *Systematics of moduli stabilisation in Calabi-Yau flux compactifications*, *JHEP* **0503** (2005) 007, hep-th/0502058.

[172] J. -P. Bruneton and G. Esposito-Farese, *Phys. Rev. D* **76** (2007) 124012 [Erratum-ibid. D **76** (2007) 129902], 0705.4043.

[173] B. de Carlos, J. A. Casas, F. Quevedo and E. Roulet, *Phys. Lett. B* **318** (1993) 447, hep-ph/9308325.

[174] P. J. Steinhardt, L. M. Wang and I. Zlatev, "Cosmological tracking solutions," Phys. Rev. D **59**, 123504 (1999) [astro-ph/9812313].

[175] I. Zlatev, L. M. Wang and P. J. Steinhardt, "Quintessence, cosmic coincidence, and the cosmological constant," Phys. Rev. Lett. **82**, 896 (1999) [astro-ph/9807002].